Disclosures
October 1, 2018

Dr. Christine Louie has disclosed a financial relationship with Grail, Inc. (consultant). South Bay Pathology Society has determined that these relationships are not relevant to the clinical cases being presented. The following planners and faculty had no financial relationships with commercial interests to disclose:

Presenters:

Erna Forgo, MD

Kevin Ko, MD, DDS

John Higgins, MD

Brittany Holmes, MD

Sebastian Fernandez-Pol, MD

Kerri Rieger, MD

Dita Gratzinger, MD, PhD

Yaso Natkunam, MD, PhD

Emily Chan, MD

Sarah Umetsu, MD

Keith Duncan, MD

Ankur Sangoi, MD

Activity Planners/Moderator:

Kristin Jensen, MD

Ankur Sangoi, MD

Megan Troxell, MD

OCT 2018 DIAGNOSIS LIST

6311: prostate paraganglion (prostate; GU pathology)
6312: oral syphilis (oral cavity; head and neck pathology)
6313: traumatic granuloma of tongue (tongue; head and neck pathology)
6314: c/w cryoglobulin deposits (skin; dermatopathology)
6315: EBV-positive mucocutaneous ulcer (oral cavity; head and neck pathology)
6316: renal cell carcinoma with ALK rearrangement (kidney; GU pathology)
6317: renal cell carcinoma, TCEB1-mutated (kidney; GU pathology)
6318: Myxoid variant nodular fascitis (soft tissuepsoft tissue pathology)
6319: crystal-negative Leydig cell tumor (ovary/GYN pathology)
6320: de-differentiated liposarcoma (kidney/GU pathology)

SB 6311

Erna Forgo/Christine Louie;
Stanford/Palo Alto VA

60-year-old male with increased PSA level. Prostate biopsy performed.

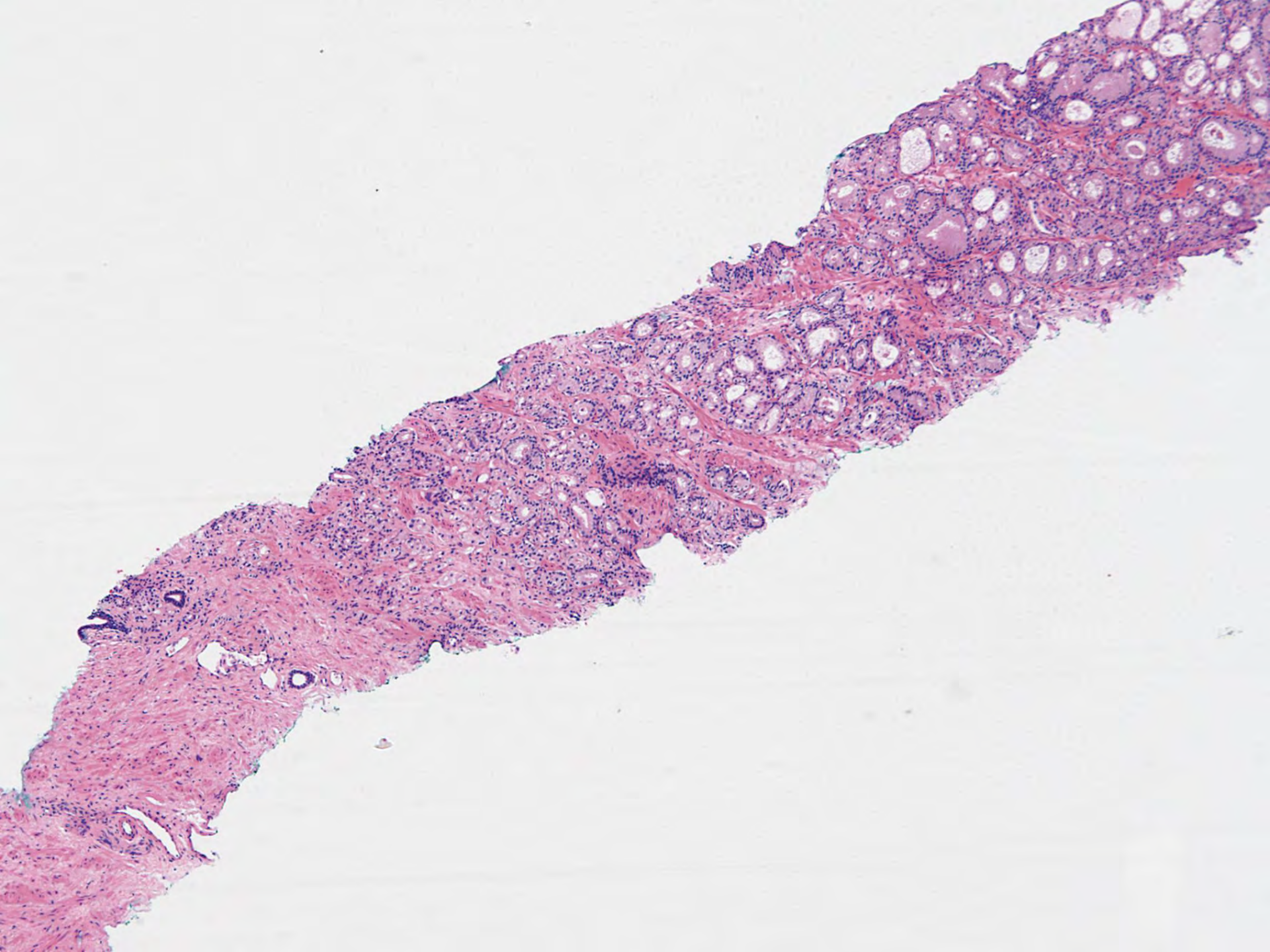

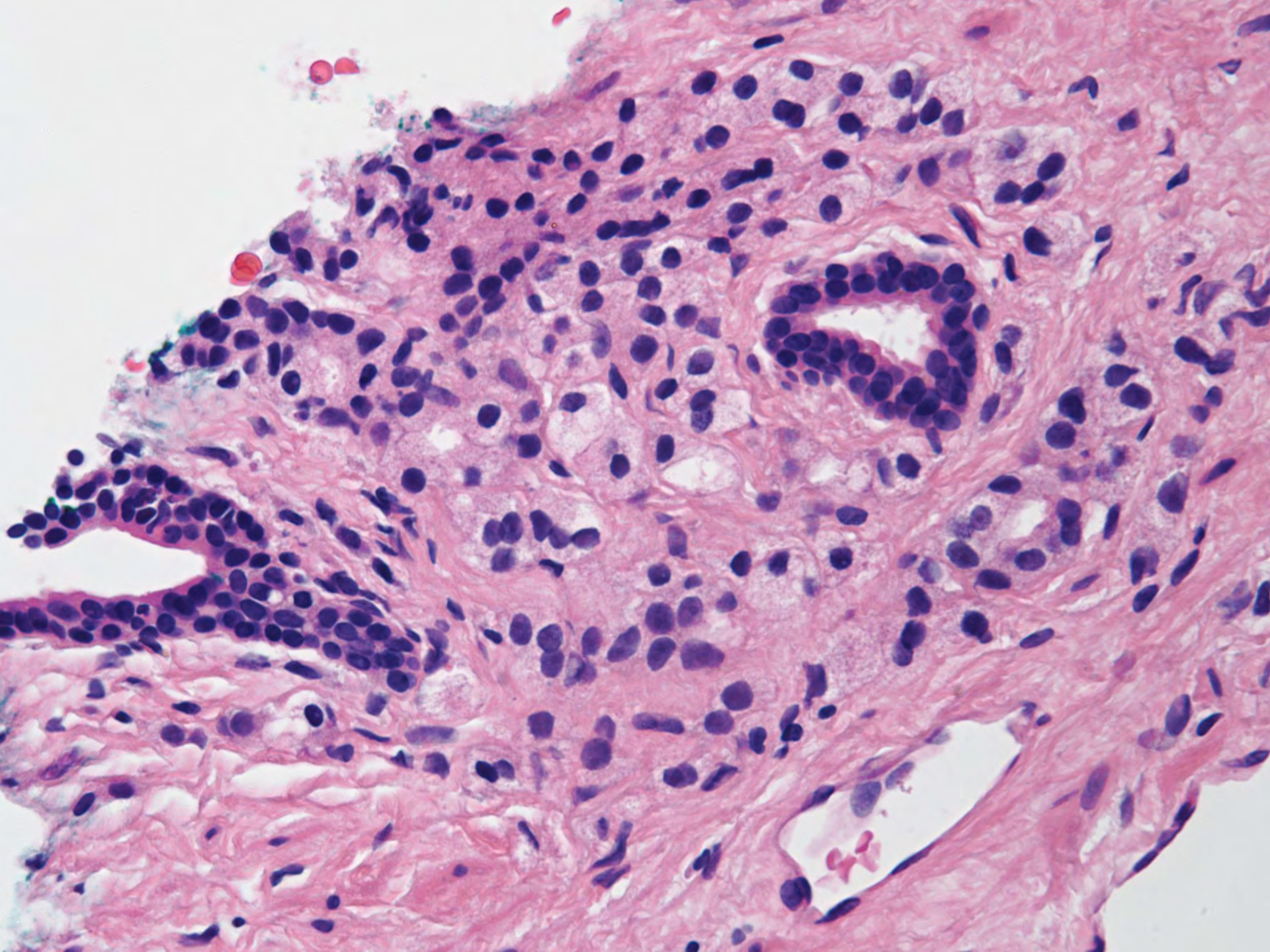

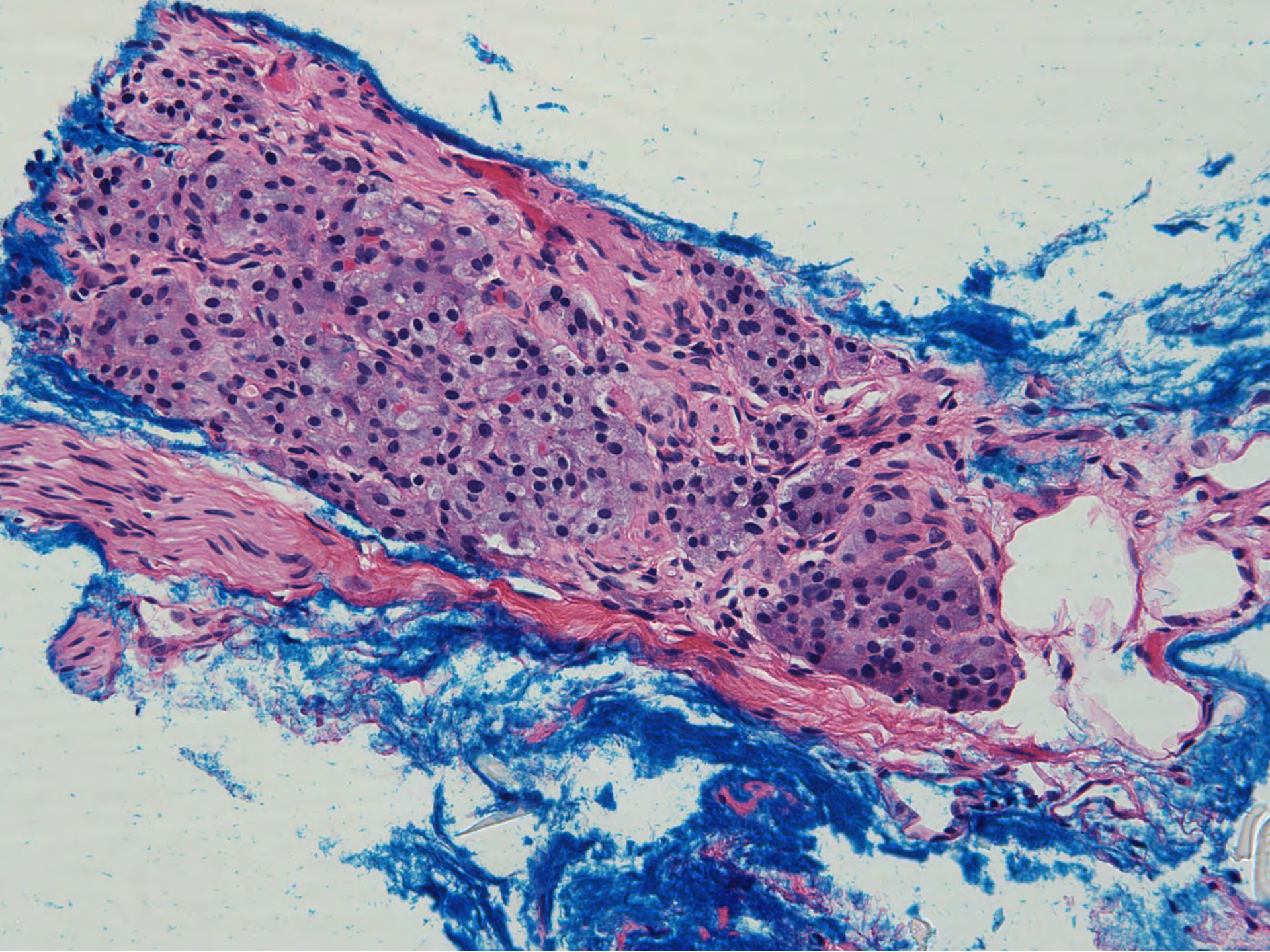

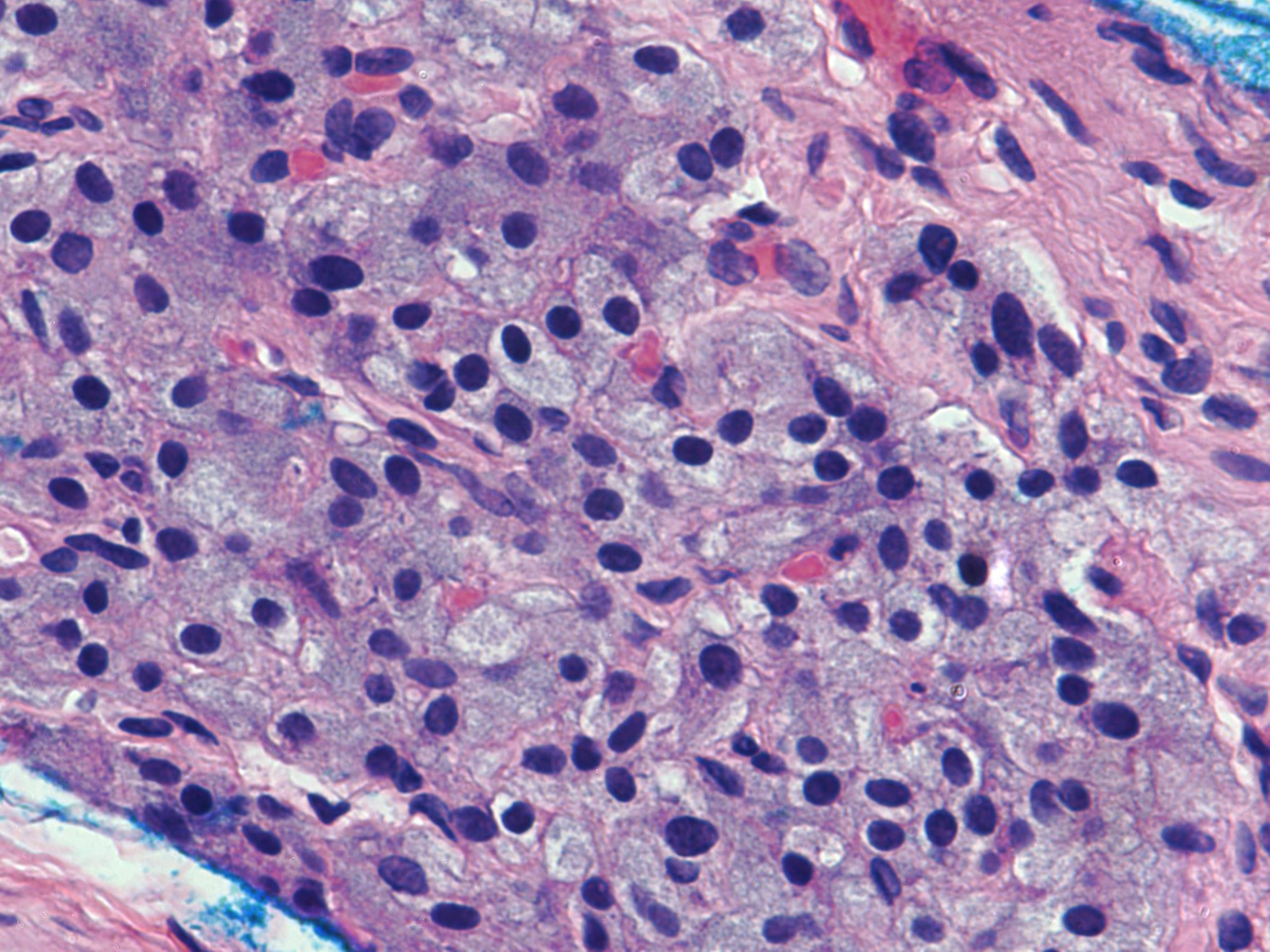

DIAGNOSIS

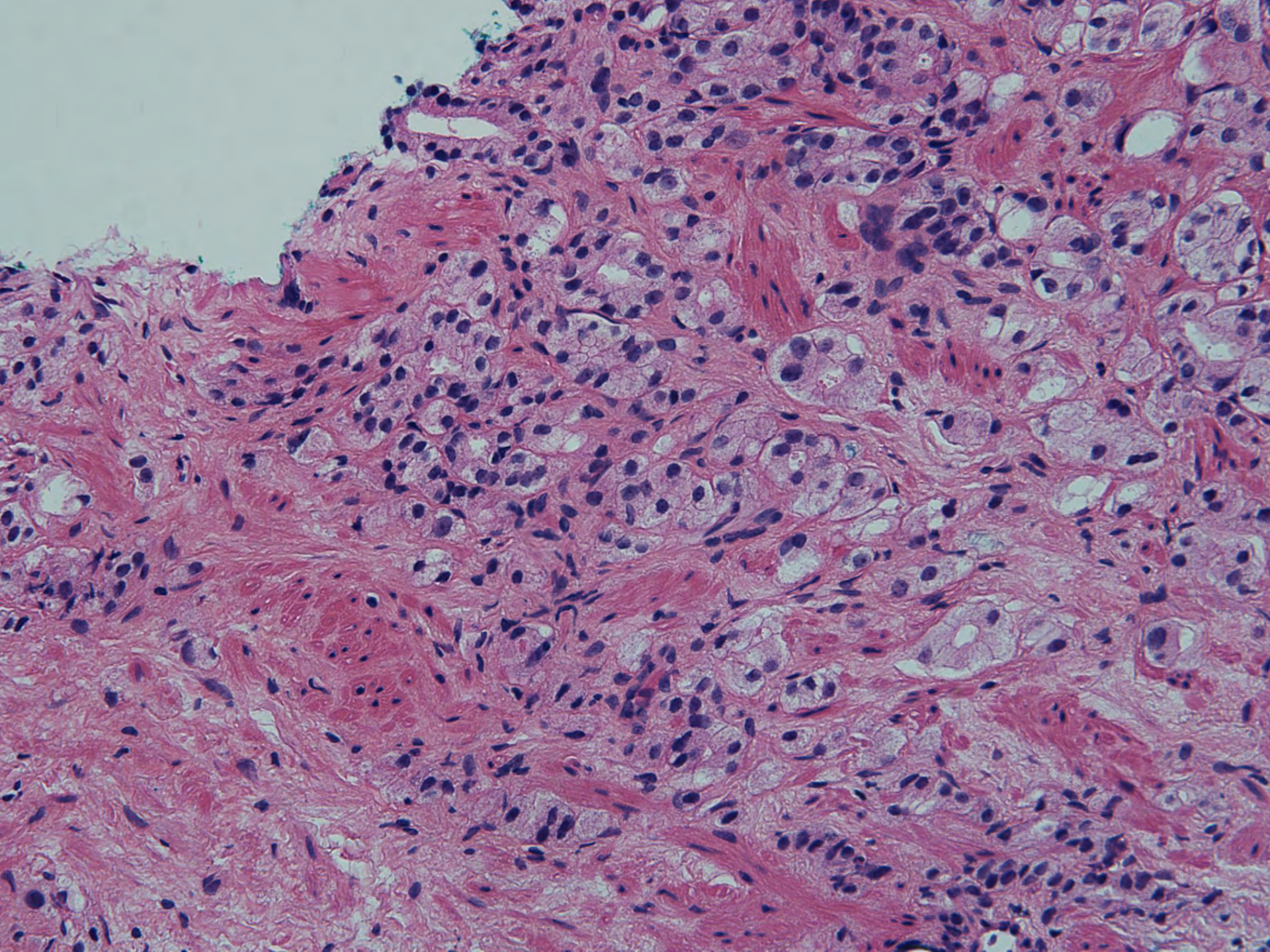

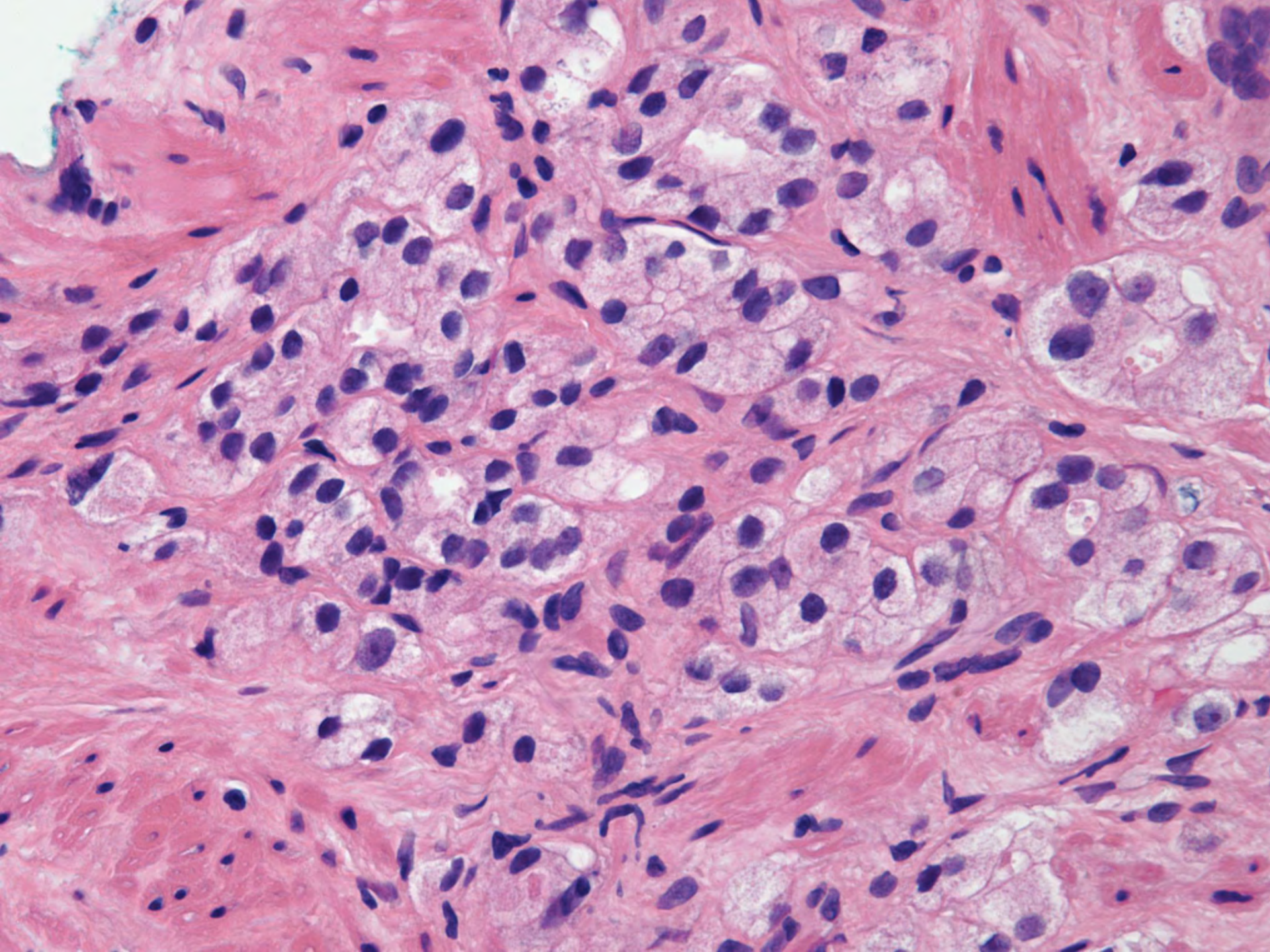

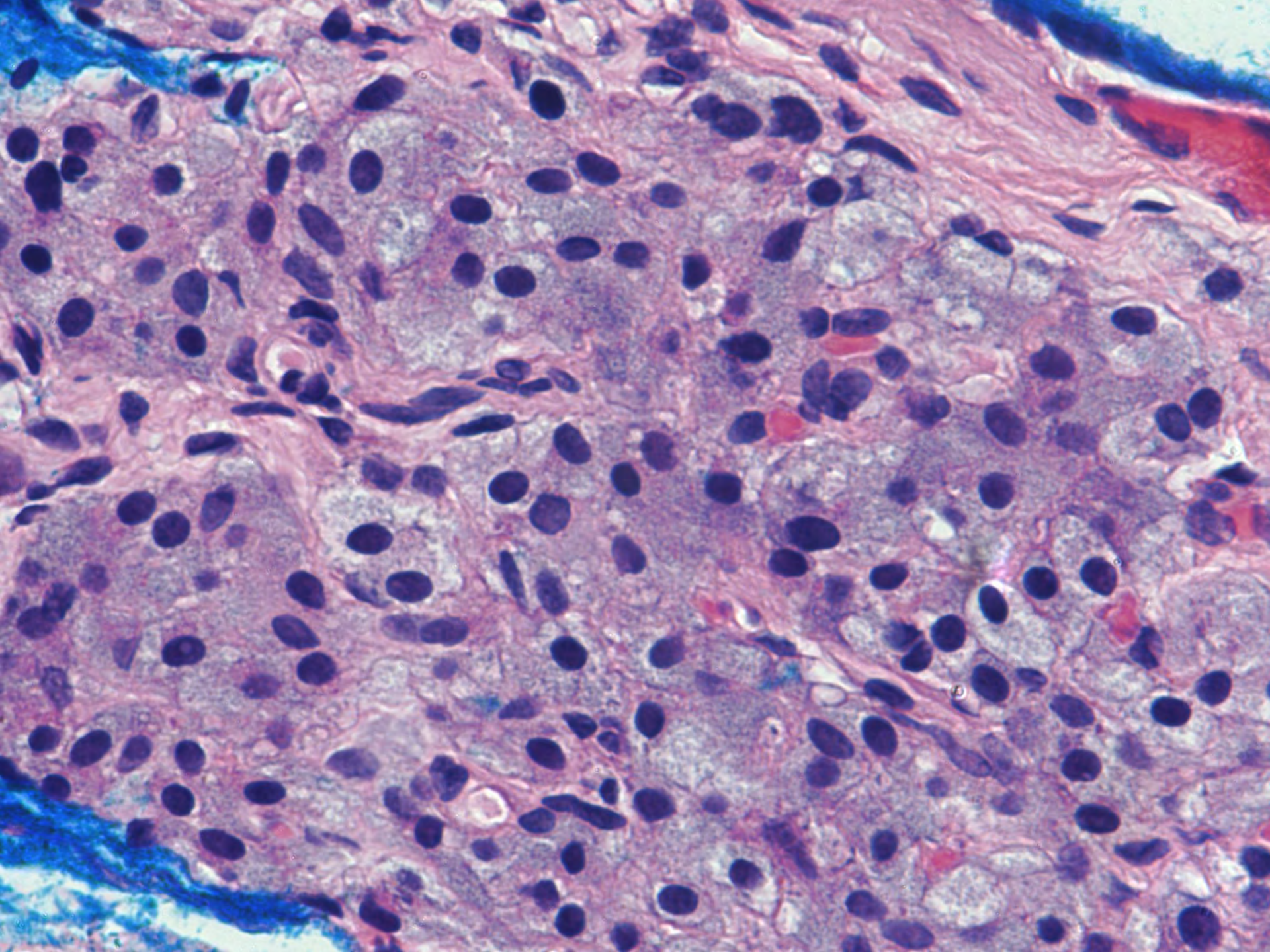

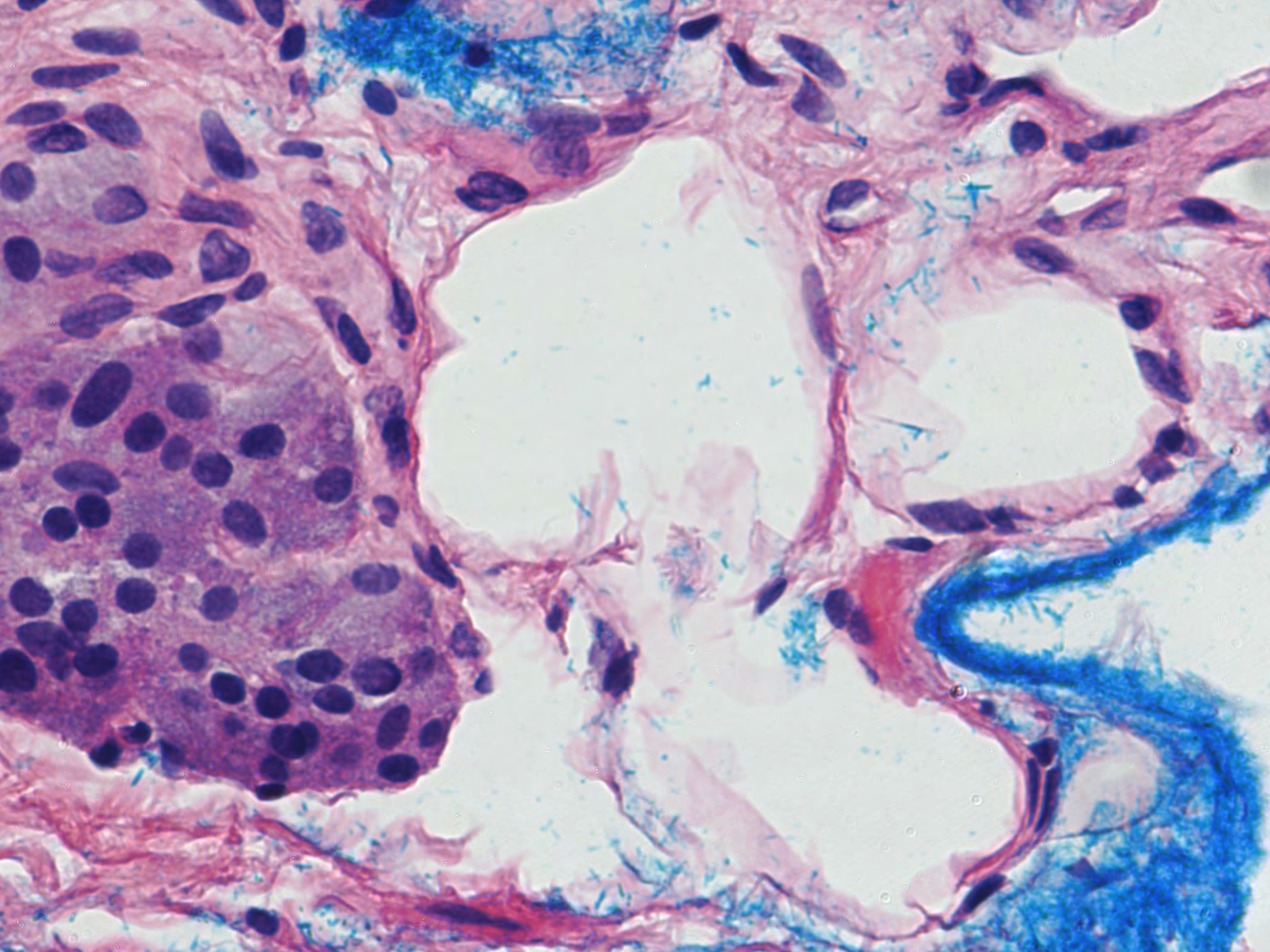

Differential Diagnosis

- Prostatic adenocarcinoma, pattern 5
- Prostatic adenocarcinoma with extraprostatic extension
- Paraganglion

Synaptophysin

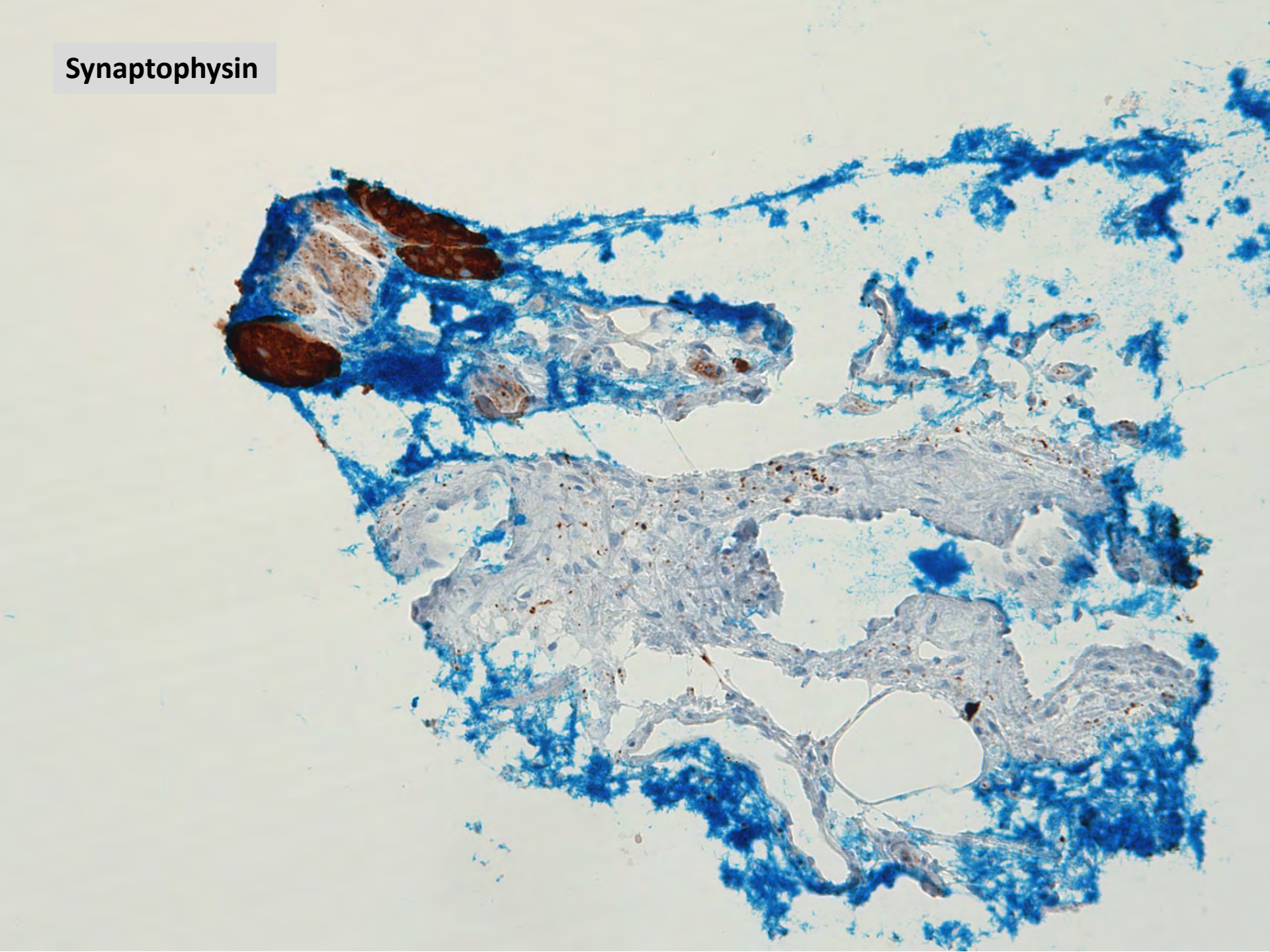

J Urol. 1975 Jun;113(6):874-5.

Normal paraganglia in the human prostate.

Freedman SR, Goldman RL.

Abstract

A normal paraganglion was discovered incidentally in prostatic fragments resected for nodular prostatic hyperplasia.

PMID: 1152165

Arch Pathol Lab Med. 1997 May;121(5):515-6.

Paraganglion of the prostate in a needle biopsy: a potential diagnostic pitfall.

Kawabata K[1].

⊕ Author information

Abstract

Paraganglionic tissue incidentally observed in a needle biopsy of the prostate is reported. The tissue was seen in the periprostatic adipose tissue obtained during a needle biopsy of the prostate of an 81-year-old man. The paraganglionic cells demonstrated round to oval nuclei and basophilic granular or vacuolated cytoplasm and were immunohistochemically positive for chromogranin A, but negative for prostatic acid phosphatase and prostate-specific antigen. Paraganglion in the periprostatic adipose tissue is a diagnostic pitfall and should be distinguished from extension of prostatic adenocarcinoma outside the prostatic capsule into the periprostatic adipose tissue.

PMID: 9167608

Paraganglion of the prostate gland: an uncommon mimic of prostate cancer in needle biopsies

Sir: Paraganglia are recognized as potential mimics of carcinoma in both bladder and prostate resections. However, they are rarely encountered in prostate needle biopsies and only a single case report of paraganglionic tissue in such specimens could be found in the English literature.[1] We describe two cases of incidental paraganglia identified in prostate needle biopsy specimens and discuss their distinction from prostate cancer.

Histopathology. 2005 Jul;47(1):114-5.

Am J Surg Pathol. 1994 Apr;18(4):412-20.

Paraganglia of the prostate. Location, frequency, and differentiation from prostatic adenocarcinoma.

Ostrowski ML[1], Wheeler TM.

⊕ Author information

Abstract

In contrast to paraganglia of the urinary bladder, prostatic paraganglia have been largely unreported. Following the discovery of paraganglia in two separate radical prostatectomy specimens, we reviewed 100 randomly selected radical prostatectomy specimens to document the location and frequency of prostatic paraganglia. Twelve additional paraganglia were identified in eight resections, for a total of 14 paraganglia in 10 cases. Most paraganglia were located in or adjacent to lateral neurovascular bundles and, rarely, in lateral prostatic stroma. The size of paraganglia ranged from 0.1 to 1.7 mm (median 0.9 mm). Paraganglia consisted of clusters of cells in patterns that ranged from lobular to diffuse, usually with a prominent stromal vascular component. The cells contained bland oval nuclei and clear cytoplasm, which was often abundant. Occasionally, larger cells with larger nuclei were present. Immunohistochemical stains for chromogranin, neuron-specific enolase, and synaptophysin were positive; those for prostatic-specific antigen were uniformly negative. In one of our cases, histologic similarity was noted between a paraganglion and an adjacent prostatic adenocarcinoma with a "hypernephroid" pattern. Recognition of prostatic paraganglia, with appropriate immunohistochemical stains when necessary, will obviate the possibility of confusing these structures with prostatic adenocarcinoma.

PMID: 8141432

J Anat. 1998 Apr;192 (Pt 3):407-15.

Immunohistochemical characteristics of human paraganglion cells and sensory corpuscles associated with the urinary bladder. A developmental study in the male fetus, neonate and infant.

Dixon JS[1], Jen PY, Gosling JA.

⊕ Author information

Abstract

Triple label immunohistochemistry was used to study the coexistence of the catecholamine-synthesising enzymes dopamine beta-hydroxylase (DBH) and tyrosine hydroxylase (TH) and several neuropeptides including neuropeptide Y (NPY), vasoactive intestinal polypeptide (VIP), substance P (SP), calcitonin gene-related peptide (CGRP), somatostatin (SOM) and galanin (GAL) as well as nitric oxide synthase (NOS) in developing pelvic paraganglion cells in a series of human male fetal, neonatal and infant specimens ranging in age from 13 wk of gestation to 3 y postnatal. 13-20 wk old fetal specimens possessed large clusters of paraganglion cells lying lateral to the urinary bladder and prostate gland which were intensely DBH-immunoreactive (-IR) but lacked TH, NOS and the neuropeptides investigated. With increasing fetal age small clusters of paraganglion cells were observed in the muscle coat of the urinary bladder. At 23 wk of gestation occasional paraganglion cells were NOS or NPY-IR while at 26 wk of gestation the majority of paraganglion cells were TH-IR and a few were SOM or GAL-IR. Some postnatal paraganglia within the bladder musculature contained cells which were all VIP, SP or CGRP-IR while others displayed coexistence of NOS and NPY, SP and CGRP, or NPY and VIP. The presence of NOS in certain paraganglion cells indicates their capacity to generate nitric oxide (NO). These results show that human paraganglion cells develop different phenotypes possibly dependent upon their location within the bladder wall. A delicate plexus of branching varicose nerves was observed in the fetal paraganglia which increased in density with increasing gestational age. The majority of these nerves were VIP-IR while others were CGRP, SP, NPY, NOS or GAL-IR. The presence of nerve terminals adjacent to the paraganglion cells implies a neural influence on the functional activity of the paraganglia. Some paraganglia in the late fetal and early postnatal specimens contained Timofeew's sensory corpuscles, resembling pacinian corpuscles in their morphology. The central nerve fibre of these corpuscles displayed immunoreactivity for SP, CGRP and NOS, the latter indicating a possible role for NO in afferent transmission from the urinary bladder. In addition, a few corpuscles were penetrated by a noradrenergic nerve fibre immunoreactive for NPY and TH, which may have a modulatory role on the sensory receptor.

PMID: 9688506 PMCID: PMC1467784

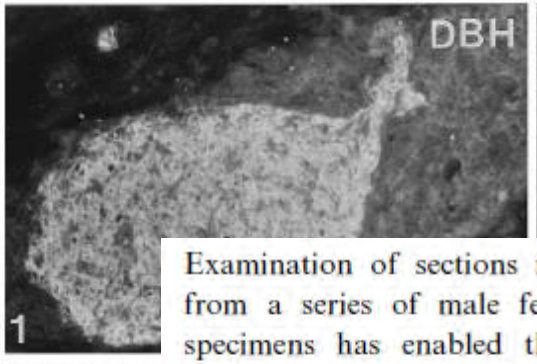

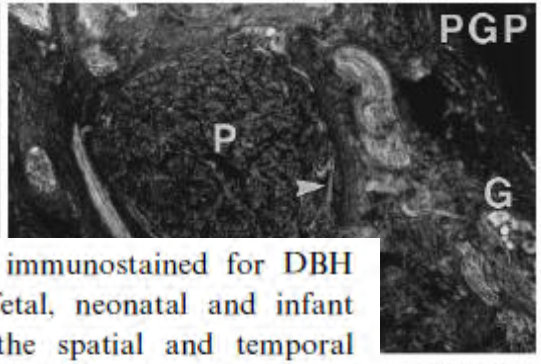

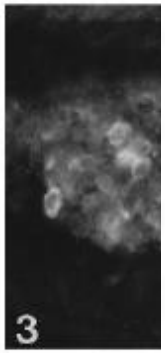

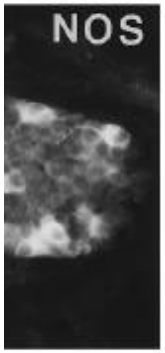

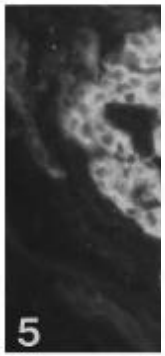

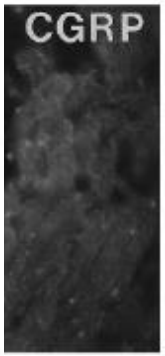

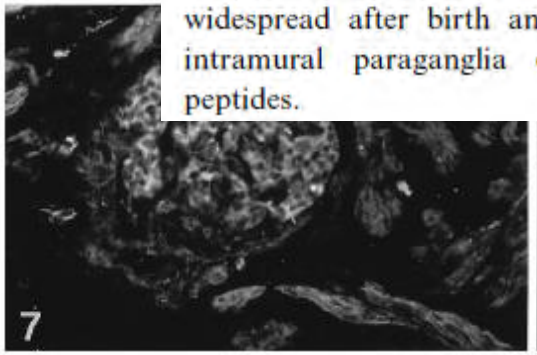

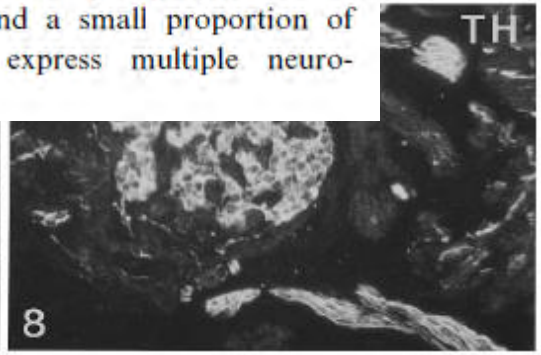

Examination of sections immunostained for DBH from a series of male fetal, neonatal and infant specimens has enabled the spatial and temporal distribution of human paraganglia associated with the urinary bladder to be determined in greater detail than has previously been reported. Since all the material examined in the present study came from males we are unable to comment on possible sex differences in the development and distribution of paraganglia. A similar study using female specimens is required to resolve this possibility. Nevertheless, it is apparent from the present observations in the male that small clusters of paraganglion cells dissociate themselves from the large aggregates lying in the adventitia of the urinary bladder and prostate gland and seemingly migrate into the bladder wall during development to become embedded among the detrusor muscle bundles. In addition the vascularity of the paraganglia becomes evident with increasing gestational age. The expression of neuropeptides and/or NOS begins in fetal paraganglia but is widespread after birth and a small proportion of intramural paraganglia express multiple neuropeptides.

J Anat. 1998 Apr;192 (Pt 3):407-15.

Urology. 2005 Jul;66(1):194.

Periprostatic phec

Perlmutter AE[1], Livengood R,

Author information

Abstract

In adults, 10% of pheochr
Occasionally, pheochromo
hypertensive man with a p
sparing the prostate from
medications.

PMID: 15961143 DOI: 10.101

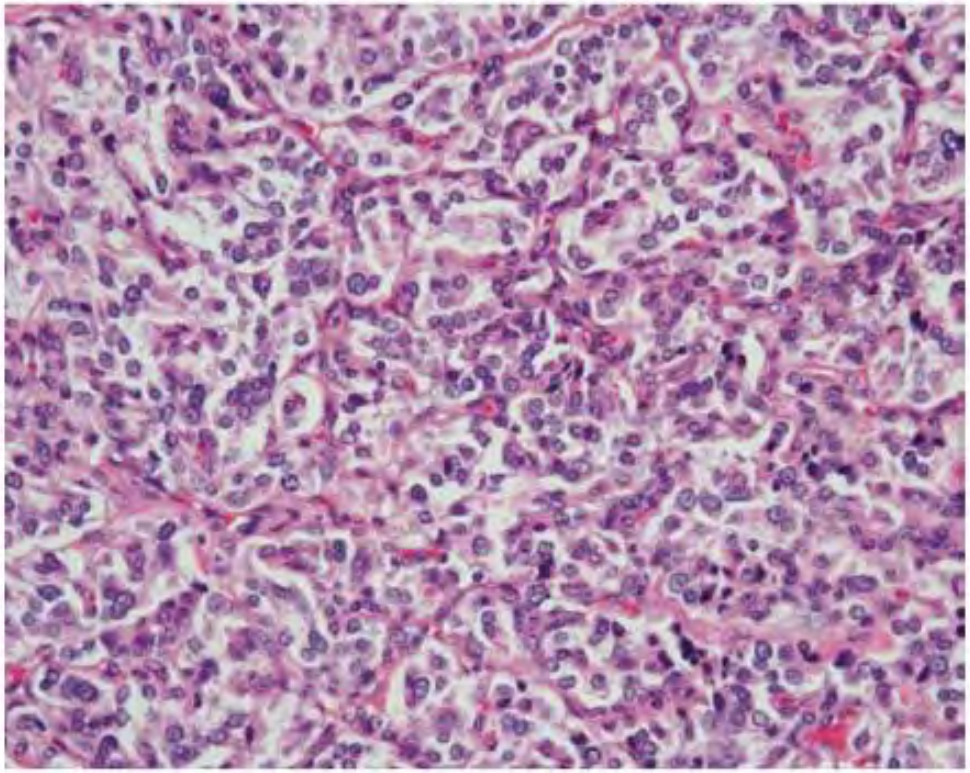

organ of Zuckerkandl.
he case of a 63-year-old
ochromocytoma, while
addition of antihypertensive

Take home points

- Paraganglia can be found incidentally in prostatic biopsy and resection specimens
- Uncommon
- Diagnostic pitfall
- Likely embryologic remnant from early development

SB 6312

Kevin Ko/John Higgins; Stanford

68-year-old male with 4cm indurated left tongue mass. Recently had 2 “negative” biopsies, 1PPDx40 years.

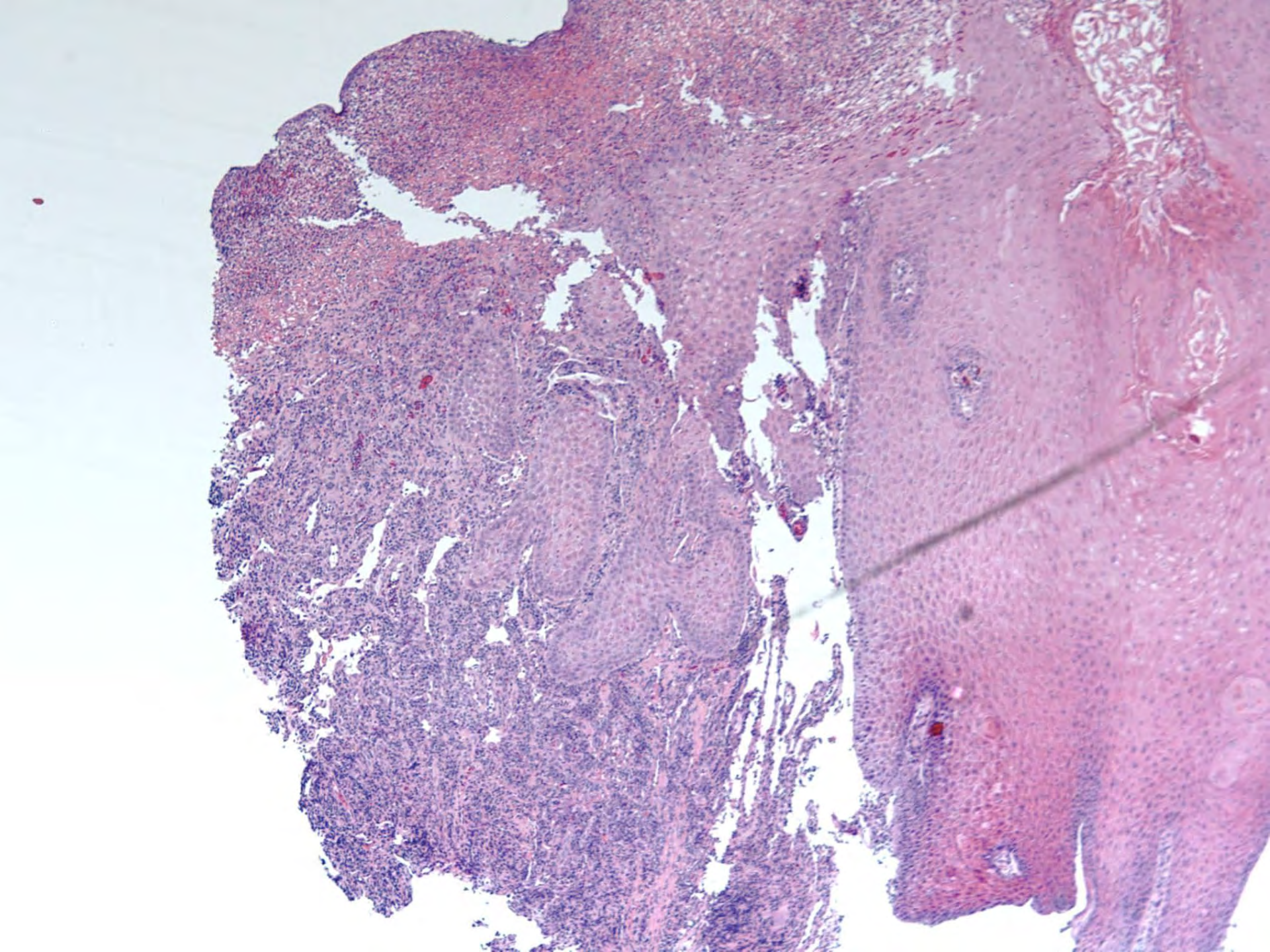

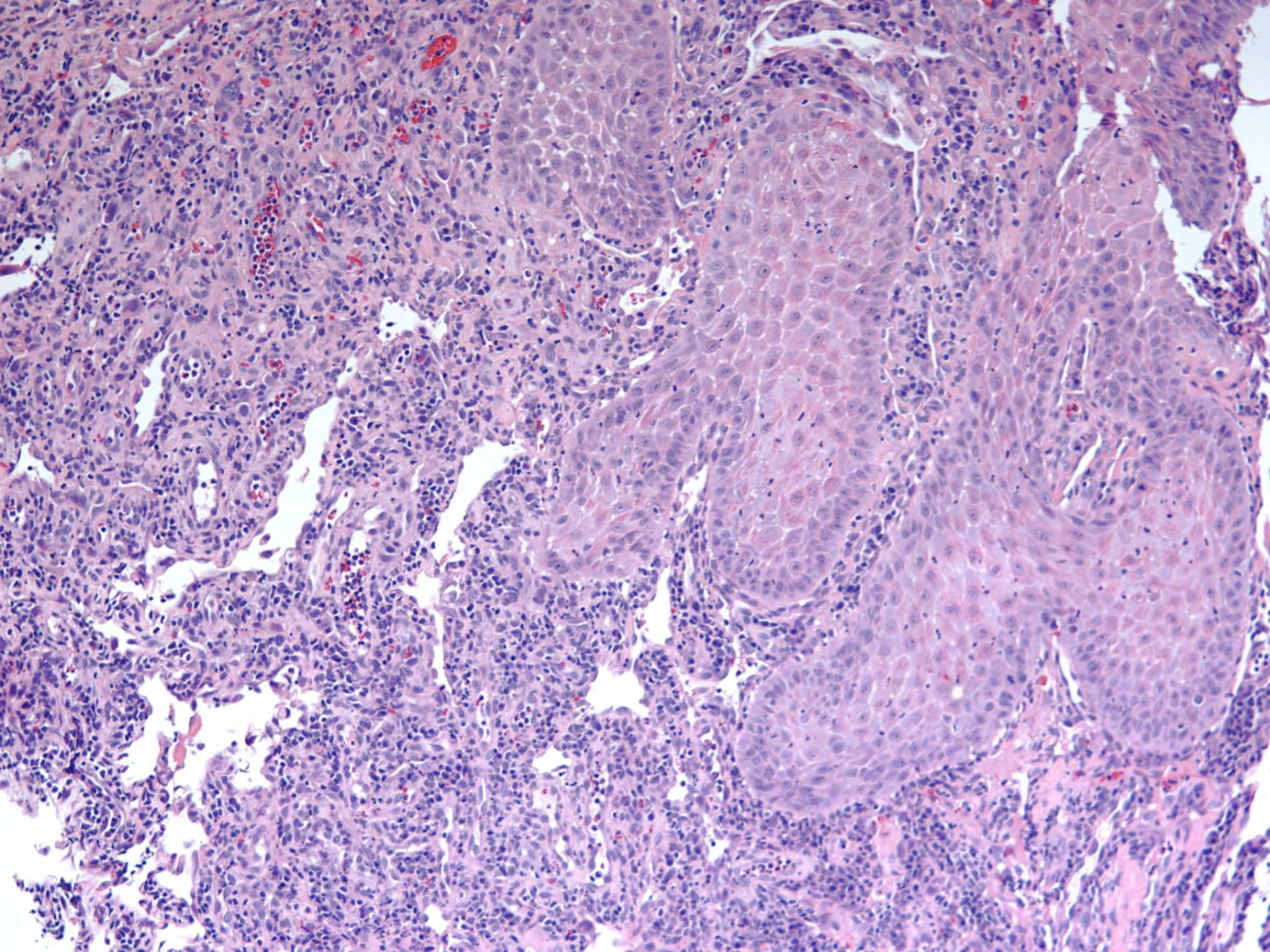

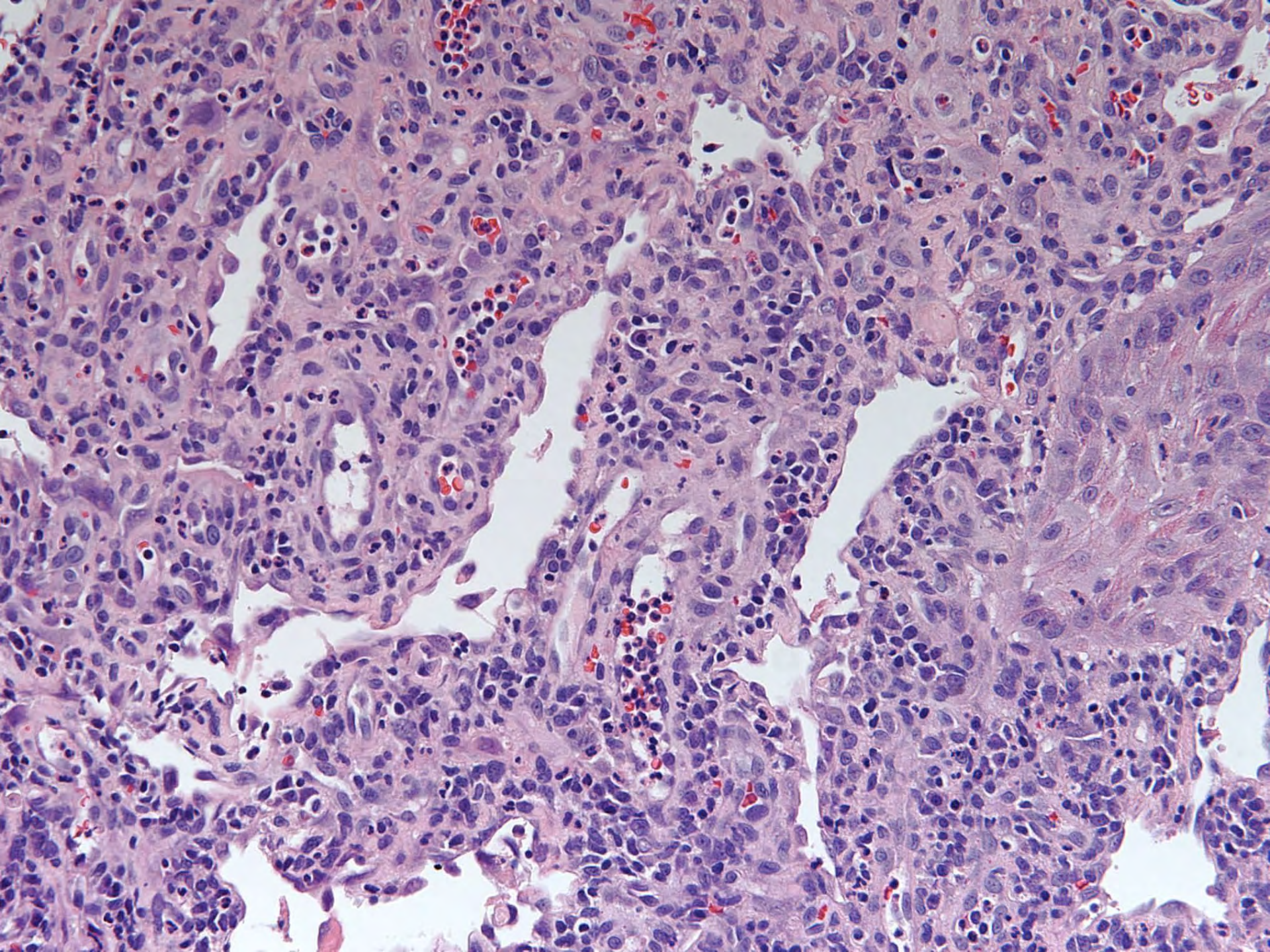

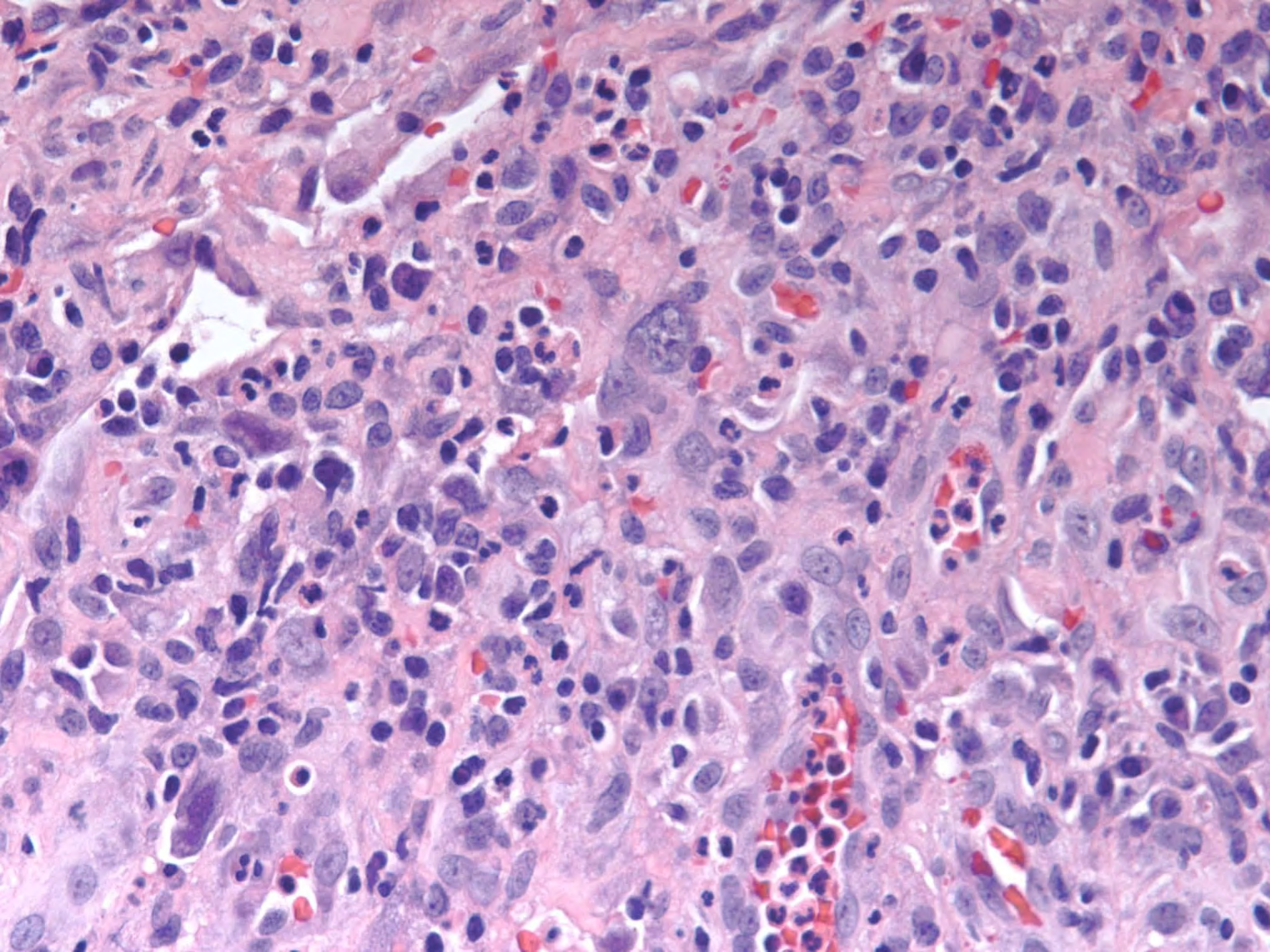

DIAGNOSIS

Initial Presentation

Biopsy #1

TONGUE, LEFT LATERAL, PUNCH BIOPSY

- **-- SQUAMOUS MUCOSA WITH ULCERATION AND GRANULATION TISSUE**
- **-- NO TUMOR SEEN**

- **COMMENT:** No tumor is seen on initial sections and deeper levels. Immunohistochemical stains demonstrate no staining for P63 or CKMIX, providing no support for an invasive carcinoma

- MRI
  - Prominent left level 1 and level 2 lymph nodes concerning for metastatic disease but not clearly meeting criteria for tumor

- Clinical impression:
  - Squamous cell carcinoma, likely T2N2 disease
  - Plan for adjuvant chemotherapy

“Extractions of teeth #2,3,5,13,14,16,18,31 recommended”

1 week post-biopsy #1

Biopsy #2

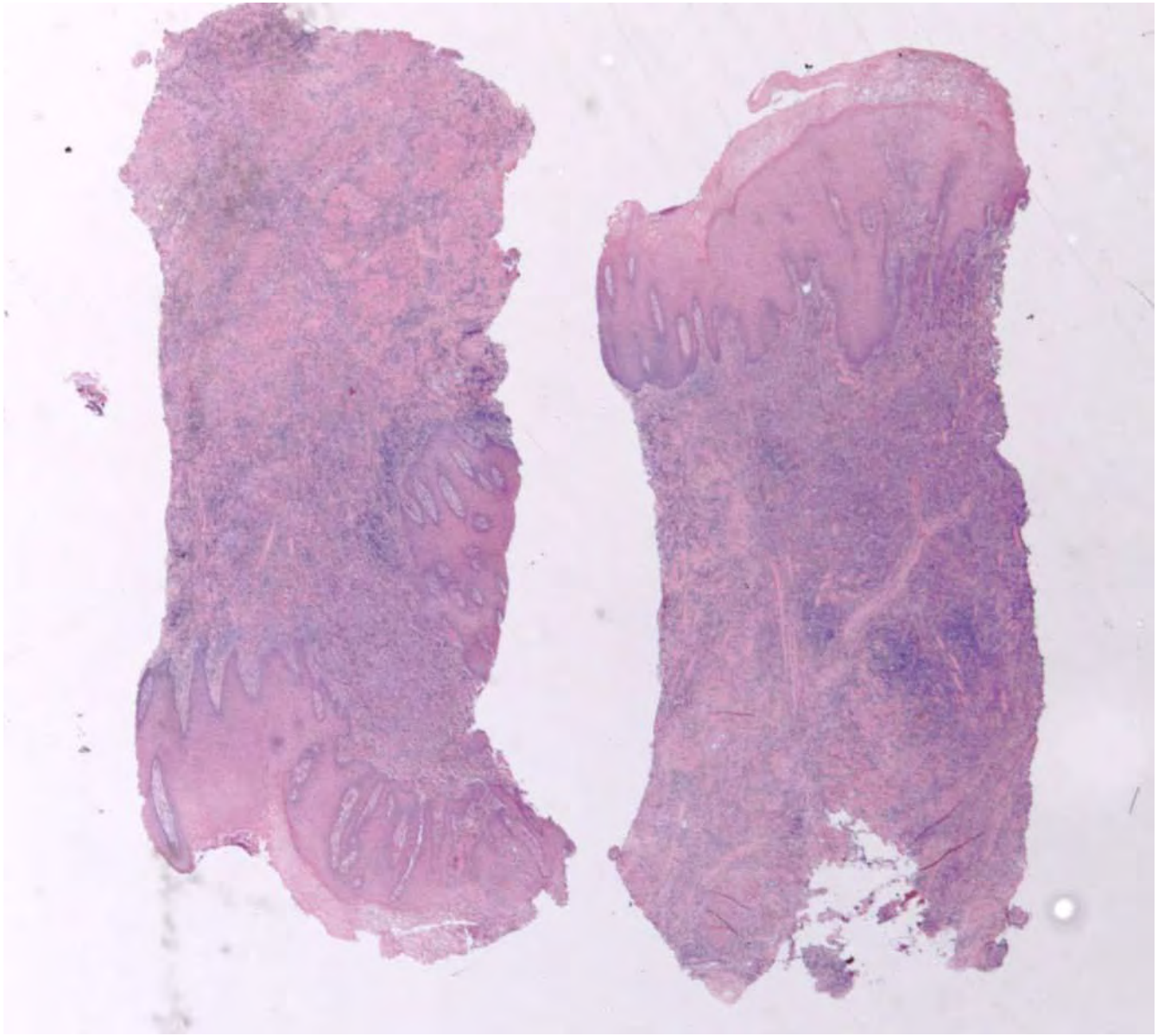

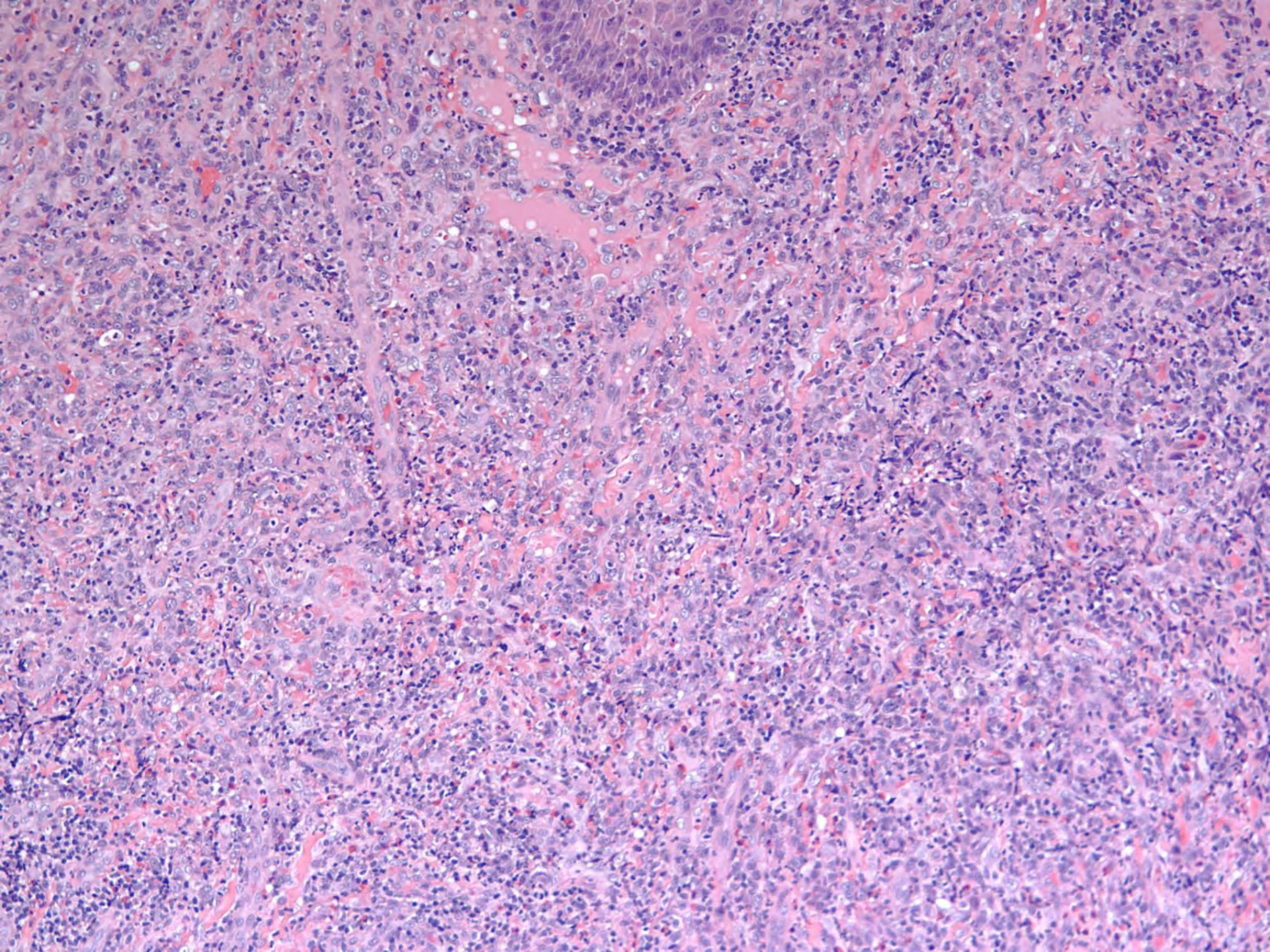

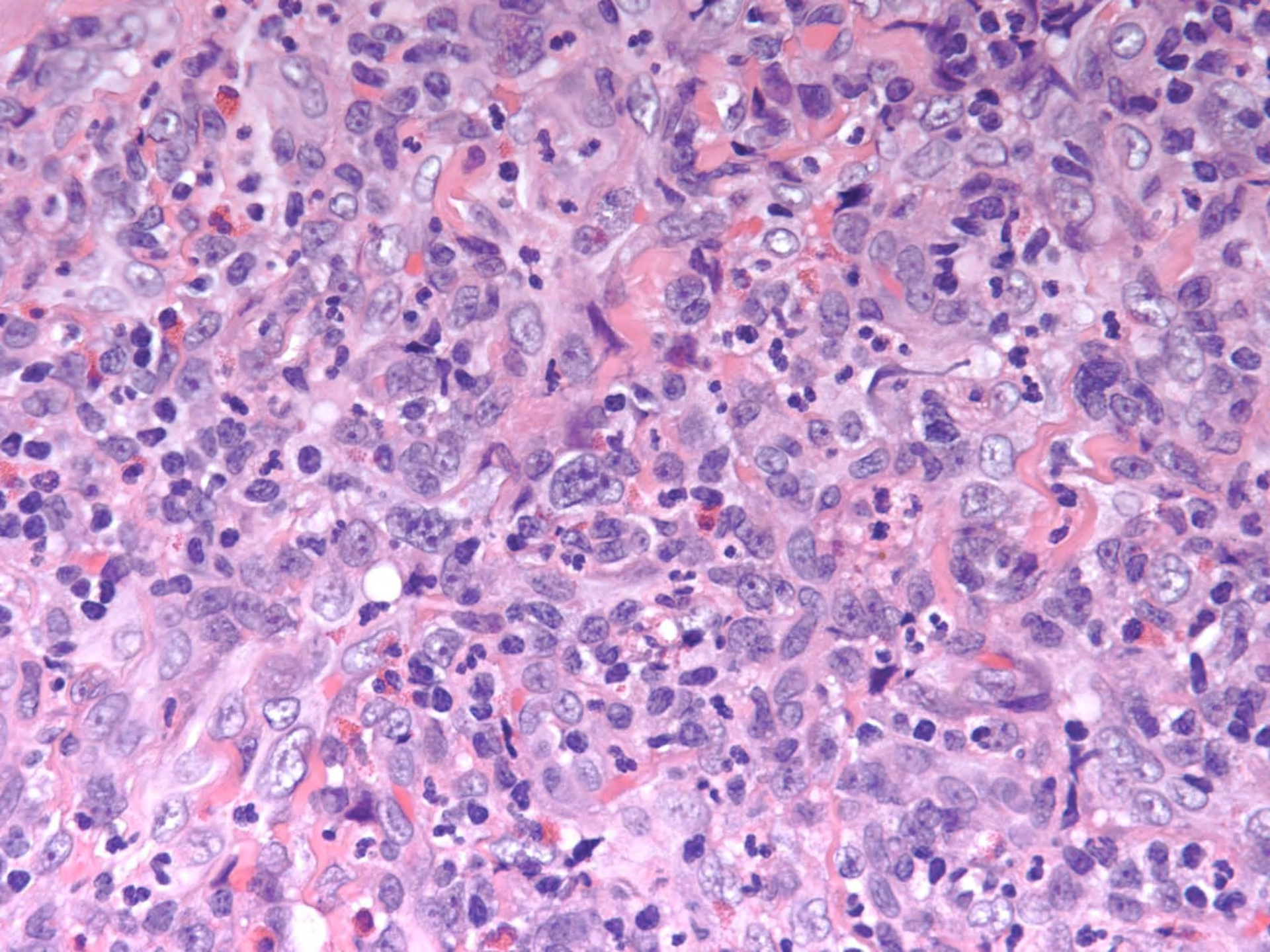

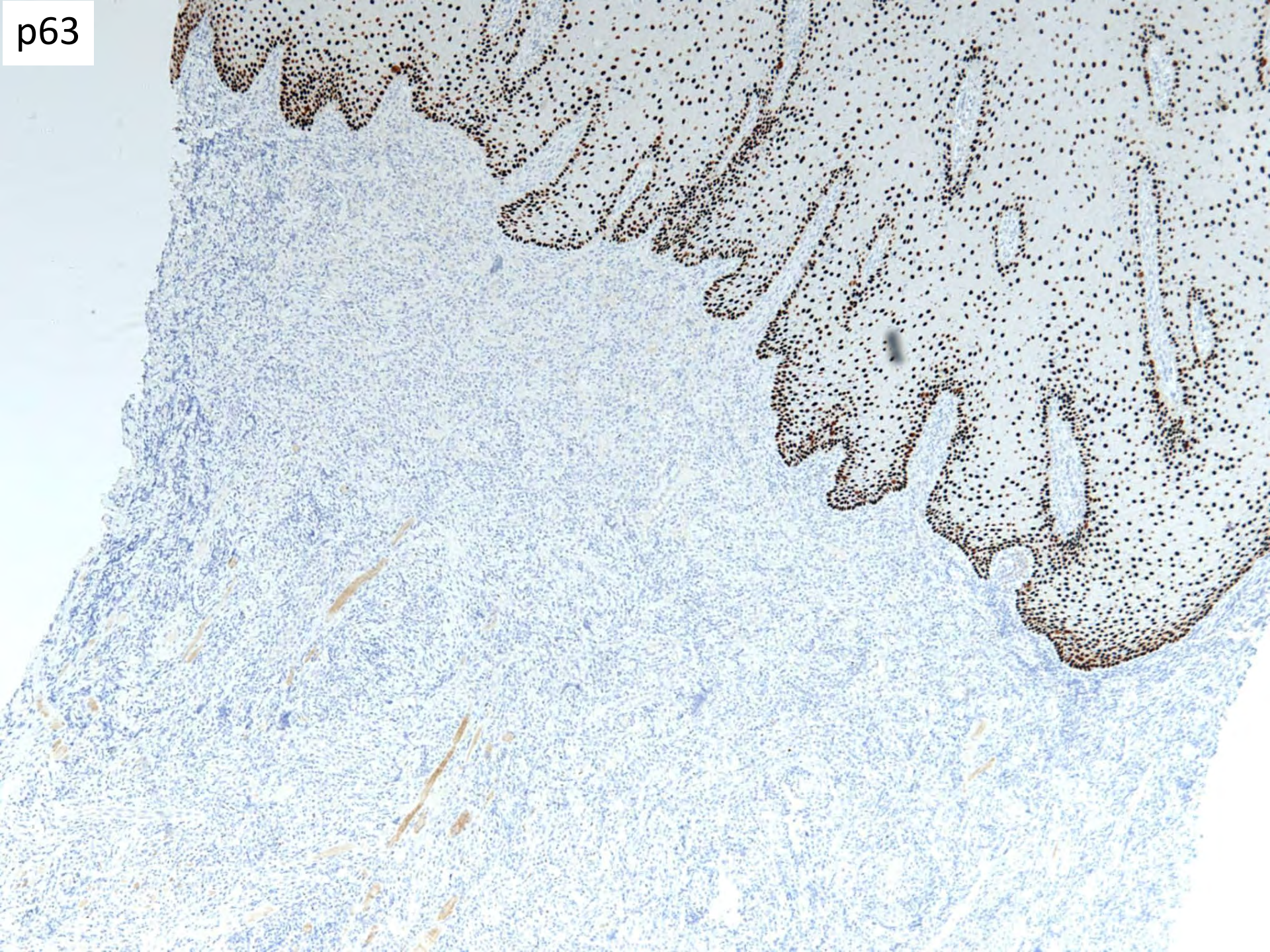
p63

Biopsy #2

- Staining with EBV ISH and CD30 are negative
- Staining with ERG highlights normal vasculature structures
- Staining with CK5/6 and p63 provide no support for carcinoma

Another 3 weeks gone by…

Biopsy #3

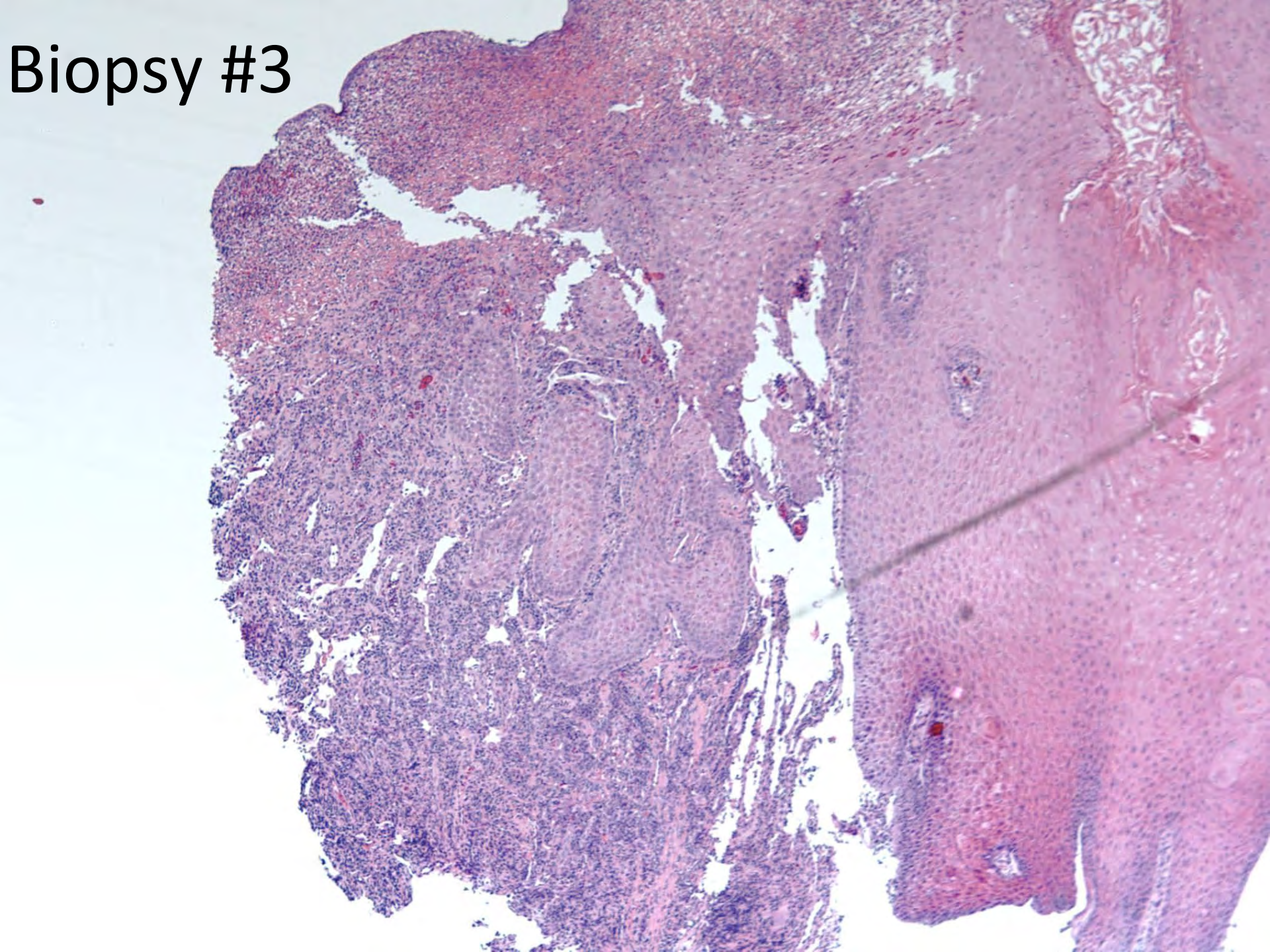

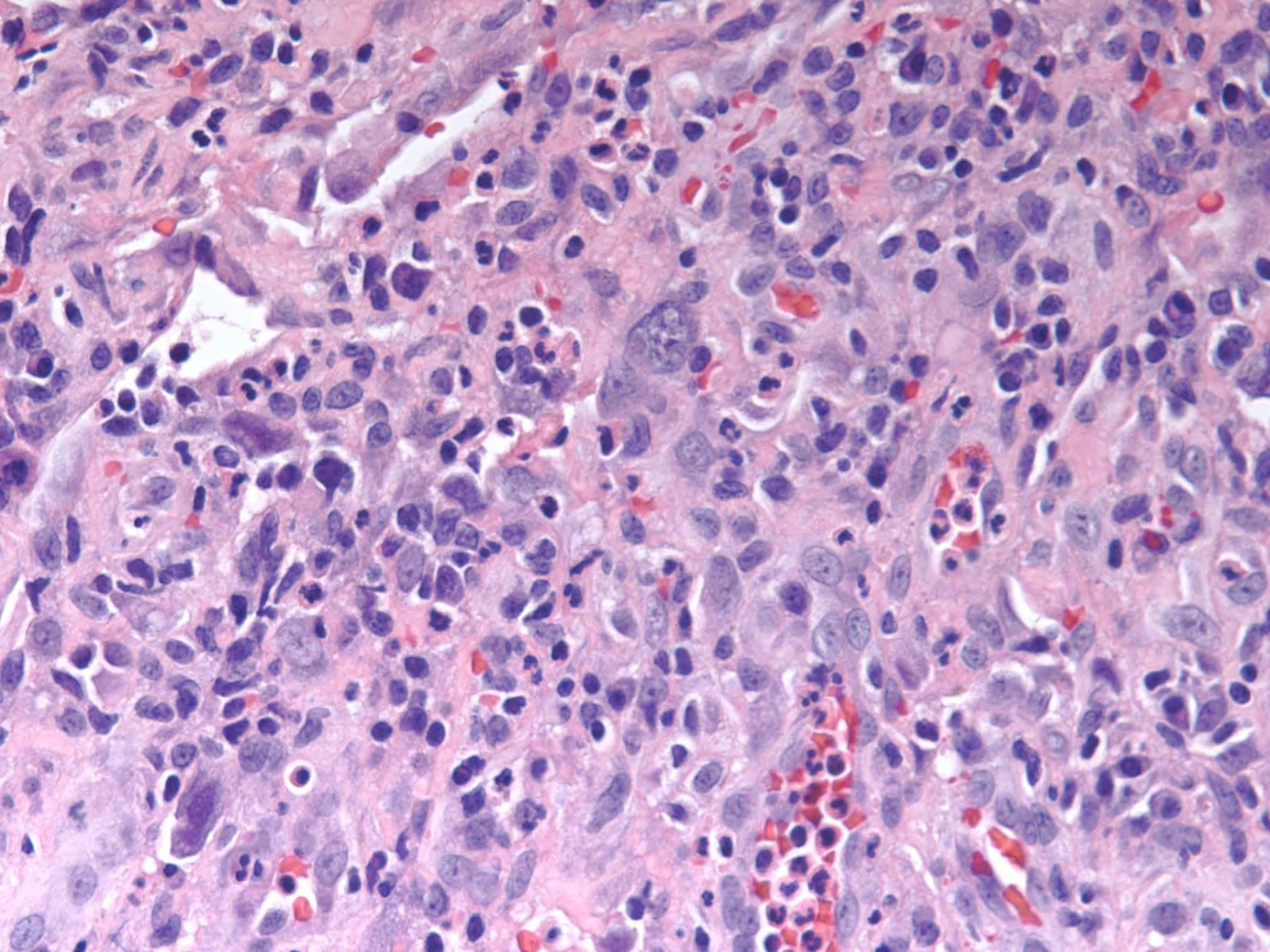

Differential Diagnosis

- Atypical vascular proliferation/angiosarcoma
- Atypical squamoproliferative lesion with extensive ulceration (vs. SCC)
- Reactive lesion
- Deep fungal infection
- Viral infection
- Syphilis

Stains

- PasD –
- GMS –
- CMV –
- HSV –
- EBV ish –
- CD30 –
- Spirochetes –

Long discussion with clinical team…

- Continued observation vs repeat biopsy

- Ultimately decided hold off on any further biopsies and follow-up in 1-2 months…

Patient Returns 4 weeks later…

- ENT clinic:
  - He feels that the lesion may be "healing”….

Final Diagnosis

TONGUE, LEFT LATERAL, PUNCH BIOPSY

-- TRAUMATIC ULCERATIVE GRANULOMA WITH STROMAL EOSINOPHILIA

Traumatic Ulcerative Granuloma with Stromal Eosinophilia

- “TUGSE”
- Accidental trauma from biting or fractured teeth
- Can occur anywhere in oral cavity
- Painful ulcer from 1 mm to > 1 cm
- Clinically mimicking squamous cell carcinoma

Traumatic ulcerative granuloma with stromal eosinophilia

- Ulcer bed composed of granulation tissue with mixed chronic inflammatory cell infiltrate
- Pseudoepitheliomatous hyperplasia of adjacent epithelium can be seen
- Scattered eosinophils extends into underlying muscle
- Subset of traumatic ulcers, atypical CD30(+) histiocytic cells are noted

Traumatic ulcerative granuloma with stromal eosinophilia

- Treatment:
  - Biopsy of ulcer can initiate complete resolution (1 week to 8 months)
  - Intralesional steroid injections
  - Ulcers that do not resolve may need total excision

TUGSE

FIGURE 1. Lesion at initial clinical presentation demonstrating a large ulcer of the dorsum of the tongue with raised, rolled borders.

FIGURE 3. Lesion 2 months postbiopsy.

Gagari E, Stathopoulos P, Katsambas A, Avgerinou G. Traumatic ulcerative granuloma with stromal eosinophilia: a lesion with alarming histopathologic presentation and benign clinical course. Am J Dermatopathol. 2011 Apr;33(2):192-4. doi: 10.1097/DAD.0b013e3181e26db0.

FIGURE 1. Traumatic ulcerative granuloma with stromal eosinophilia consisting of a 1.7×1.3-cm vascular-appearing nodule with a collarette of mucosal epithelium on the left side of the dorsal surface of the tongue.

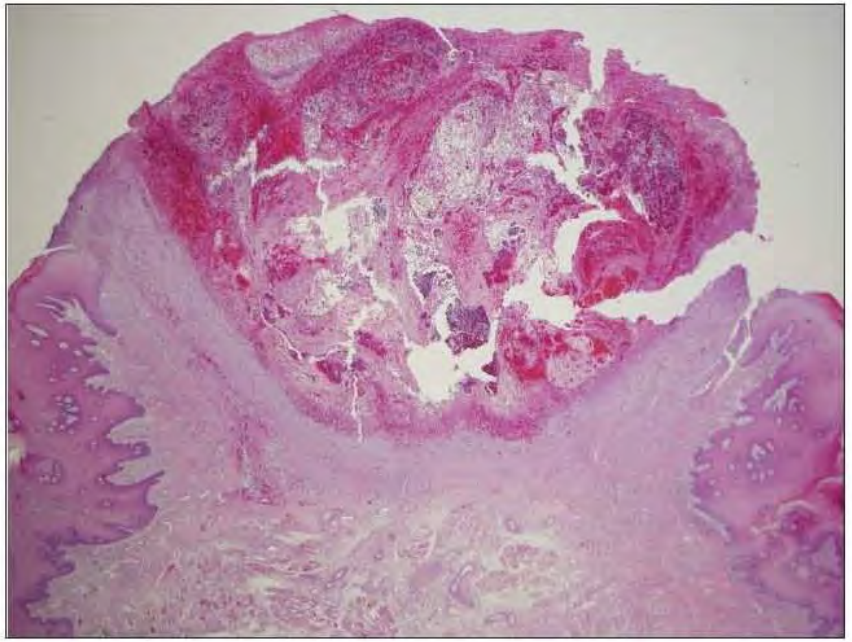

FIGURE 2. Traumatic ulcerative granuloma with stromal eosinophilia histopathology consisting of fibrinoid hemorrhagic necrosis overlying an ulcerated nodule with a collarette of epithelium at the base (H&E, original magnification ×20).

Butler JN, Kobayashi TT. Traumatic ulcerative granuloma with stromal eosinophilia: a malignant-appearing benign lesion. Cutis. 2017 Aug;100(2):E28-E31.

SB 6313

Kevin Ko/Brittany Holmes; Stanford

48-year-old male with multiple recurring tongue ulcers.

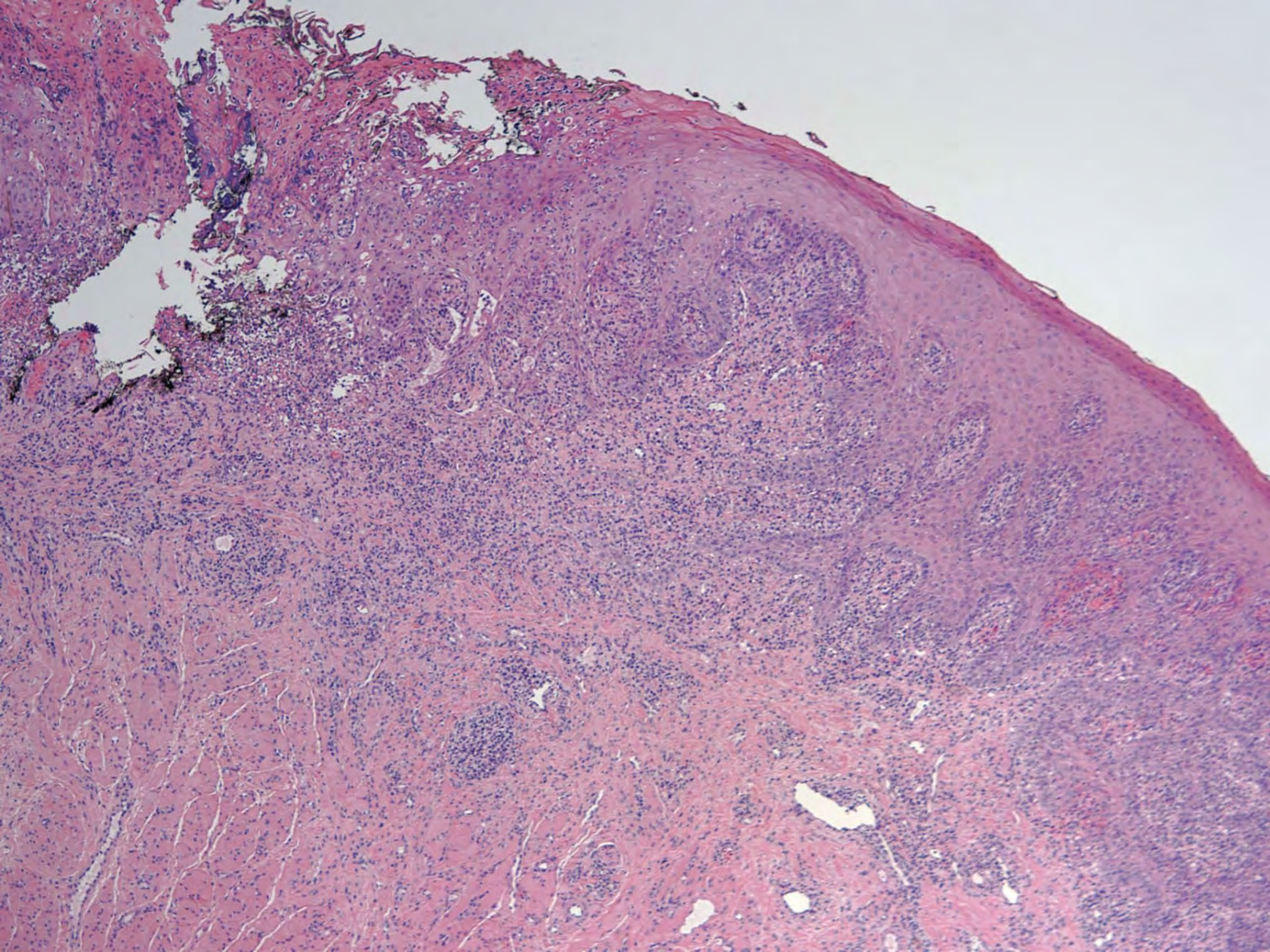

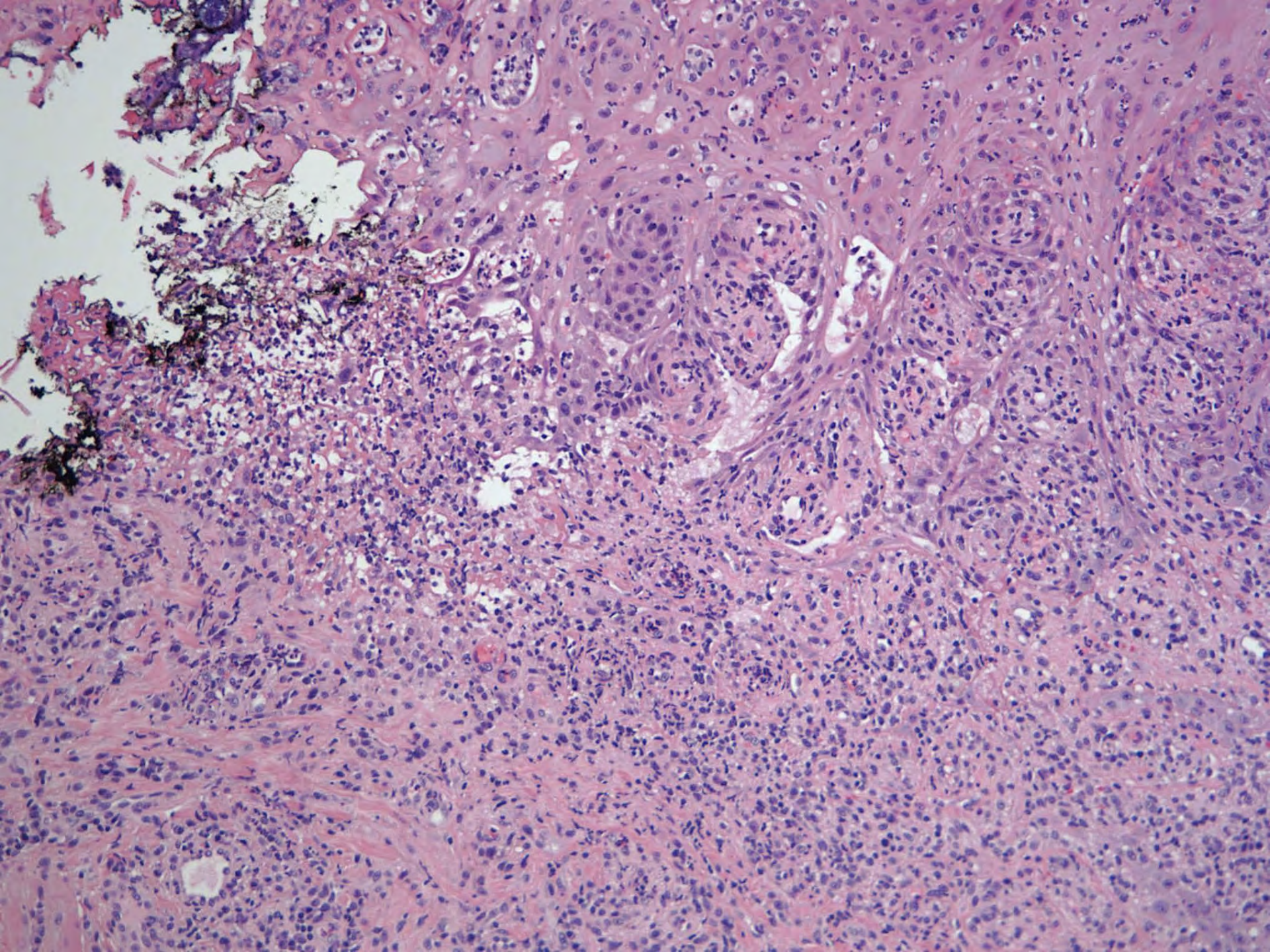

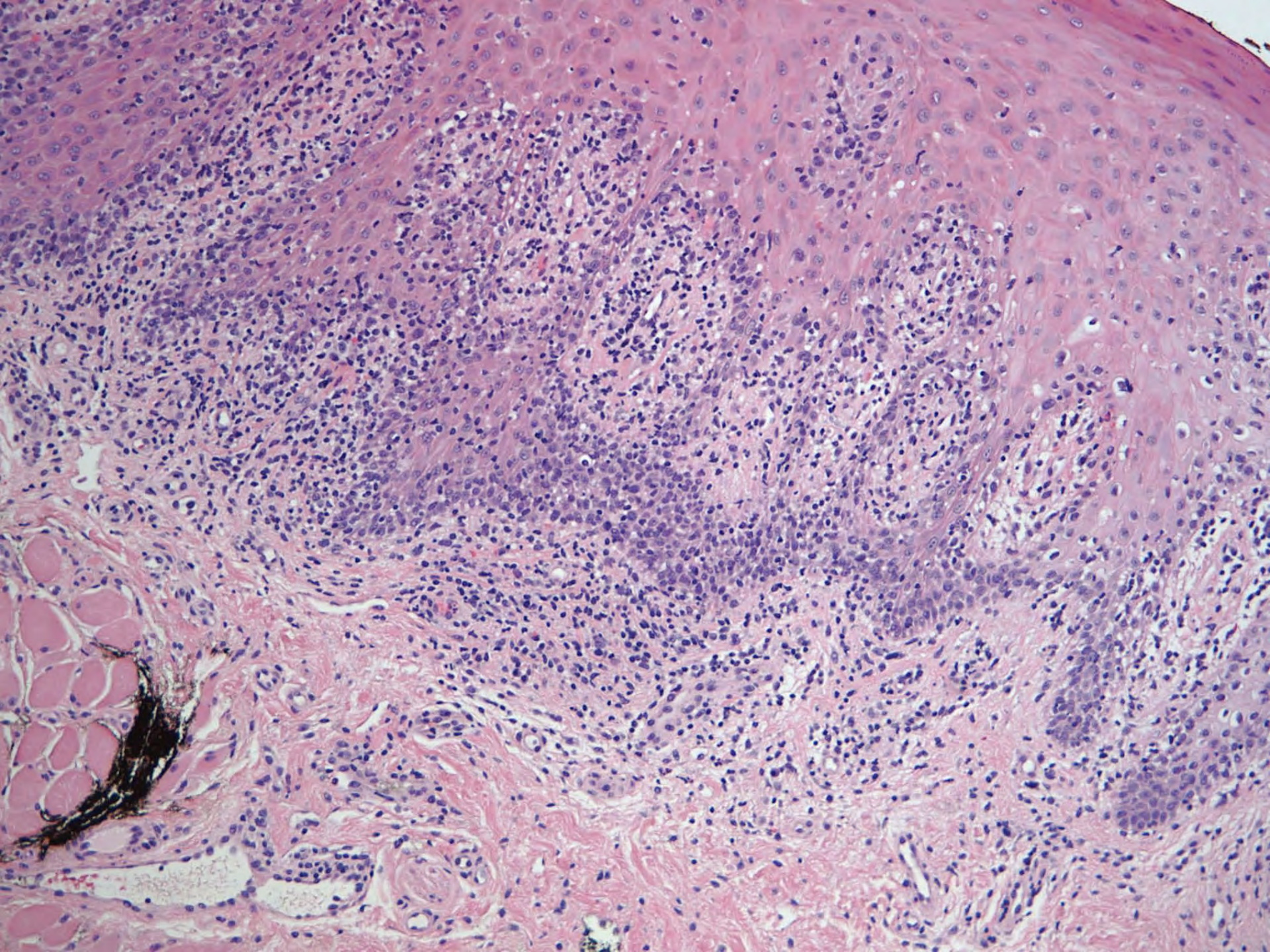

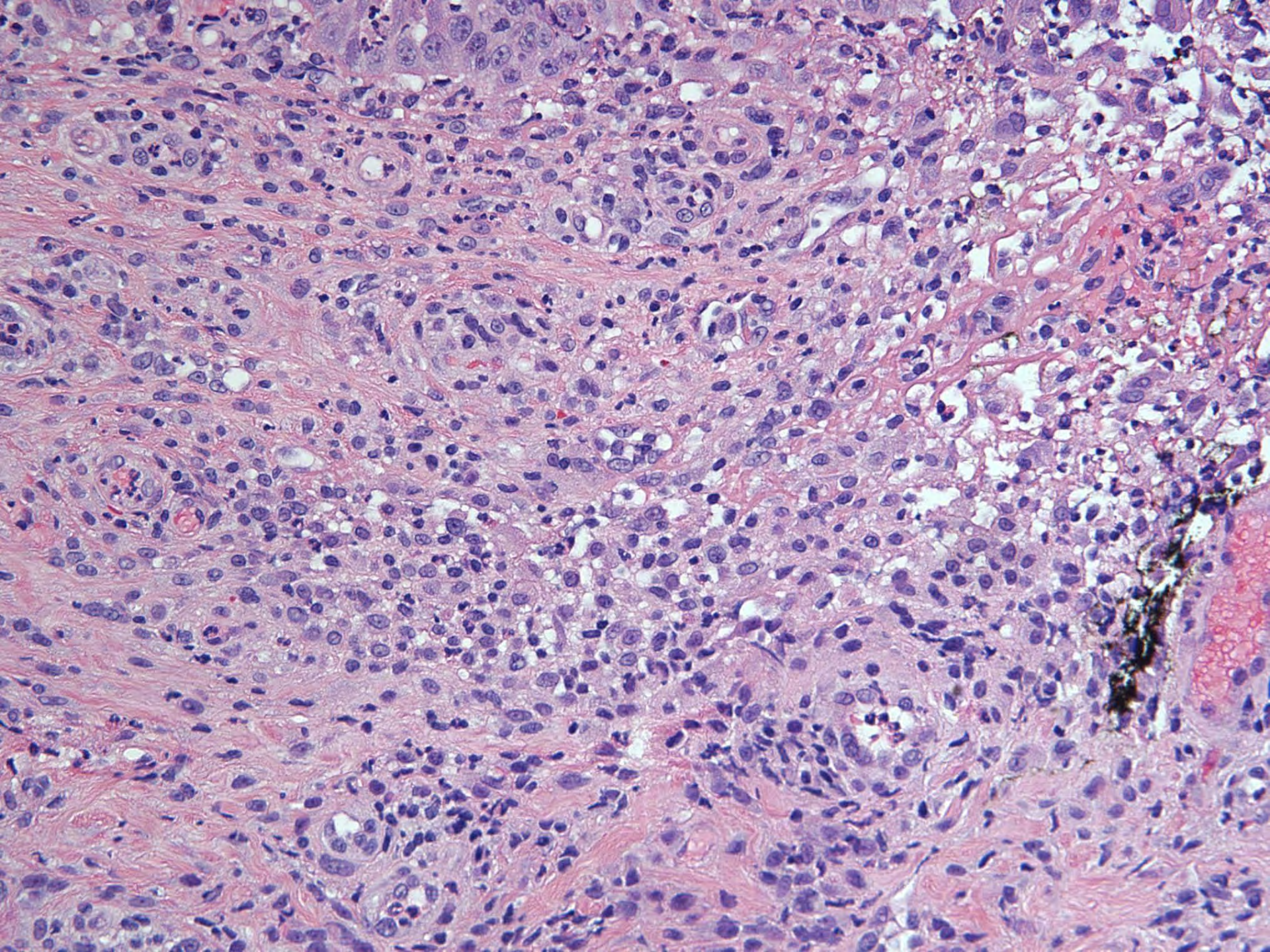

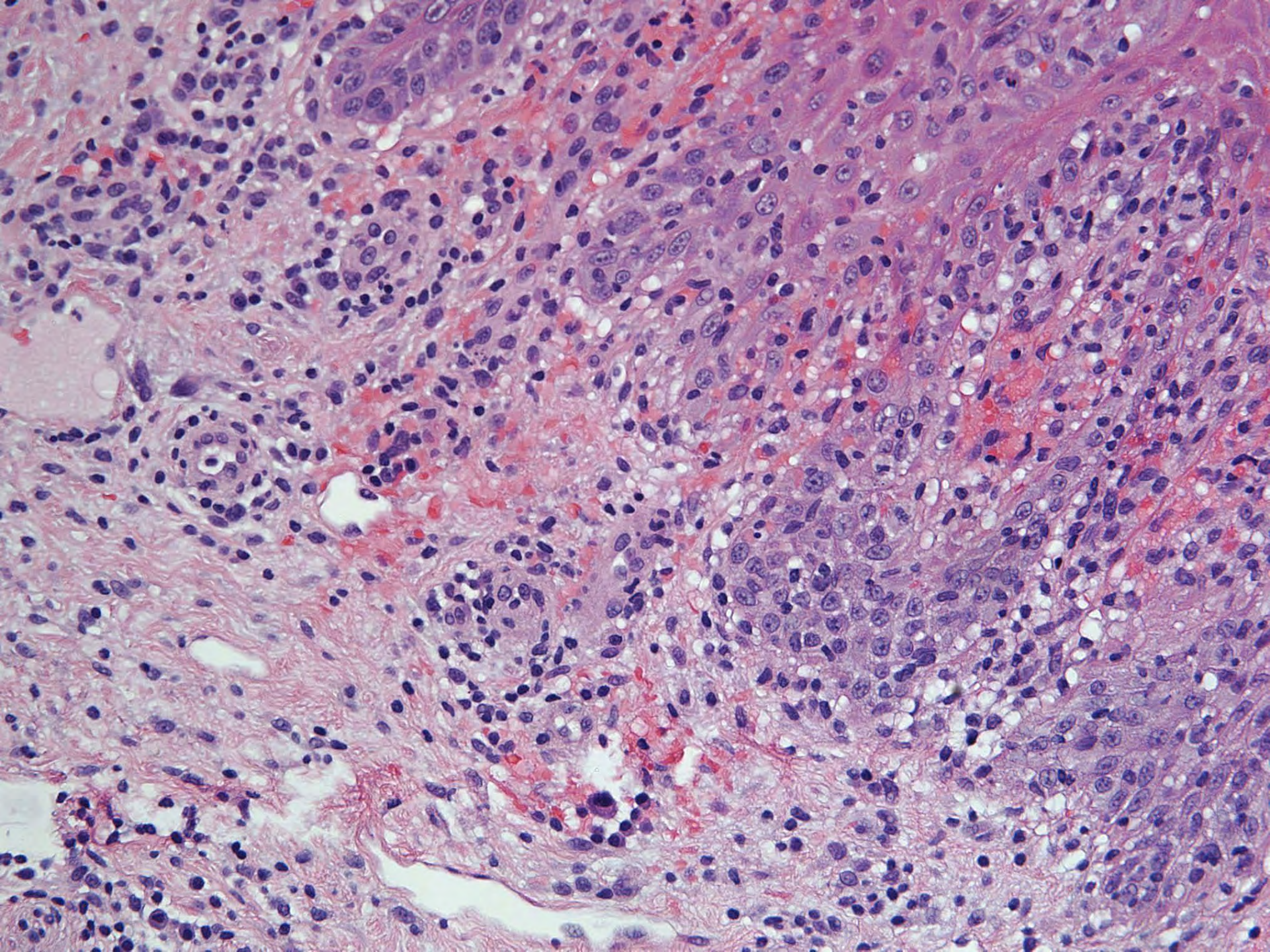

DIAGNOSIS

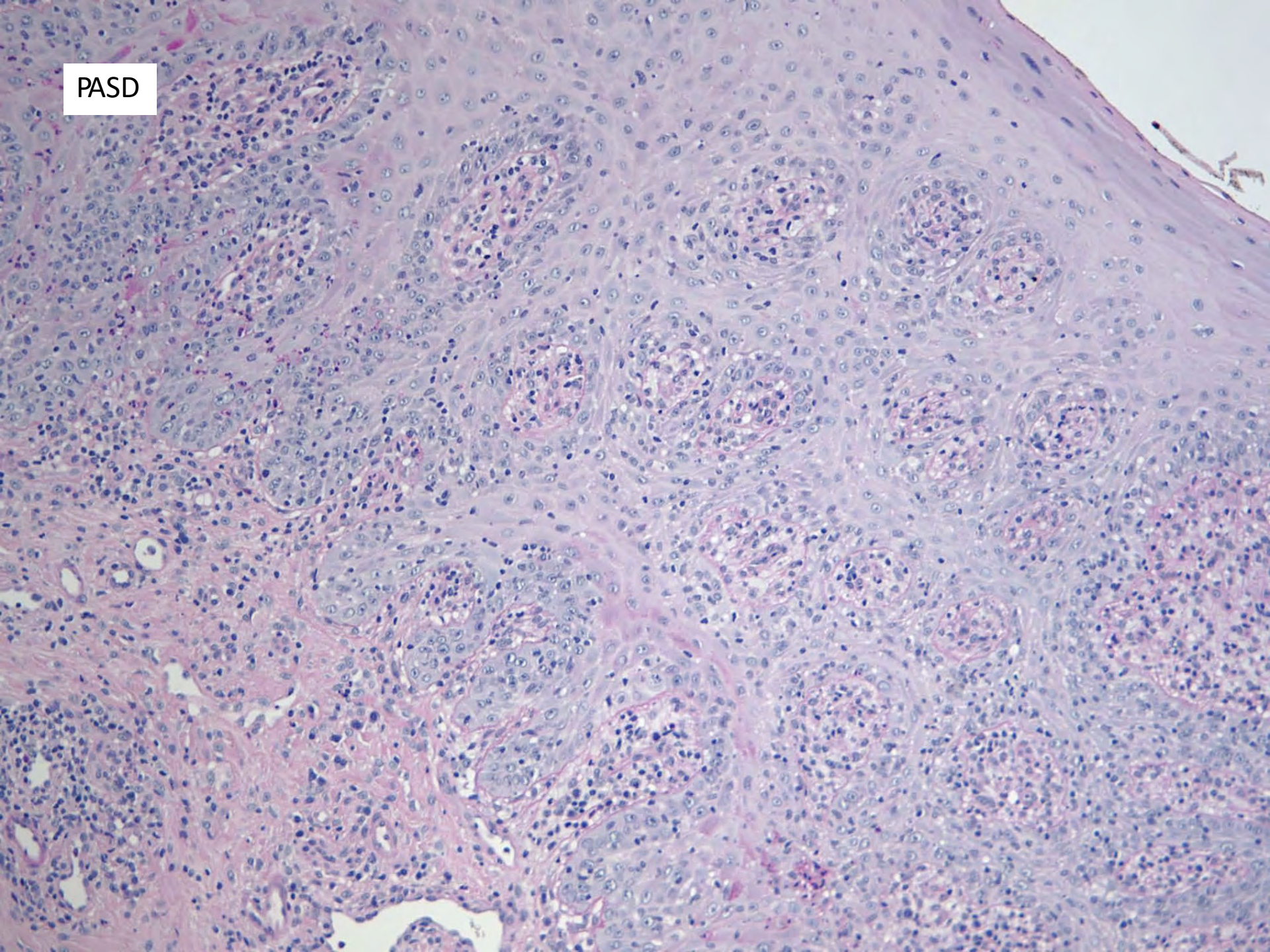
PASD

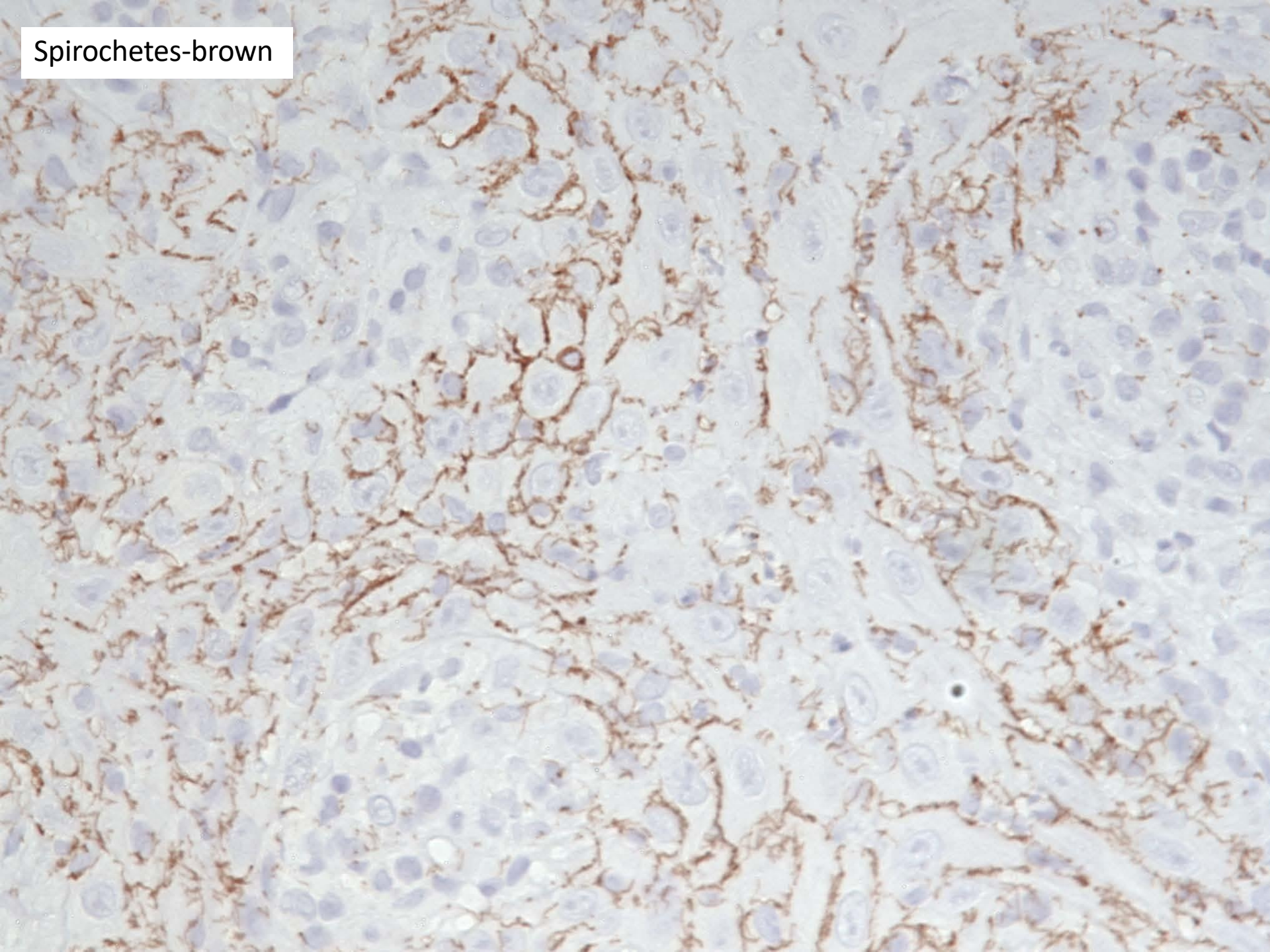
Spirochetes-brown

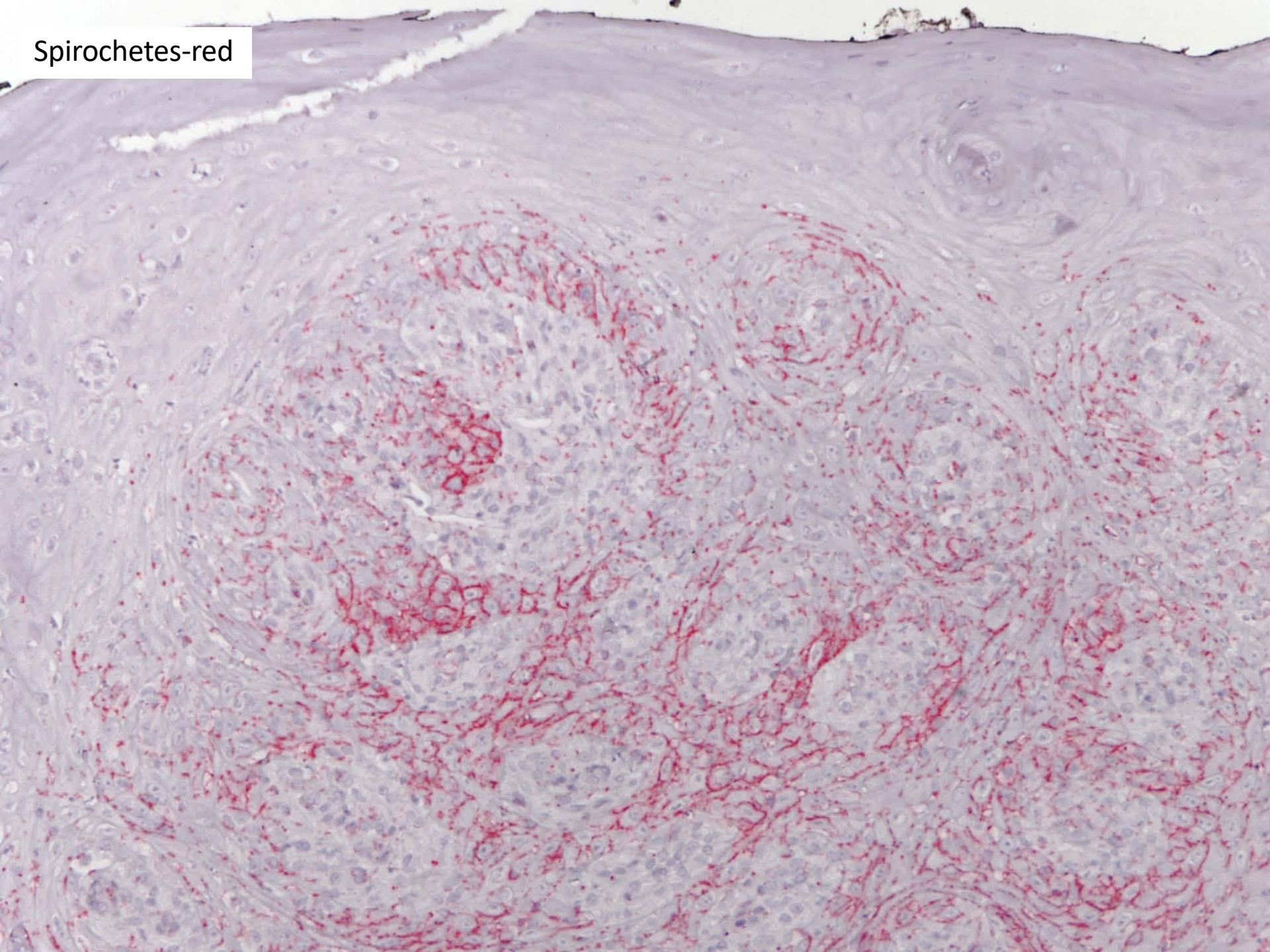
Spirochetes-red

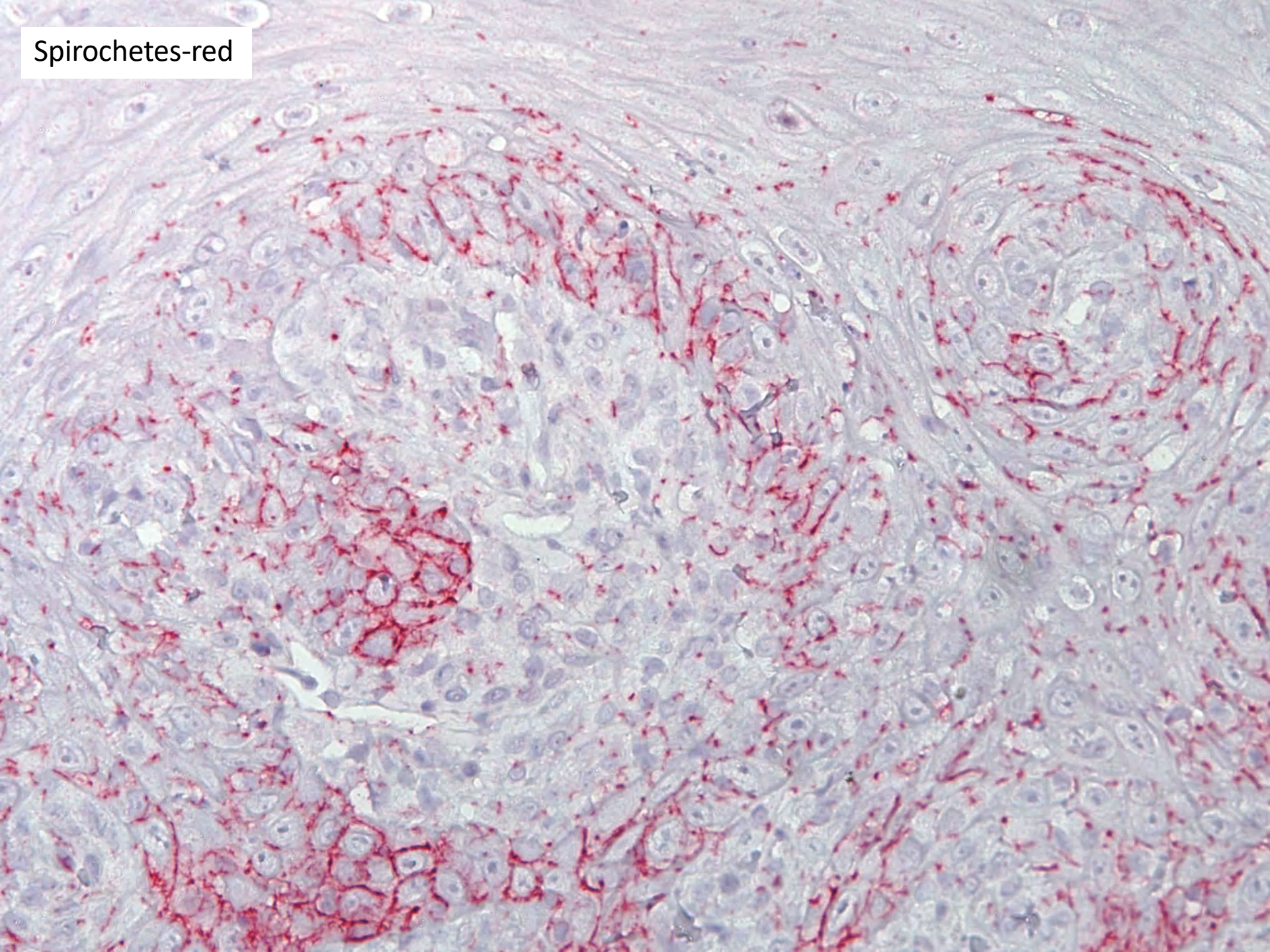
Spirochetes-red

Final Diagnosis

TONGUE, LEFT LATERAL, BIOPSY

-- SQUAMOUS MUCOSA WITH LICHENOID MUCOSITIS

-- TREPONEMAL SPIROCHETE STAINING POSITIVE BY IMMUNOHISTOCHEMISTRY

Oral Syphilis

- Primary syphilis- Chancre
  - Site of inoculation
  - 3-90 days after exposure
  - Solitary; papular; central ulceration
  - 85% genital regions; 10% anal; 4% oral
  - Men: upper lip more common; Women: lower lip more common
- Heals within 3- 8 weeks (if untreated)

Oral Syphilis

- Secondary syphilis
  - 4-10 weeks after initial infection
  - Painless lymphadenopathy, sore throat, malaise
  - Maculopapular cutaneous rash
    - Palmar and plantar areas
  - Mucous patch; split papules
  - Spontaneous resolution 3-12 weeks

Thakrar P et al. Oral ulcers as a presentation of secondary syphilis. Clin Exp Dermatol. 2018 Jul 23.

Thakrar P et al. Oral ulcers as a presentation of secondary syphilis. Clin Exp Dermatol. 2018 Jul 23.

Oral Syphilis

- Tertiary syphilis
  - Aneurysm of ascending aorta
  - CNS involvement
  - Argyll Robertson pupils
  - Gumma (indurated, nodular, ulcerated lesions)
  - Perforation of the hard palate

Oral Syphilis: Histology

- Ulcerated surface epithelium
- Extensive exocytosis
- Intense chronic inflammatory cellular infiltrate
  - Lymphocytes; Plasma cells
- Granulomatous inflammation
- IHC/Warthin-Starry
  - Corkscrew-like spirochetal organisms within surface epithelium and at interface between epithelium and the superficial stroma

False-positive results are possible in the oral cavity

Treponema microdentium
Treponema macrodentium
Treponema mucosum

Questions ?

SB 6314

Sebastian Fernandez-Pol/Kerri Rieger; Stanford

64-year-old female with purpuric papules coalescing into plaques on lower legs, with atrophic scars on left and right medial ankle, also on forearms with recent extension to upper arms.

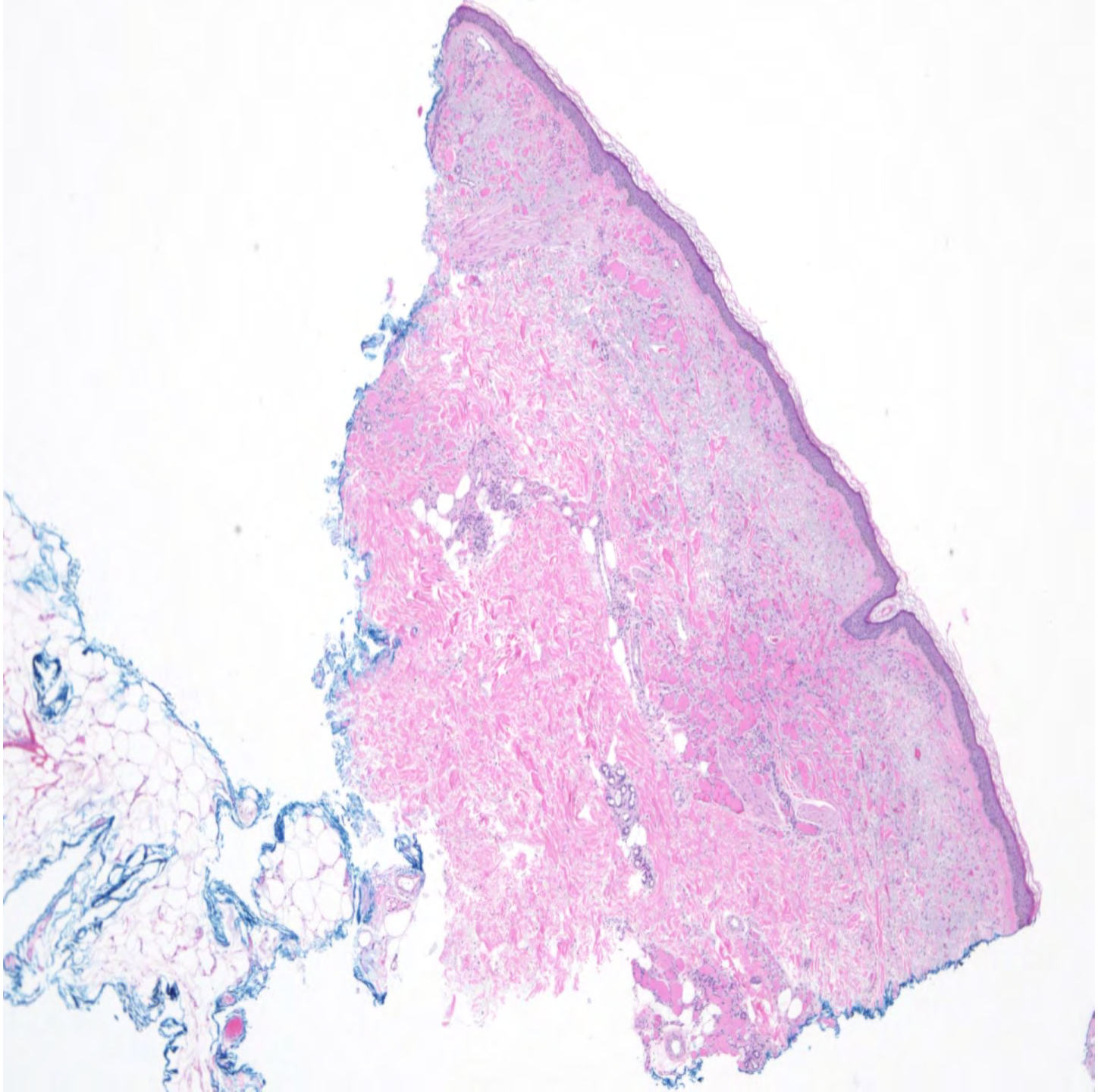

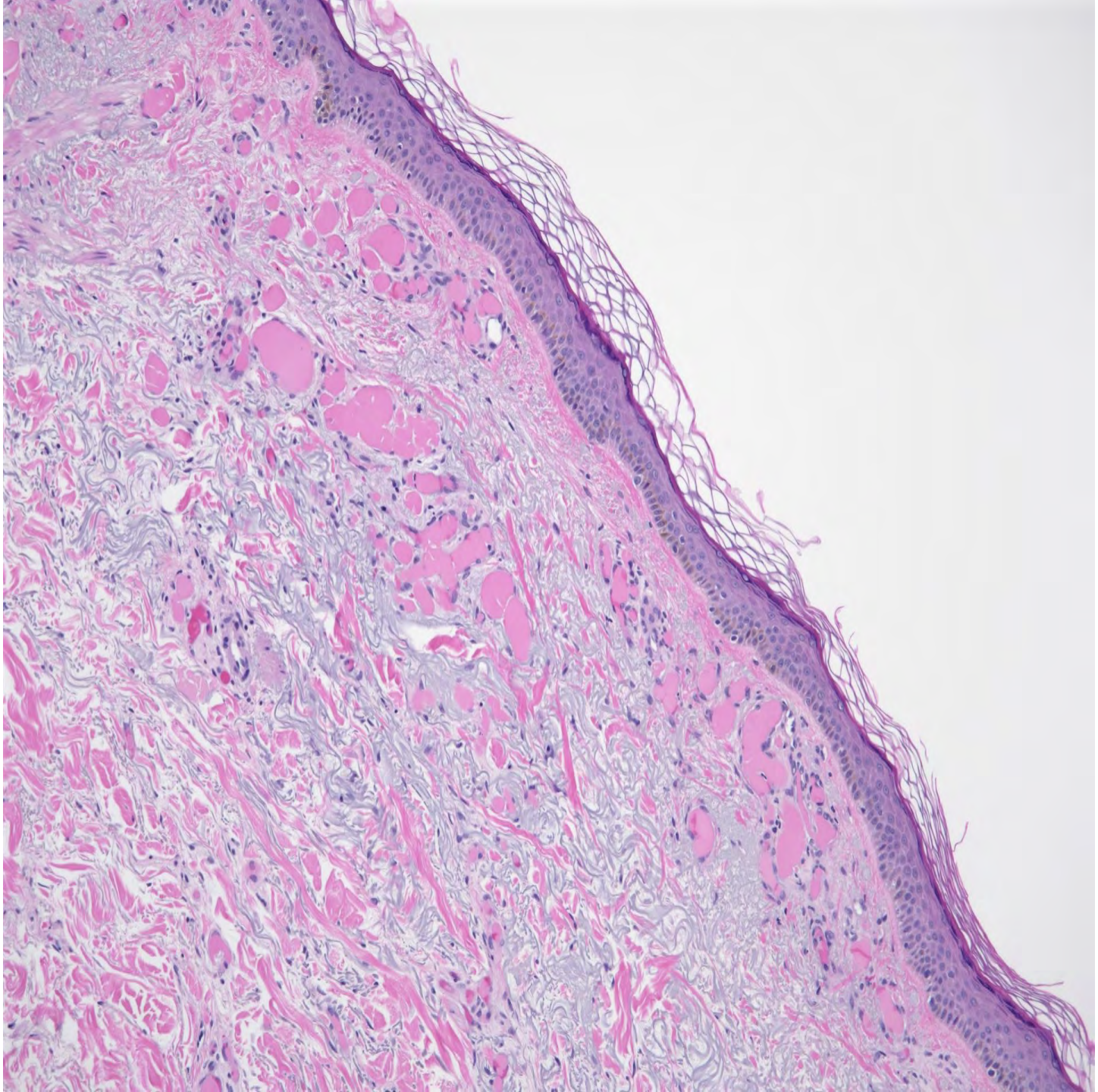

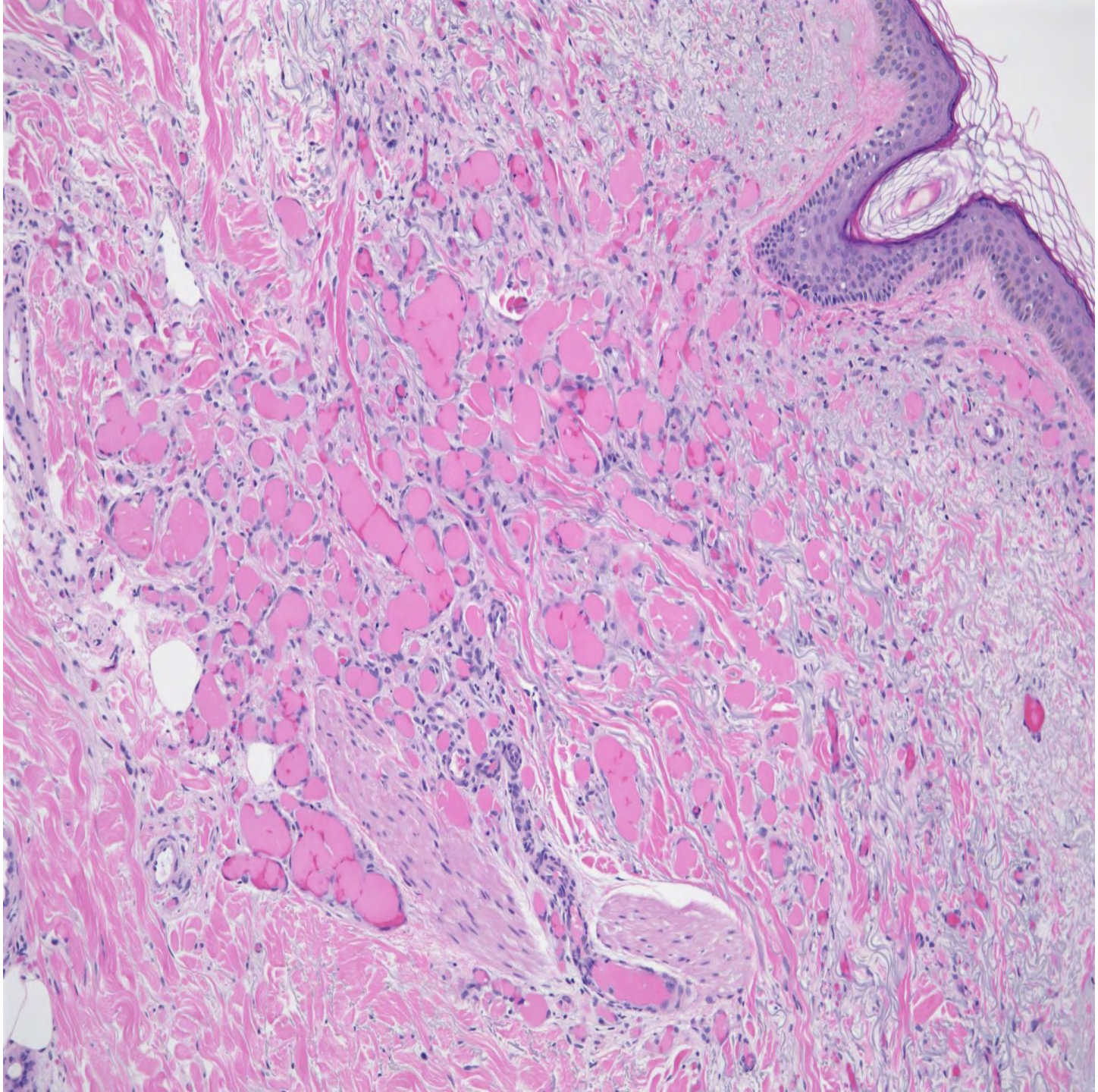

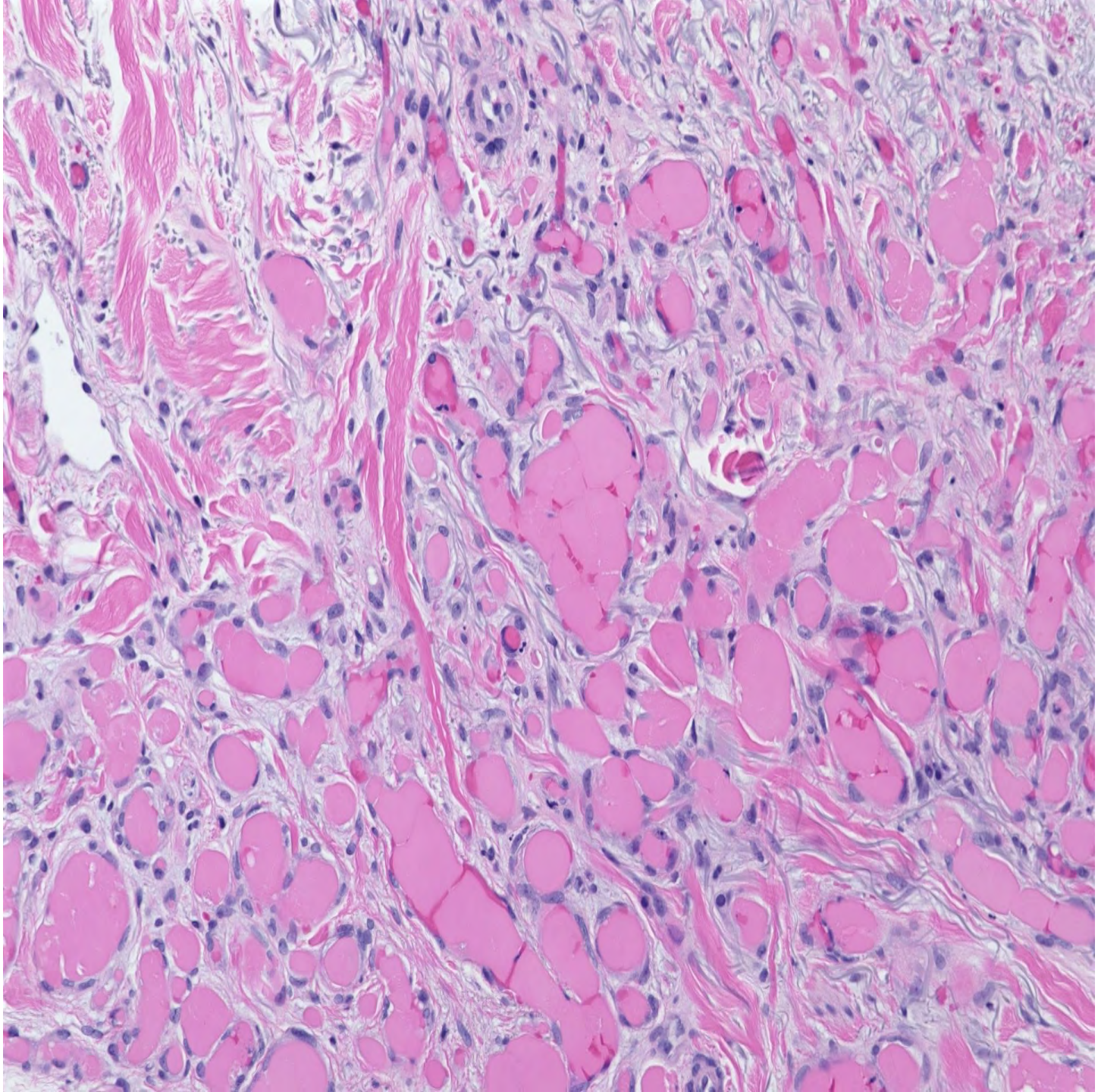

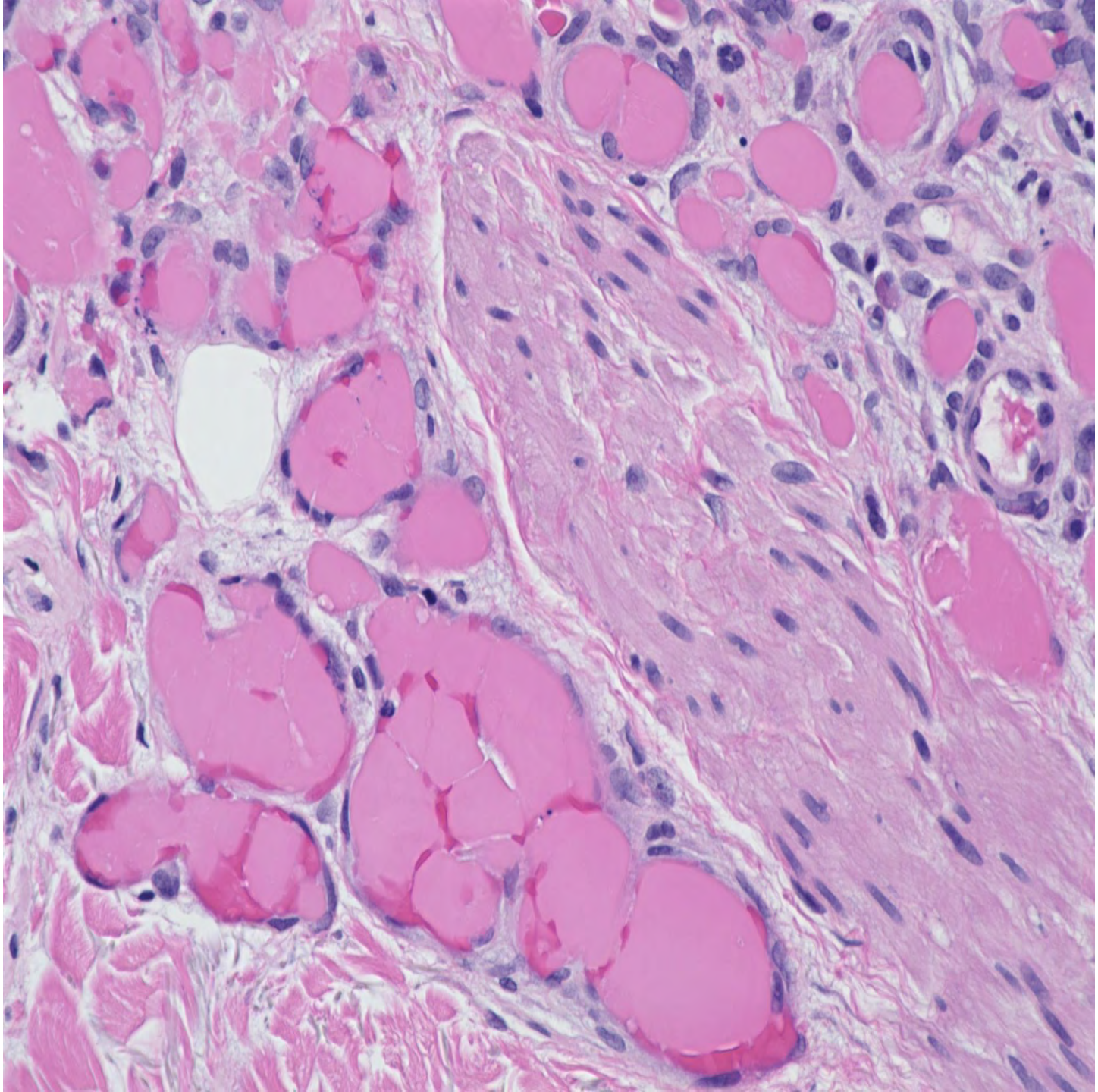

DIAGNOSIS

PASd

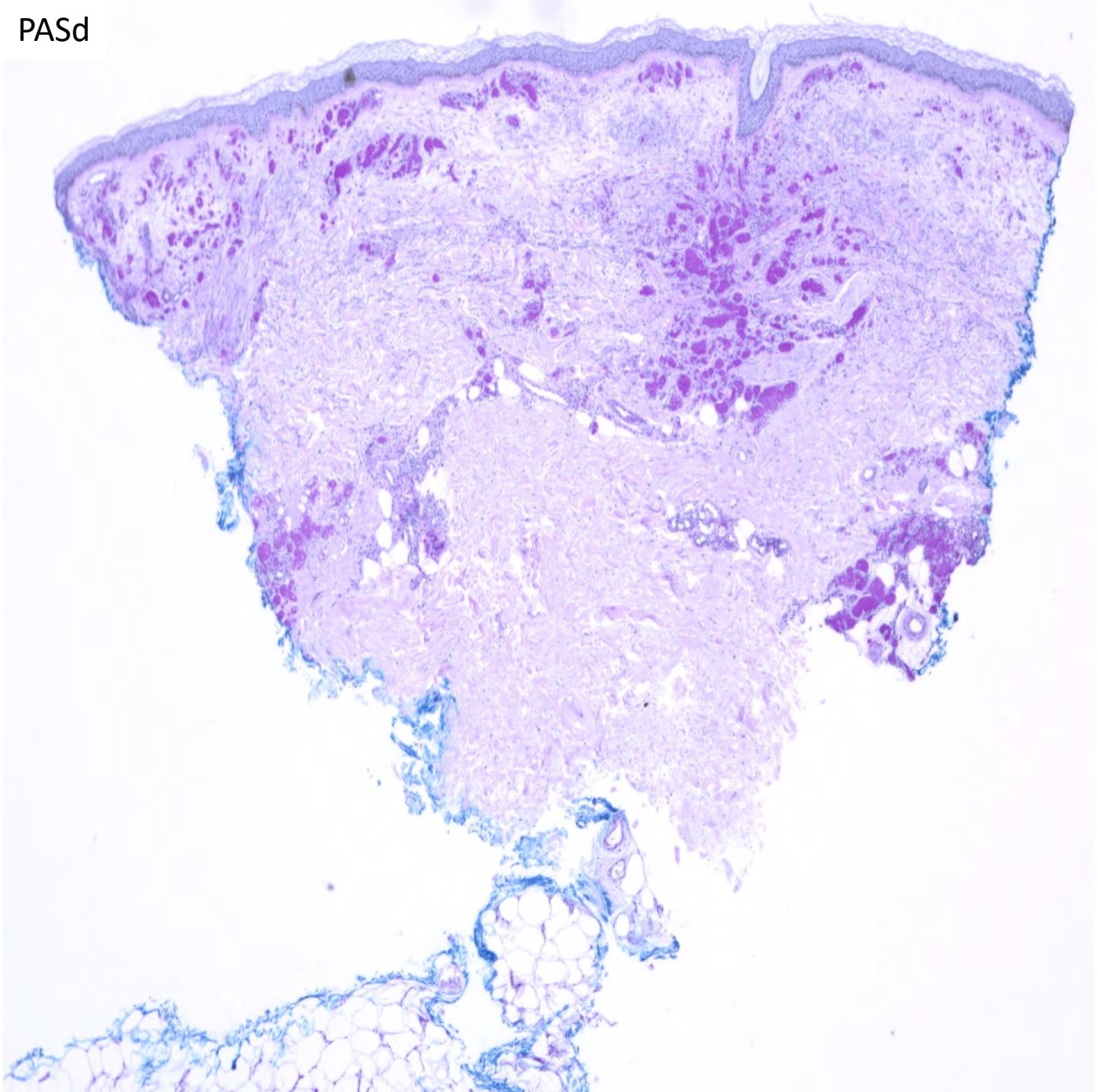

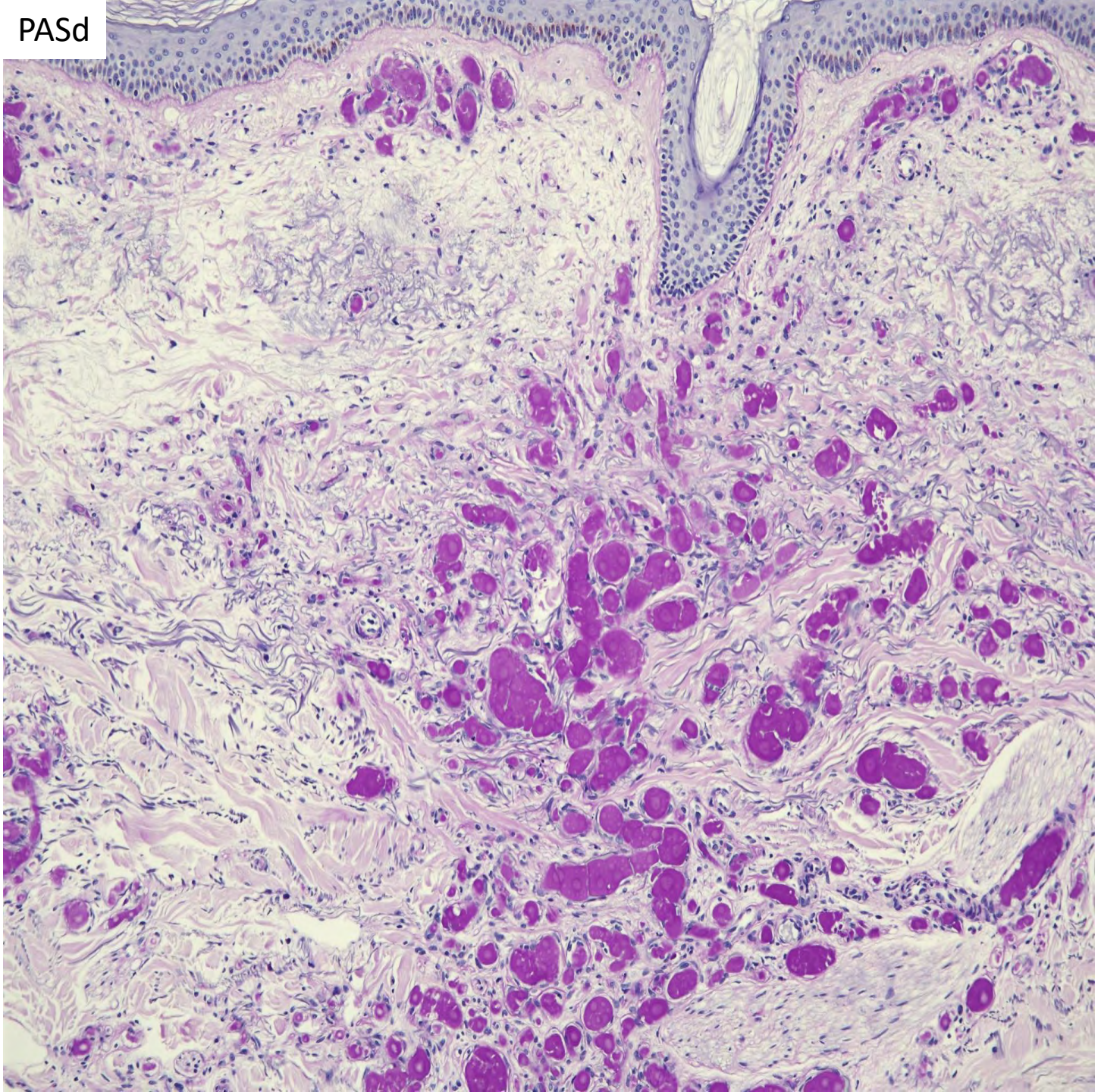
PASd

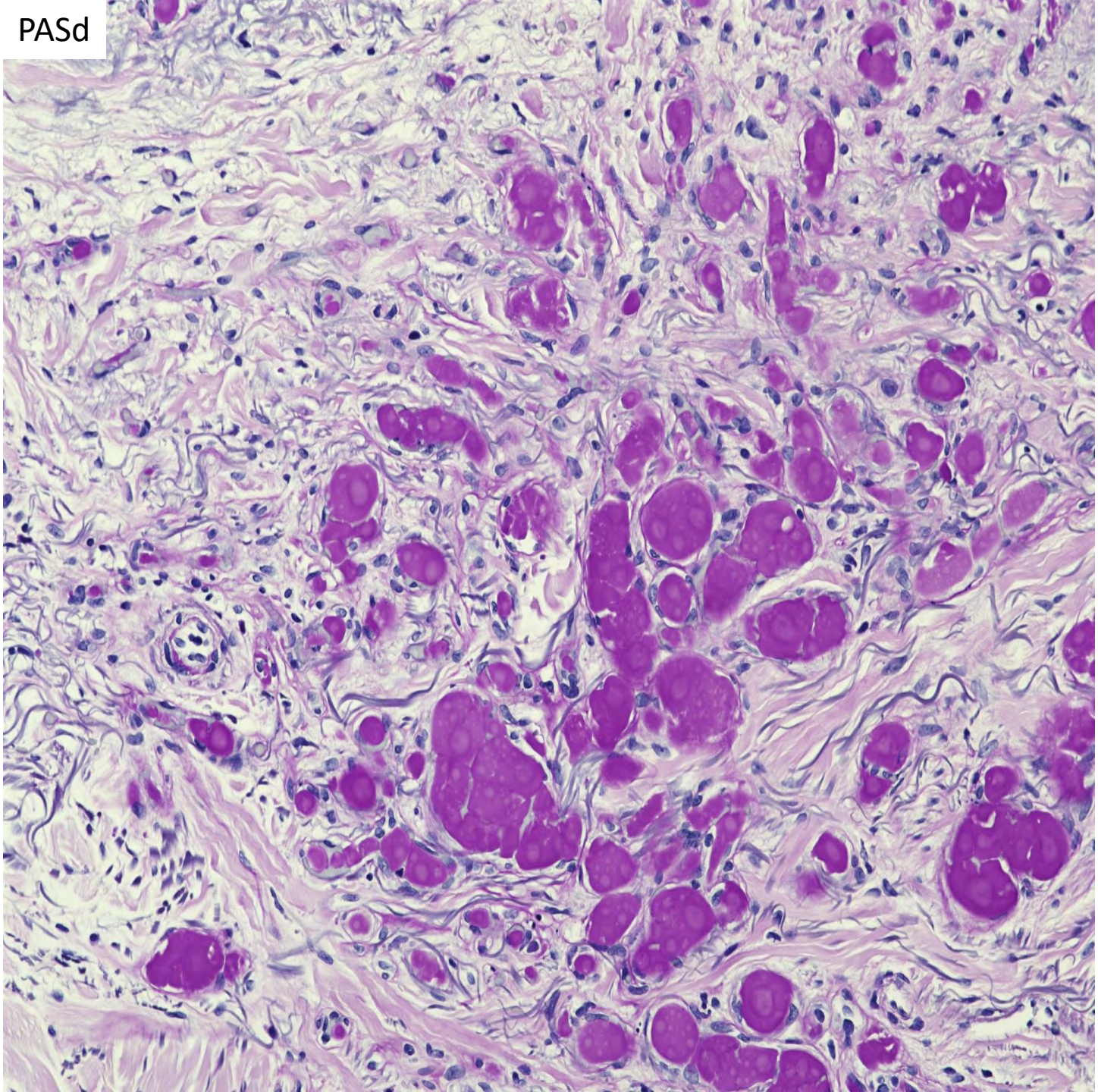
PASd

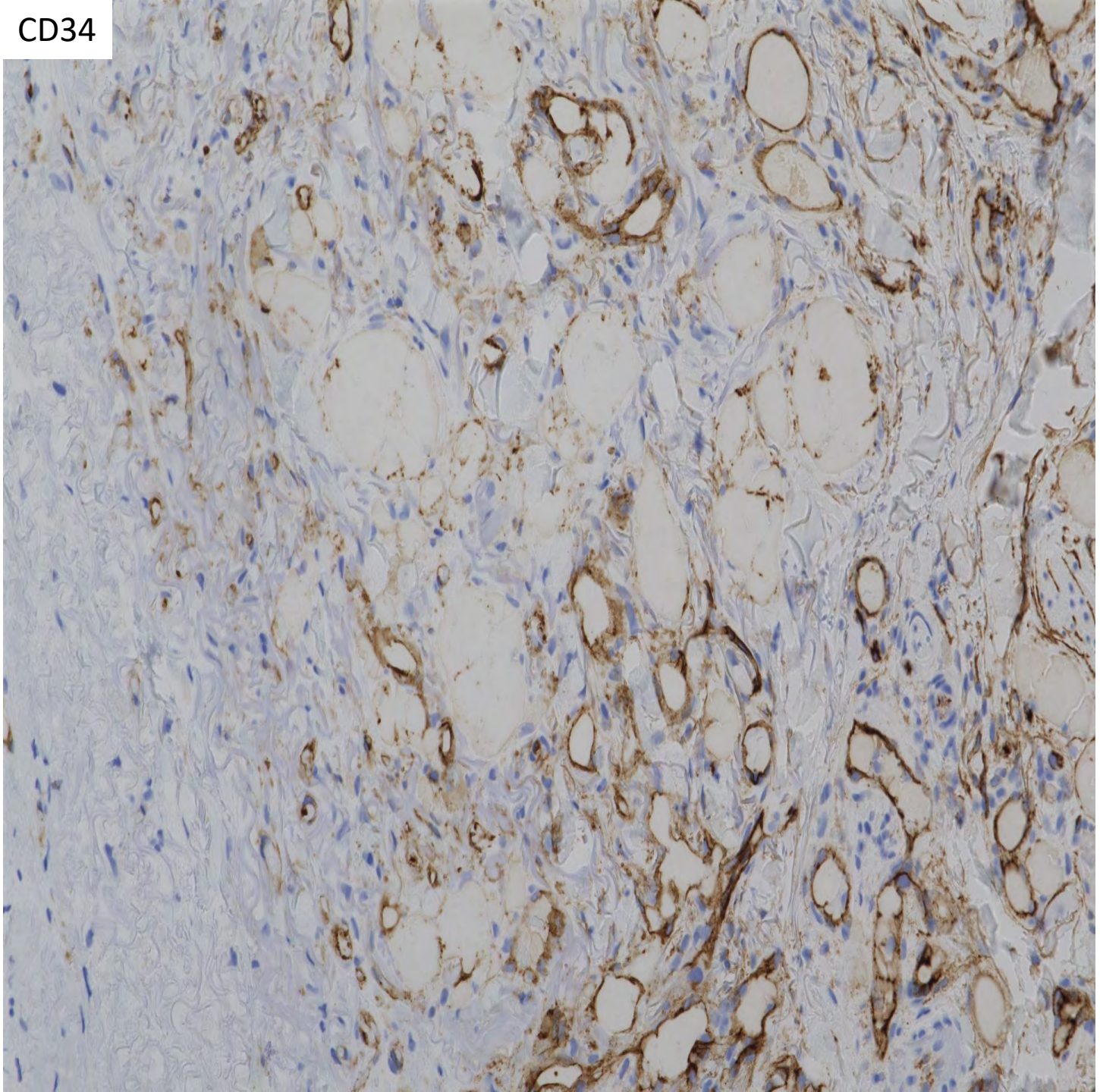
CD34

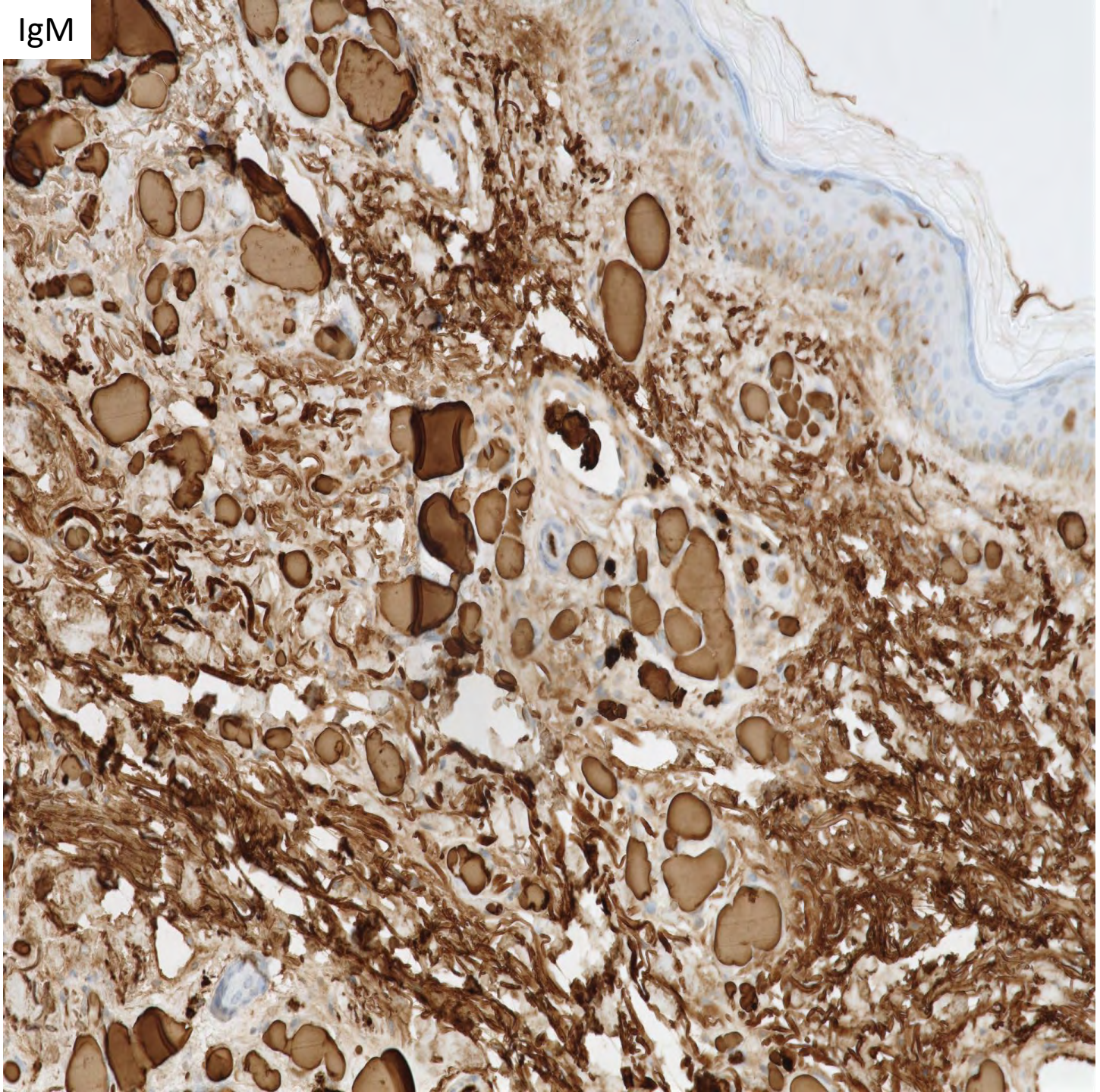
IgM

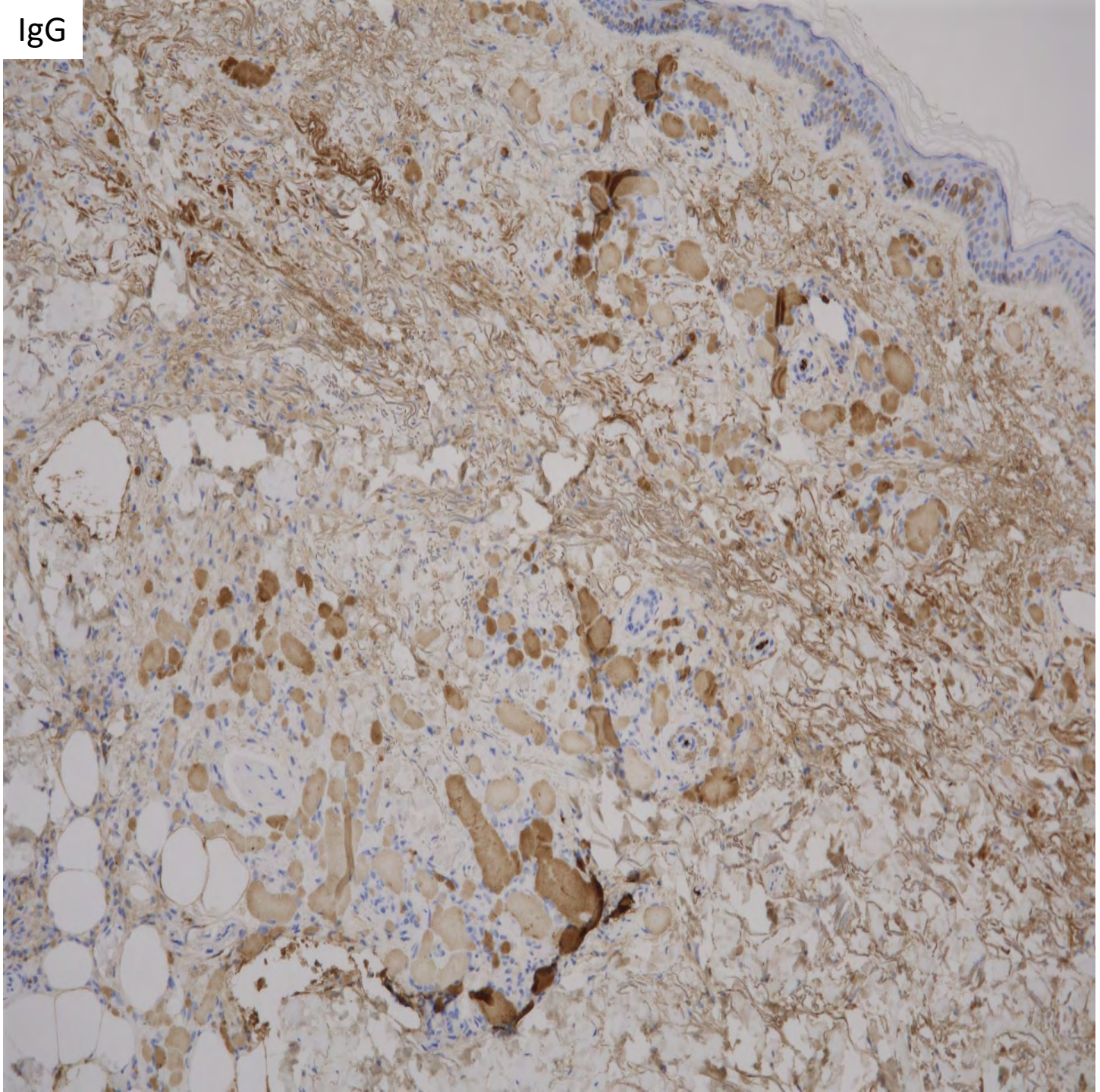
IgG

Signed out

- Increase dermal vascularity with intravascular and extravascular eosinophilic PASd-positive deposits

- Favored to represent cryoglobulin vasculopathy and reactive angiomatosis


DATE
AREA
www.deltasco.com
1-800-831-6273

Follow up

- Serum protein electrophoresis and immunofixation
  - IgM kappa monoclonal band, 0.4 g/dL
- Rheumatoid factor assay: negative
- Anti-HCV test: negative
- Referred to hematology

Type I cryoglobulinemia

- ~50% show skin manifestations
  - Necrosis
  - Raynaud syndrome
  - Urticaria
  - Livedo
- ~20% develop renal manifestations
  - Albuminuria
  - Nephrotic syndrome
  - Renal impairment
- ~20% defvelopeNeurologic manifestations
  - Polyneuropathy
  - Acute inflammatory demyelinating polyradiculoneuropathy
  - Ischemic stroke
  - Consciousness disorder

Harel et al. Clinico-biological characteristics and treatment of type I monoclonal

Type I cryoglobulinemia

- 40% had MGUS
- 60% had an overt lymphoproliferative disorder

- IgM
  - Lymphoplasmacytic lymphoma (62%)
  - MGUS (31%)

- IgG
  - MGUS (47%)
  - Indolent multiple myeloma (29%)
  - Chronic lymphocytic leukemia (13%)
  - Symptomatic multiple myeloma (5%)
  - Lymphoplasmacytic lymphoma (5%)

Harel et al. Clinico-biological characteristics and treatment of type I monoclonal

Summary

- Type I cryoglobulinemia frequently presents in the skin

- IgM cryoglobulinemia is associated with lymphoplasmacytic lymphoma or MGUS

SB 6315

Sebastian Fernandez-Pol/Dita Gratzinger/Yaso Natkunam; Stanford

88-year-old male with presents with ulcer of midine lower gingiva for 5 weeks after biting on a tortilla chip.

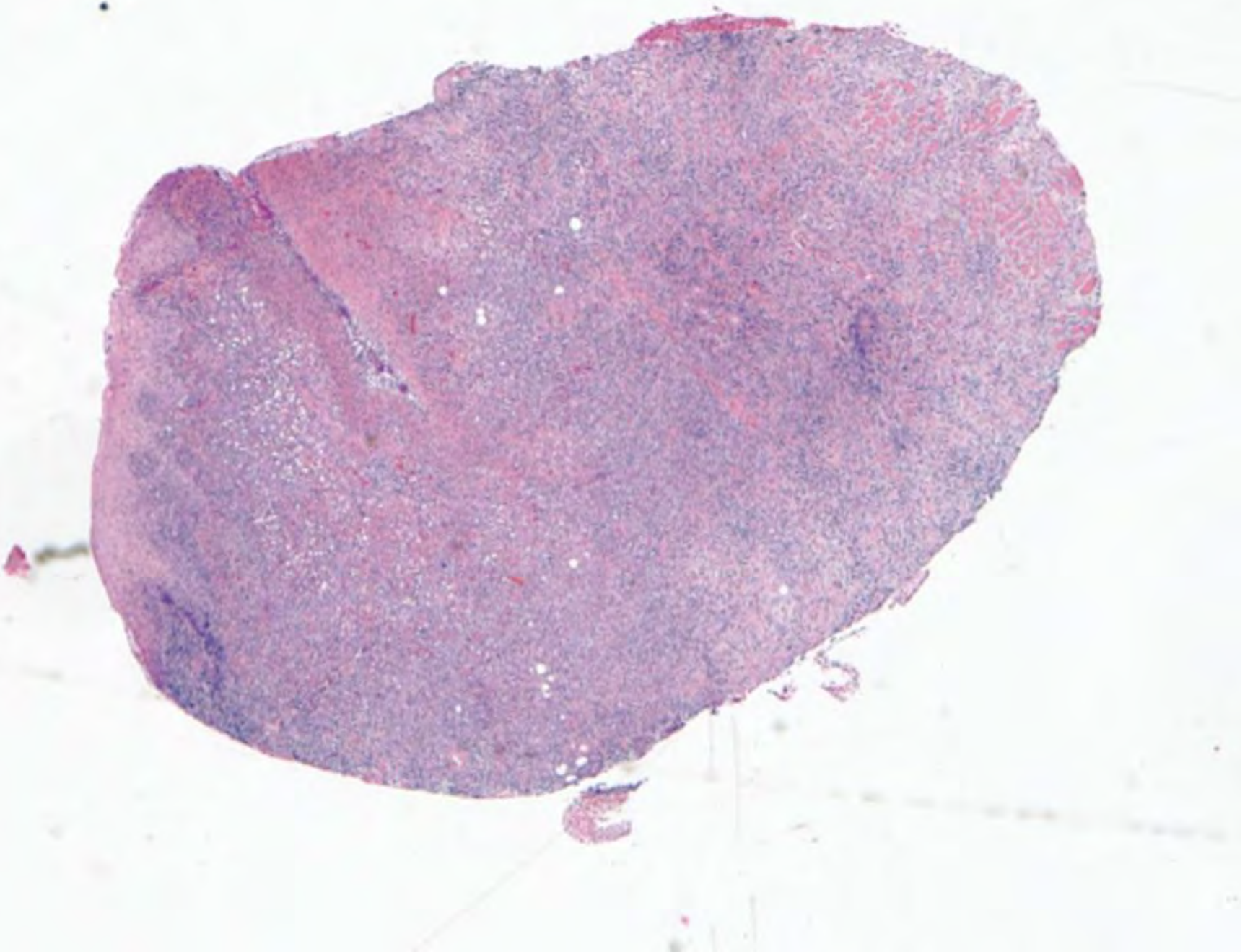

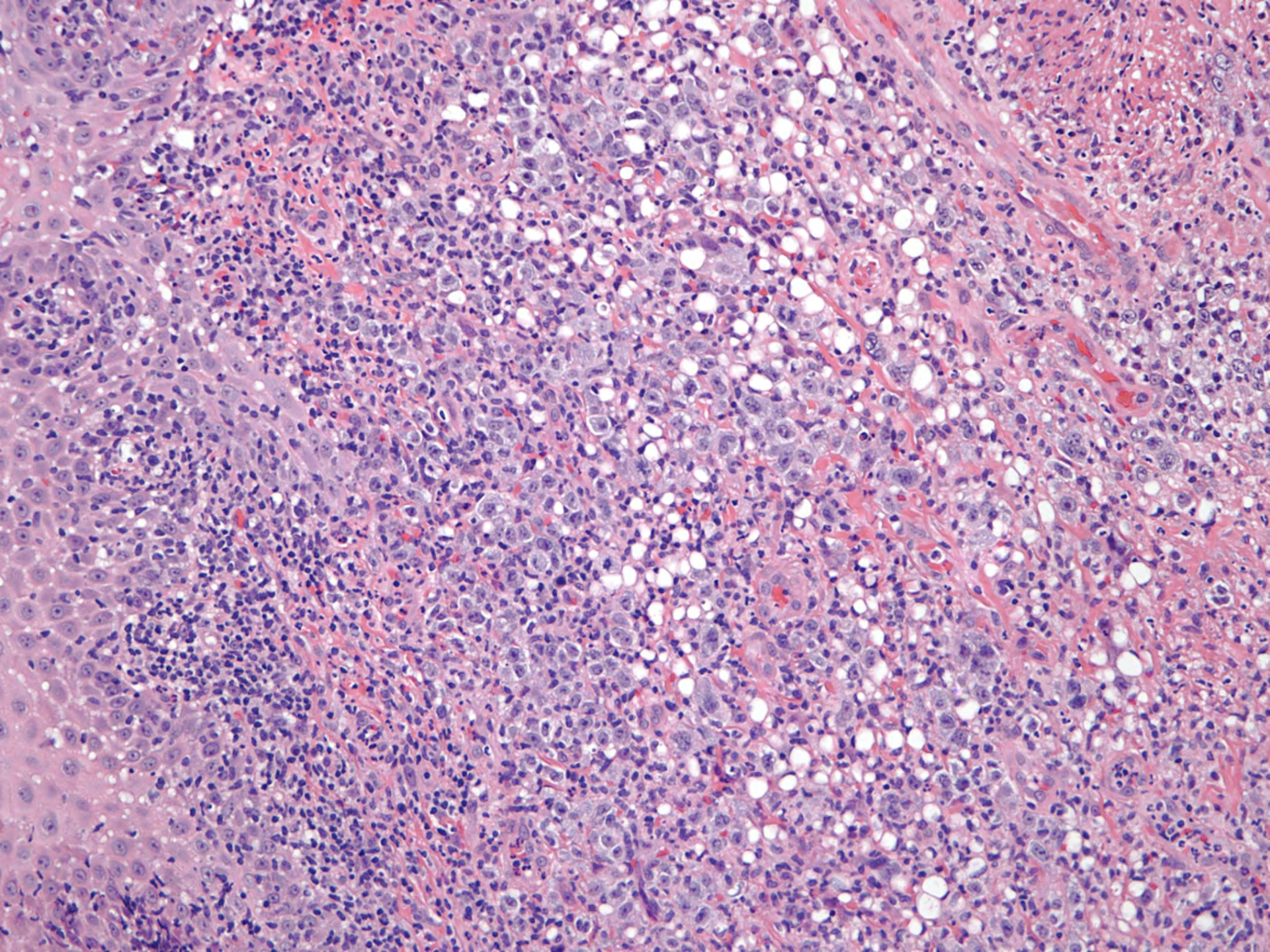

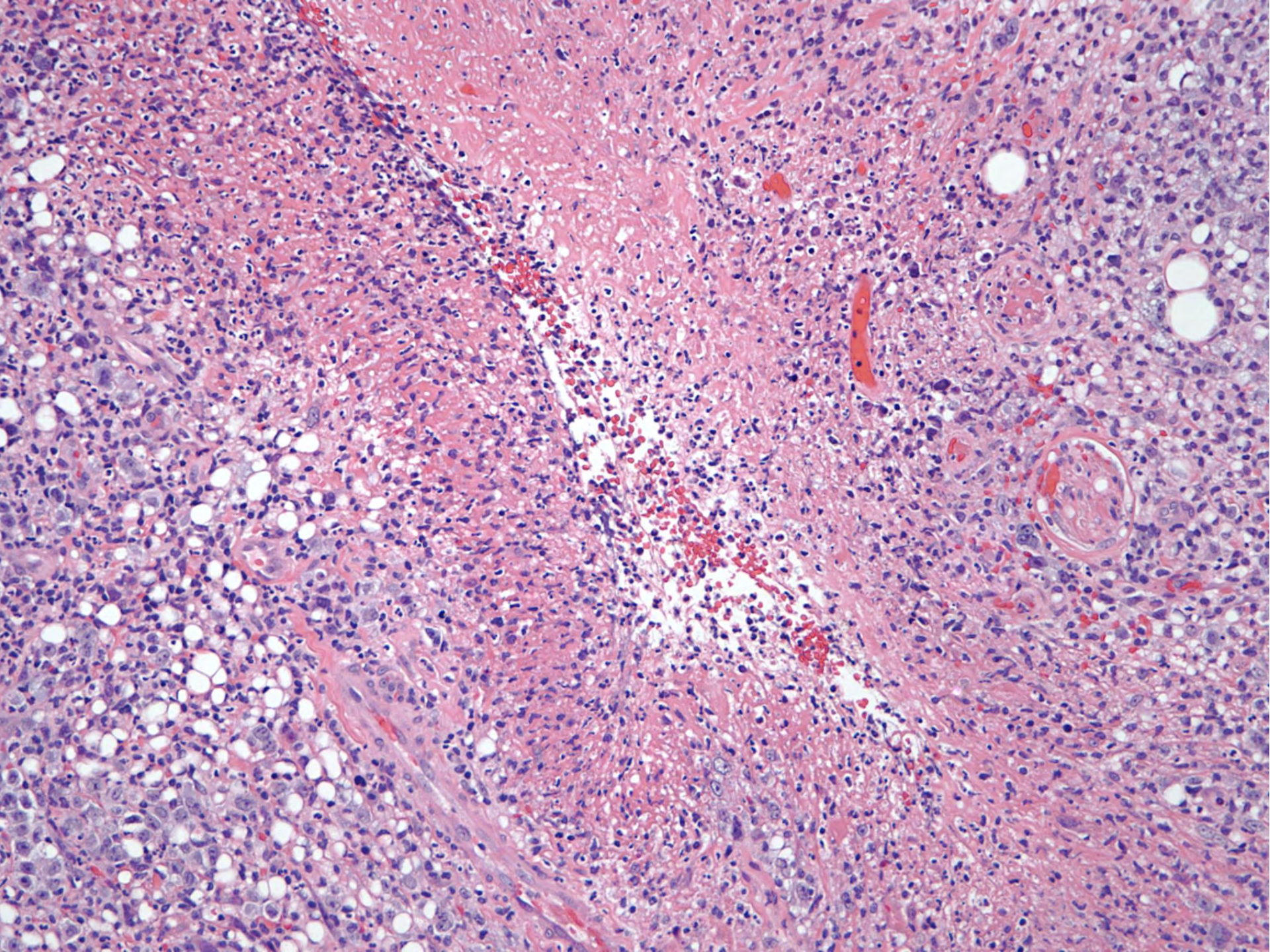

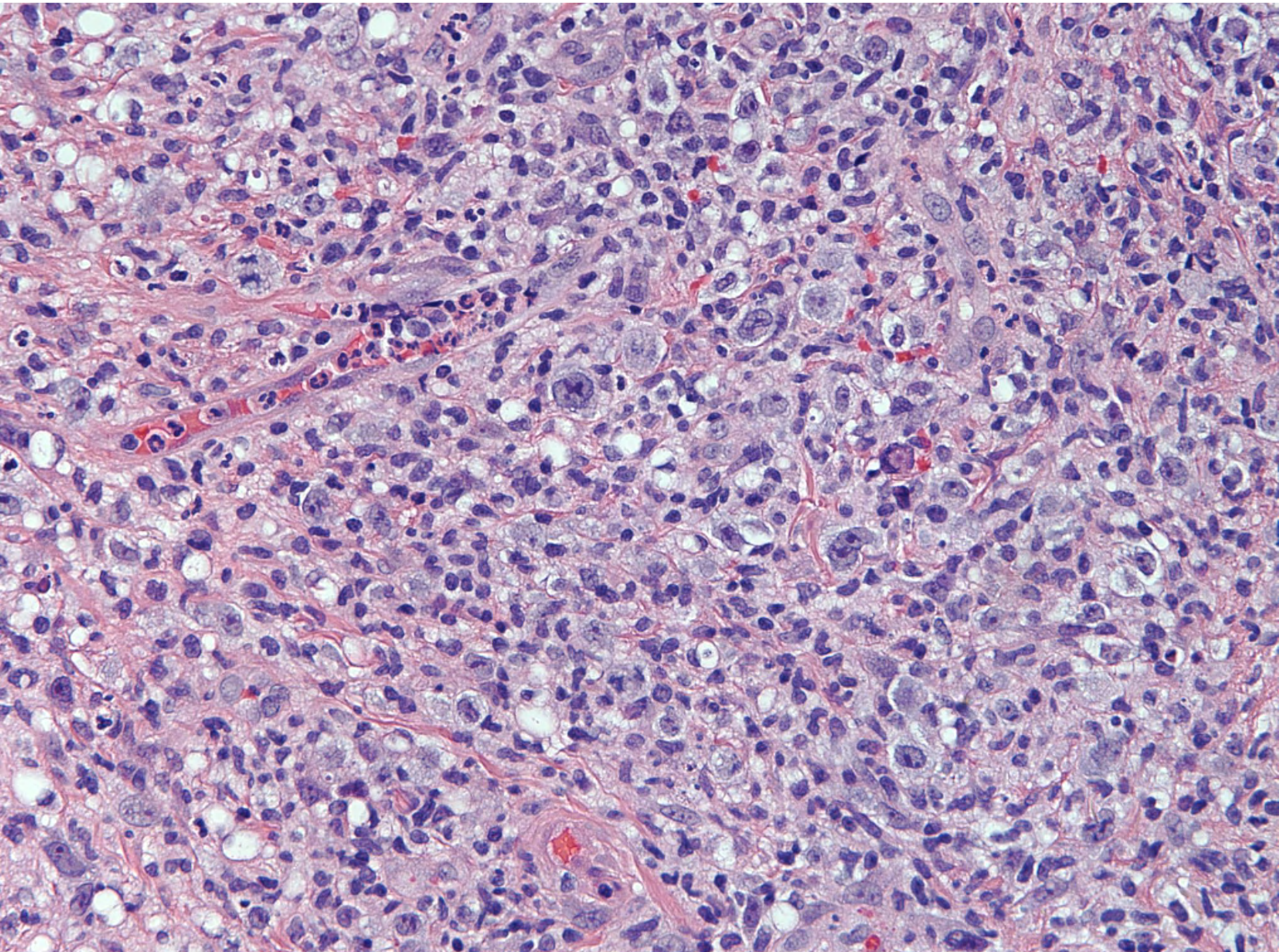

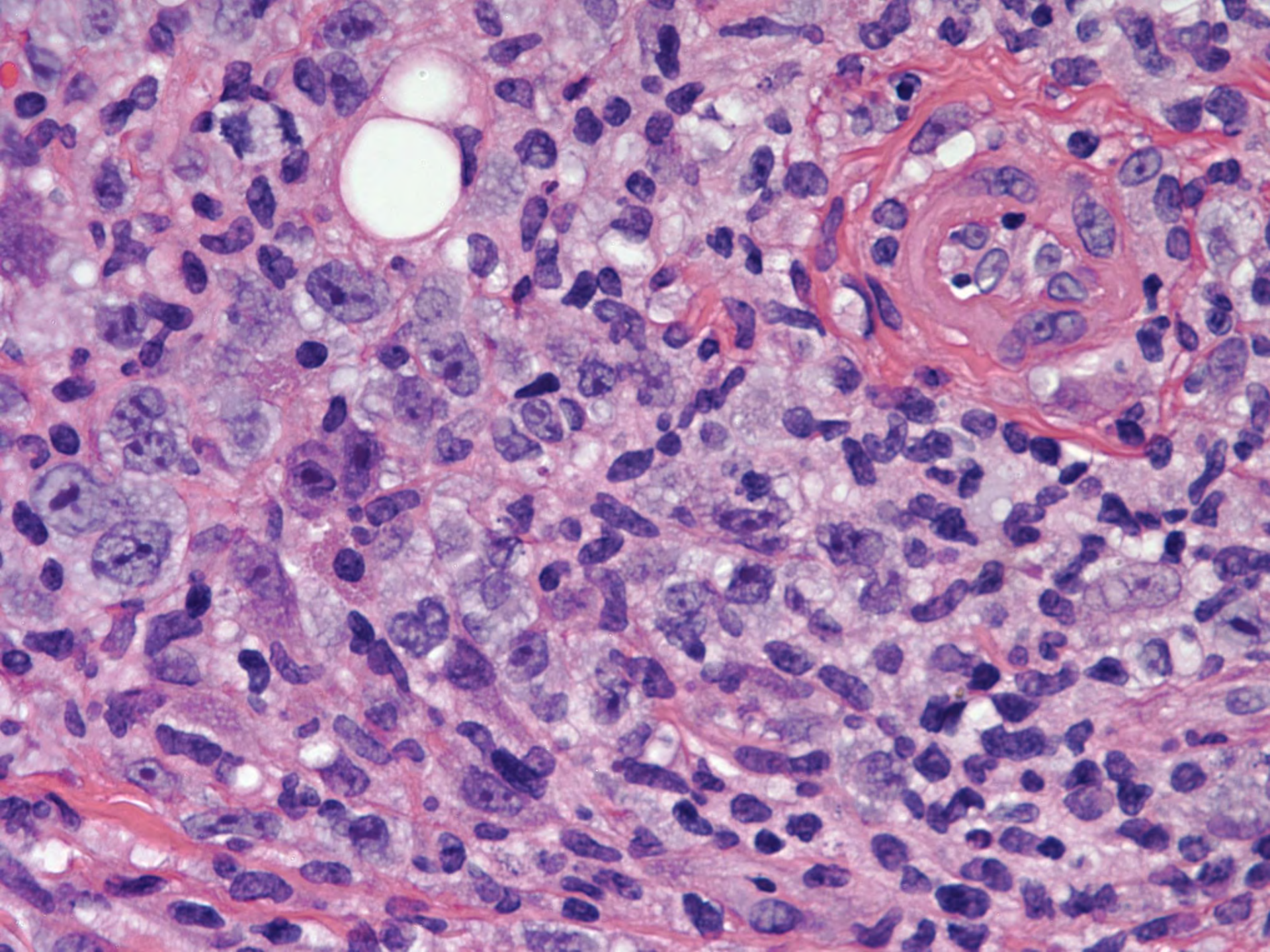

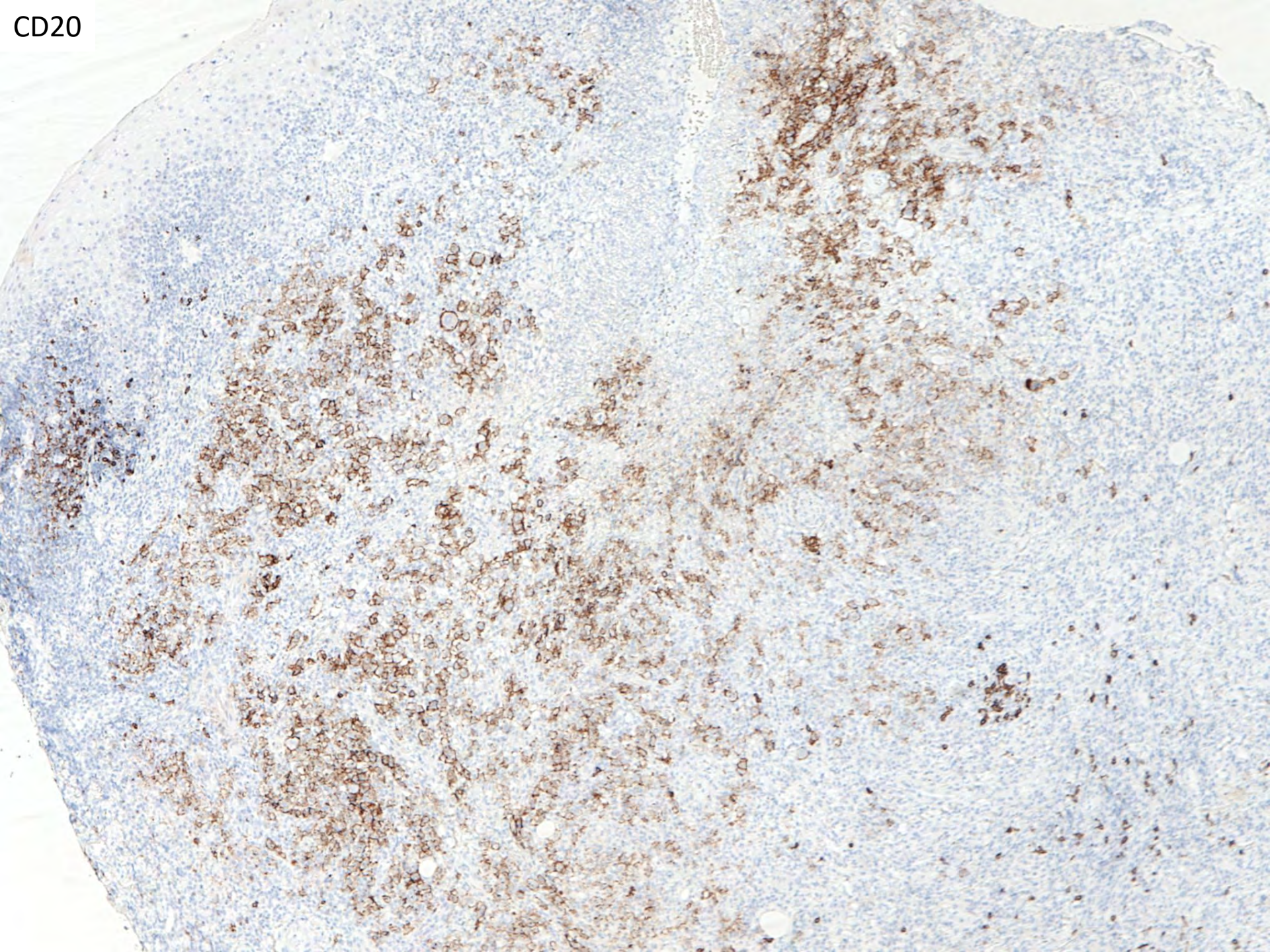
CD20

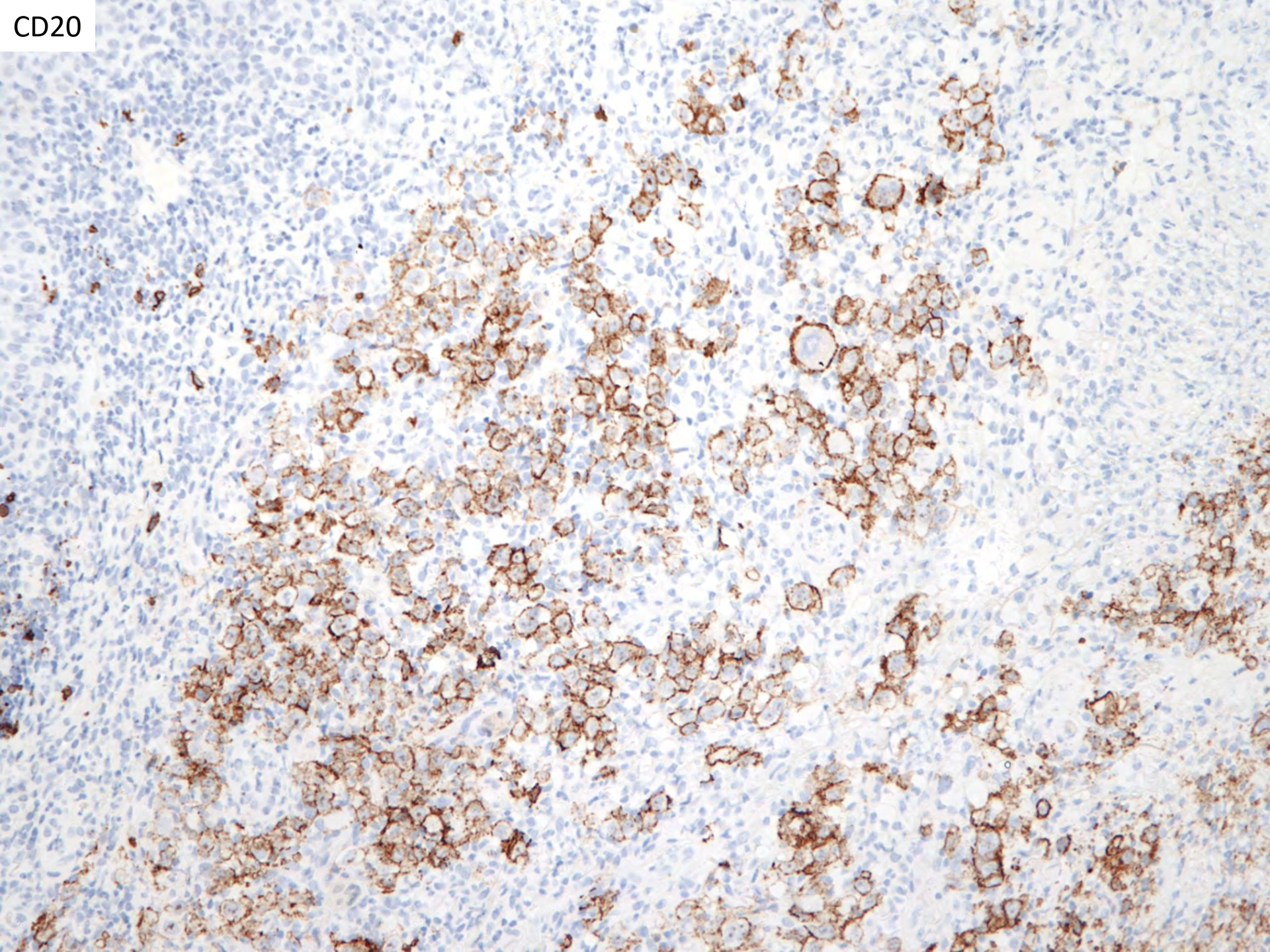
CD20

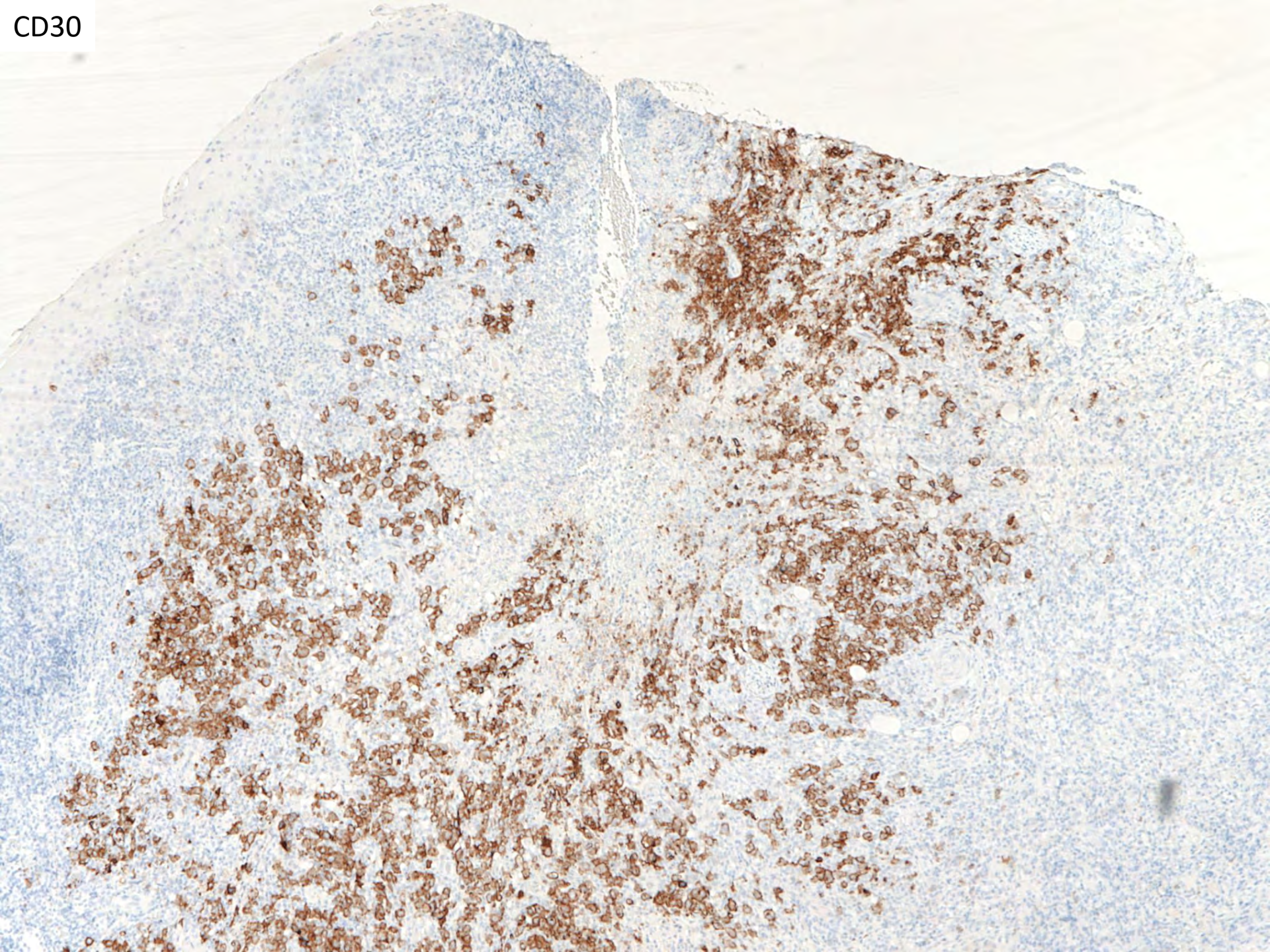
CD30

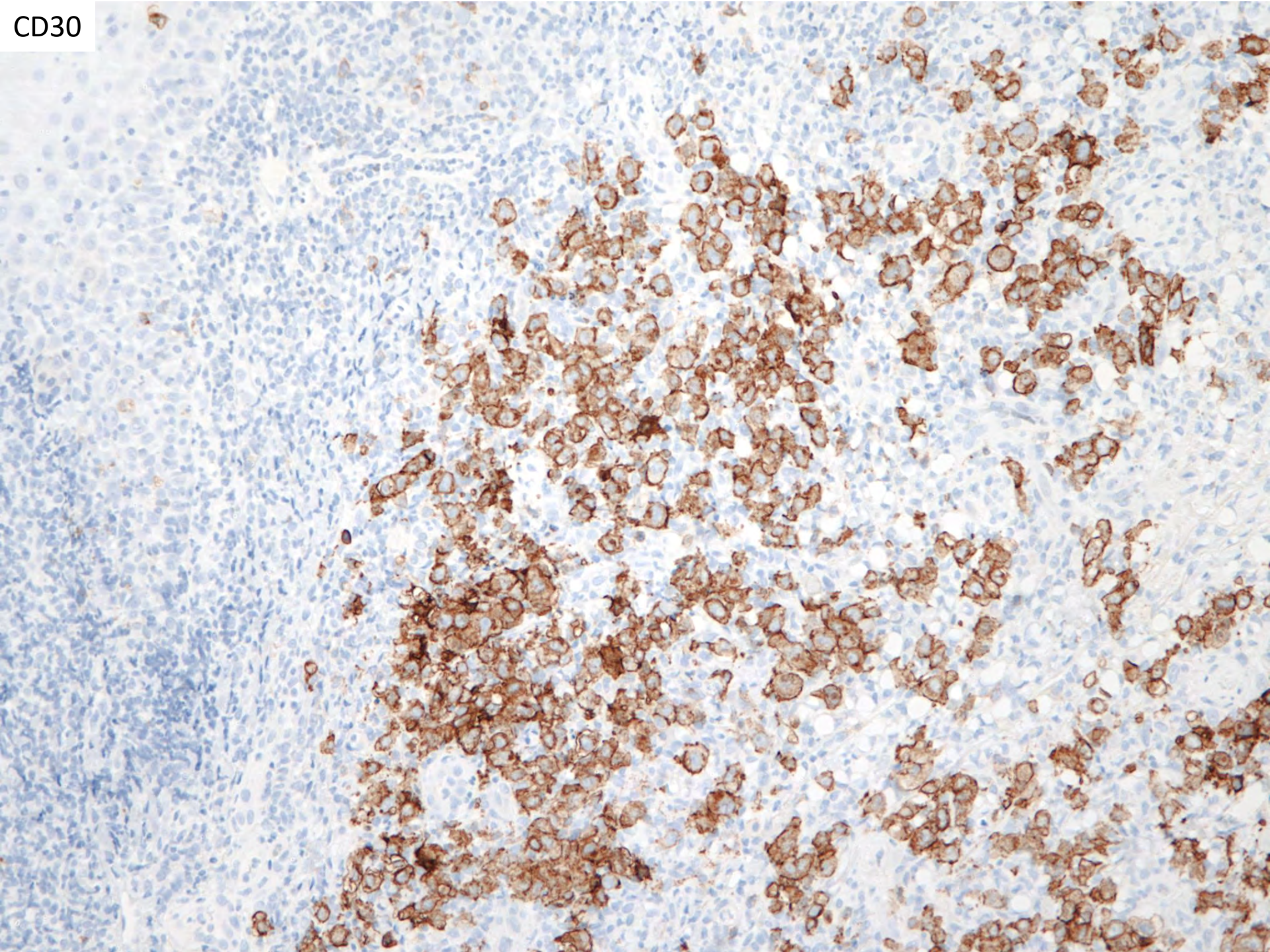
CD30

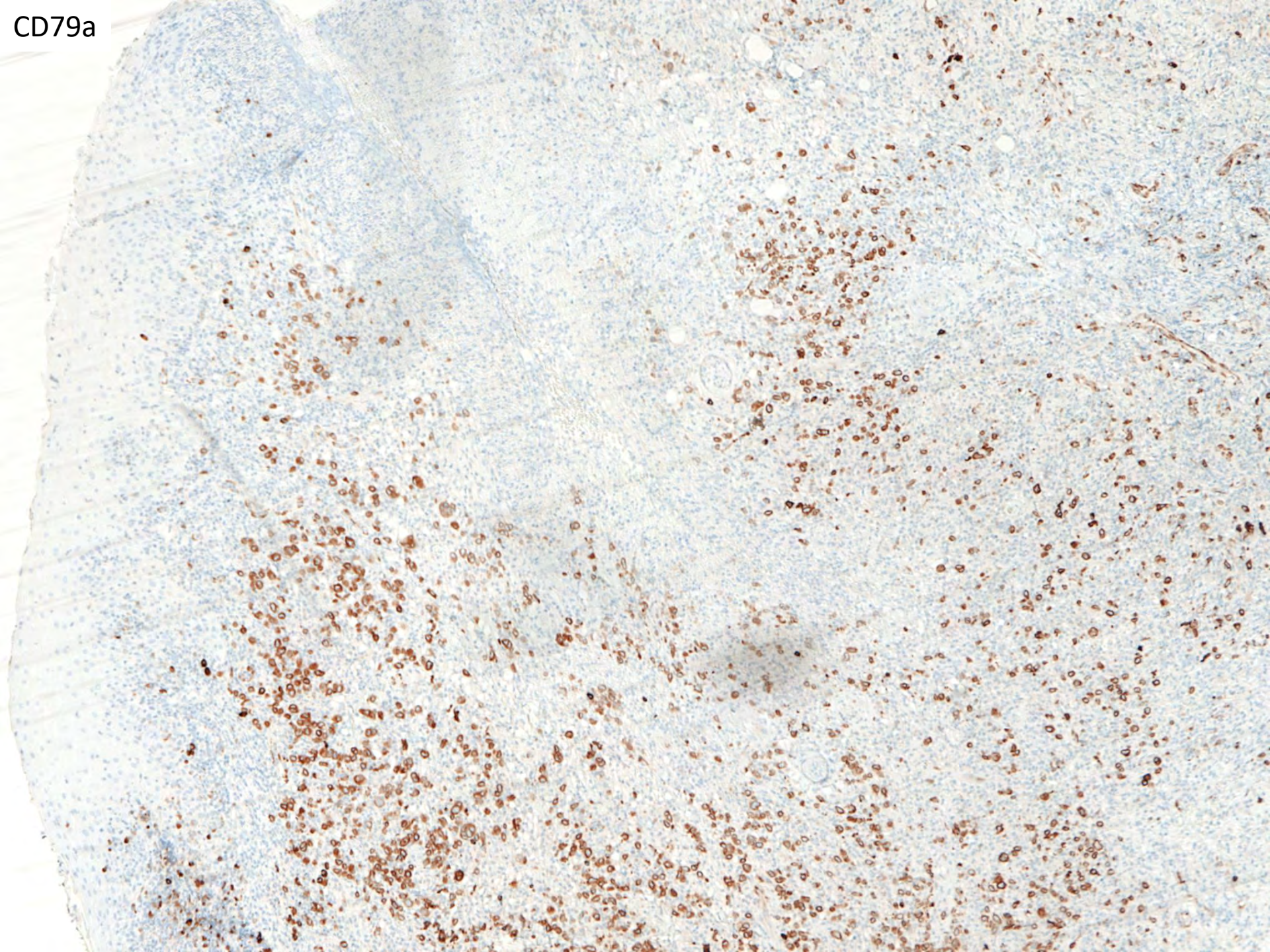
CD79a

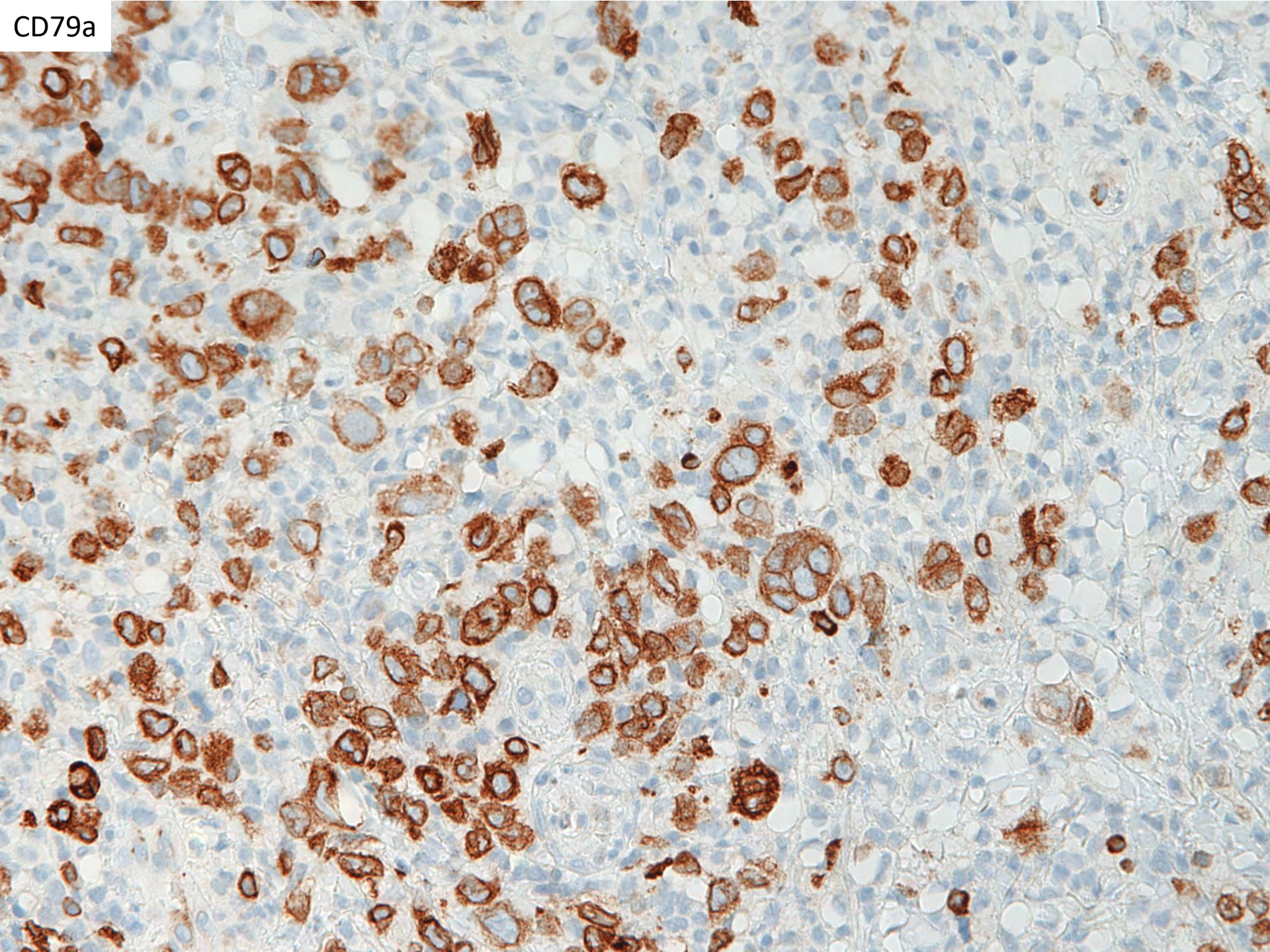
CD79a


CD3

DIAGNOSIS

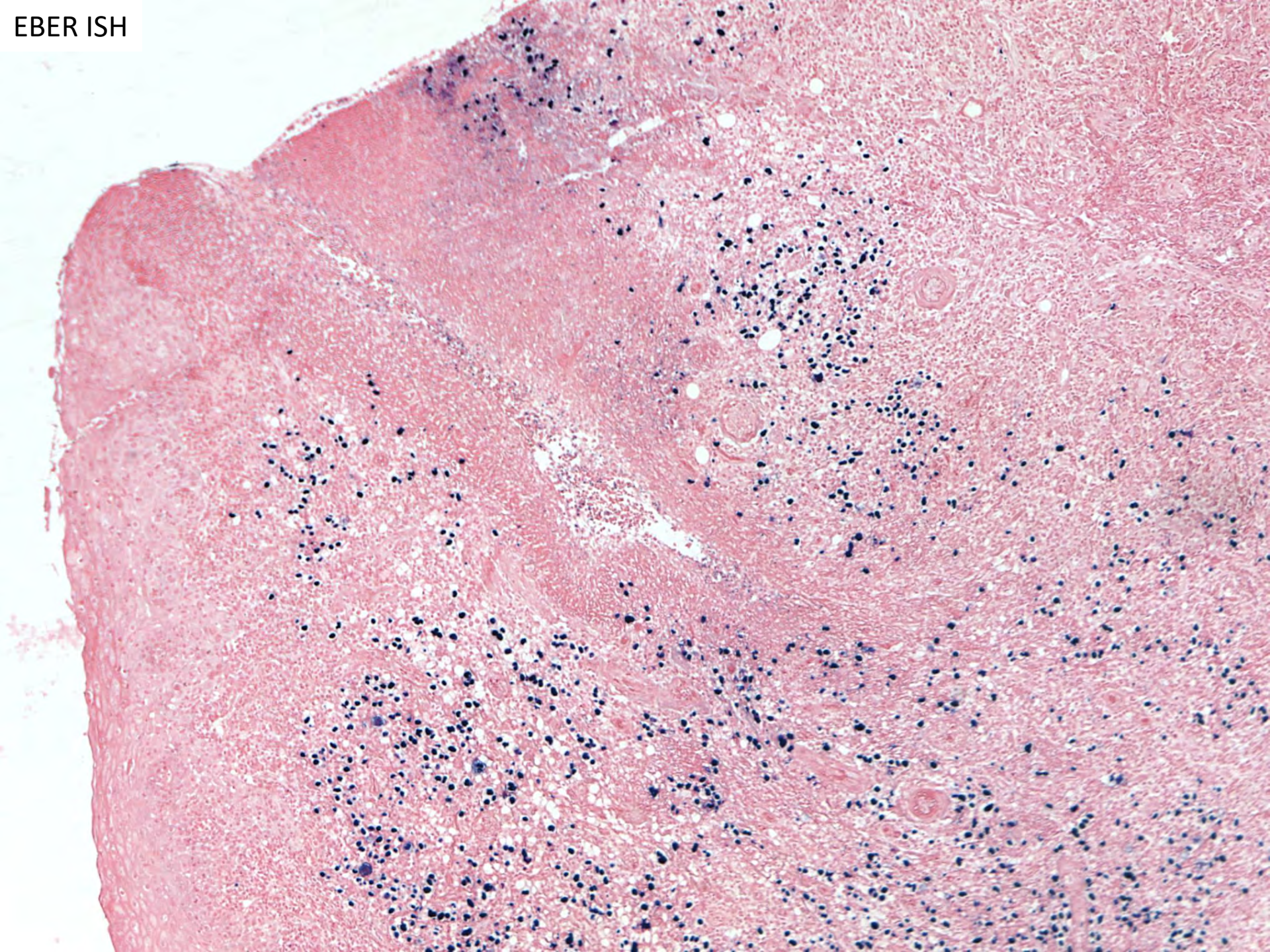
EBER ISH

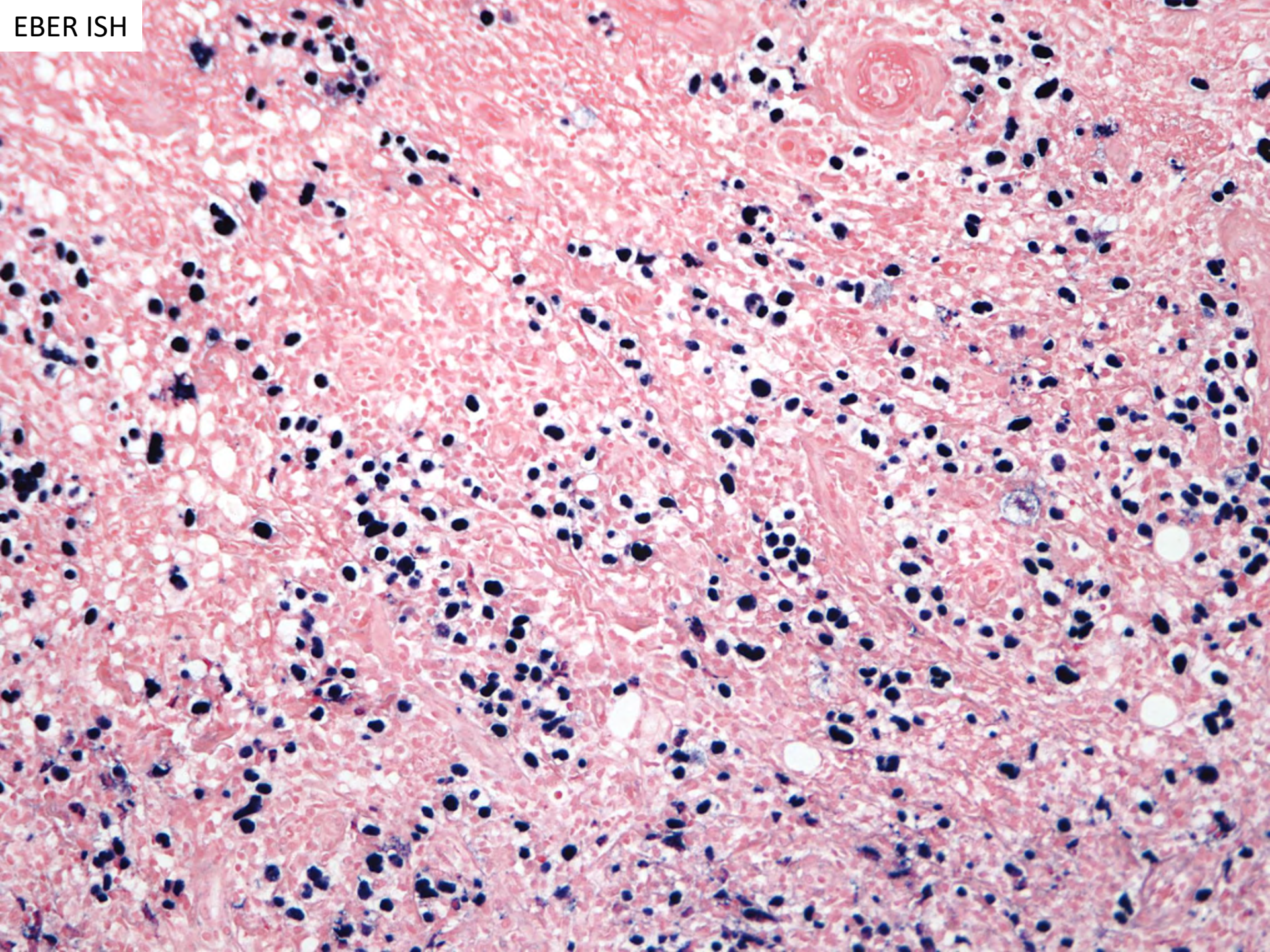
EBER ISH

EBV Positive Mucocutaneous Ulcer—A Study of 26 Cases Associated With Various Sources of Immunosuppression

Stefan D. Dojcinov, MD, FRCPath, Girish Venkataraman, MD,† Mark Raffeld, MD,† Stefania Pittaluga, MD, PhD,† and Elaine S. Jaffe, MD†*

- 26 patients - 10 males and 16 females
- Median age 77 years (range 42 to 101)
- Cause of immunosuppression:
  - 17 patients had age-related immunosenescence
  - 9 patients included azathioprine (AZA), methotrexate (MTX) or cyclosporin-A (CyA)
- Presented with isolated sharply circumscribed ulcers:
  - Oropharyngeal mucosa (16)
  - Skin (6)
  - Gastrointestinal tract (4)

EBV Positive Mucocutaneous Ulcer—A Study of 26 Cases Associated With Various Sources of Immunosuppression

Stefan D. Dojcinov, MD, FRCPath, Girish Venkataraman, MD,† Mark Raffeld, MD,† Stefania Pittaluga, MD, PhD,† and Elaine S. Jaffe, MD†*

- Polymorphous infiltrate and atypical large B-cell blasts often with Hodgkin/Reed-Sternberg (HRS) cell-like morphology
- The B cells showed strong CD30 and EBER positivity, some with reduced CD20 expression, in a background of abundant T cells
- CD15 was positive in 43% of cases (10/23)
- Polymerase chain reaction revealed 39% (7/18) clonal Ig gene rearrangements with 38% (6/16) and 31% (5/16) clonal and restricted T-cell patterns, respectively.

EBV Positive Mucocutaneous Ulcer—A Study of 26 Cases Associated With Various Sources of Immunosuppression

Stefan D. Dojcinov, MD, FRCPath, Girish Venkataraman, MD,†*
Mark Raffeld, MD,† Stefania Pittaluga, MD, PhD,† and Elaine S. Jaffe, MD†

- Therapy:
  - 25% (5/20) received standard chemotherapy and/or radiotherapy.
  - 45% (9/20) regressed spontaneously with no treatment
  - 15% (3/20) were characterized by a relapsing and remitting course
  - All iatrogenic lesions (6/6) with available follow-up responded to reduction of immunosuppression
  - All patients achieved complete remission with no disease-associated deaths over a median follow-up period of 22 months (range 3 to 72)

On methotrexate for rheumatoid arthritis

Perforation from the buccal sulcus
Methotrexate withdrawn

Summary

- EBV^+ mucocutaneous ulcer is a newly recognized clinicopathologic entity in the 2017 revision of World Health Organization (WHO) classification.
- Often occurs in elderly patients with or without iatrogenic immunosuppression
- Usually presents as an isolated ulcerative lesion, most commonly involving the **oral mucosa** but also appearing in **skin** or **gastrointestinal tract**
- The disease typically follows an indolent clinical course.

SB 6316
(scanned slide available)

John Higgins; Stanford

15-year-old male with sickle cell trait and 1 month h/o intermittent gross hematuria.

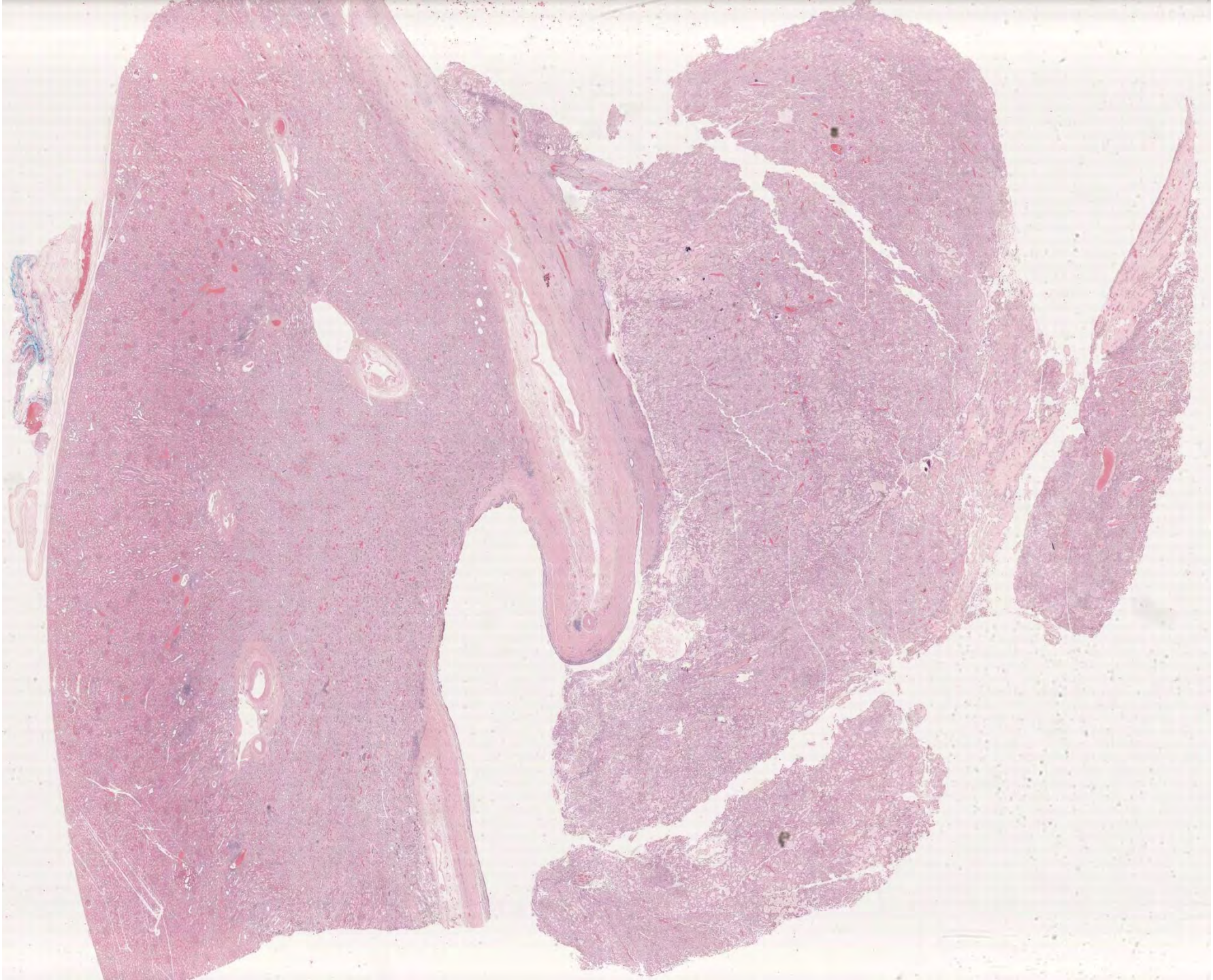

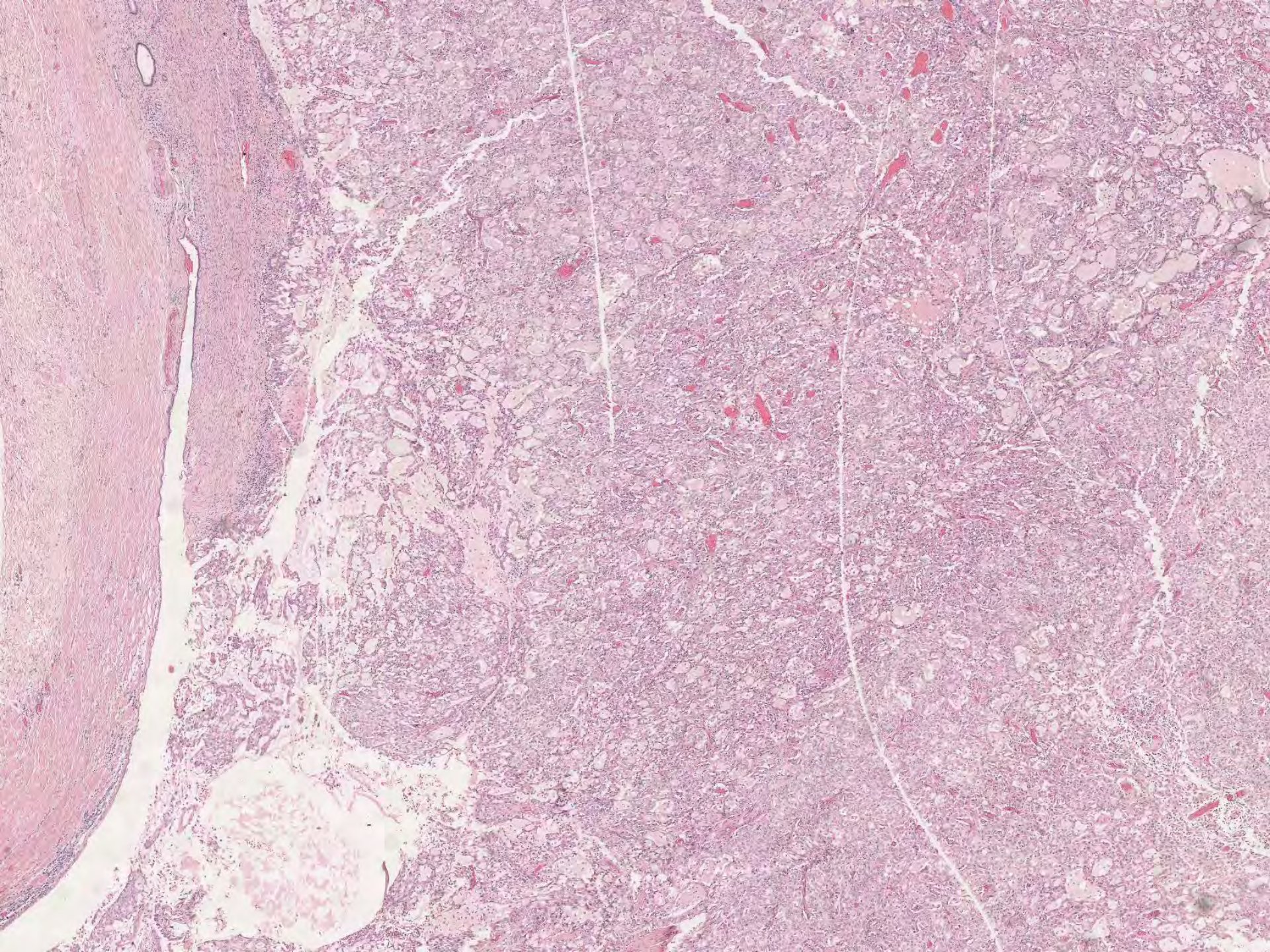

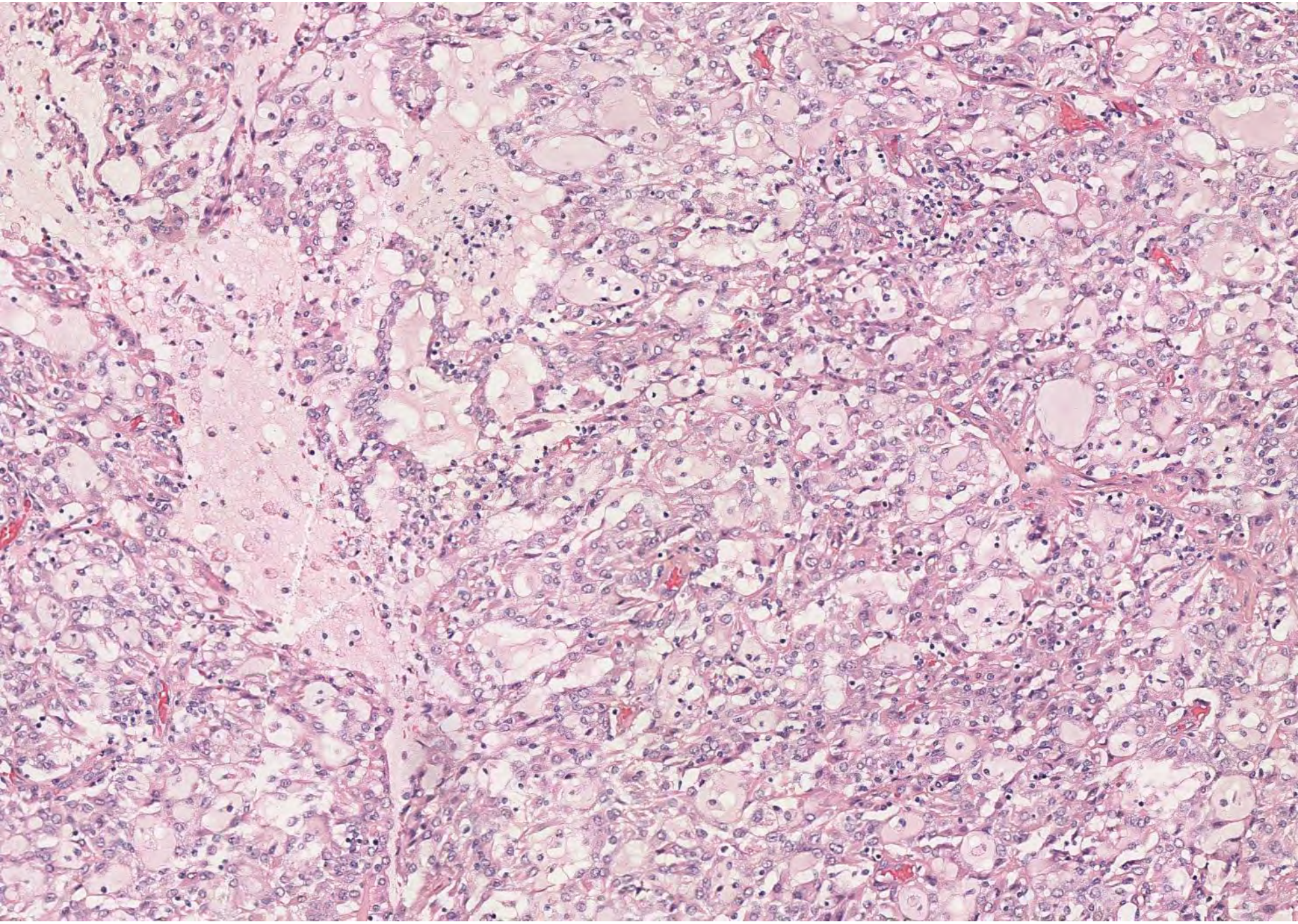

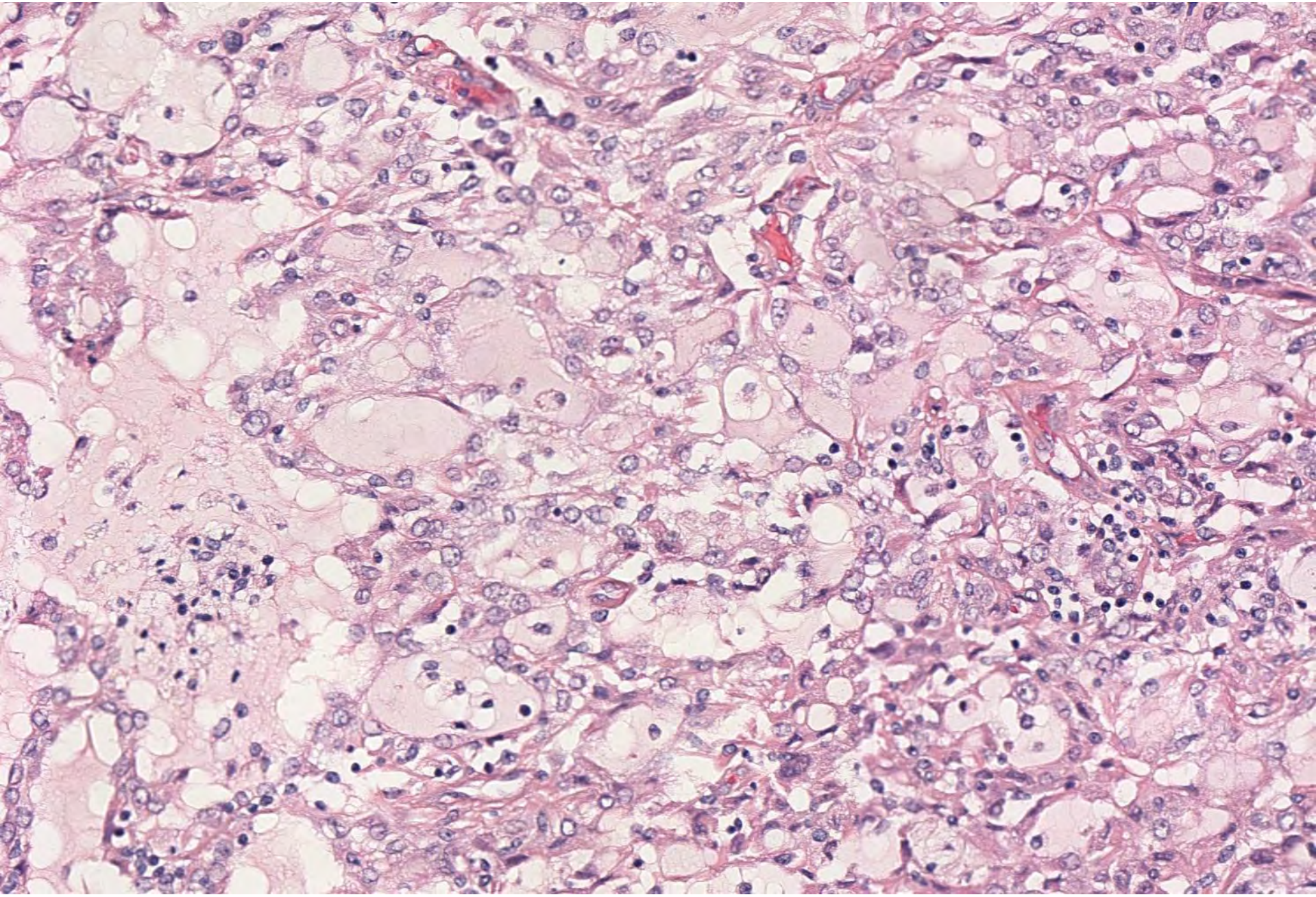

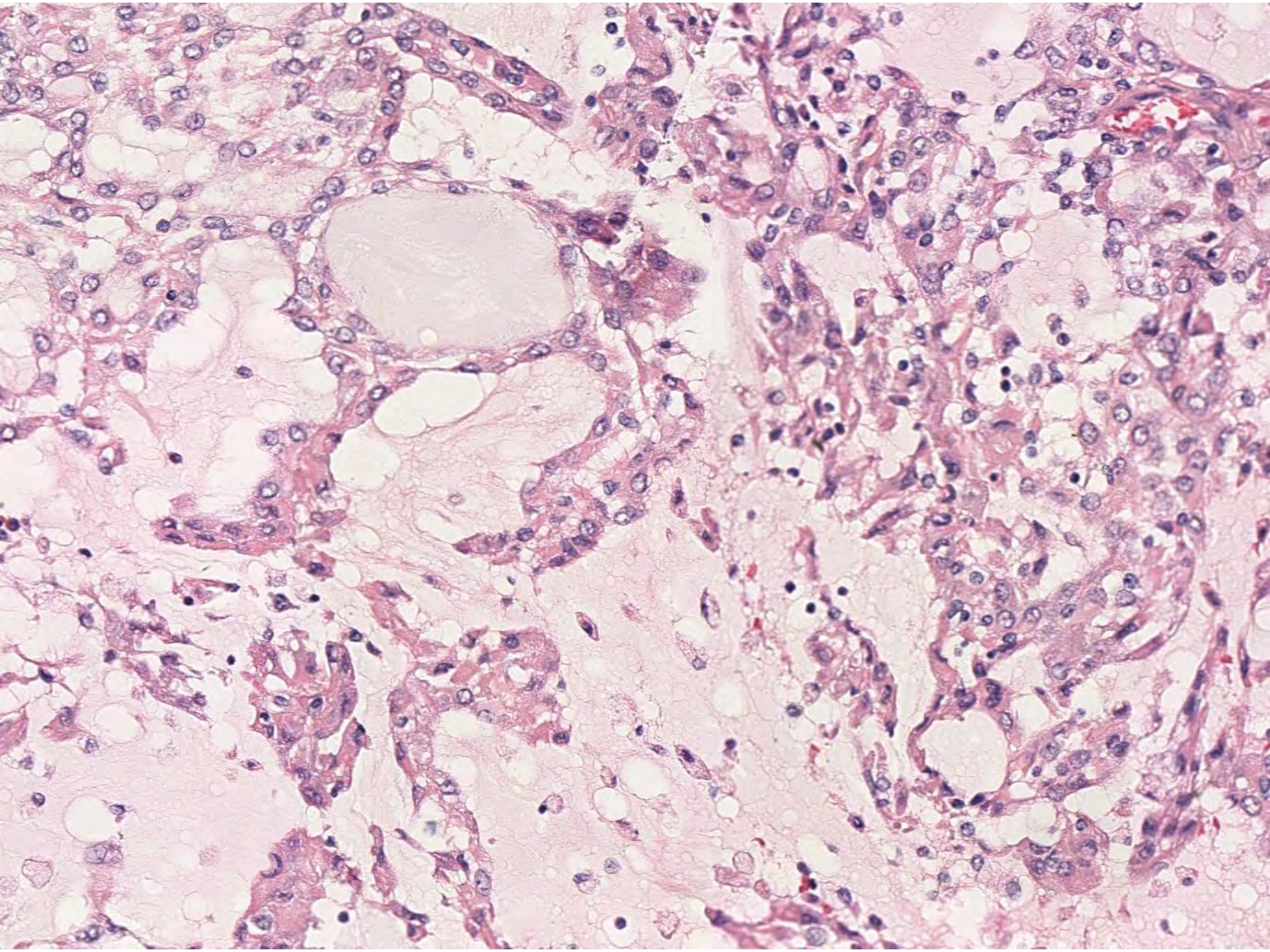

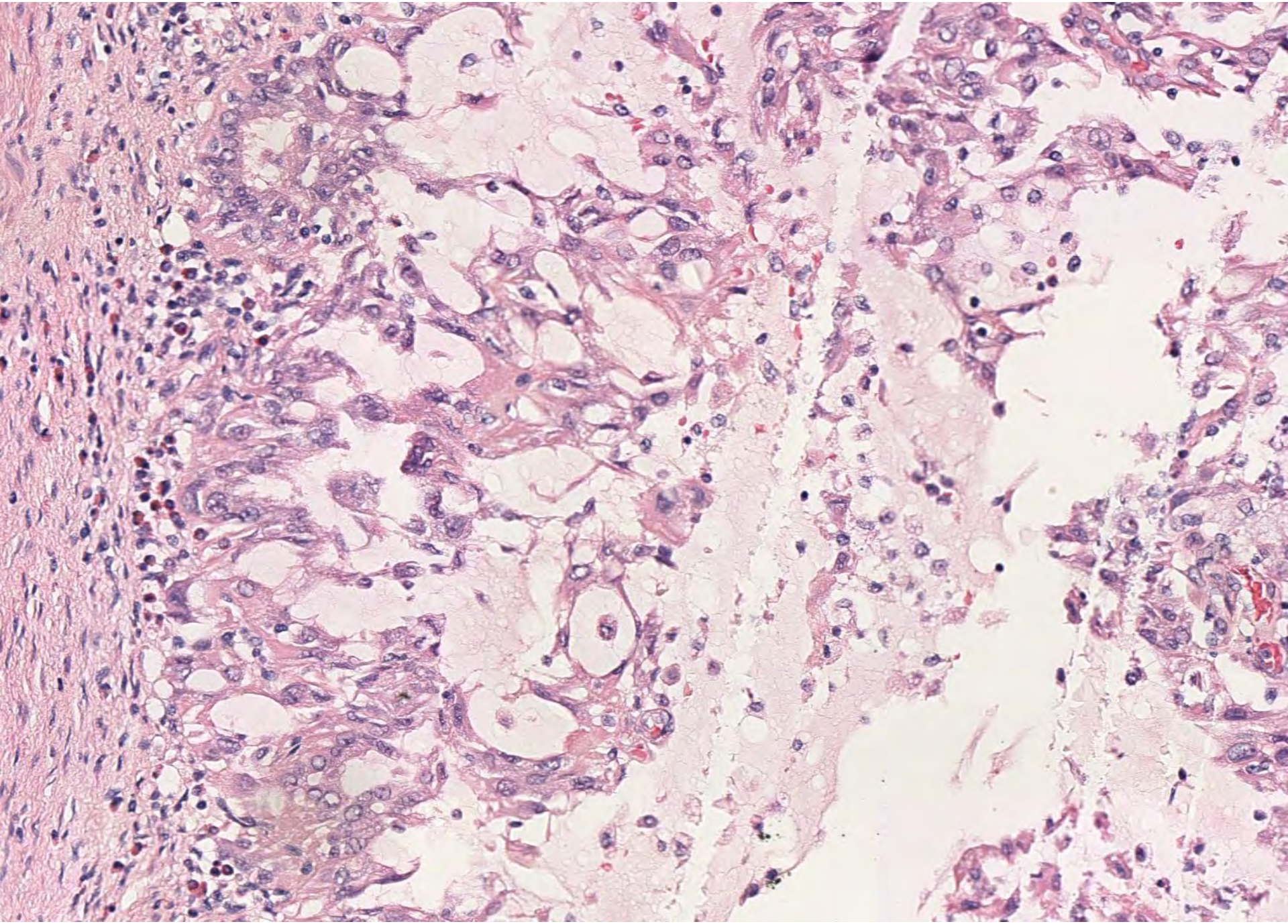

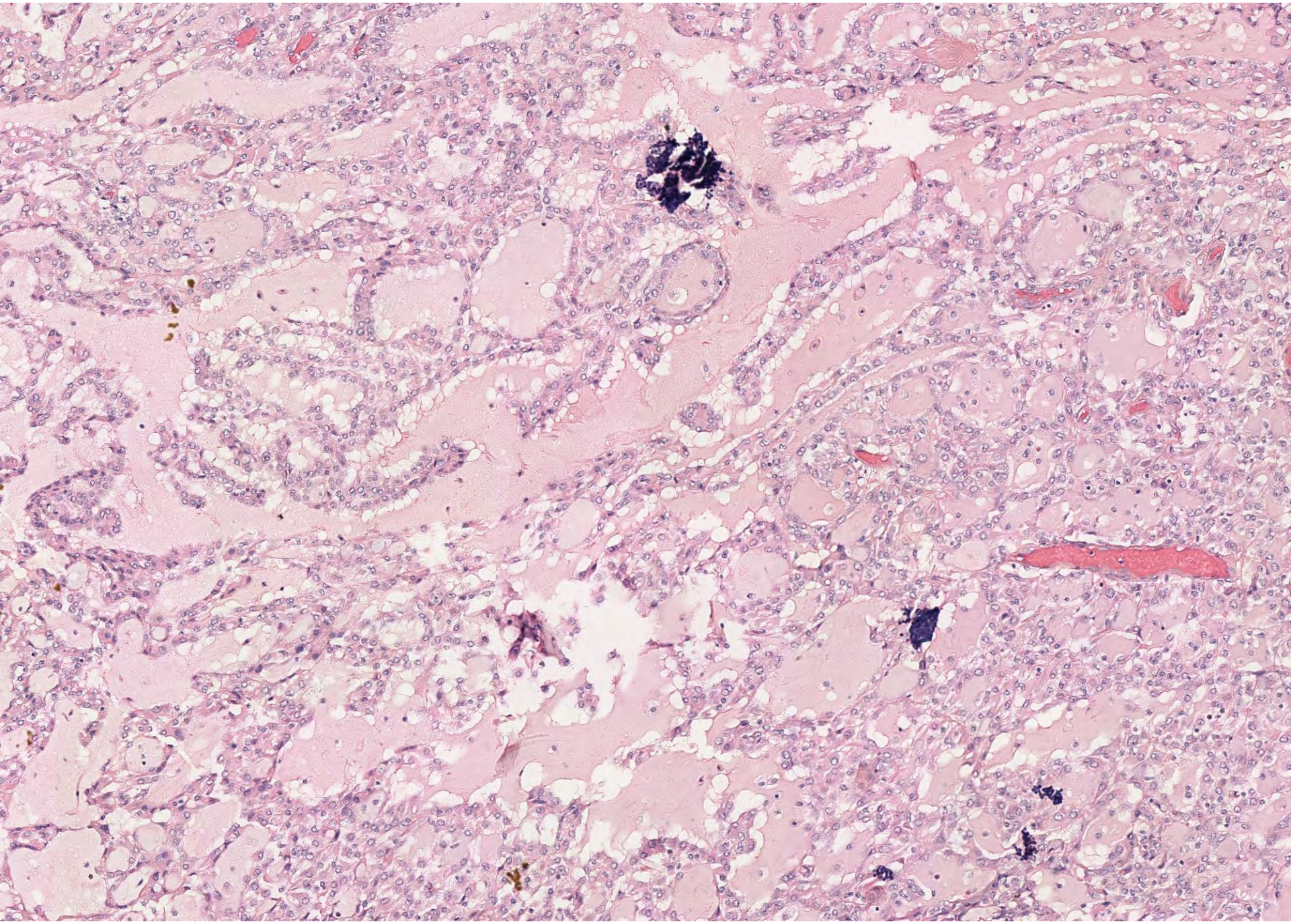

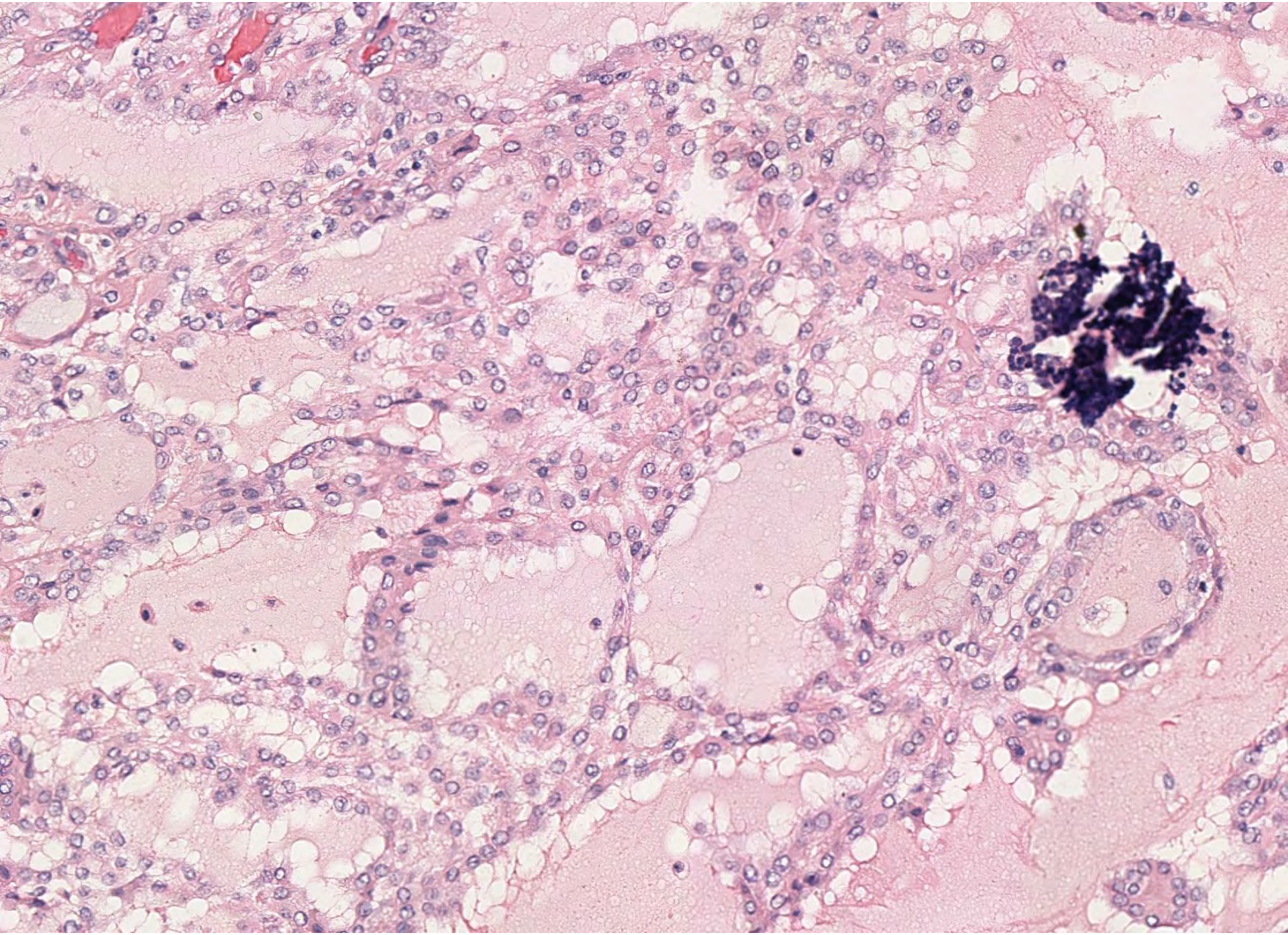

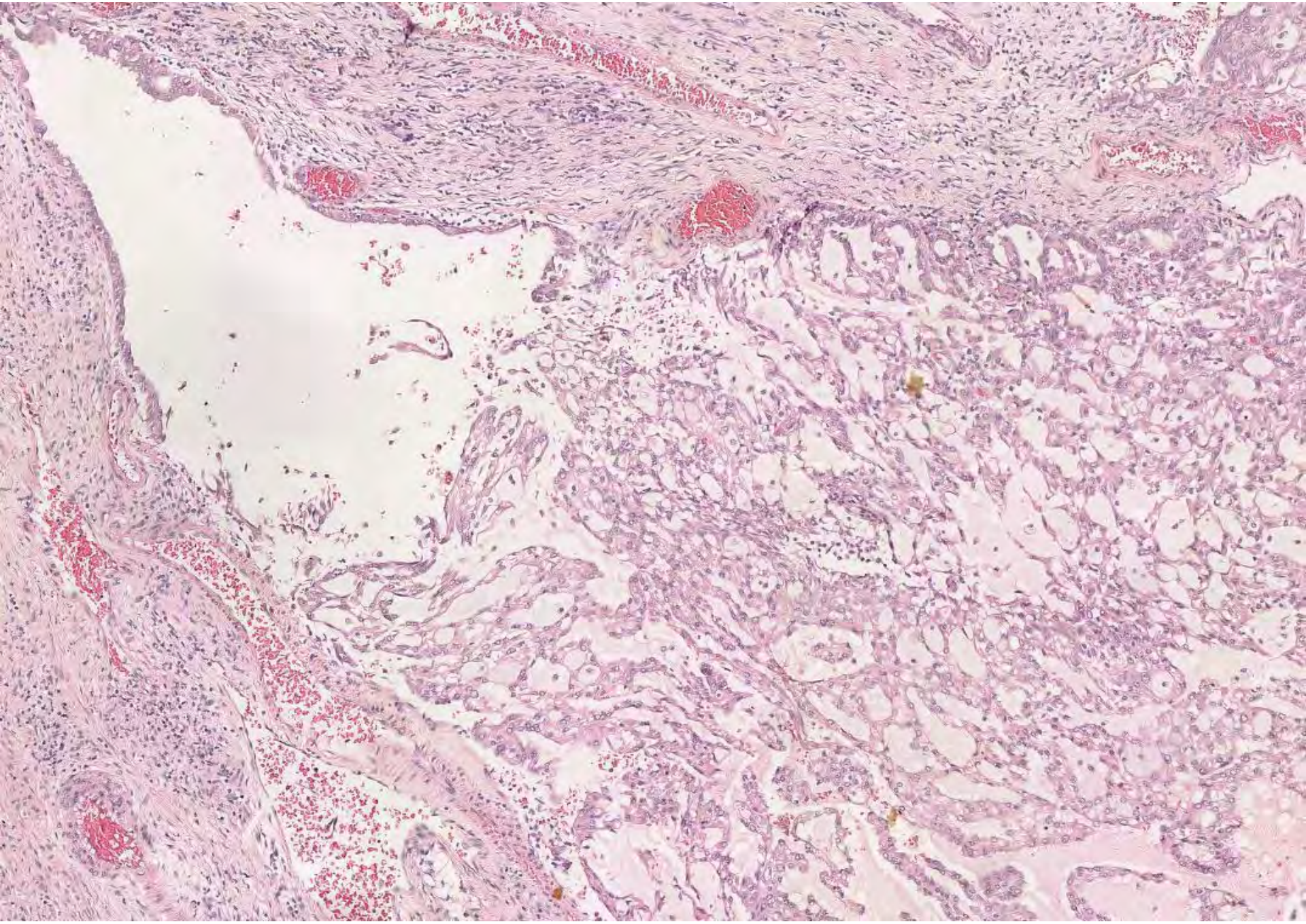

DIAGNOSIS

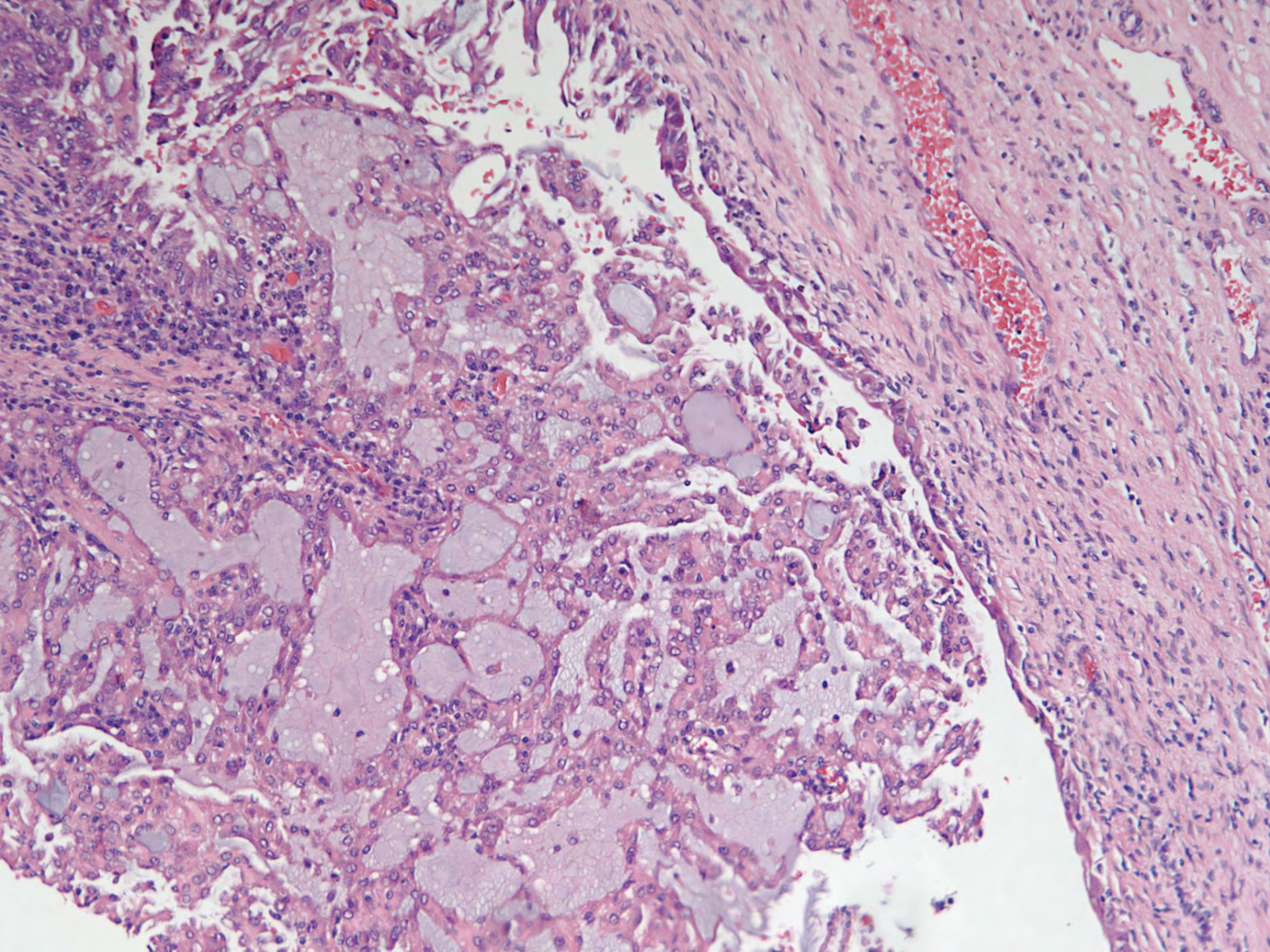

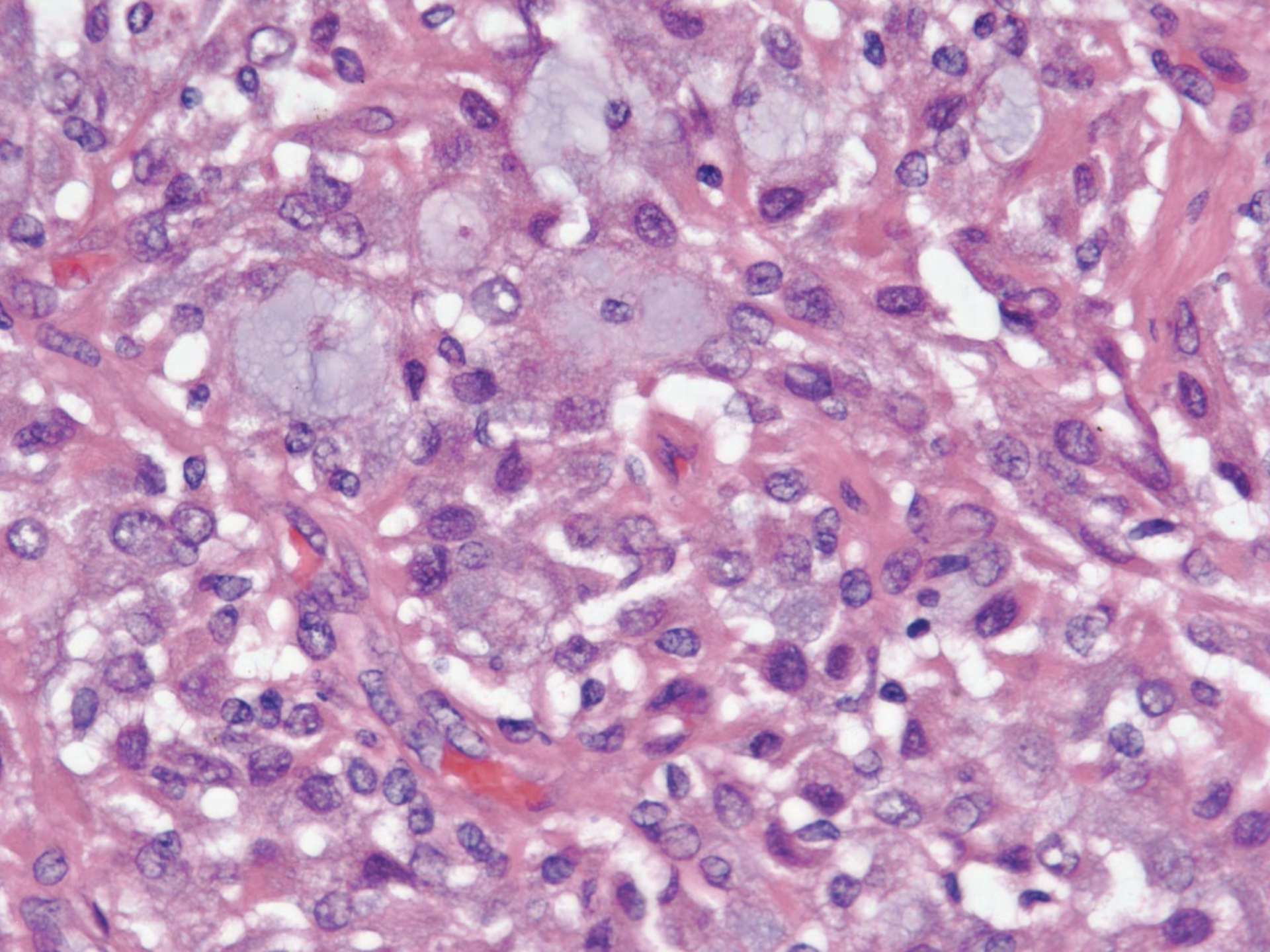

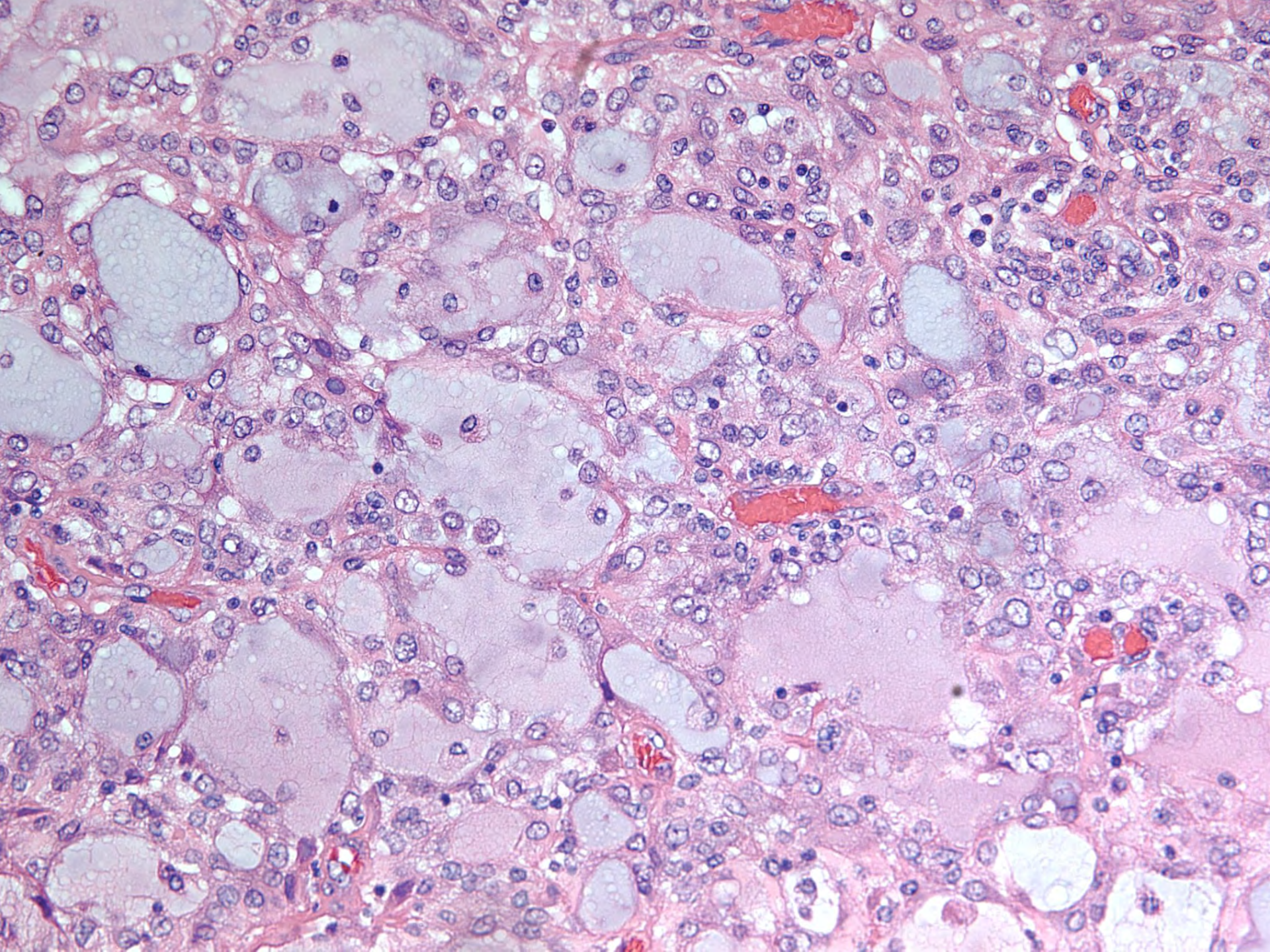

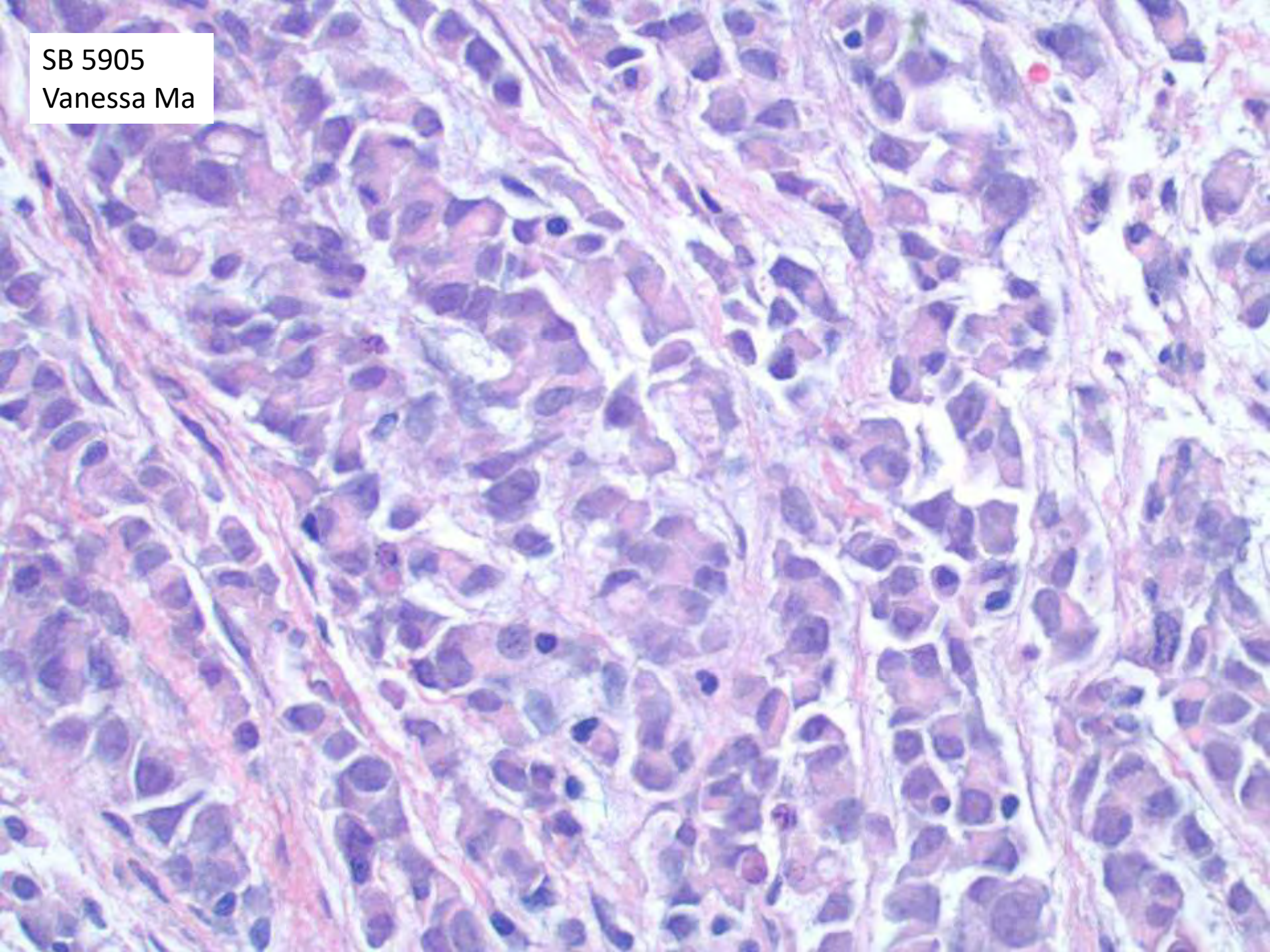
SB 5905
Vanessa Ma

Immunostains

- Positive
  - CK7 (patchy)
  - CK19
  - PAX8
  - INI-1 (retained)
- Negative
  - CK20
  - p63
  - AMACR
  - HMB45
  - MelanA

Renal cell carcinoma with novel VCL–ALK fusion: new representative of ALK-associated tumor spectrum

Debelenko LV, Raimondi SC, Daw N, Shivakumar BR, Huang D, Nelson M, Bridge JA

Mod Pathol. 2011 Mar;24(3):430-42.

- 6 pediatric patients with renal cell carcinoma
- 2 cases demonstrated structural karyotypic abnormalities involving the ALK locus on chromosomal band 2p23
- Both patients were African Americans with sickle cell trait

VCL-ALK Renal Cell Carcinoma in Children With Sickle-cell Trait: The Eighth Sickle-cell Nephropathy?

Nathaniel E. Smith, MD , Andrea T. Deyrup, MD, PhD, Adrian Marinño-Enriquez, MD, Jonathan A. Fletcher, MD, PhD, Julia A. Bridge, MD, Peter B. Illei, MD , George J. Netto, MD, and Pedram Argani, MD

Am J Surg Pathol. 2014 June ; 38(6): 858–863.

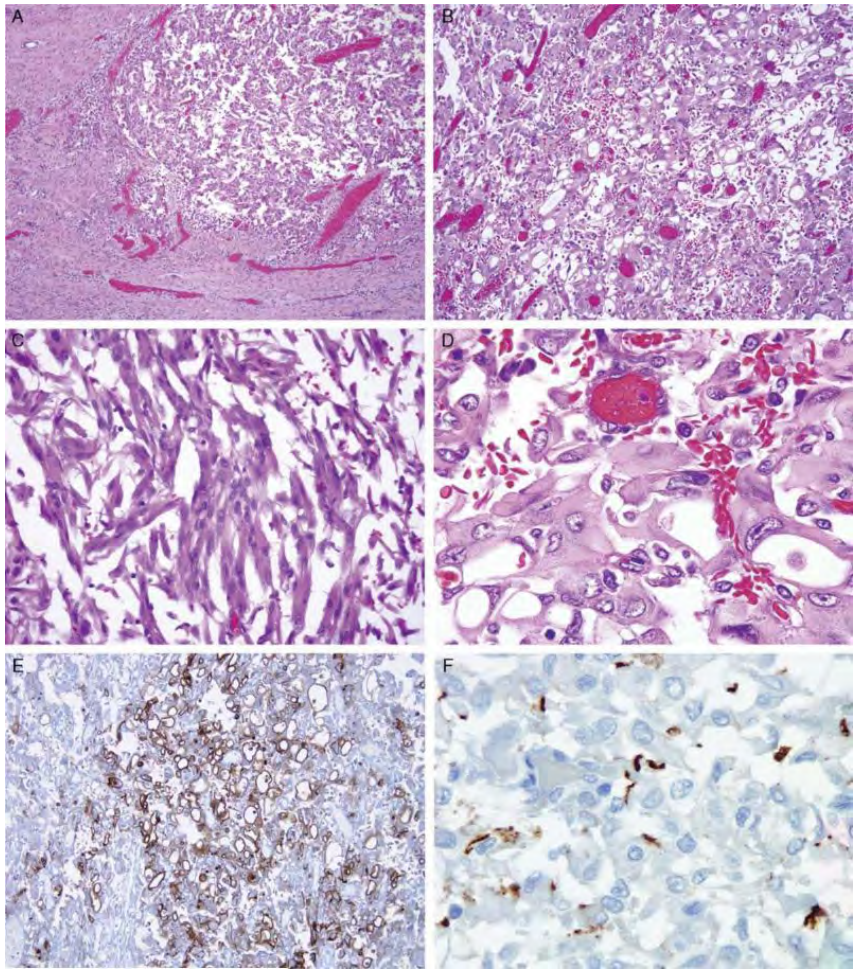

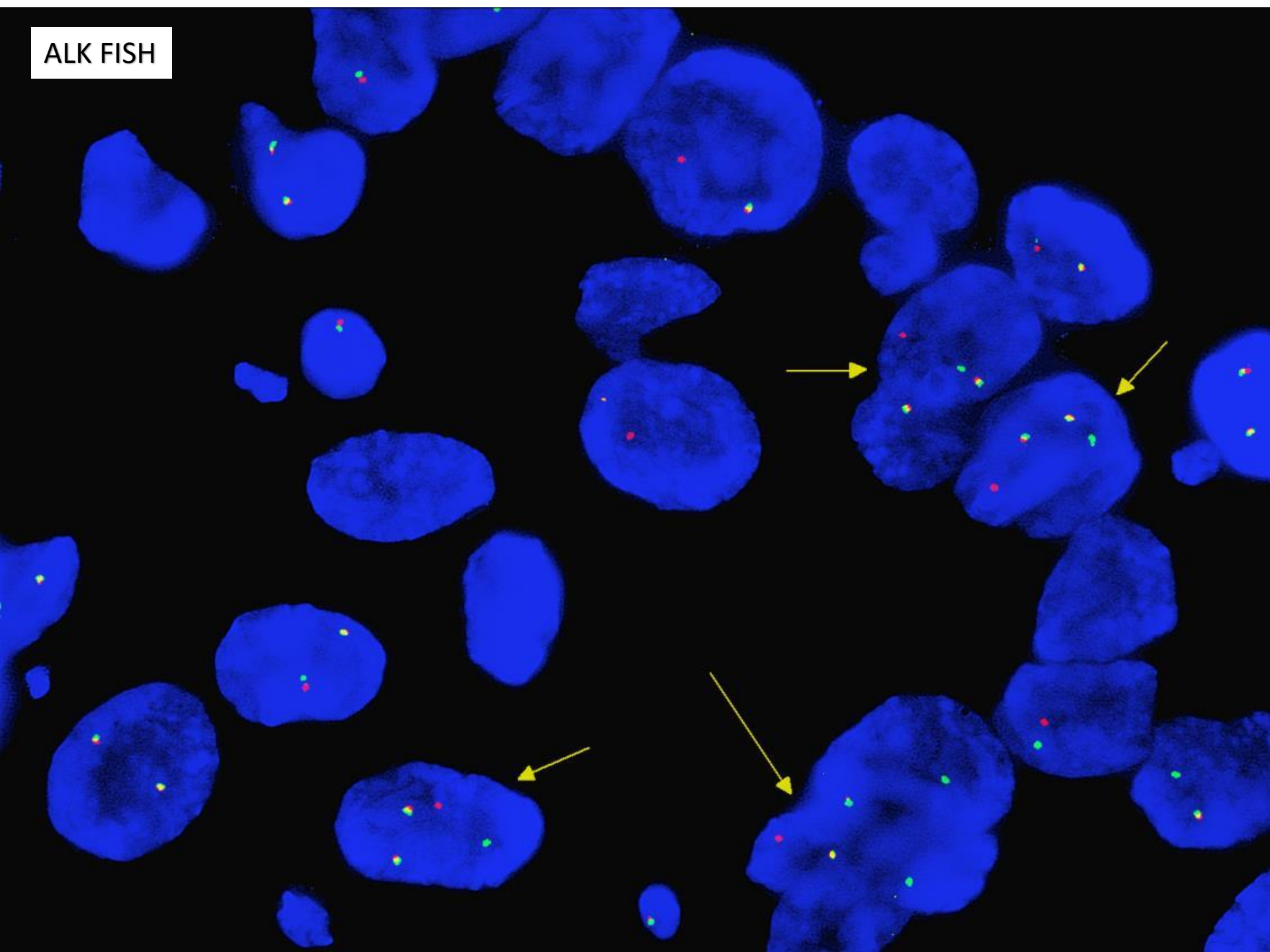
ALK FISH

Diagnosis:
Renal cell carcinoma with ALK gene rearrangement

The classification of pediatric and young adult renal cell carcinomas registered on the children's oncology group (COG) protocol AREN03B2 after focused genetic testing.

Cajaiba MM, Dyer LM, Geller JI, Jennings LJ, George D, Kirschmann D, Rohan SM, Cost NG, Khanna G, Mullen EA, Dome JS, Fernandez CV, Perlman EJ

Cancer. 2018 Aug;124(16):3381-3389.

TABLE 1. Classification of 212 Renal Cell Carcinomas Into Distinct Histologic Subtypes, Clinical Demographics, and Stage

Diagnosis	No. of Patients (%)	Age Range [Mean], y	No. of Patients per Age Group			Sex	TNM Stage Grouping, No. of Patients				
			0-10 y	11-20 y	≥21 y		I	II	III	IV	Unknown
MiT-RCC	8 (41.5)	0.9-20 [11.6]	31	57	0	55 F, 33 M	24	3	48	13	0
Papillary RCC	35 (16.5)	2.4-28 [11.9]	17	15	3	15 F, 20 M	15	7	11	1	1
Renal medullary carcinoma	26 (12.3)	6.8-21 [13.2]	7	19	0	6 F, 20 M	2	0	2	22	0
Chromophobe RCC	14 (6.6)	13-27 [15.4]	2	11	1	7 F, 7 M	8	3	3	0	0
Clear cell RCC	7 (3.3)	13-20 [16.3]	0	7	0	5 F, 2 M	7	0	0	0	0
Fumarate hydratase-deficient RCC[a]	3 (1.4)	17-18 [17.3]	0	3	0	2 F, 1 M	0	0	2	1	0
Succinate dehydrogenase-deficient RCC[a]	1 (0.5)	19	0	1	0	M	0	0	0	1	0
Other entities[a]	22 (10.4)										
Tuberous sclerosis-associated RCC	9 (4.2)	6.2-14 [10.1]	5	4	0	3 F, 6 M	6	3	0	0	0
ALK-rearranged RCC	8 (3.8)	3.8-16 [11.8]	3	5	0	1 F, 7 M	2	0	5	1	0
Thyroid-like RCC	3 (1.4)	5.3-14 [10.4]	1	2	0	2 F, 1M	2	1	0	0	0
Myoepithelial carcinoma	2 (0.9)	2-4 [3]	2	0	0	2 F	0	0	0	1	0
Unclassified[a]	16 (7.5)	2.4-19 [11.5]	6	10	0	9 F, 7 M	4	4	2	5	1

Abbreviations: *ALK*, anaplastic lymphoma kinase; F, female; M, male; MiT-RCC, renal cell carcinoma with translocations involving members of the microphthalmia transcription factor (MiT); RCC, renal cell carcinoma; TNM, tumor, lymph node, metastasis

[a] These tumors initially were classified as RCC not otherwise specified.

SB 6317
(scanned slide available)

Emily Chan/Sarah Umetsu; UCSF

37-year-old male with 2cm left upper pole renal mass.

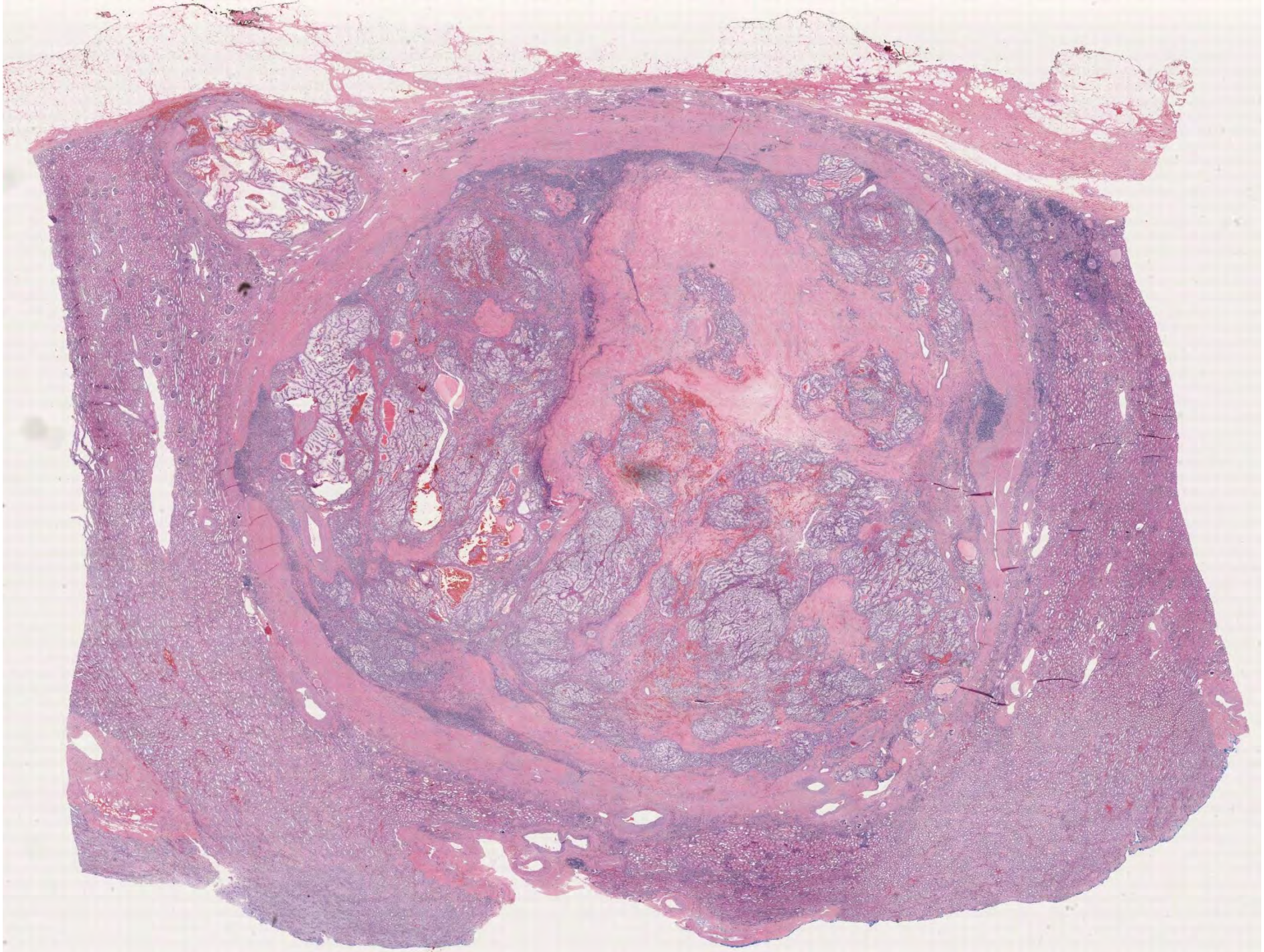

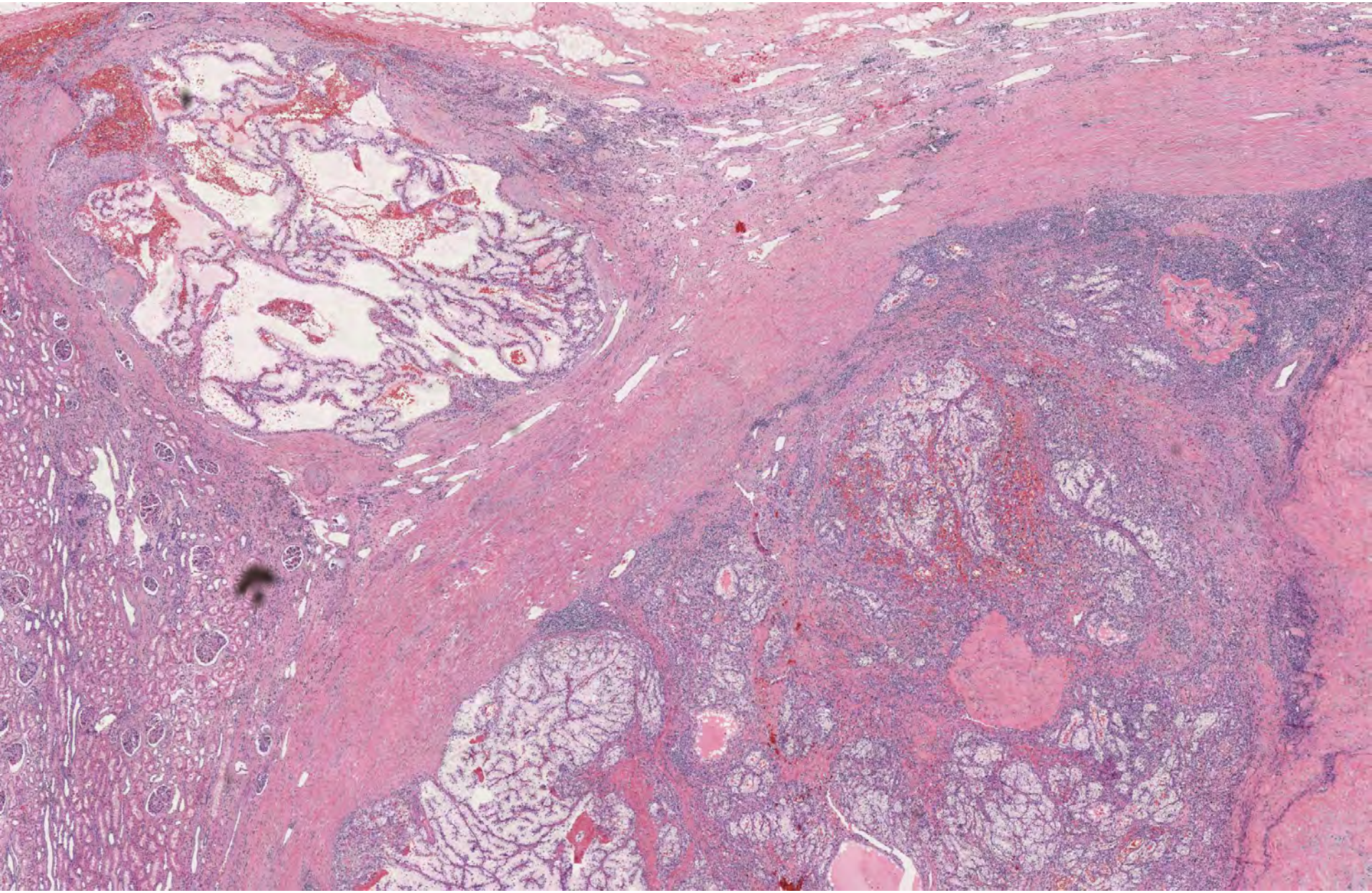

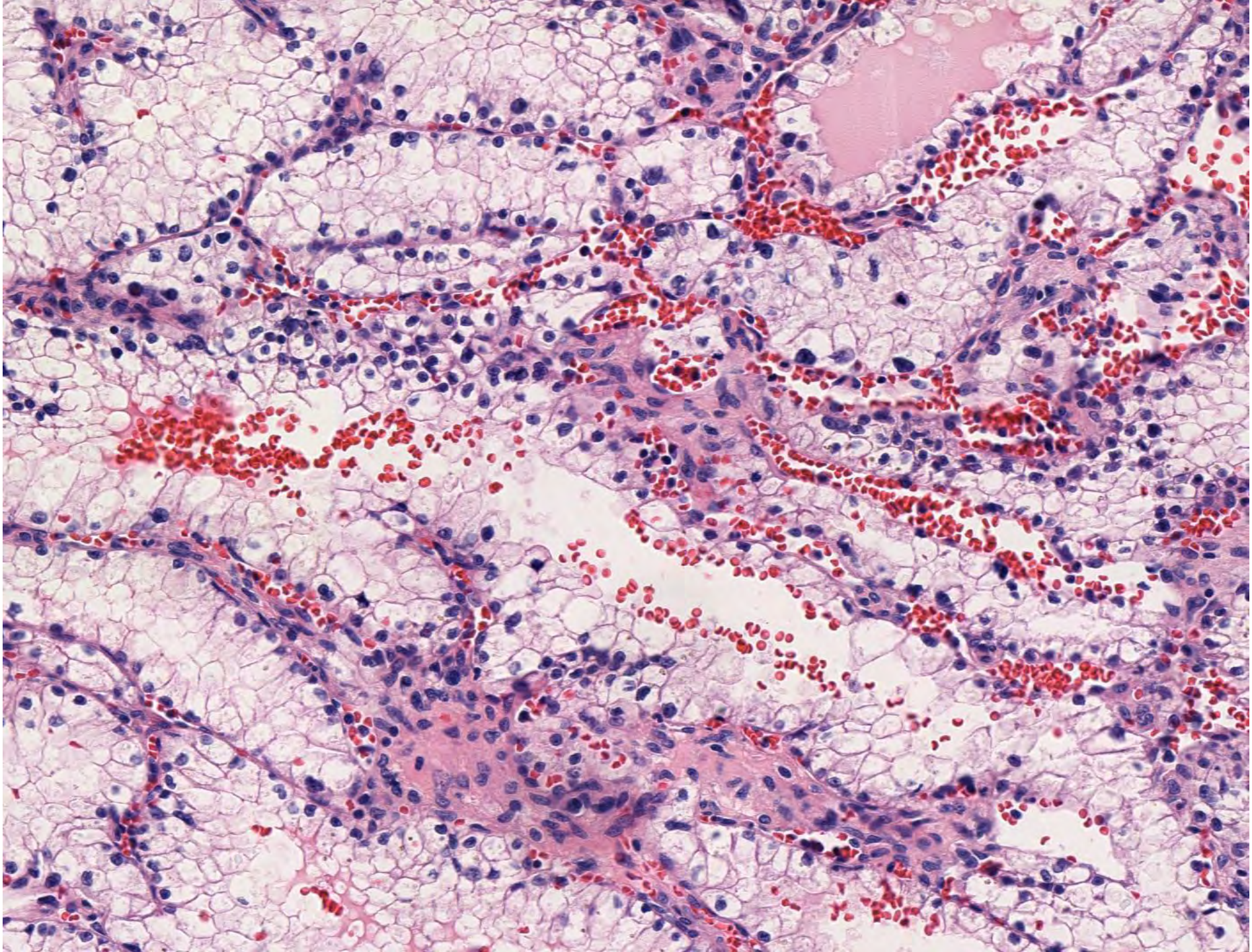

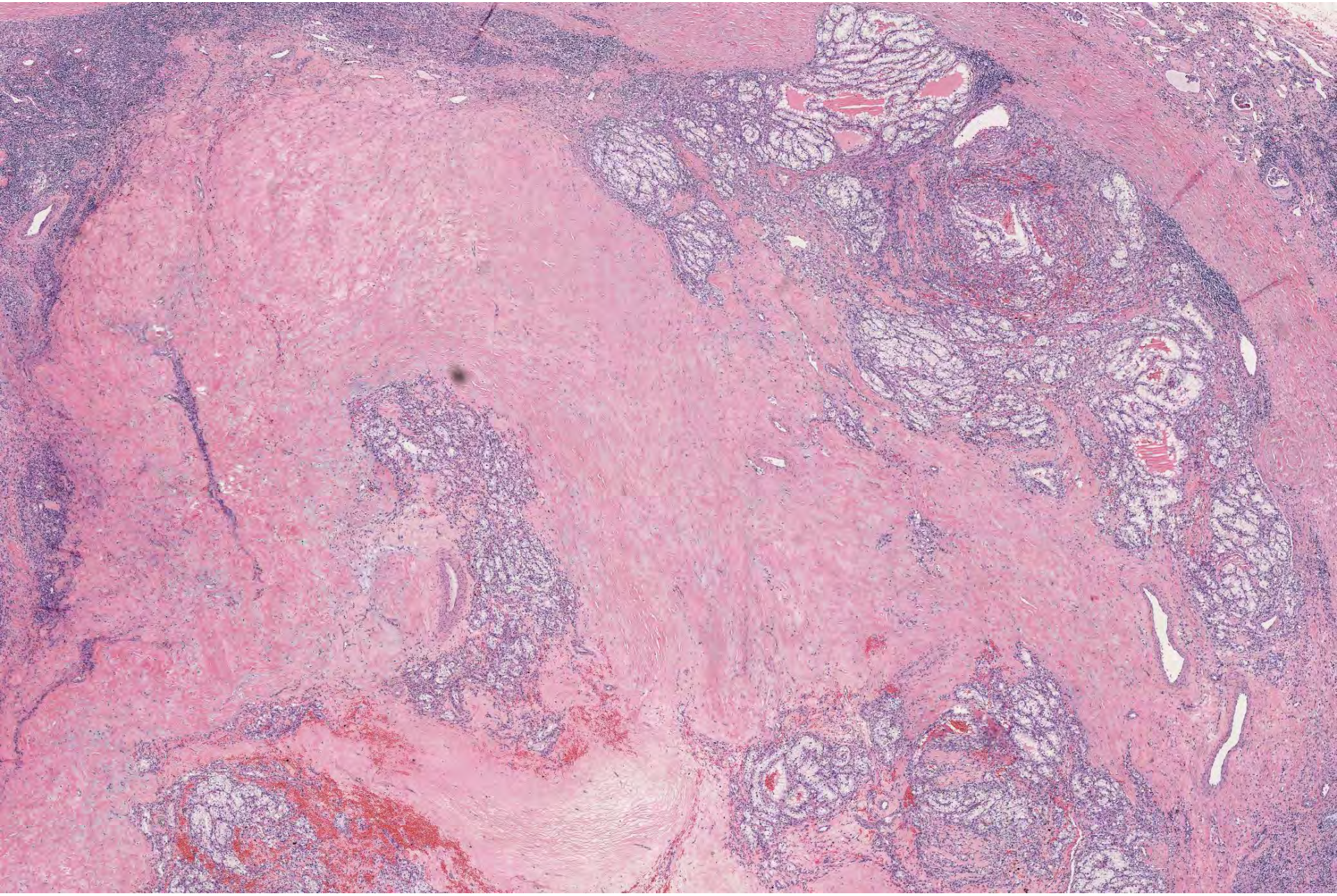

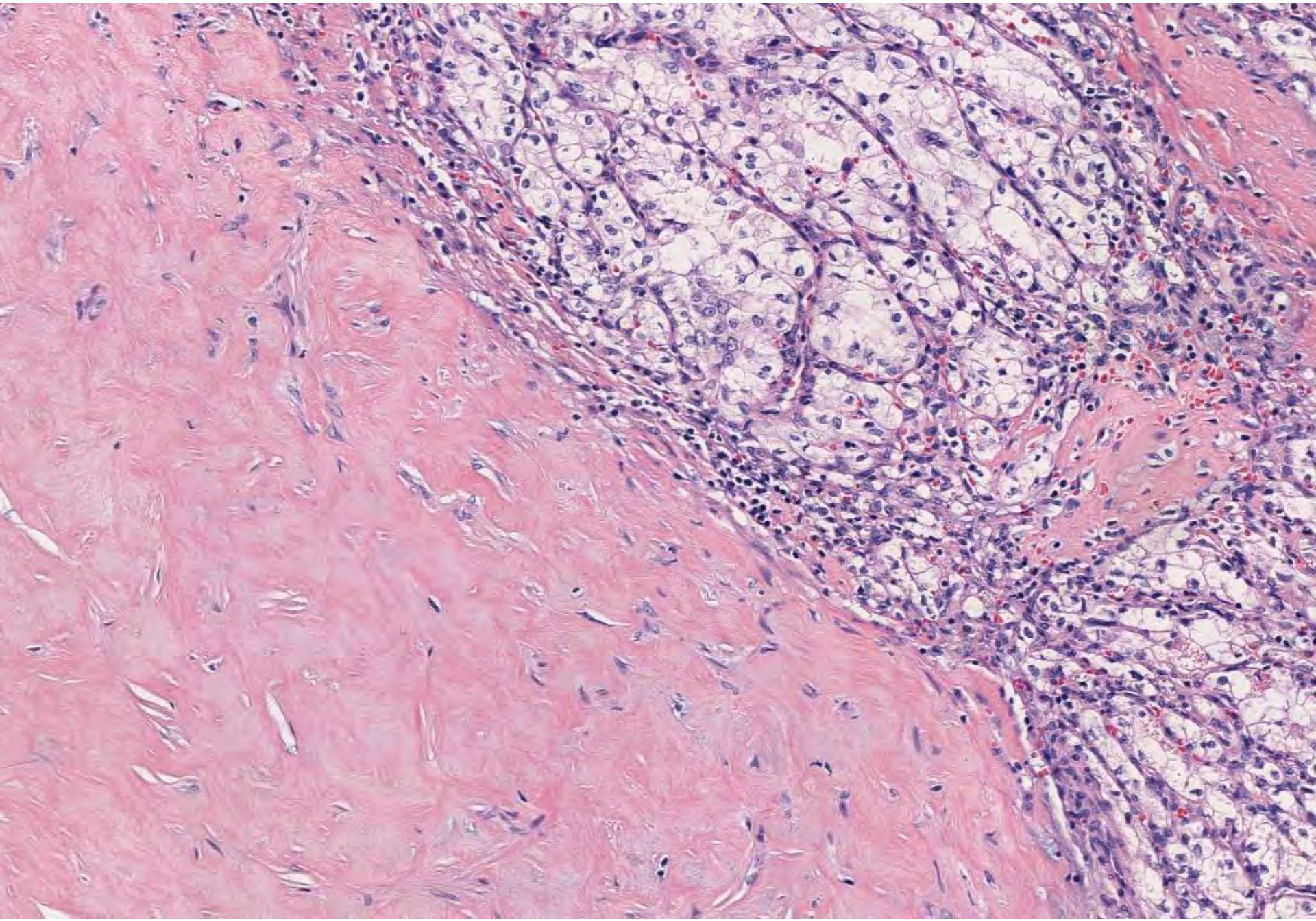

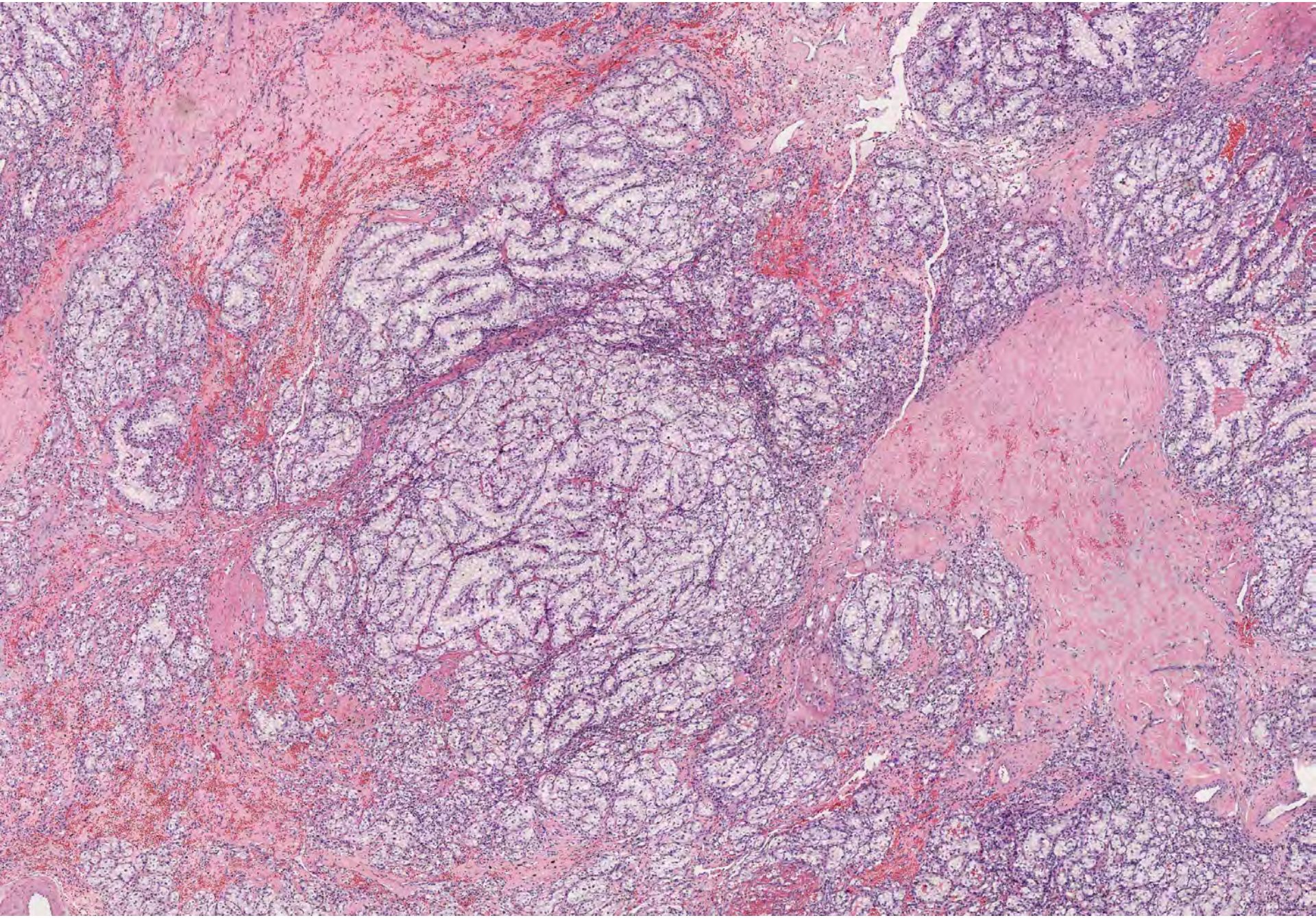

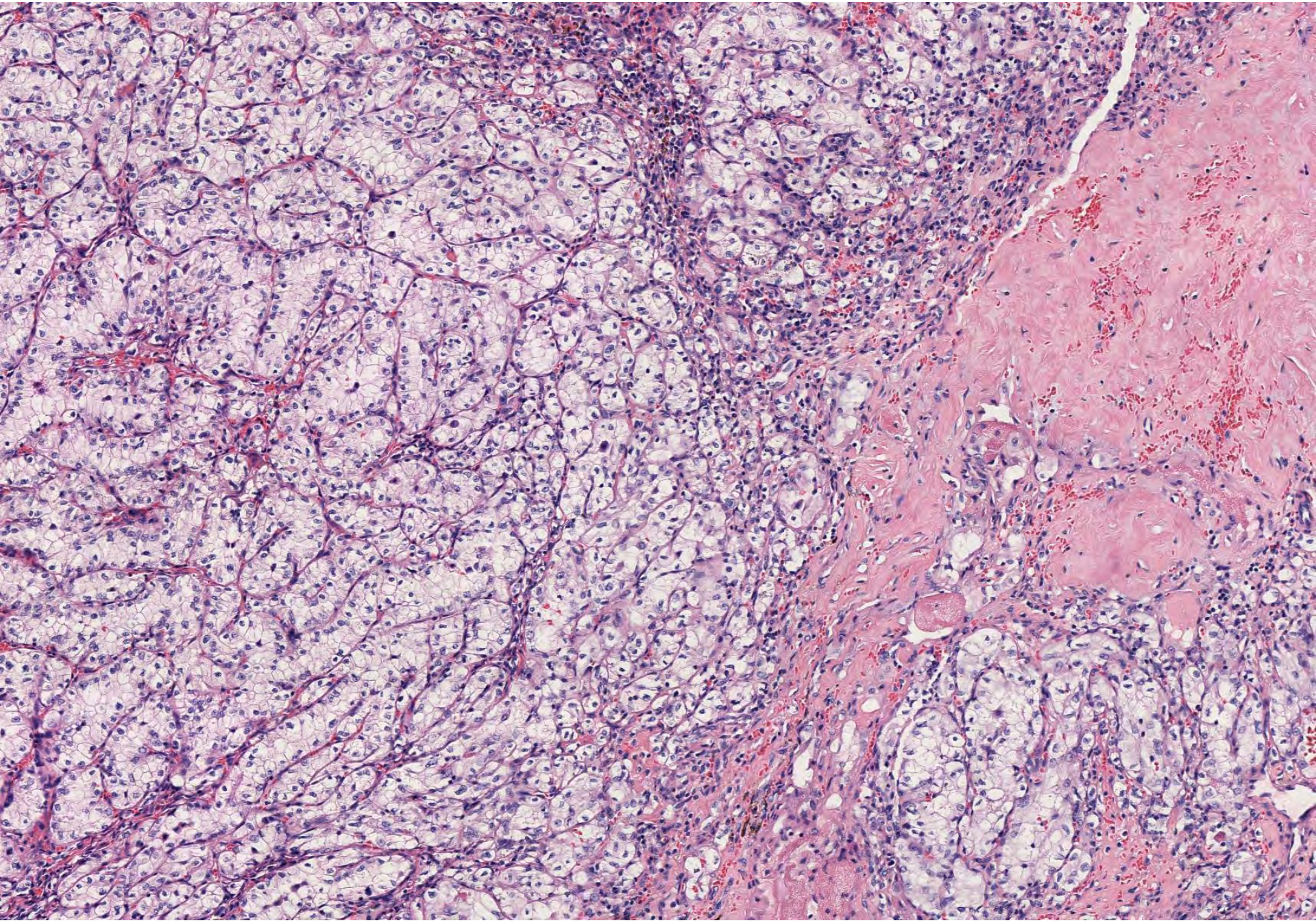

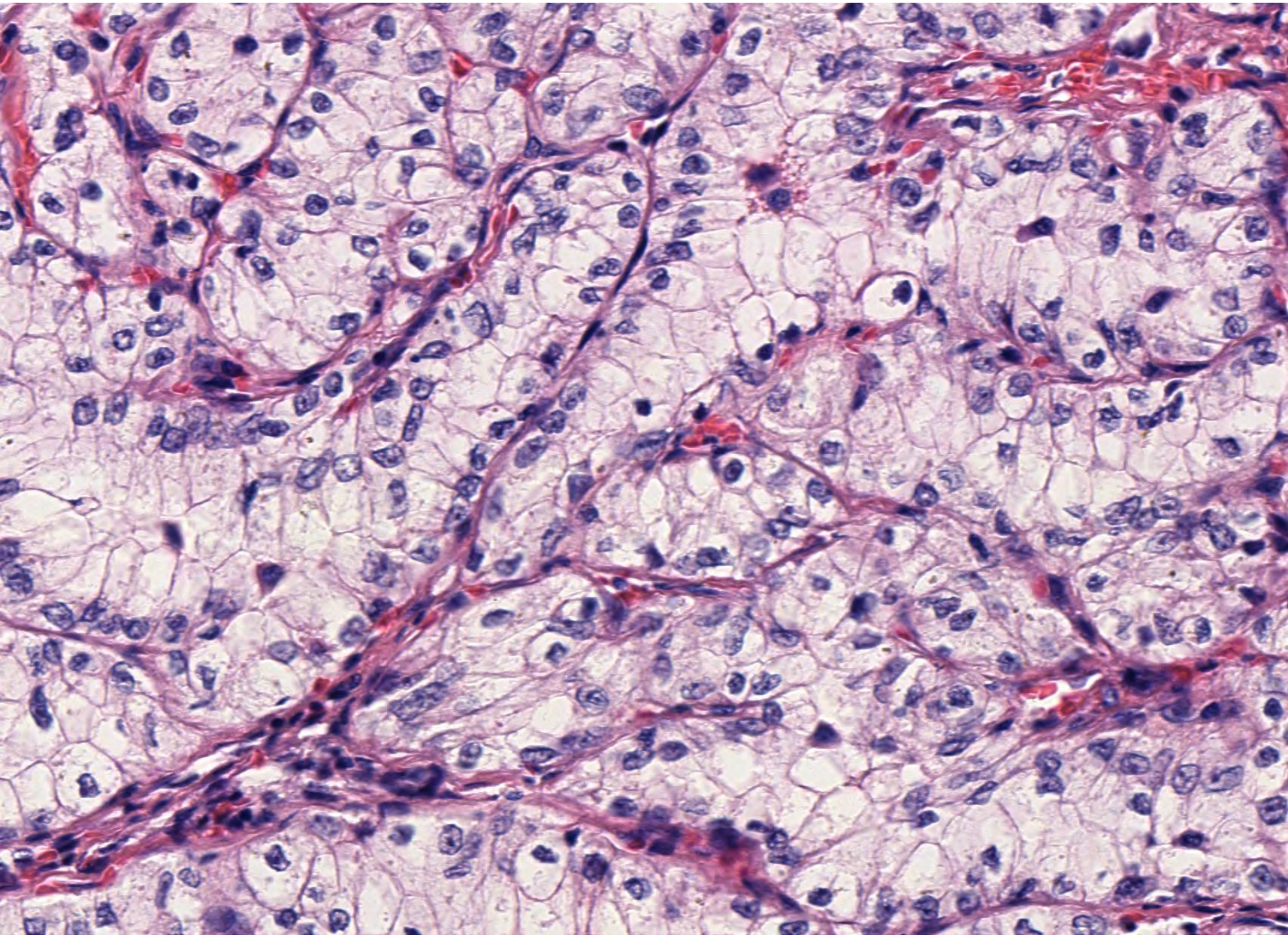

DIAGNOSIS

37-year-old man with 2 cm left upper pole renal mass

Southbay Meeting

October 2, 2018

Emily Chan/Sarah Umetsu

UCSF

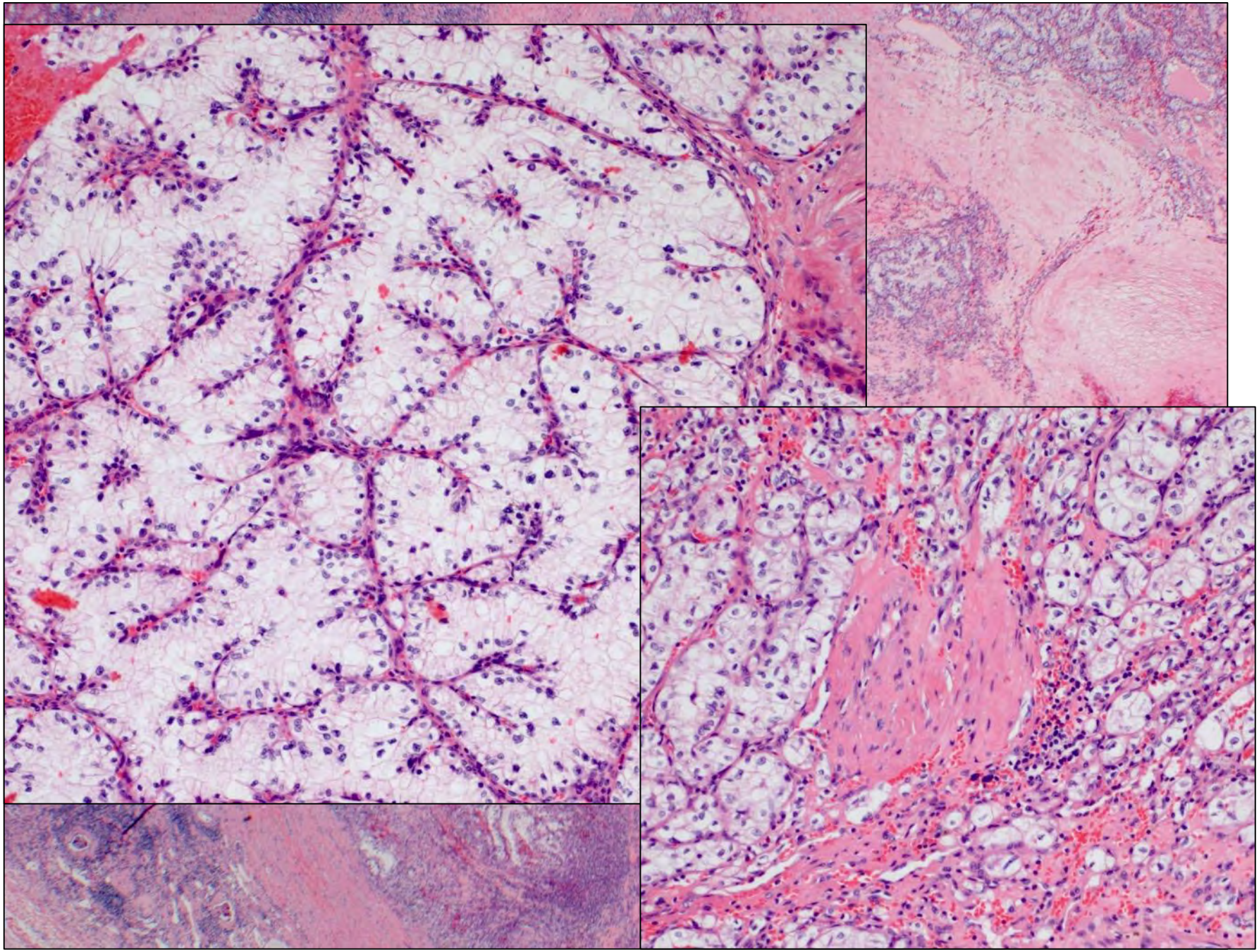

Differential diagnosis of Renal angiomyoadenomatous tumor (RAT)

- Clear cell renal cell carcinoma (ccRCC)
- Clear cell papillary RCC (ccpRCC)
- RCC, unclassified
- **RCC with angioleiomyomatous stroma**

Williamson SR et al, Modern Pathology, 2015

Renal cell carcinoma with angioleiomyomatous stroma:

- 2016 WHO emerging/provisional entity
- Encompasses (identical morphology!):
  - TSC germline associated
  - TCEB1 mutated RCC
  - ?somatic TSC mutation
- Histology: Branching tubules lined by clear to granular cells surrounded by abundant vascular and smooth muscle stroma

RCC with smooth muscle stroma in TSC

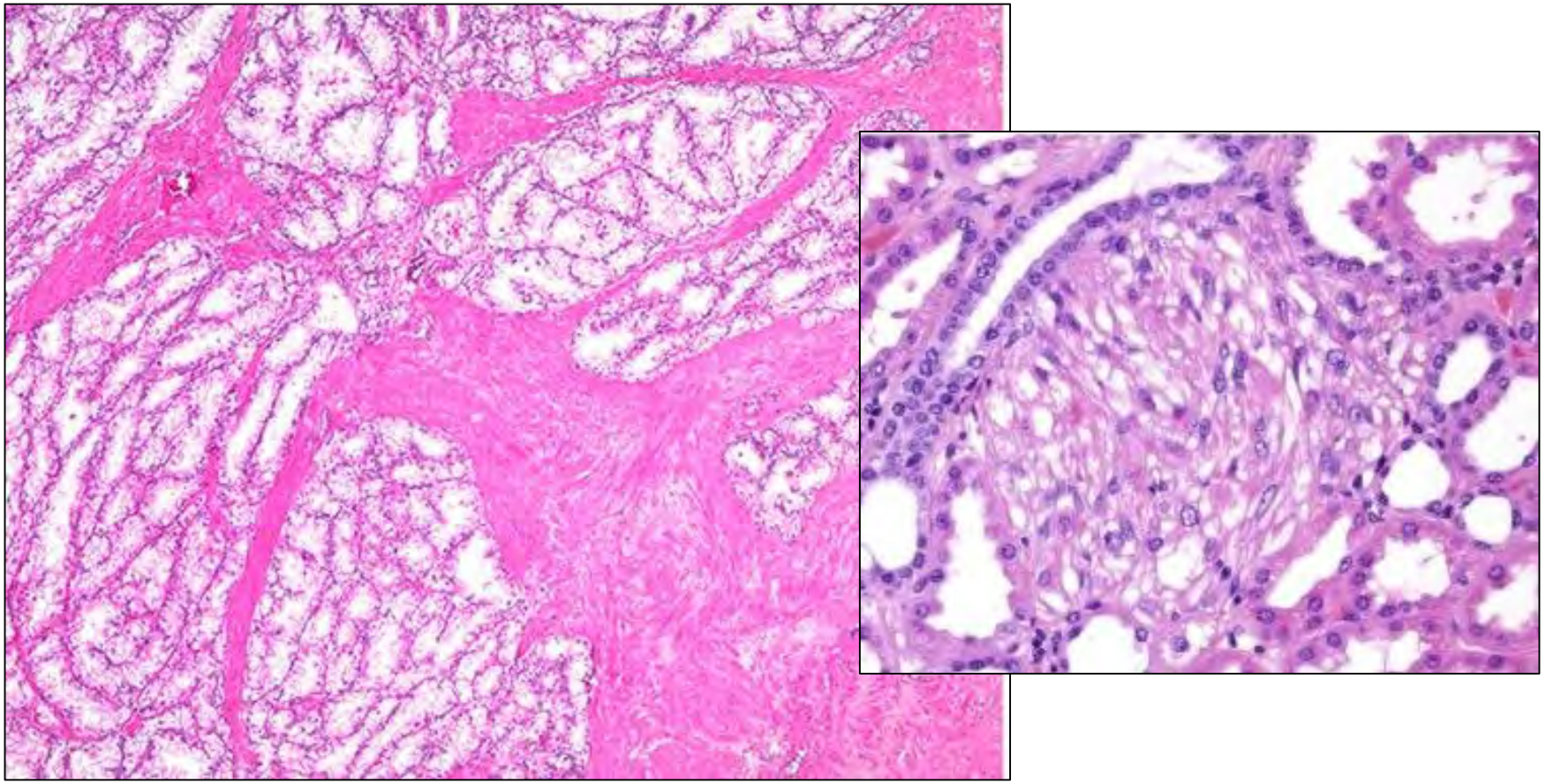

Guo et al, AJSP, 2014
Bonsib SM et al. Pathol Res Pract 2016

TCEB1 mutated RCC

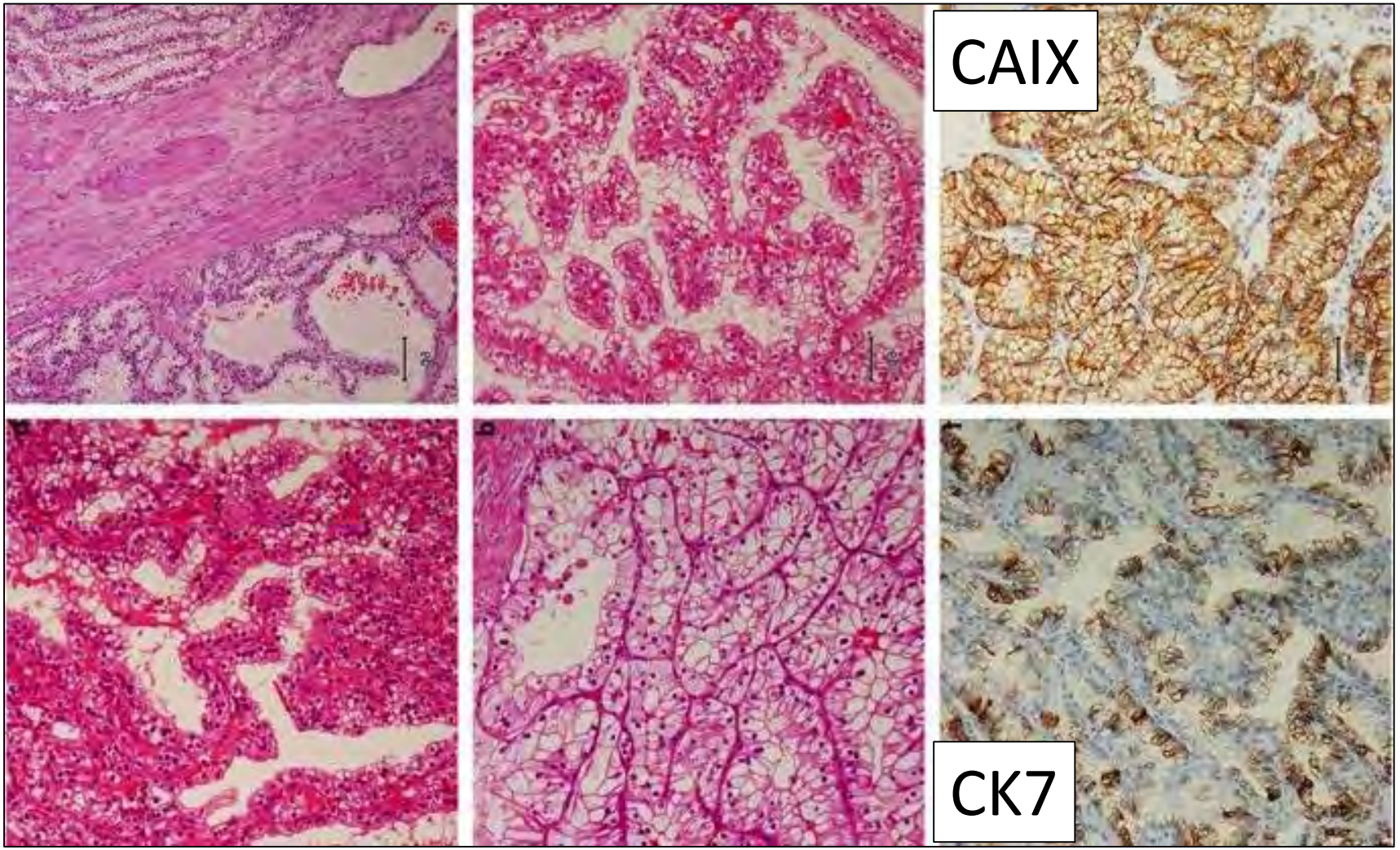

Hakimi AA et al. Mod Pathol 2015

TCEB1 (Elongin C) and VHL

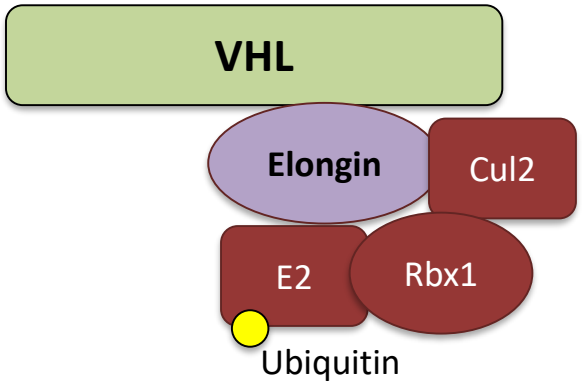

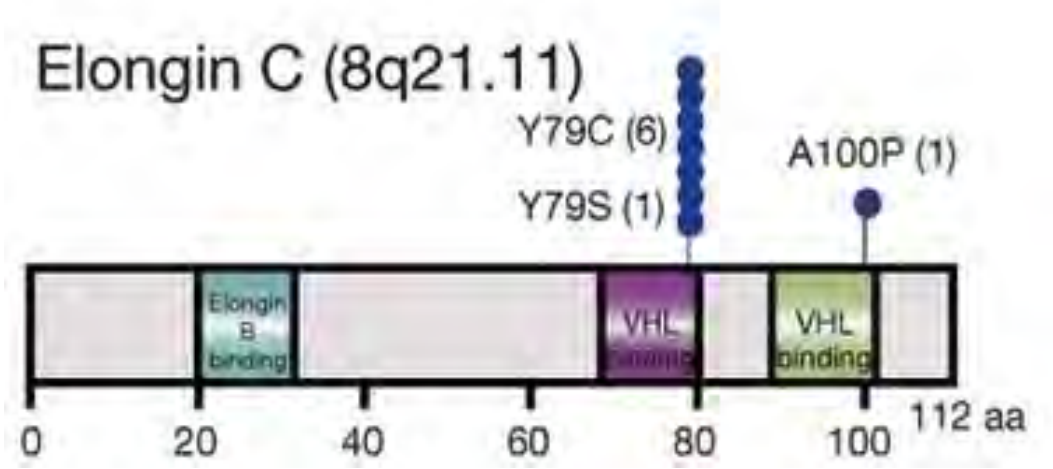

Sato et al Nature Genetics 2013

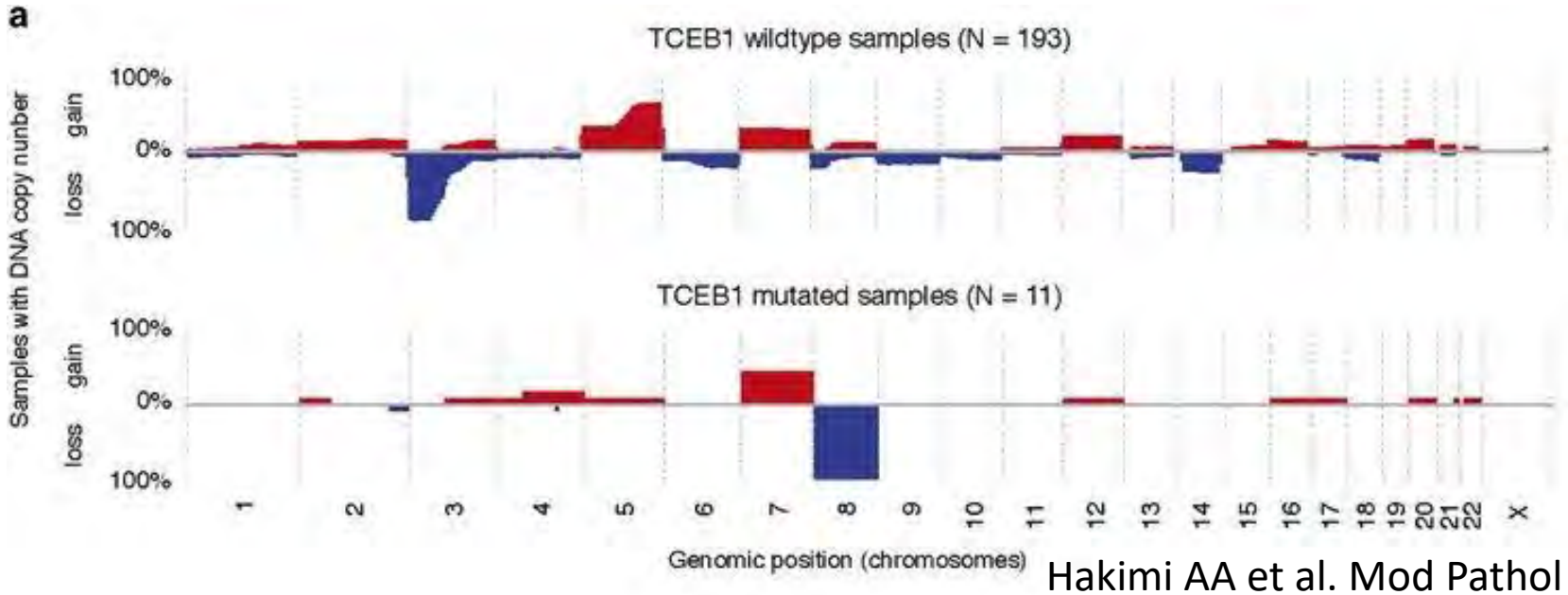

Hakimi AA et al. Mod Pathol 2015

Morphologic distinction from ccRCC and ccpRCC

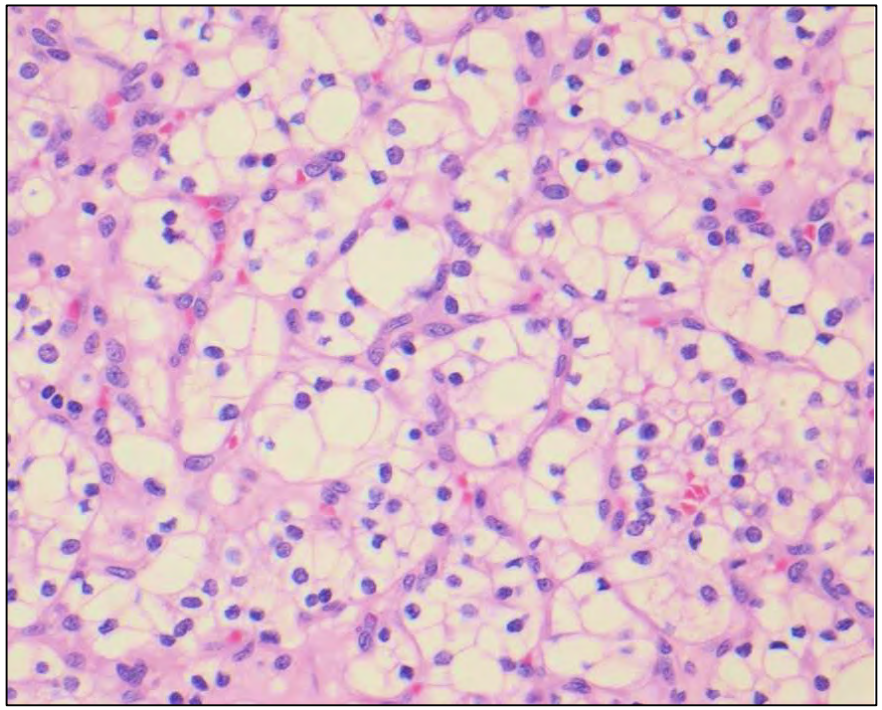

ccRCC
Small nests
Fine vascular meshwork
Loss of chromosome 3p (VHL)

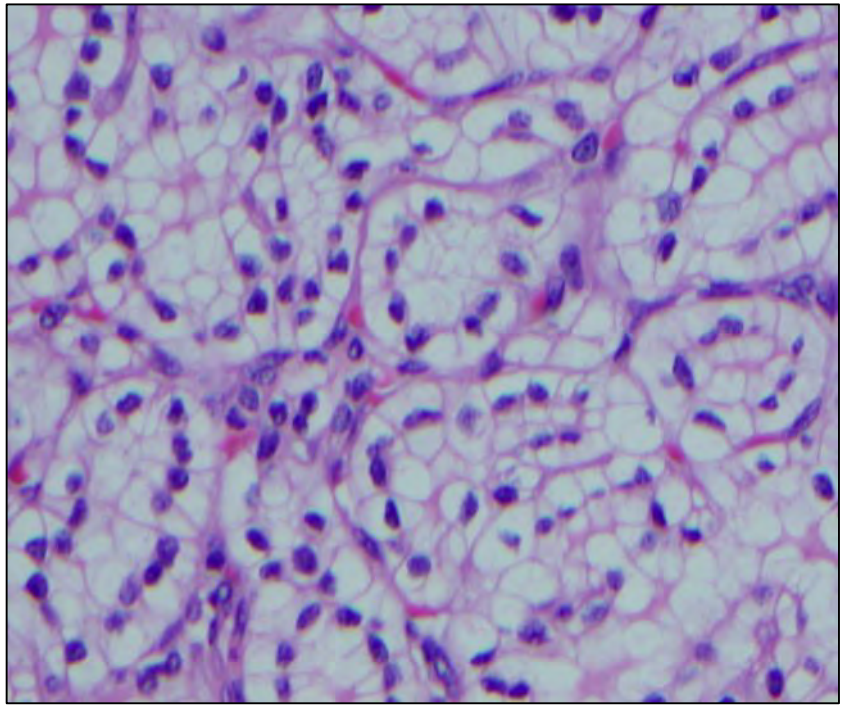

ccpRCC
Open tubules or papillary
Linear arrangement of nuclei

IHC Panel for RCC with clear cells

	CK7	CAIX	CD10	Cytogenetics
ccRCC	Neg	Pos	Pos	-3p
ccpRCC	Pos	Pos (“cuplike”)	Neg	Diploid/disomy
TCEB1 RCC	Pos	Pos	Pos	-8

Current case: IHC workup

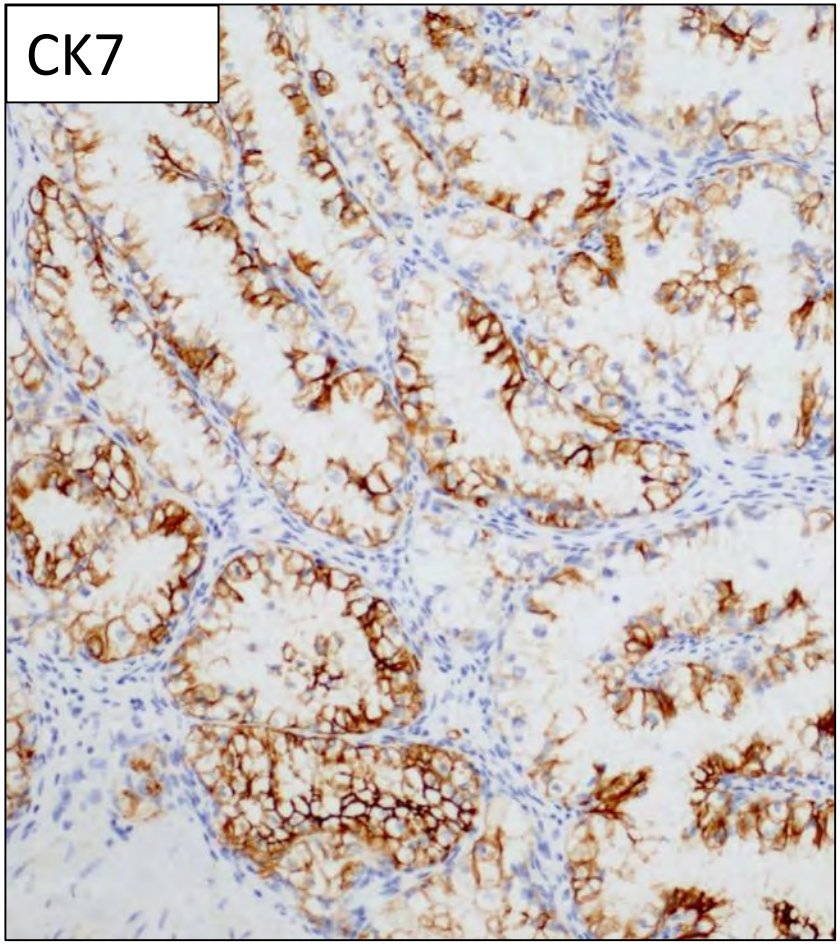

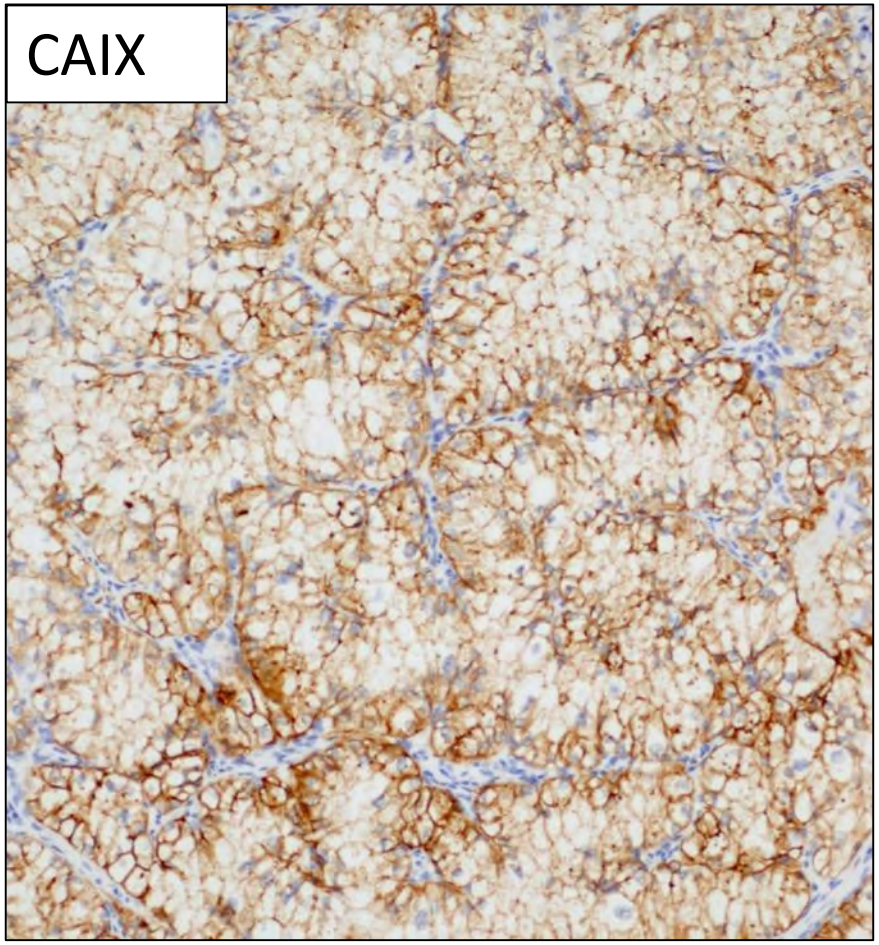

CD10 negative

Current case: Copy number and mutational analysis by UCSF500

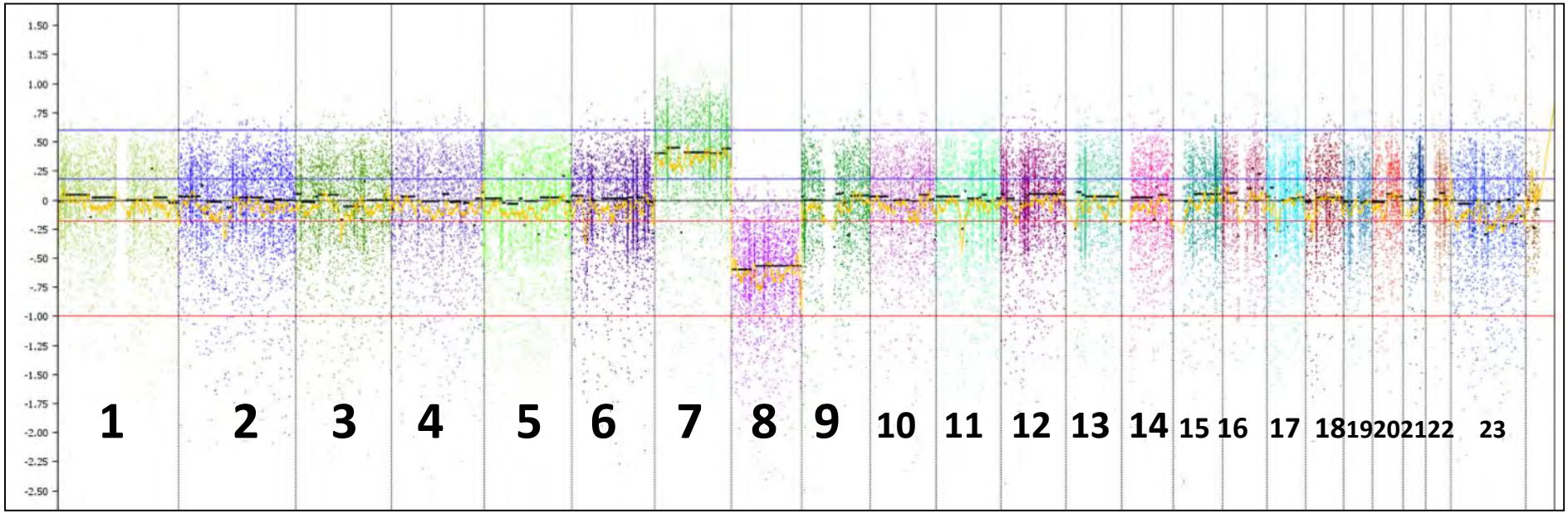

3 base pair insertion at pT78 in TCEB1

Summary

- RCCs with prominent smooth muscle stroma can be diagnosed as “RCC with angioleiomyomatous stroma”
- Morphologically, immunohistochemically, and molecularly distinct from ccRCC and ccpRCC
- If not suspecting tuberous sclerosis, can say these tumors have been shown to have underlying TCEB1 mutations and more clinically indolent than ccRCC

SB 6318
(scanned slide available)

Keith Duncan; Mills-Peninsula Hospital

70-year-old male with history of rapidly developing hand mass, now 5.7cm.

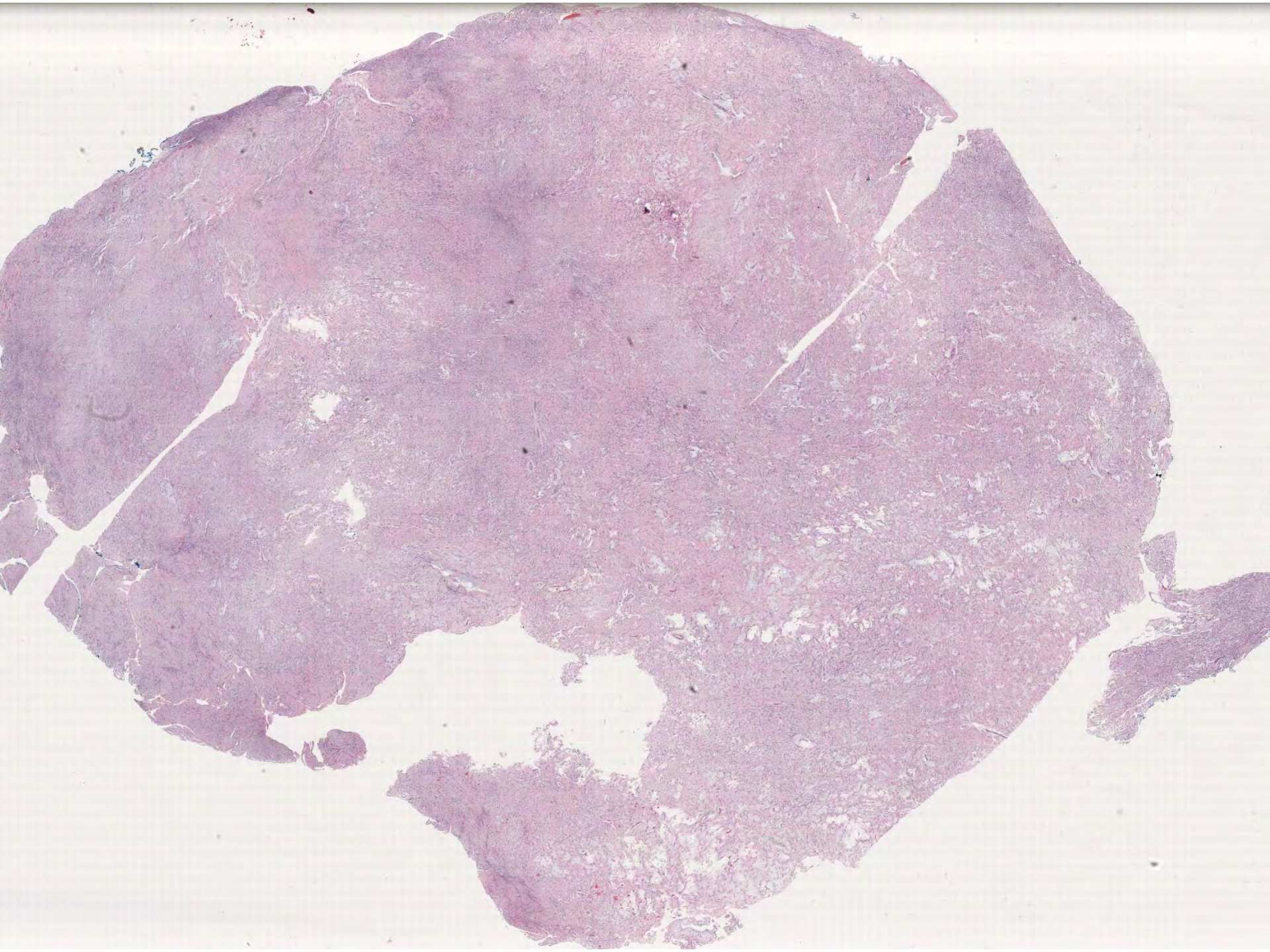

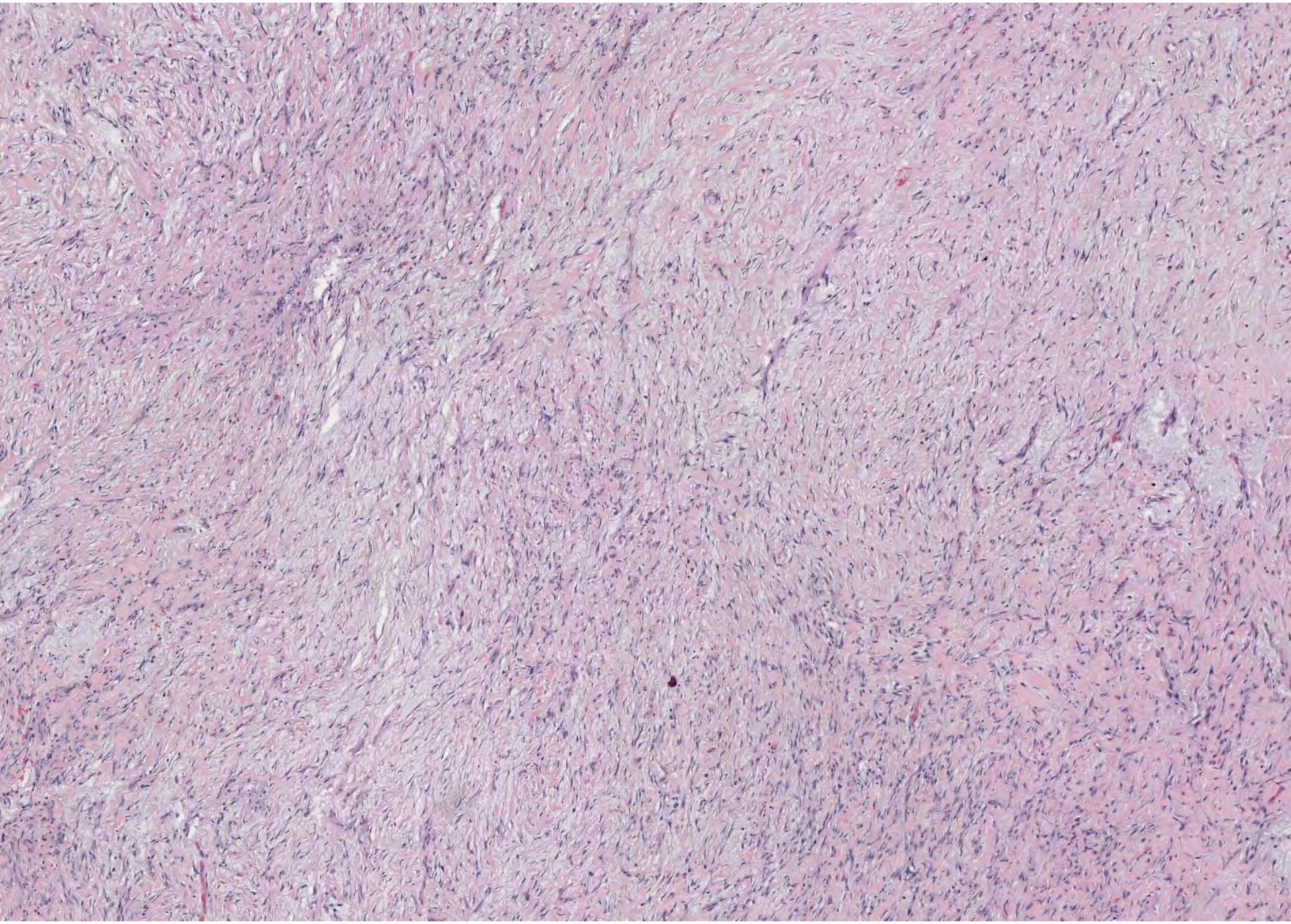

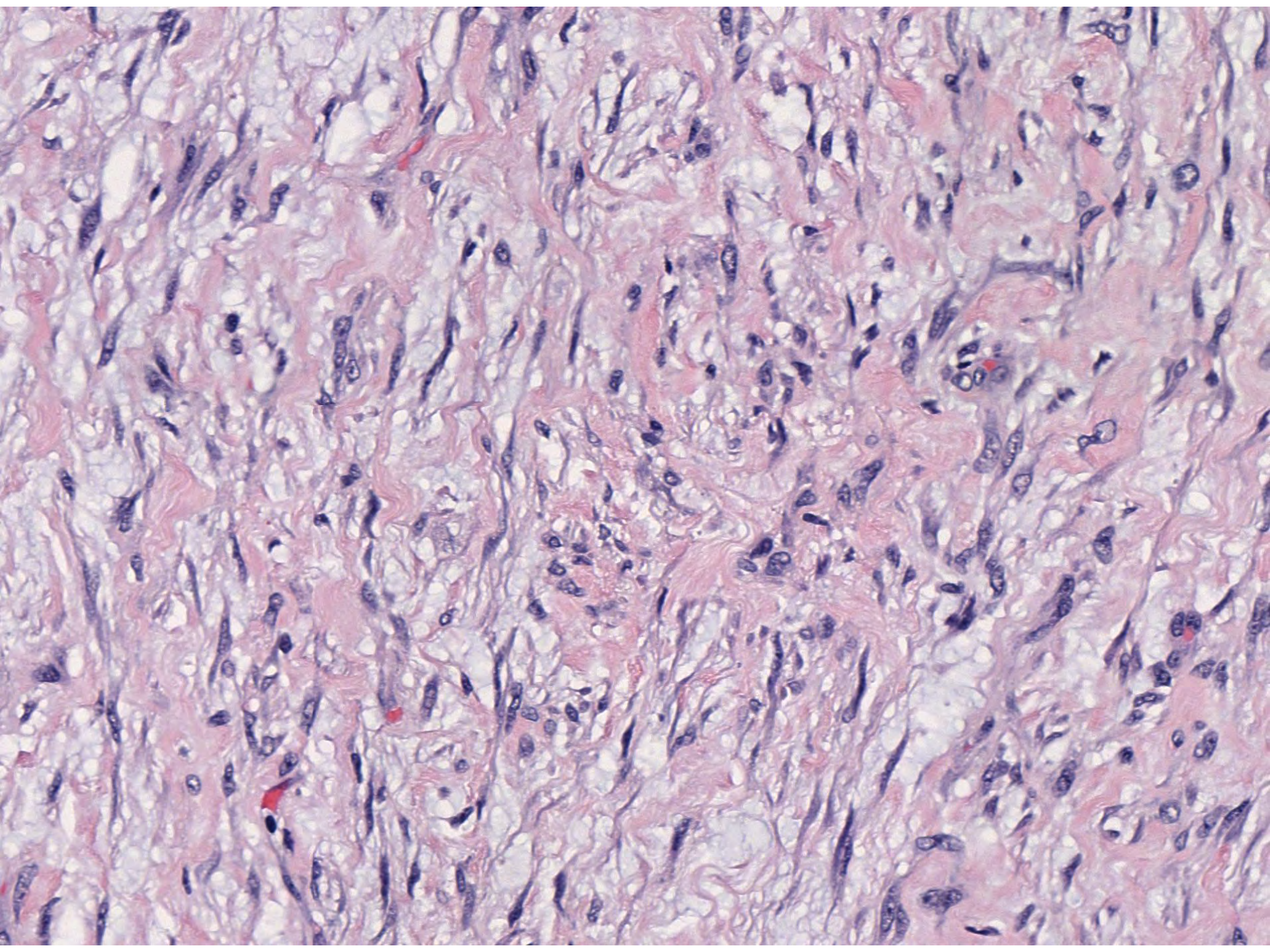

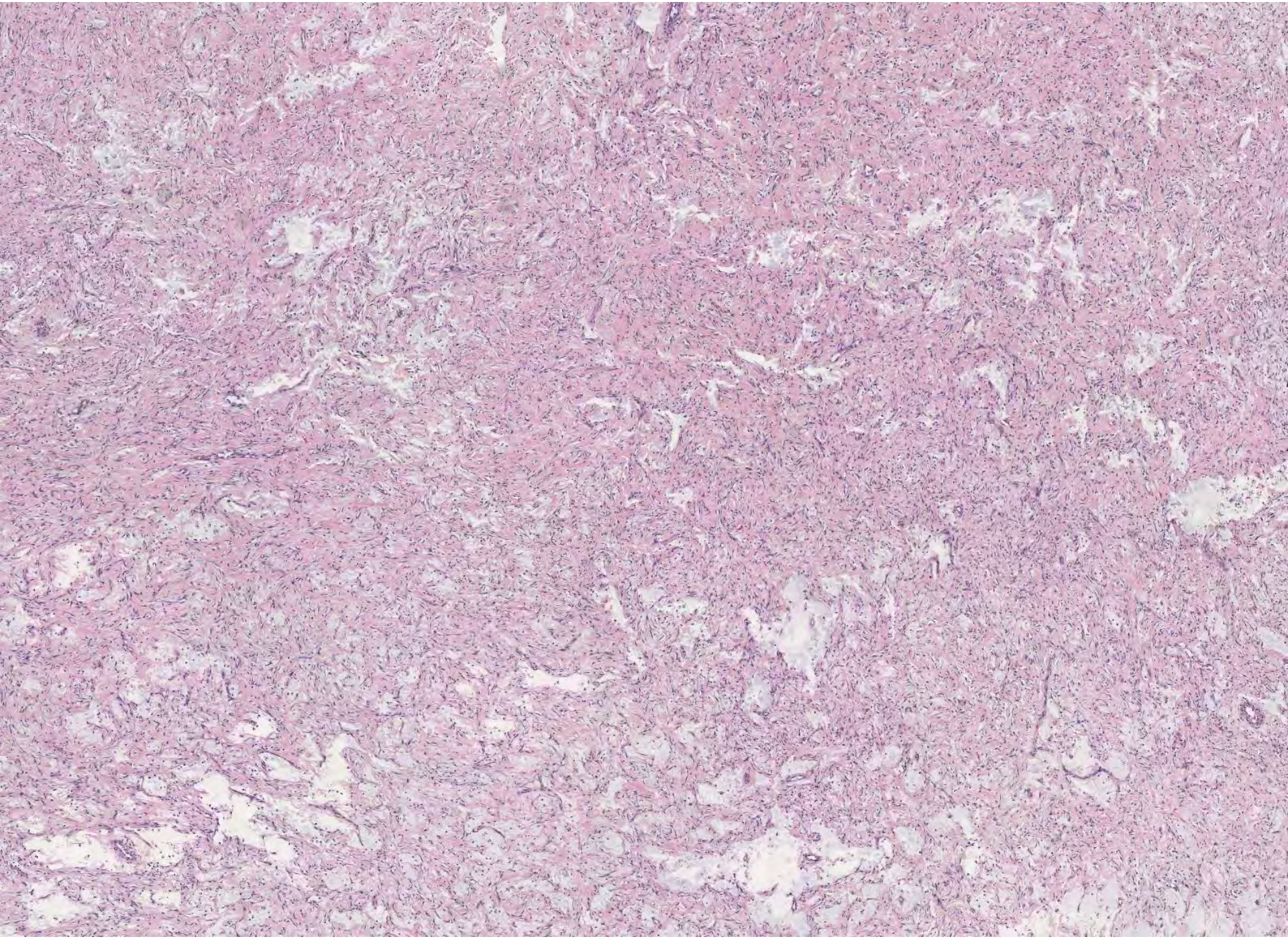

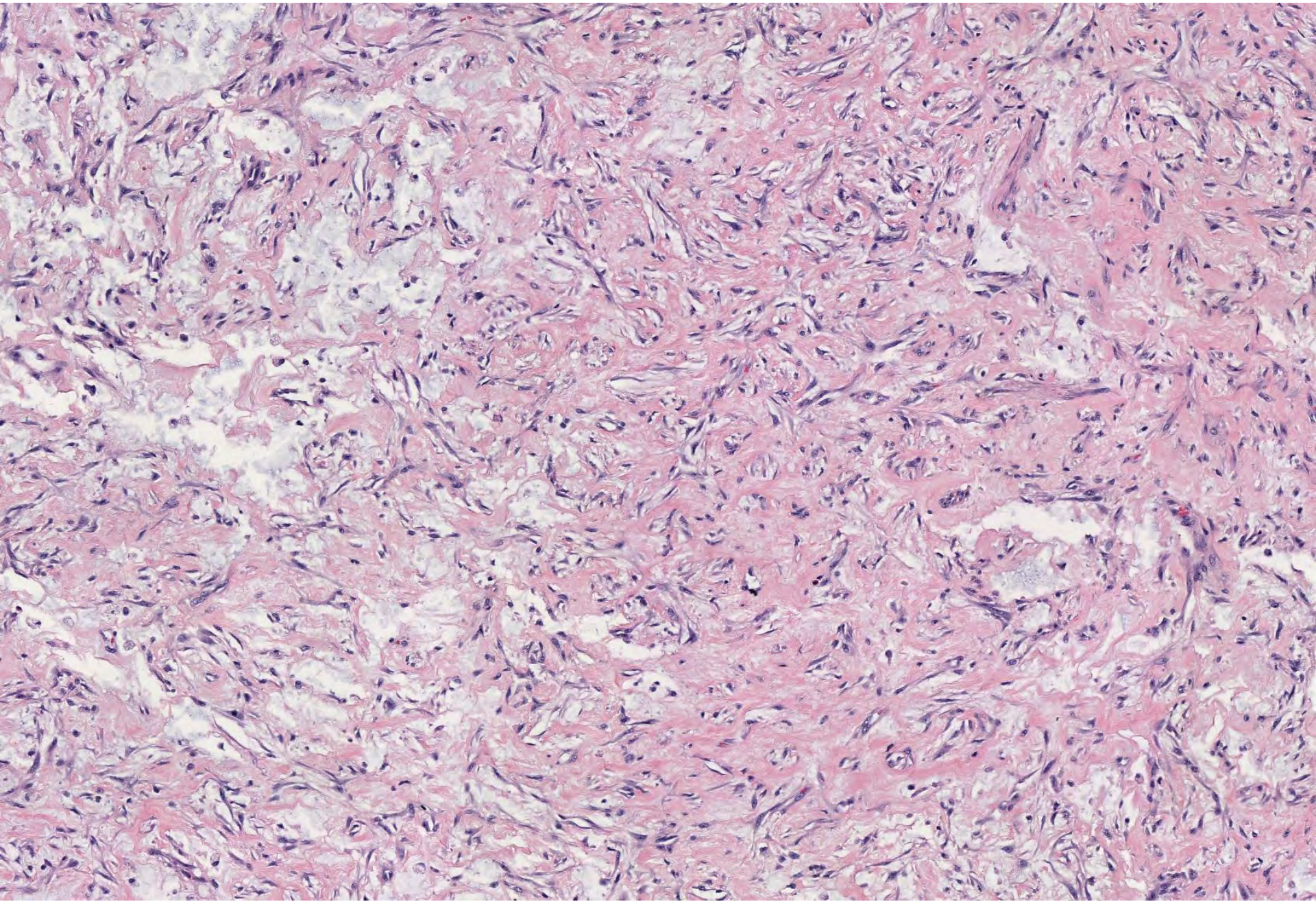

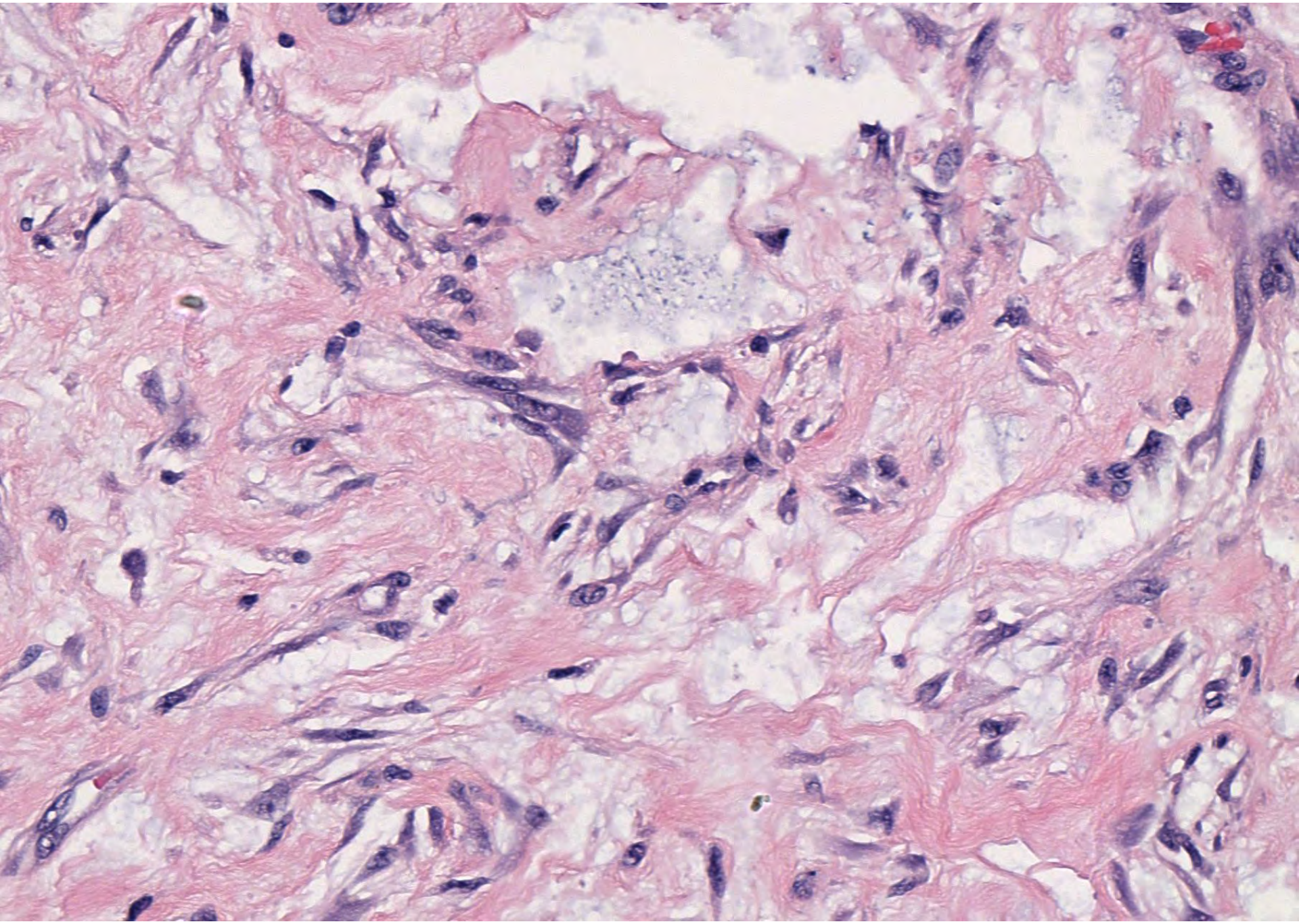

DIAGNOSIS

NODULAR FASCIITIS

- Reactive appearing proliferation of fibroblasts and myofibroblasts in myxoid stroma with granulation tissue-like vascular proliferation, lymphs and extravasated RBC's,
- Usually in young adults in fascia and SQ, rapid growth to 2 - 3 cm. Peaks at age 40 years; prior trauma in 10% of cases
- Common lesion that typically presents on the flexor forearm, chest, back
- Arises from superficial fascia, occasionally intramuscular or intravascular

MICROSCOPIC DESCRIPTION

- Zonation effect with hypocellular central region and hypercellular periphery
- Composed of uniform, plump, immature, spindled to stellate fibroblasts or myofibroblasts without atypia, with a feathery, "tissue-culture" like growth pattern due to abundant ground substance
- Often with mucoid / myxoid pools (microcysts)
- Uniform elongated nuclei with punctate nucleoli -without atypia
- May have storiform or fascicular patterns (S or C shaped)
- Often frequent mitotic figures (none atypical), lymphs and macrophages, RBC extravasation, bands of keloid-type collagen
- Vasculature often prominent

NODULAR FASCIITIS

- **Positive stains**
- **Fibroblasts / myofibroblasts: smooth muscle actin**, **muscle specific actin**, **vimentin** and **calponin**
- **Macrophages: CD68**

DIFFERENTIAL DIAGNOSIS

- **Benign fibrous histiocytoma**: based in dermis, storiform pattern, infiltrative borders with collagen trapping, xanthoma cells and Touton giant cells, no myxoid microcysts
- **Fibromatosis**: usually large tumor that infiltrates surrounding soft tissue, spindled cells are parallel and separated by abundant collagen and arranged in broad sweeping fascicles, no loose tissue culture appearance or myxoid microcysts
- **Inflammatory myofibroblastic tumor**: large tumor size, mixed inflammatory infiltrate, ALK expression; no rapid growth, no zonation, no prominent myxoid stroma
- **Myositis ossificans**: centered in muscle, calcification
- **Other sarcoma**: nuclear atypia is prominent, may have necrosis, larger size usually
- **Reactive spindle cell nodules:** post-biopsy
- **Treatment:** Excision (curative even if incomplete resection); recurs in 1% after incomplete excision but recurrence should suggest review of diagnosis; no mets

SB 6319
(scanned slide available)

Ankur Sangoi; El Camino Hospital

64-year-old female presenting with hirsutism, 2cm ovarian mass found. Rule out malignancy.

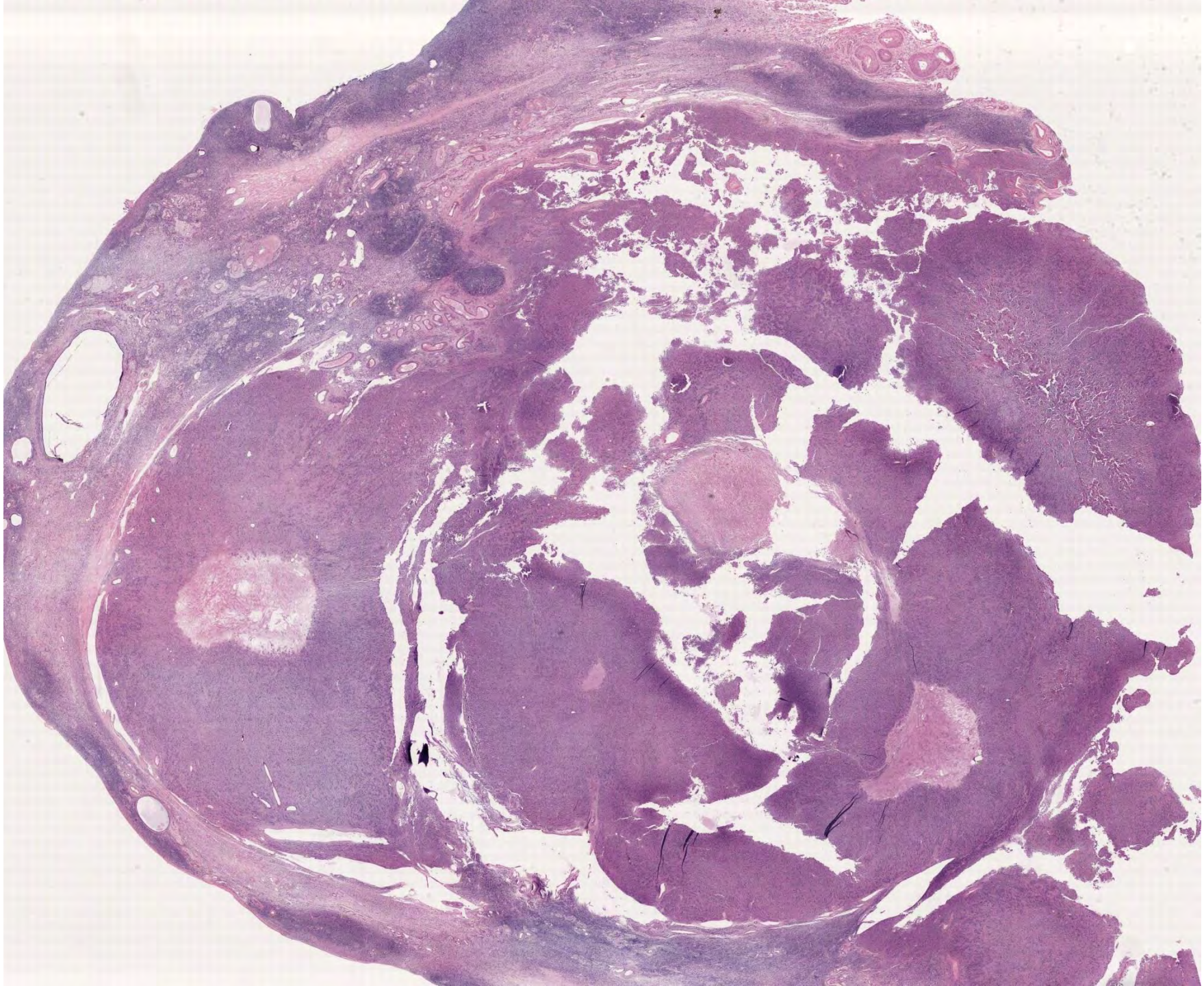

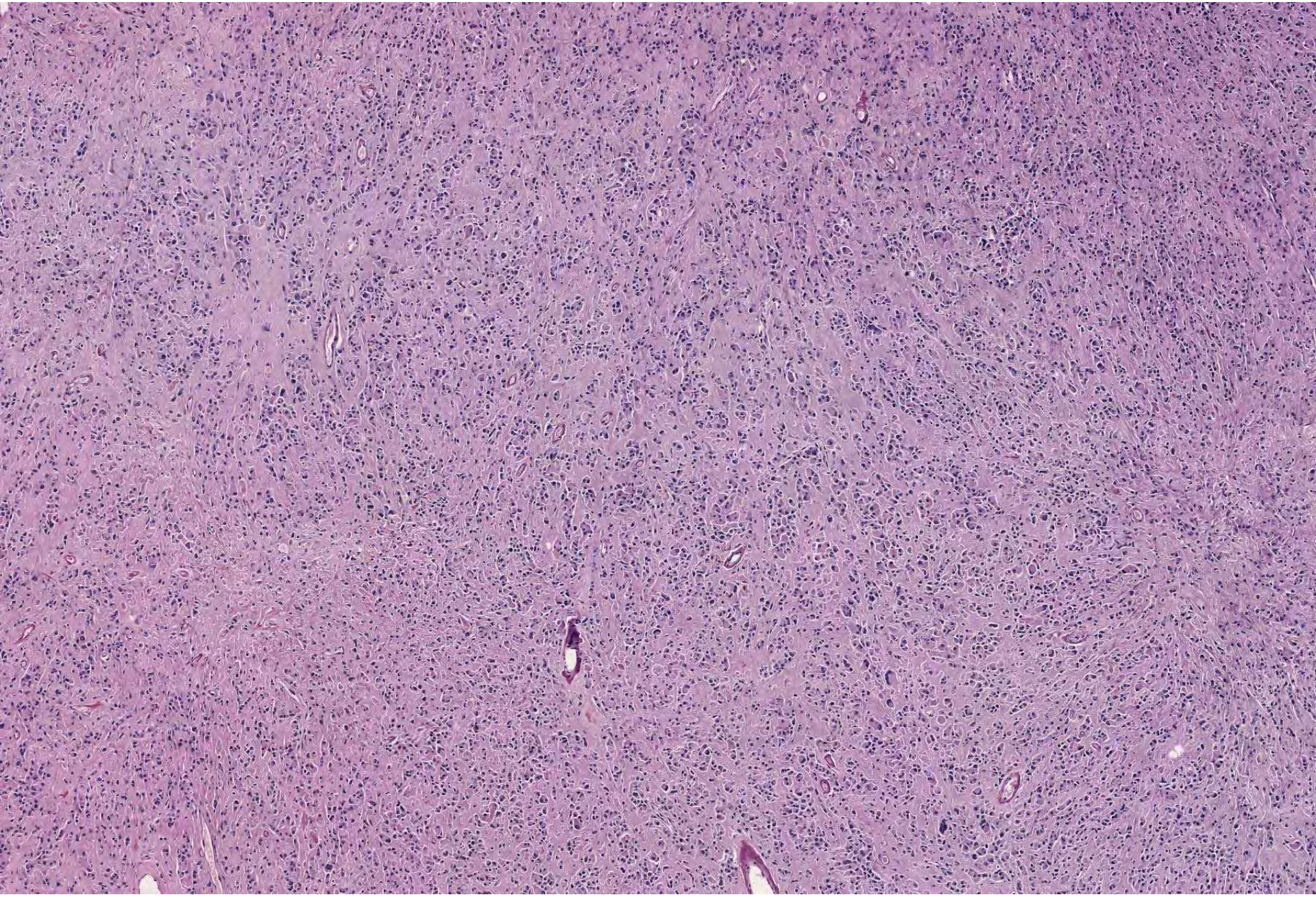

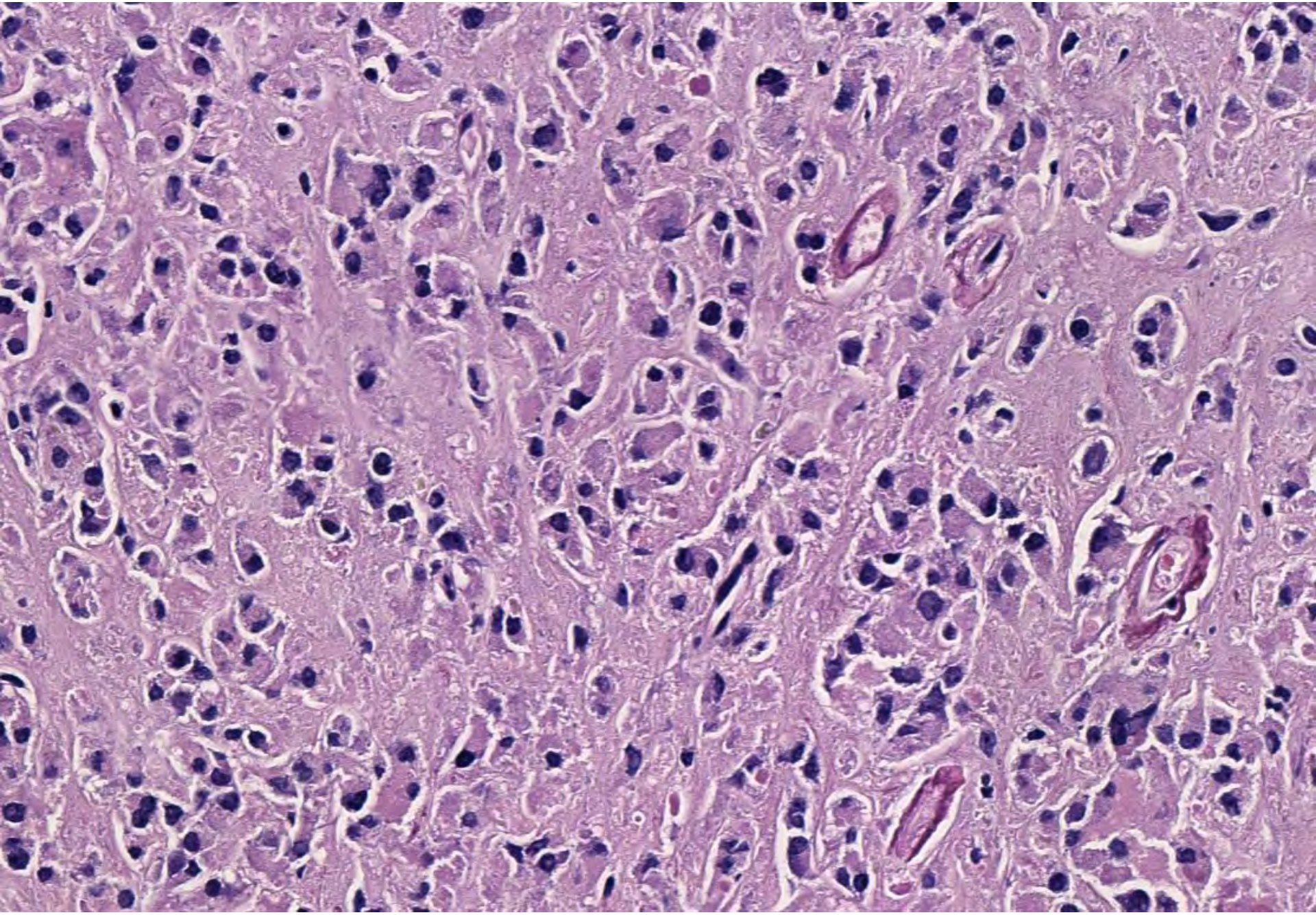

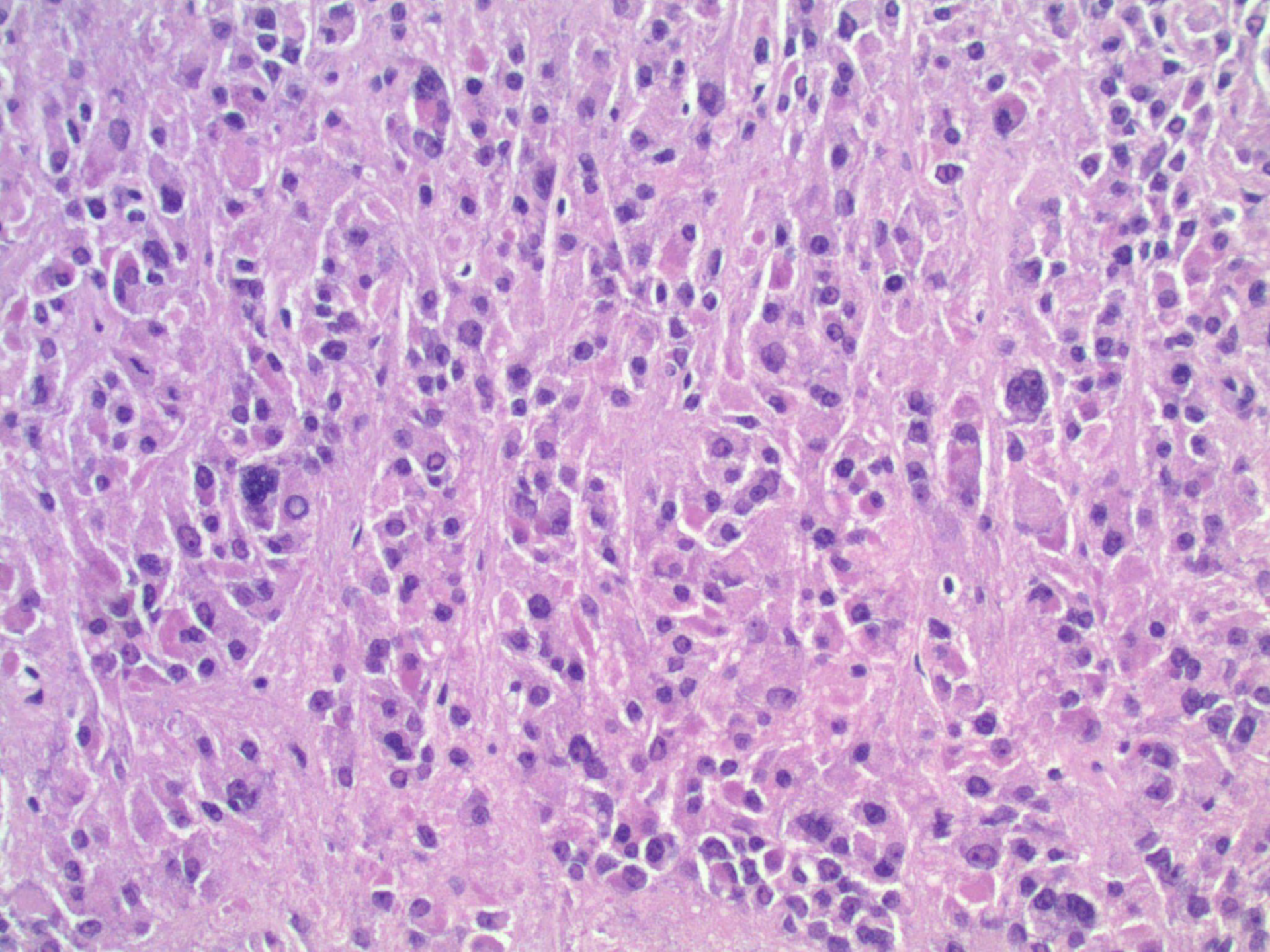

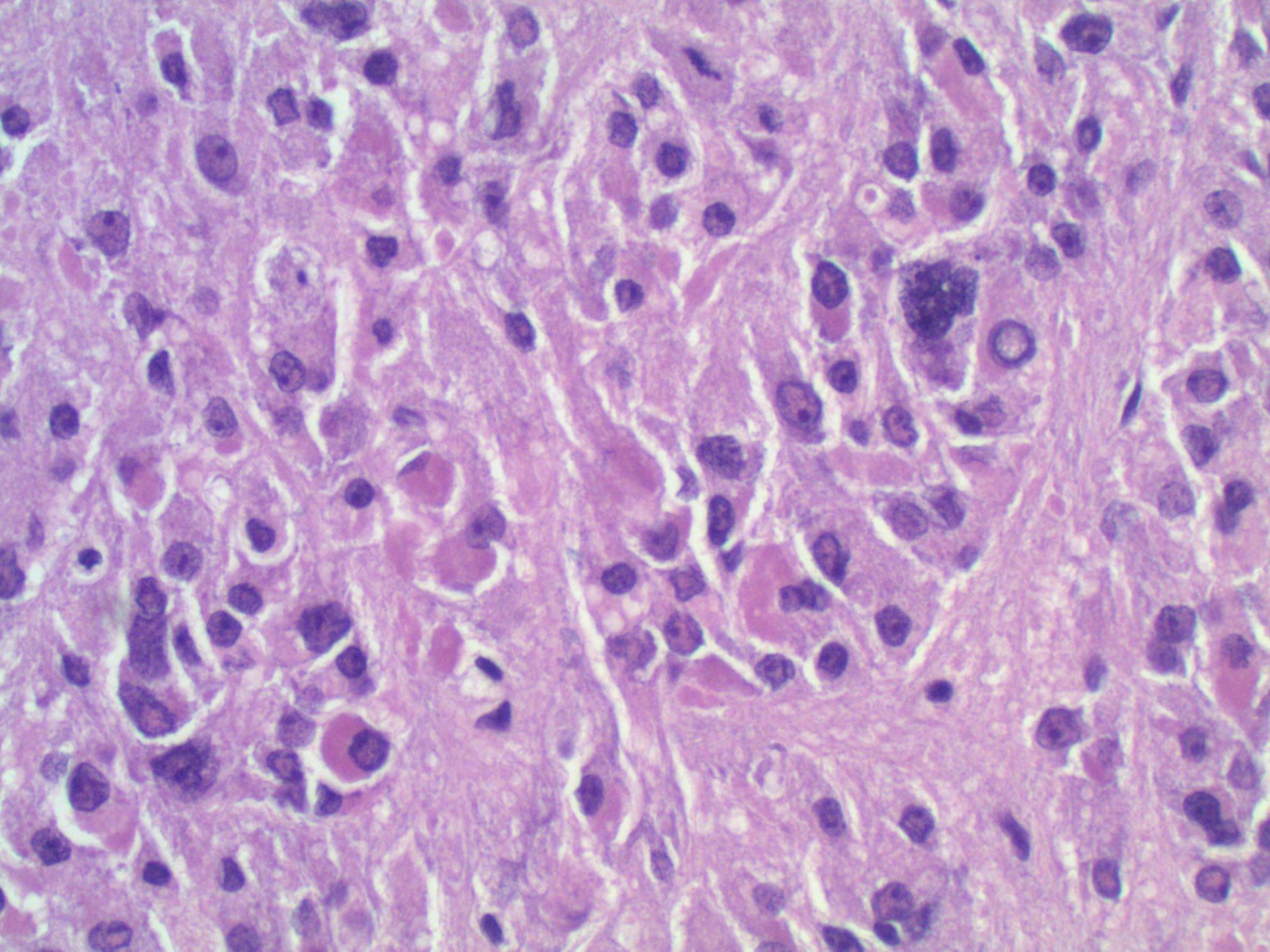

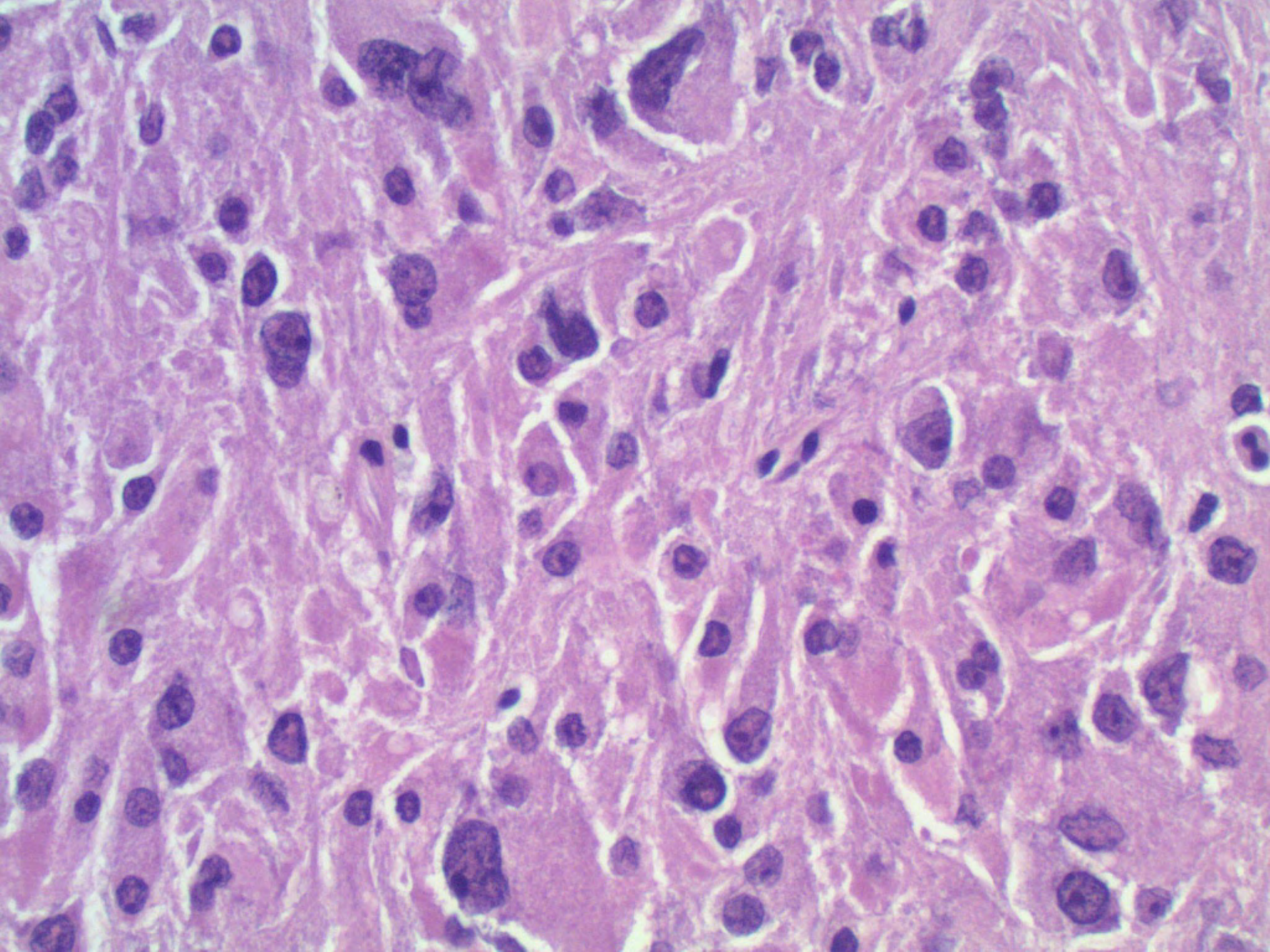

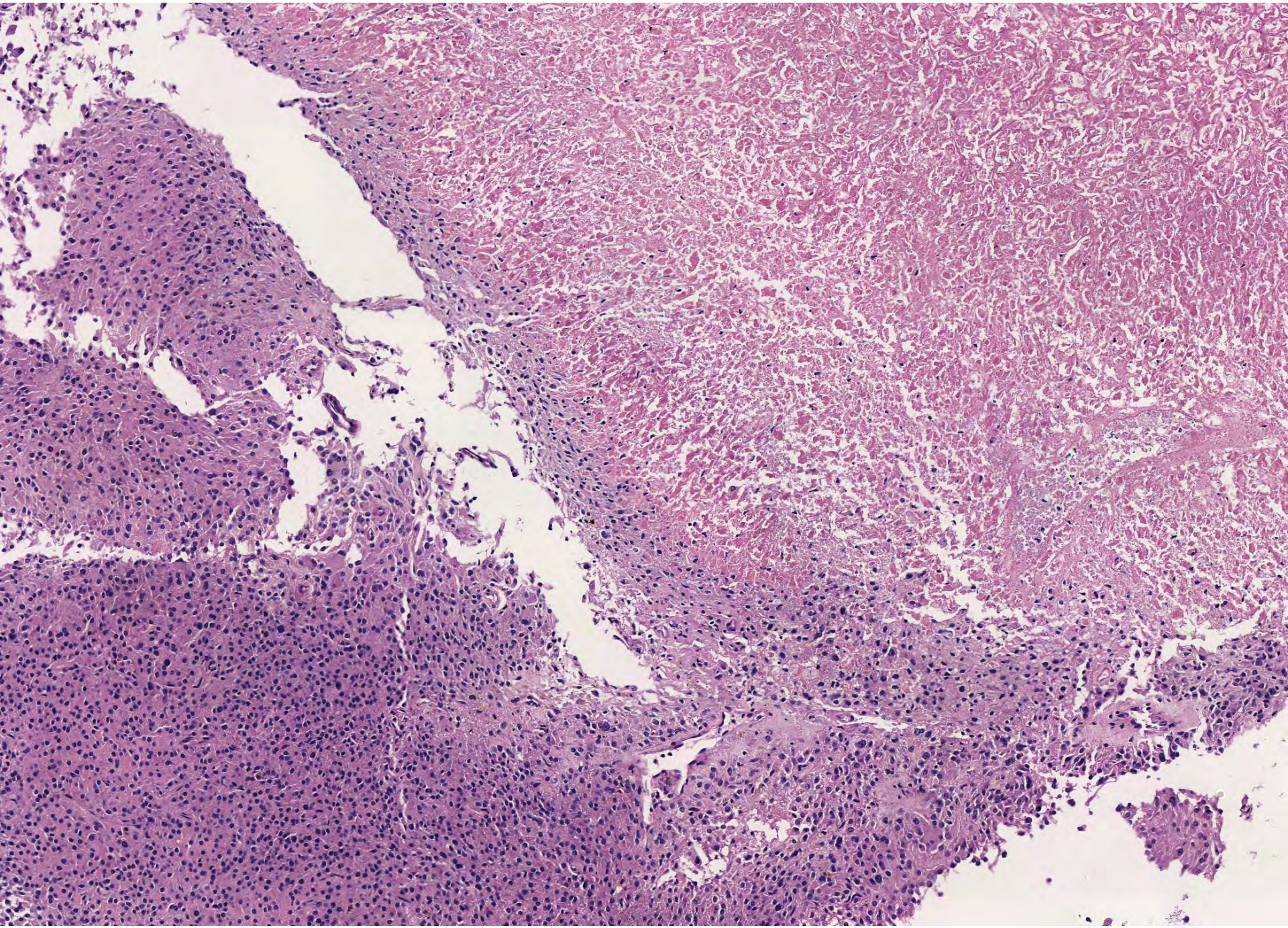

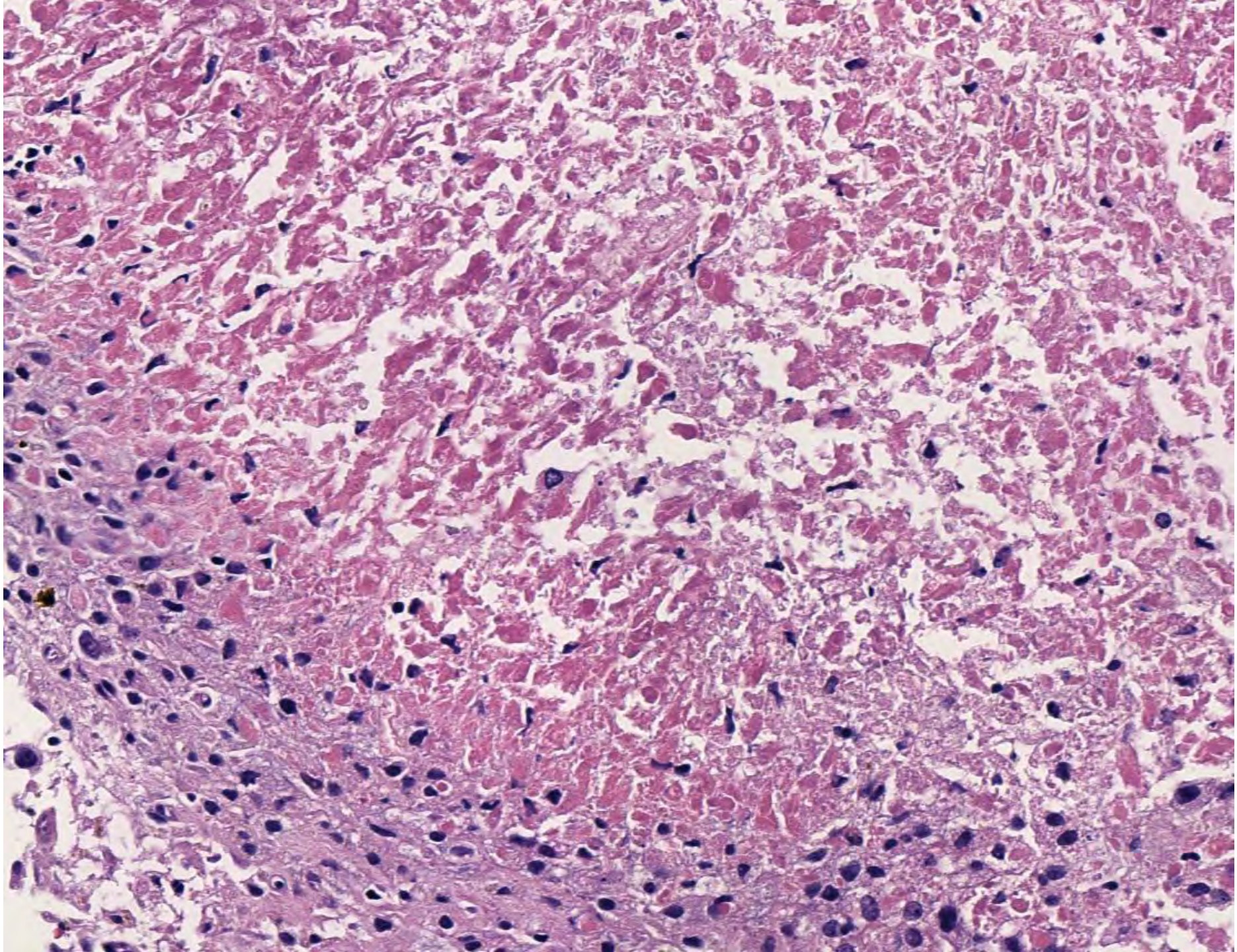

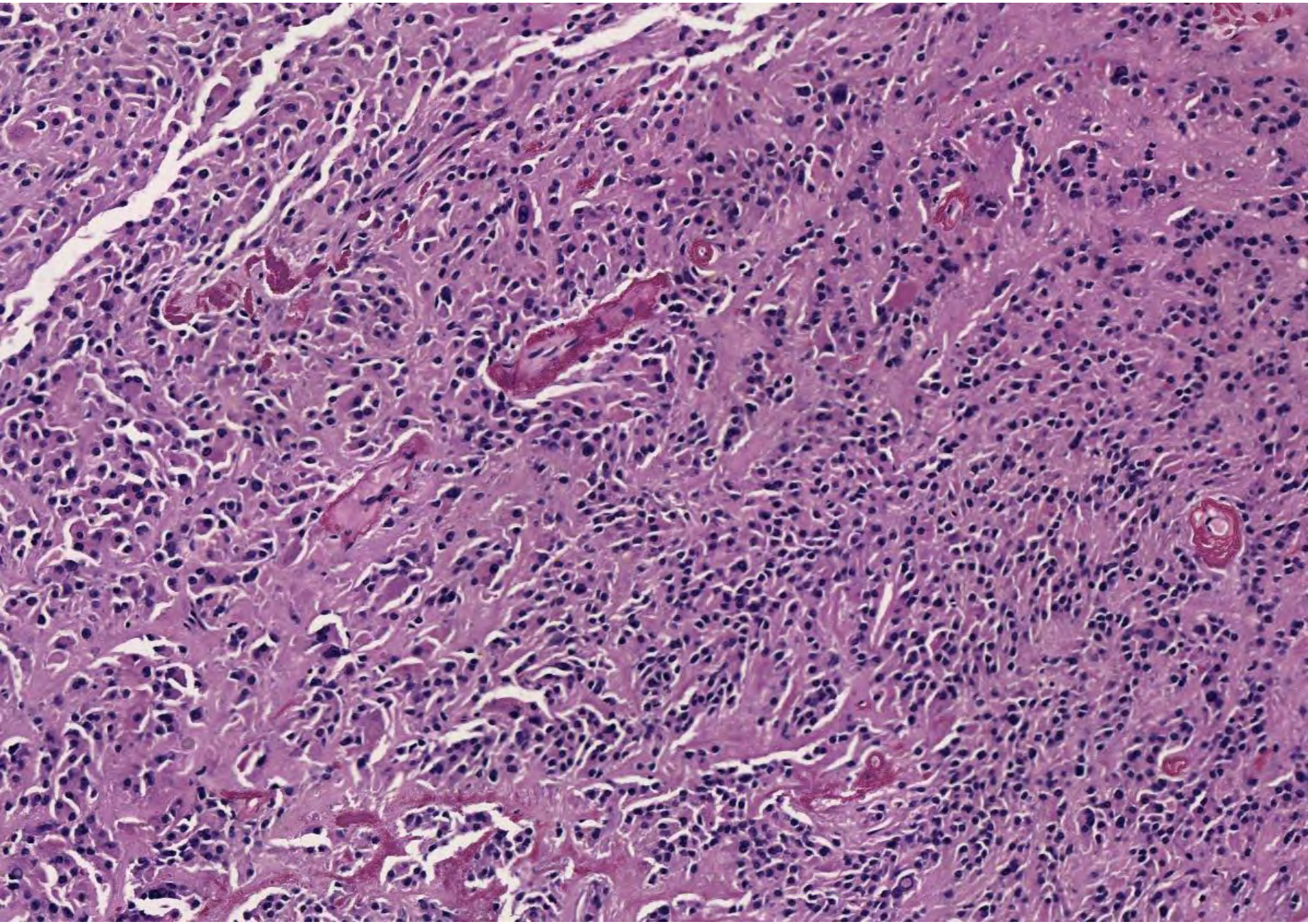

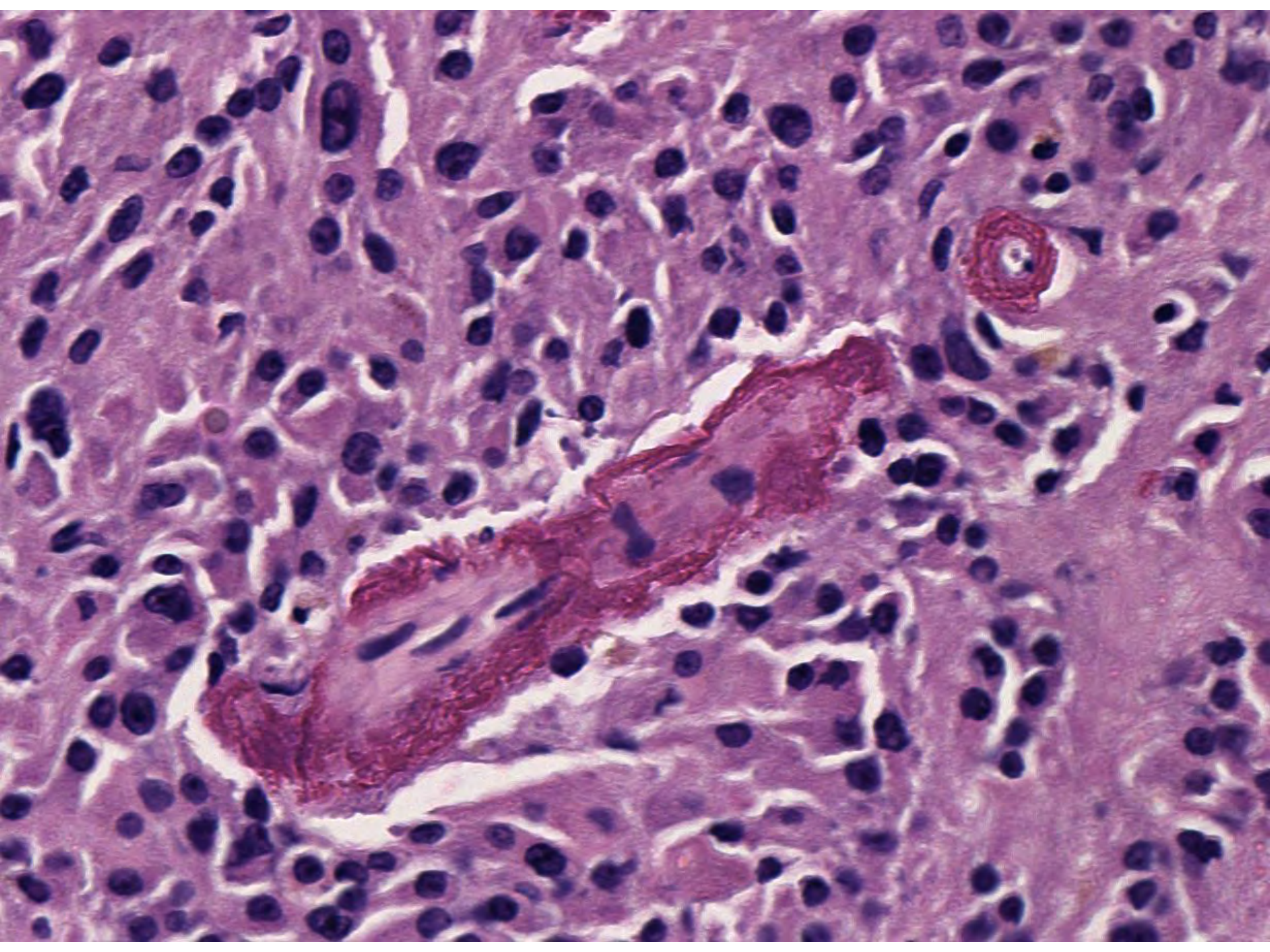

DIAGNOSIS

DDx

- **Leydig cell tumor (crystal negative)**
- **Steroid cell tumor NOS**
- **Stromal luteoma**
- **Oxyphilic struma ovarii**
- **Primary ovarian carcinoma**
  - clear cell carcinoma
- **Metastasis**
  - renal cell carcinoma, hepatocellular carcinoma

DDx

- **Leydig cell tumor (crystal negative)**
- **Steroid cell tumor NOS**
- **Stromal luteoma**
- **Oxyphilic struma ovarii**
- **Primary ovarian carcinoma**
  - clear cell carcinoma
- **Metastasis**
  - renal cell carcinoma, hepatocellular carcinoma

Consult to Dr. Robert Young

- As you know from the email I excitedly dictated to my assistant to you, this Leydig cell tumor is <u>the best</u> example of a crystal negative Leydig cell tumor I have ever seen
- Fibrinoid necrosis of vessel walls, spotty nuclear atypia, and what Dr. Scully used to call "abnuclear clustering" of cytoplasm is characteristic
  - *candidly I never knew what he quite meant by that*, but he was basically referring to the zones of cell-free eosinophilic material

Consult to Dr. Robert Young

- No good example of Leydig cell tumor that has been clinically malignant
  - So unlikely in this case
- I hope very much to keep slides X, Y, Z for teaching purposes
  - *Let me know if that is not acceptable*

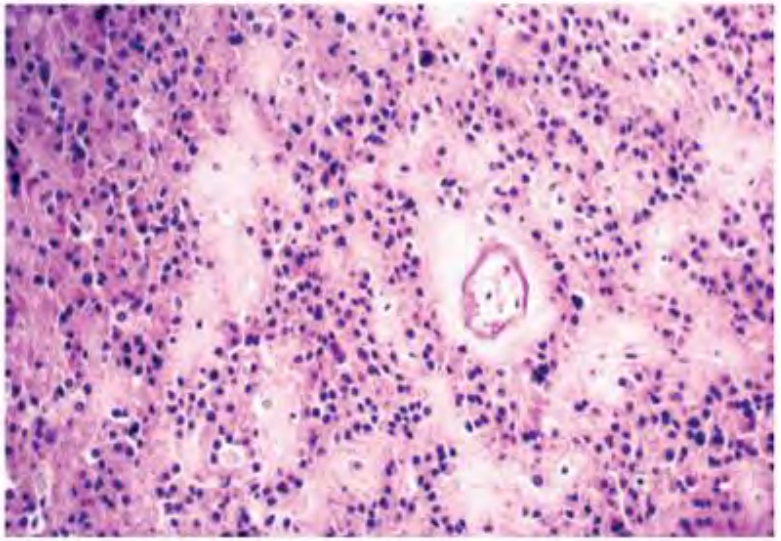

Fig. 16.57 Leydig cell tumor. Note clustering of nuclei and intervening acellular zones.

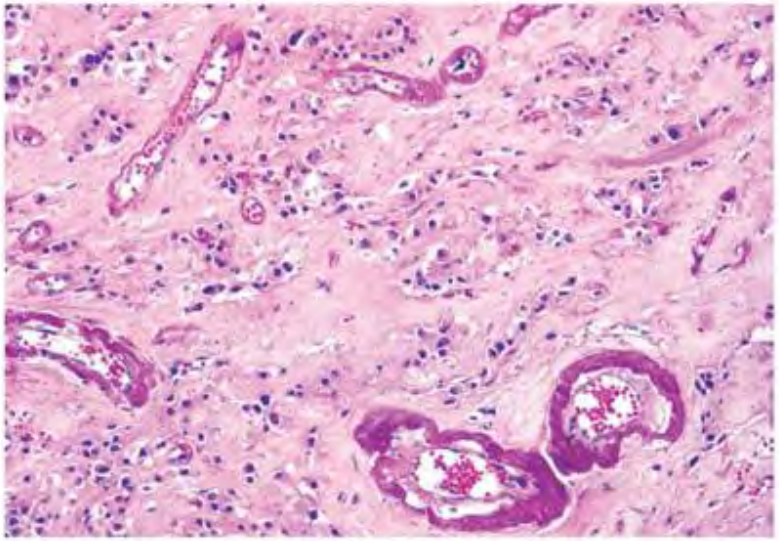

Fig. 16.58 Leydig cell tumor. Note fibrinoid necrosis of blood vessel walls that is a feature of some Leydig cell tumors in contrast to other steroid cell tumors.

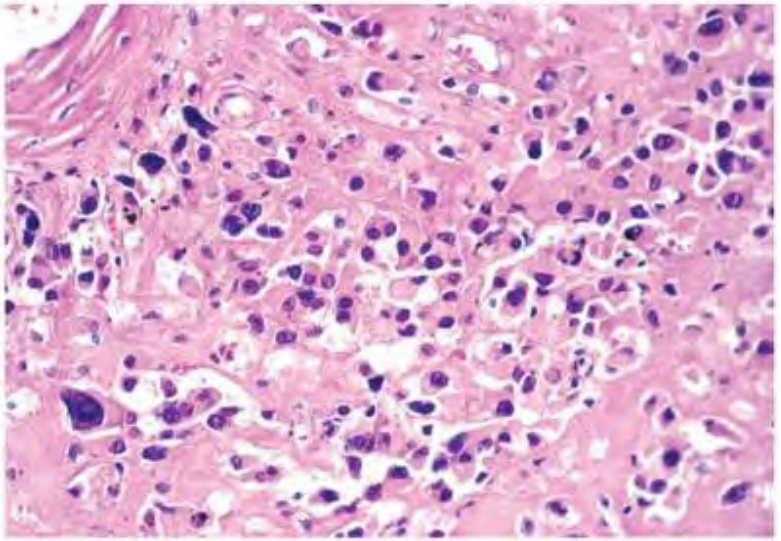

Fig. 16.59 Leydig cell tumor. There is bizarre nuclear atypicality.

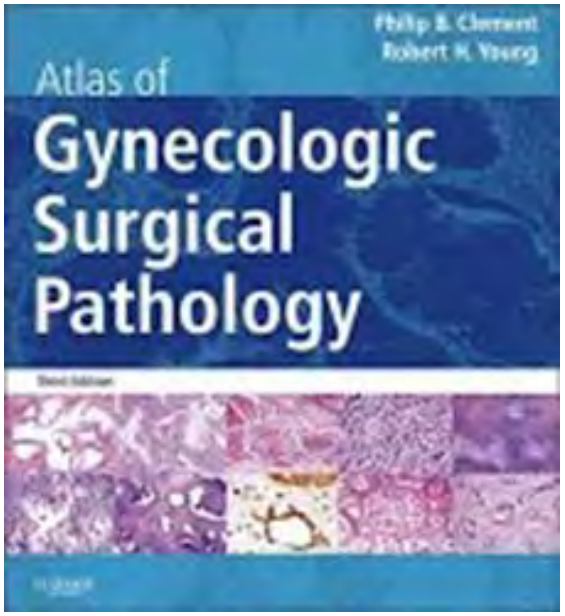

SB 6320
(scanned slide available)

Ankur Sangoi; El Camino Hospital

76-year-old male with renal mass, nephrectomy performed.

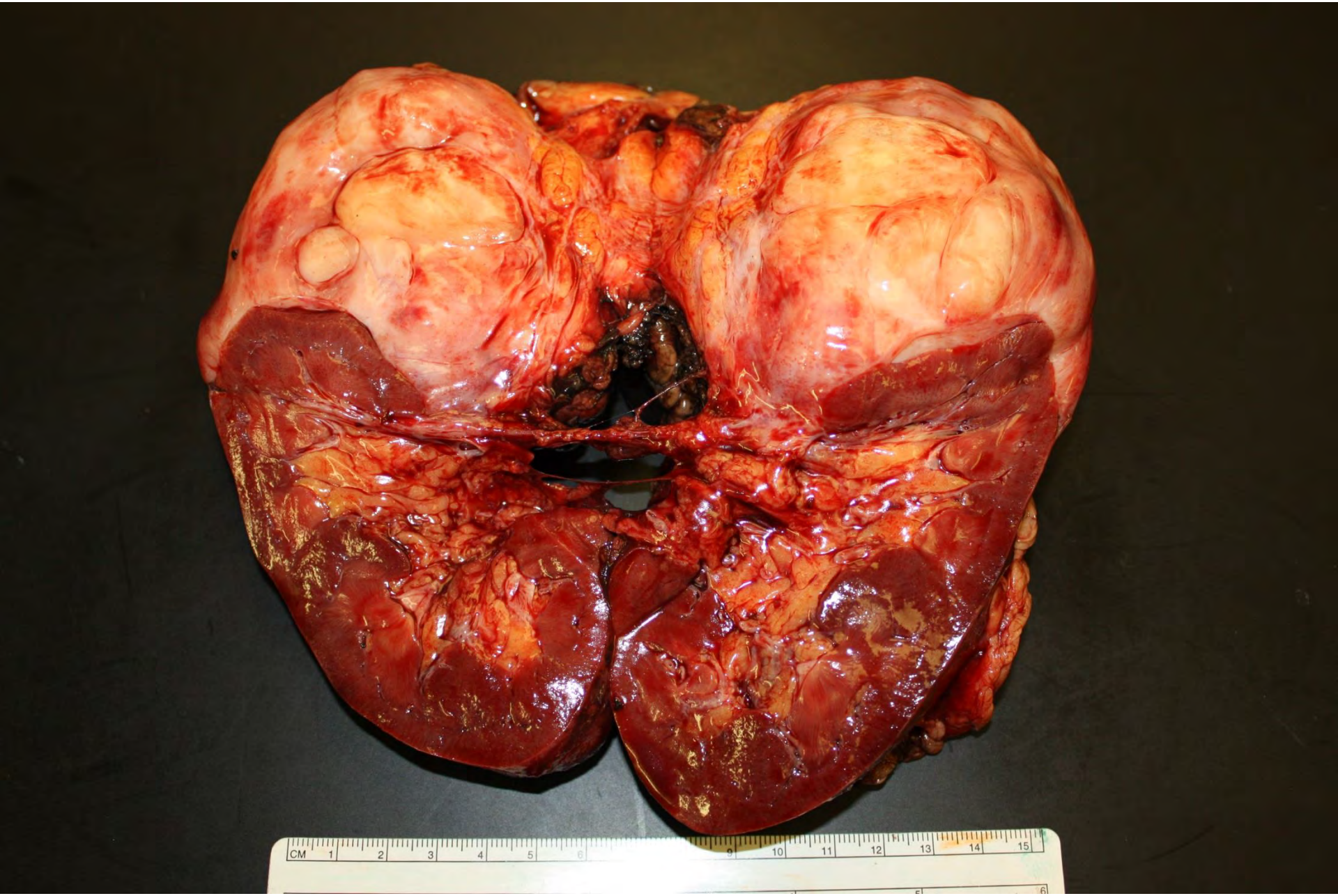
CM
1
2
3
4
5
6
9
10
11
12
13
14
15

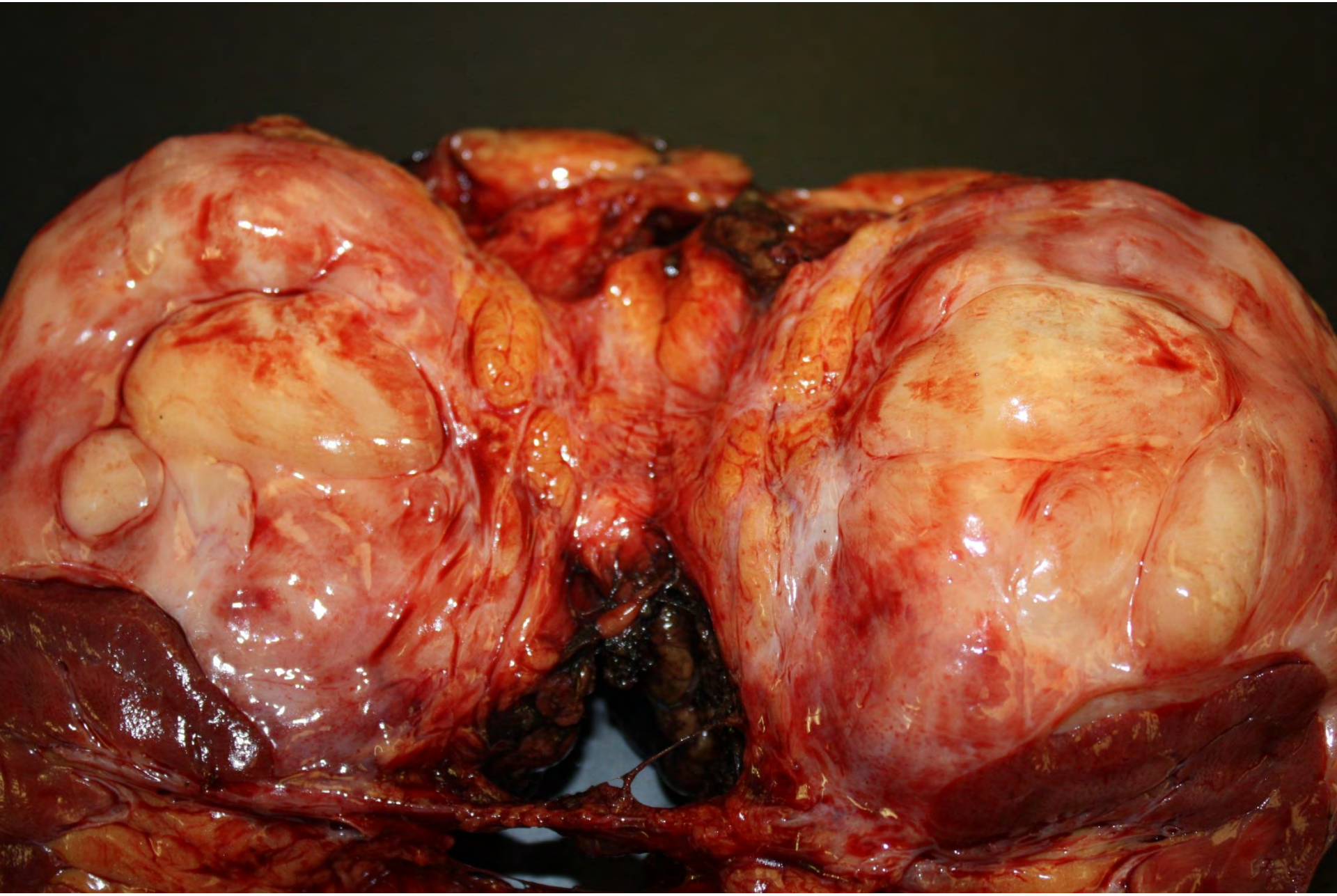

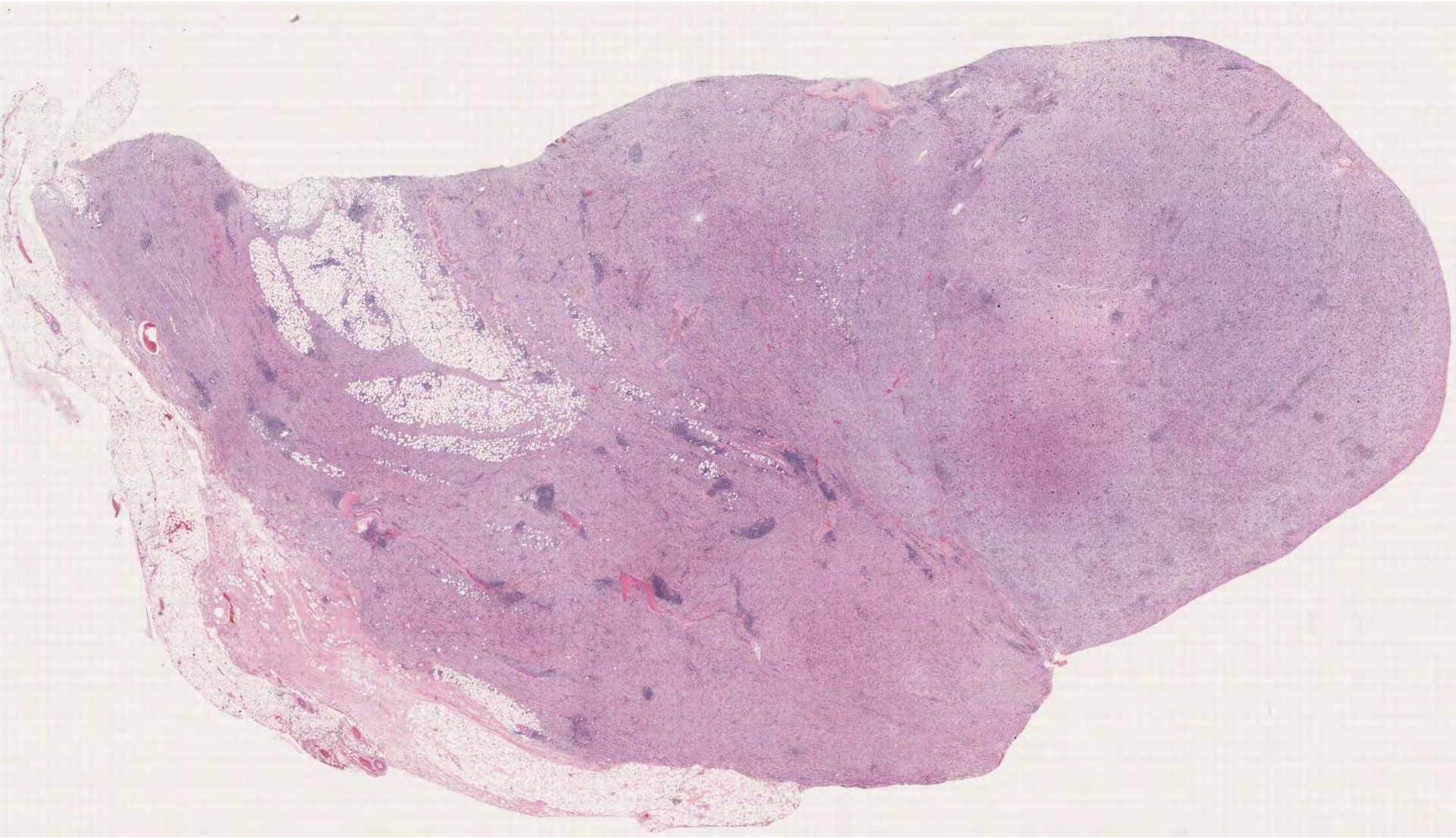

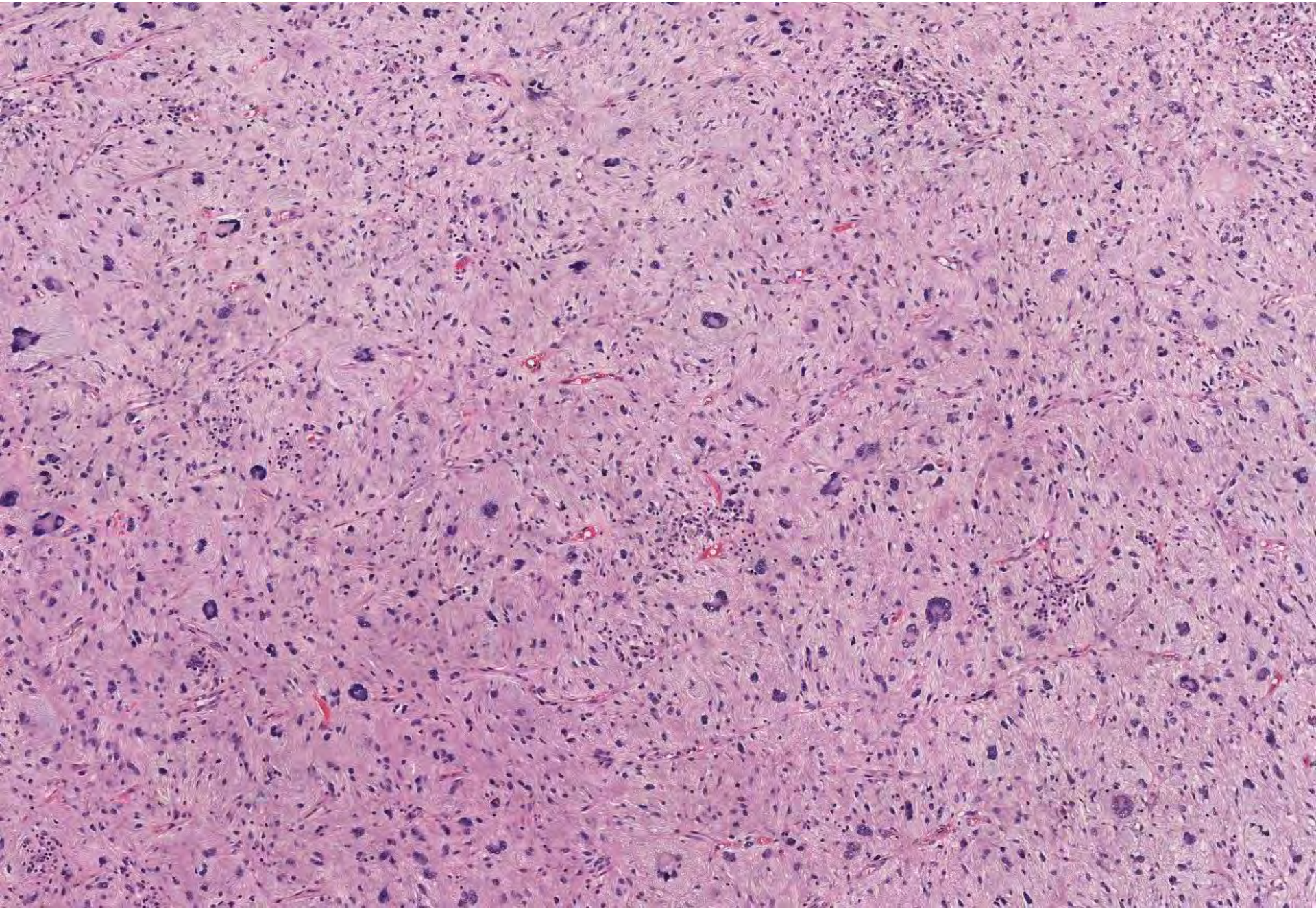

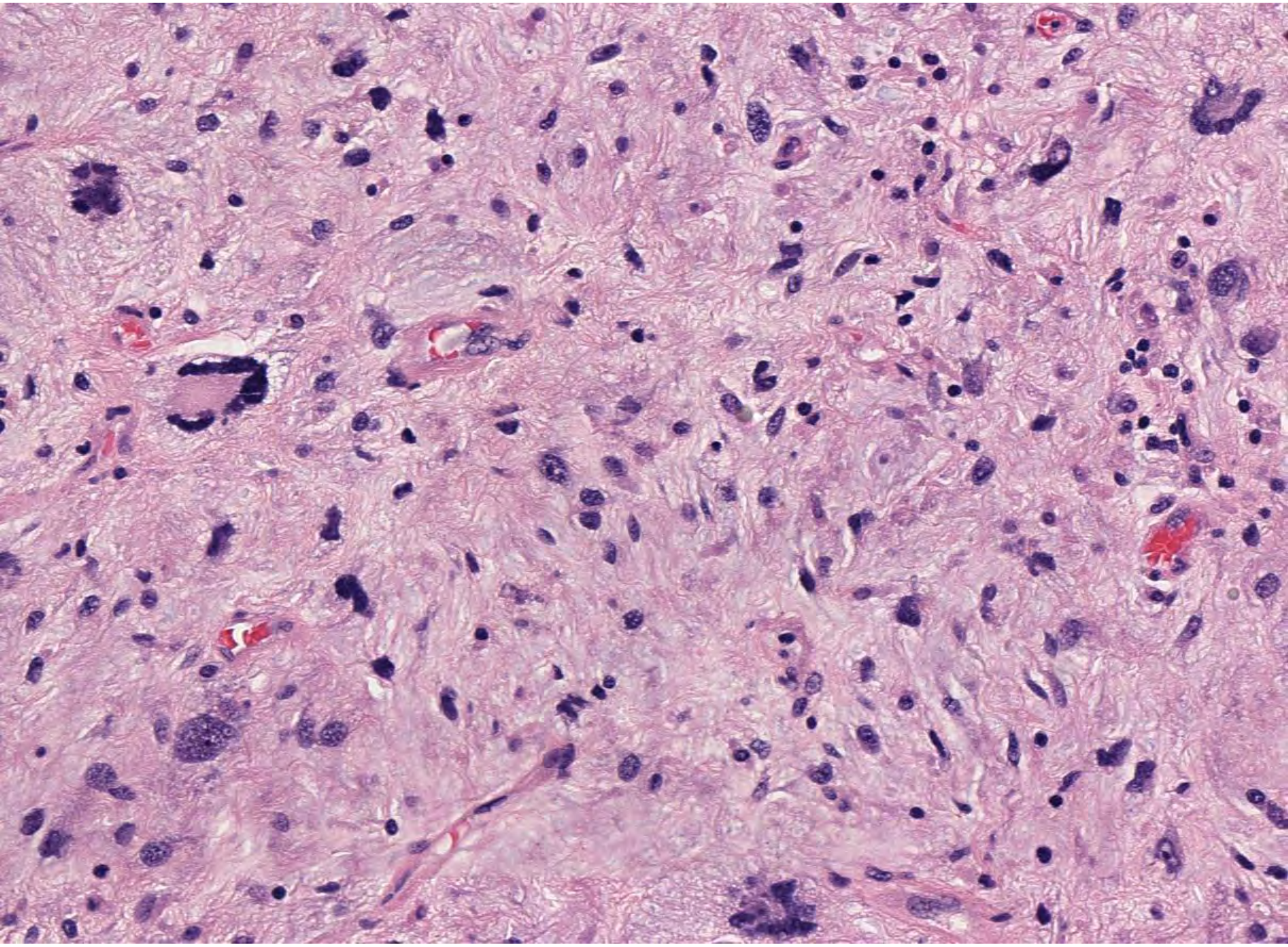

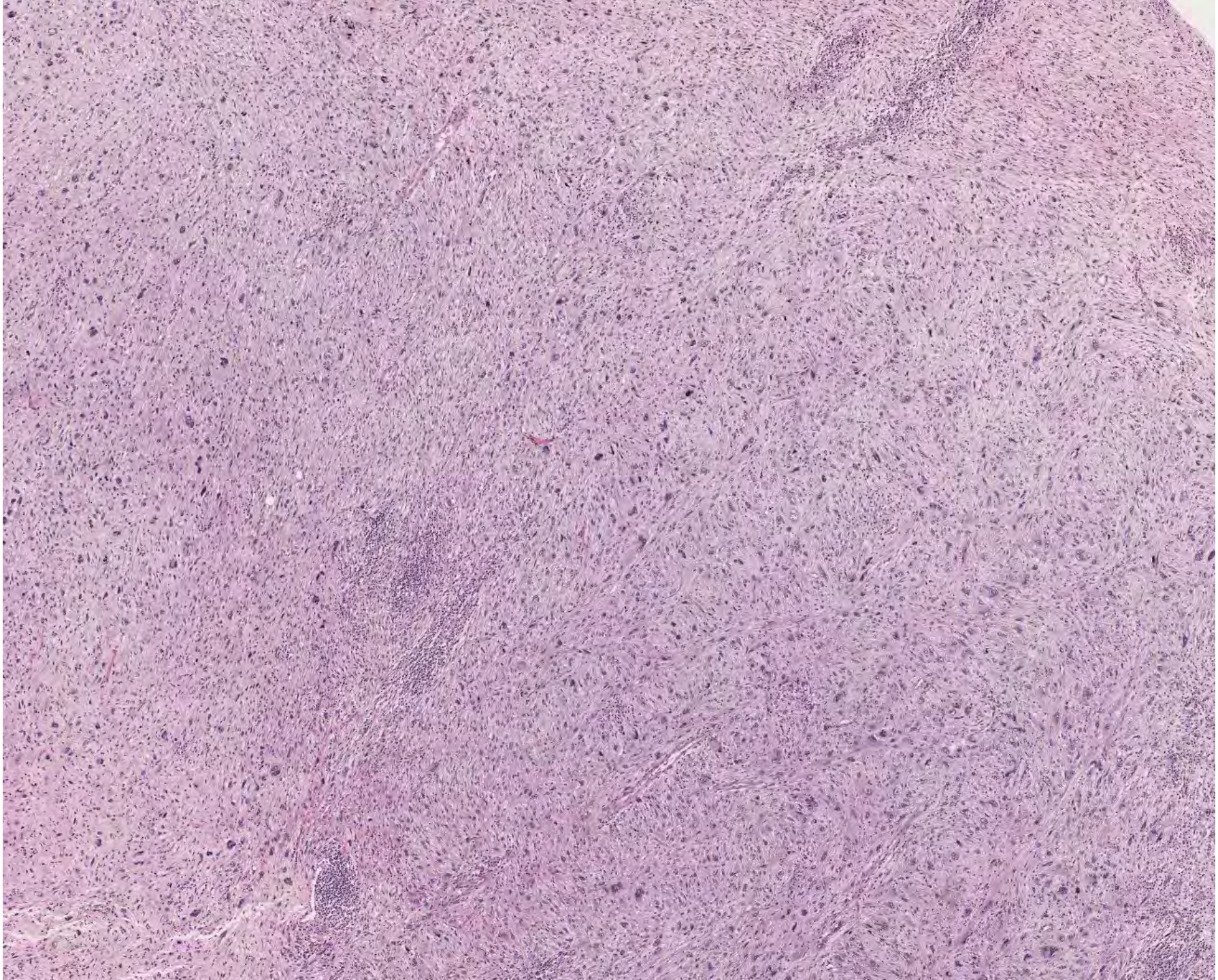

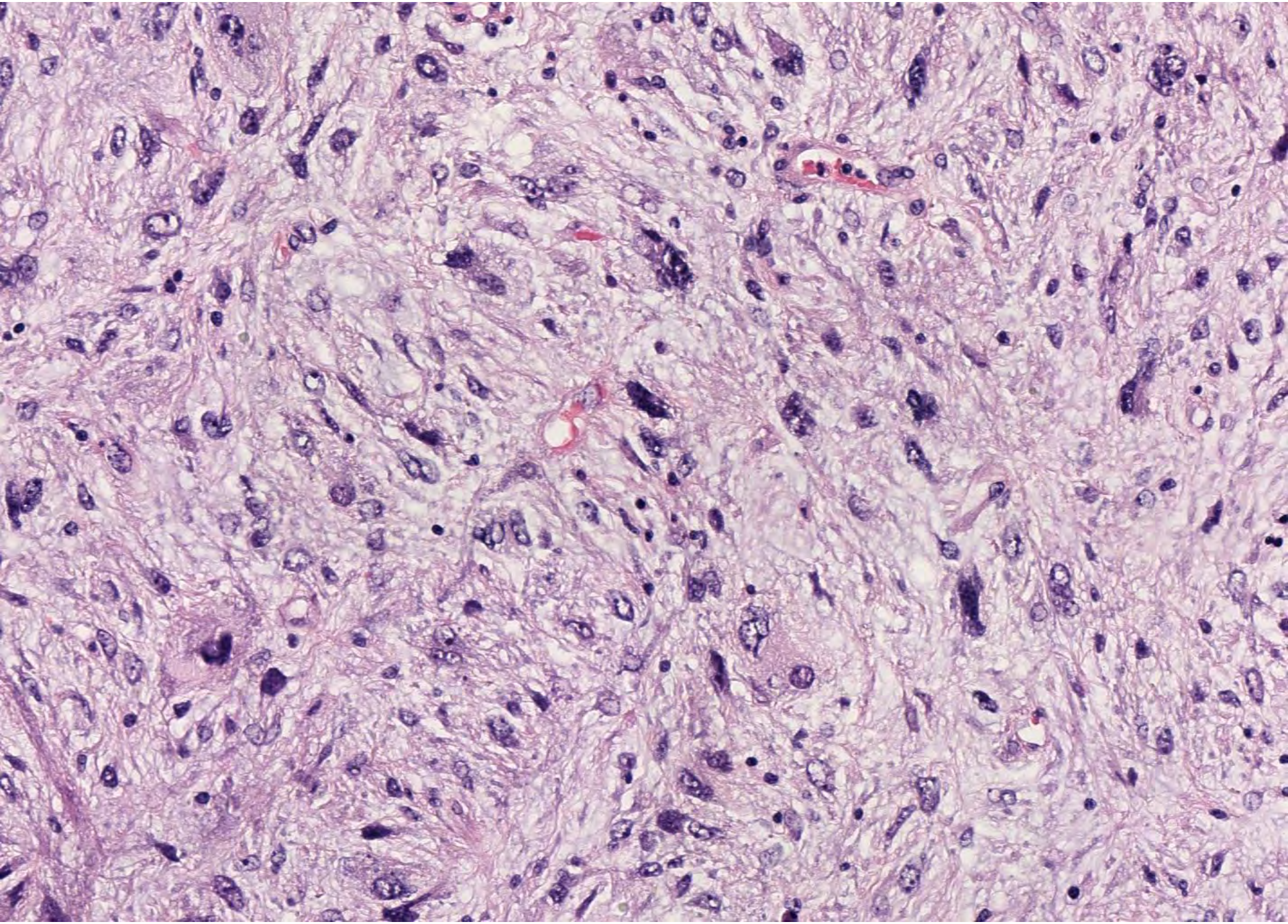

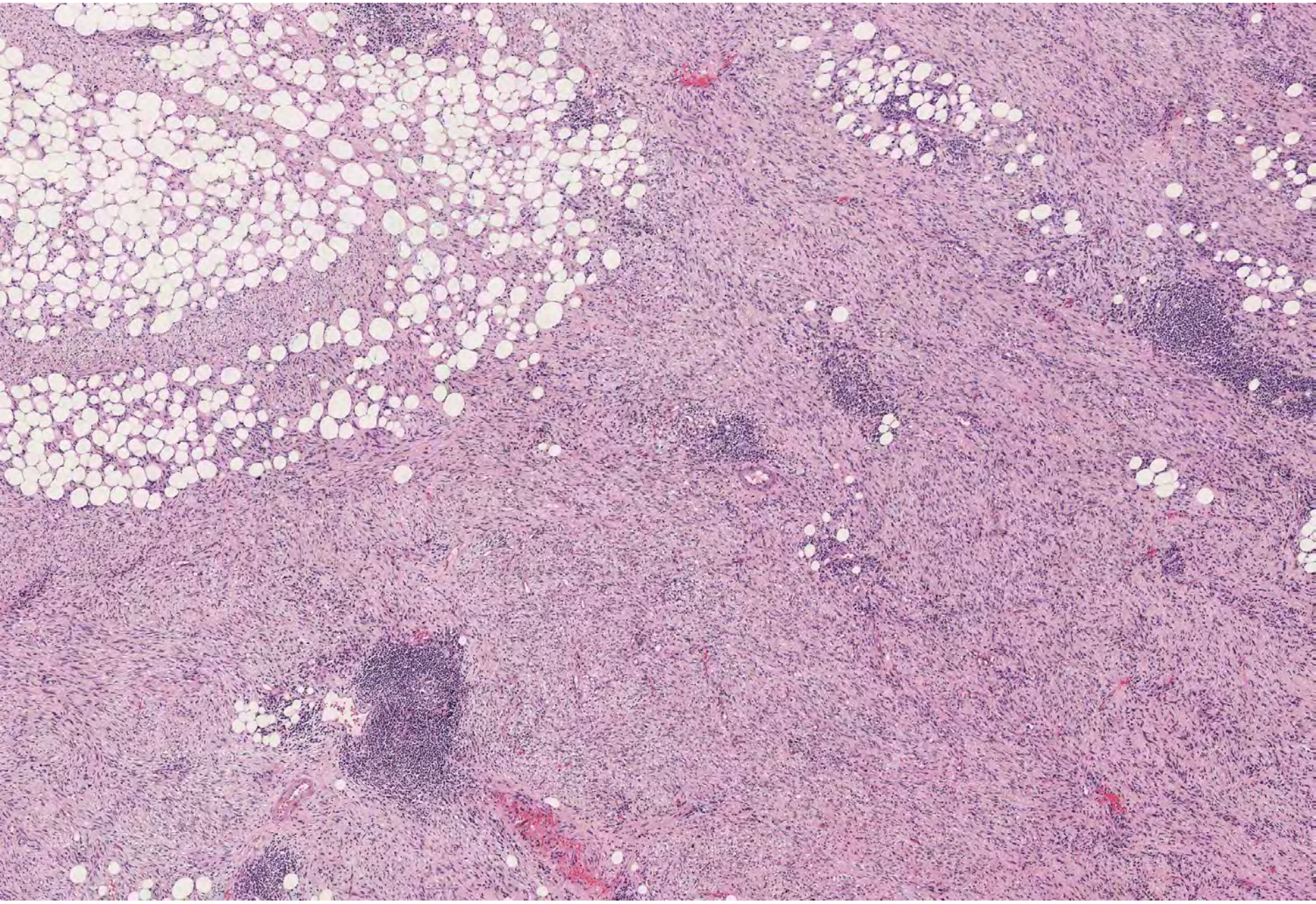

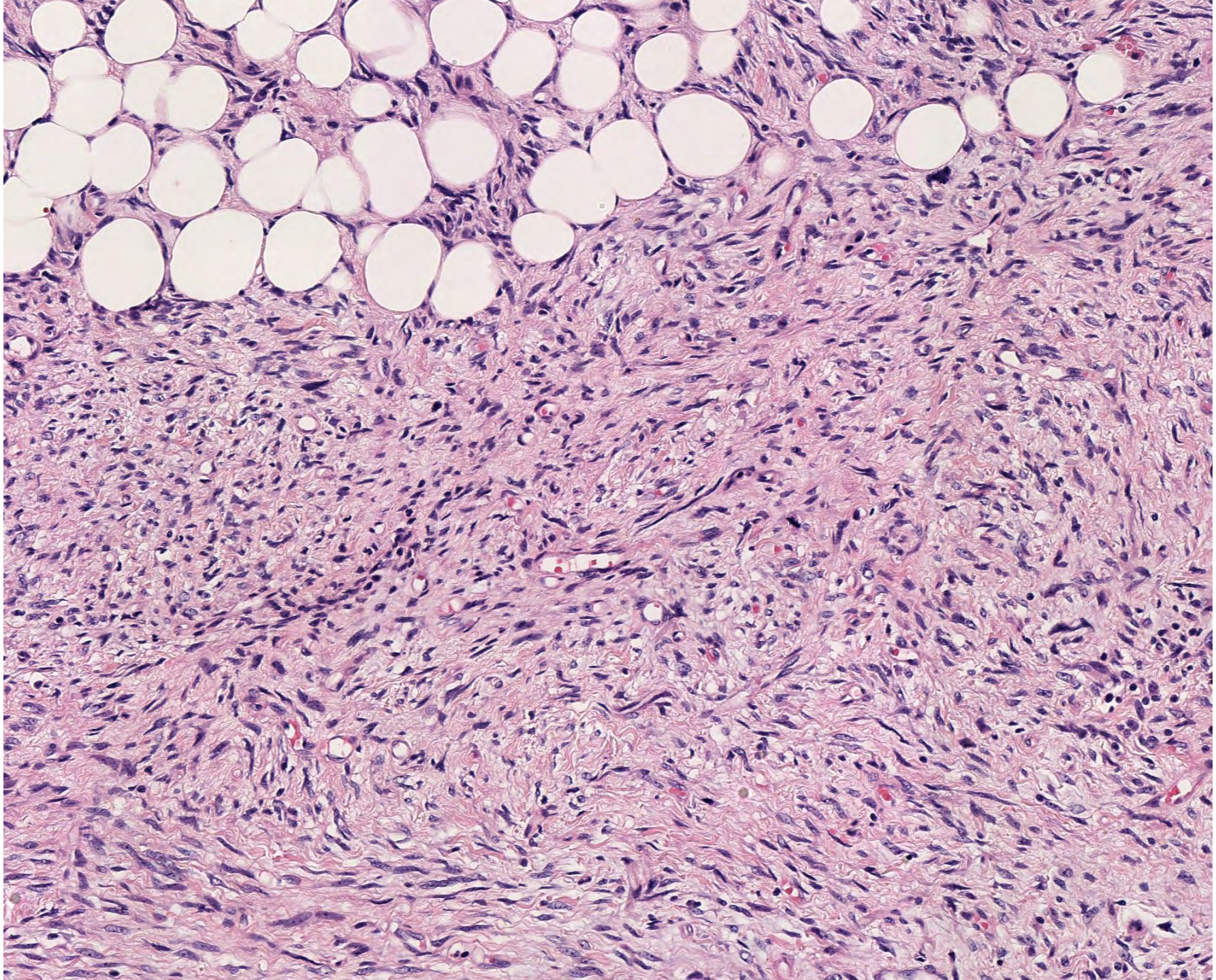

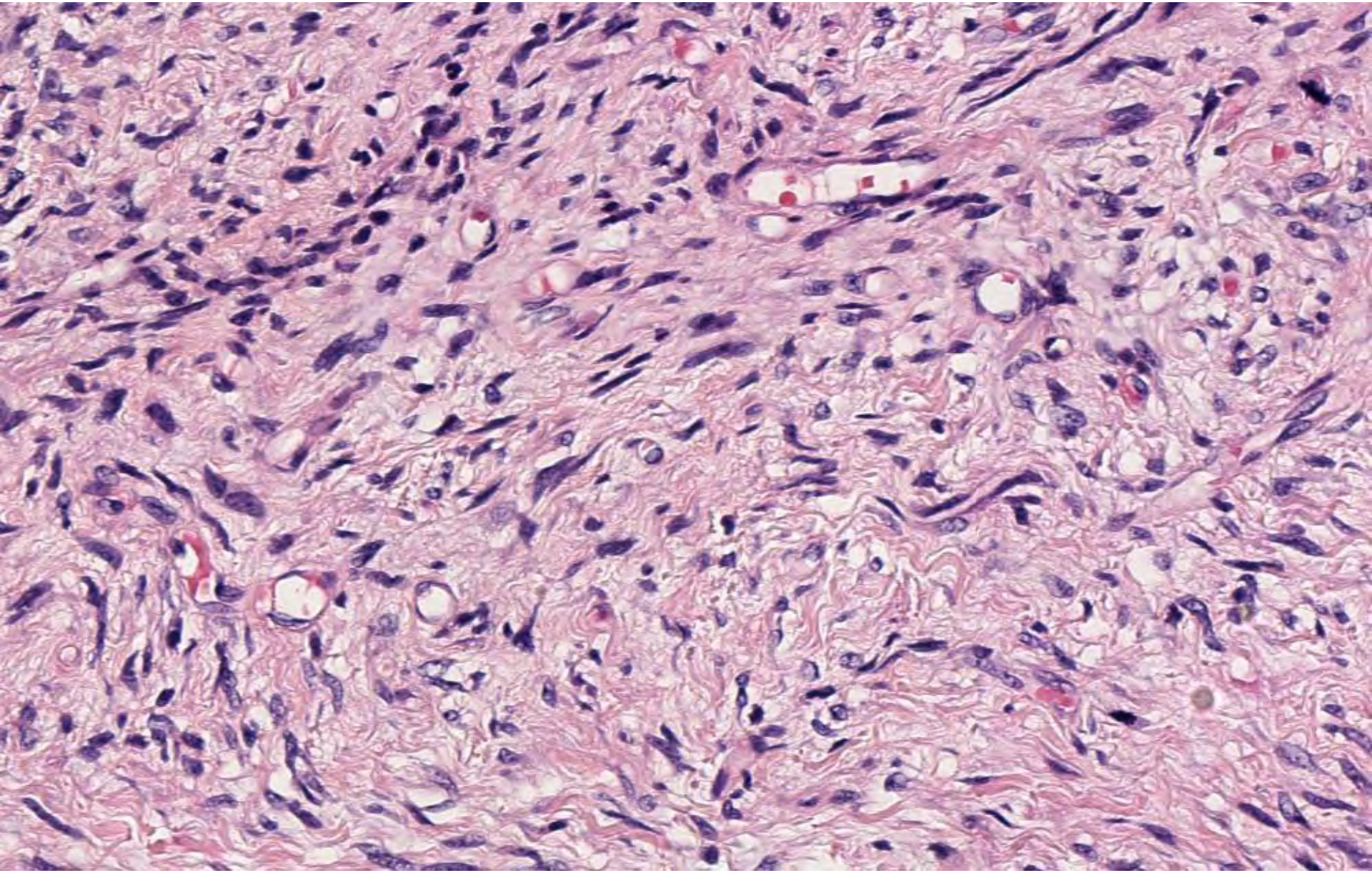

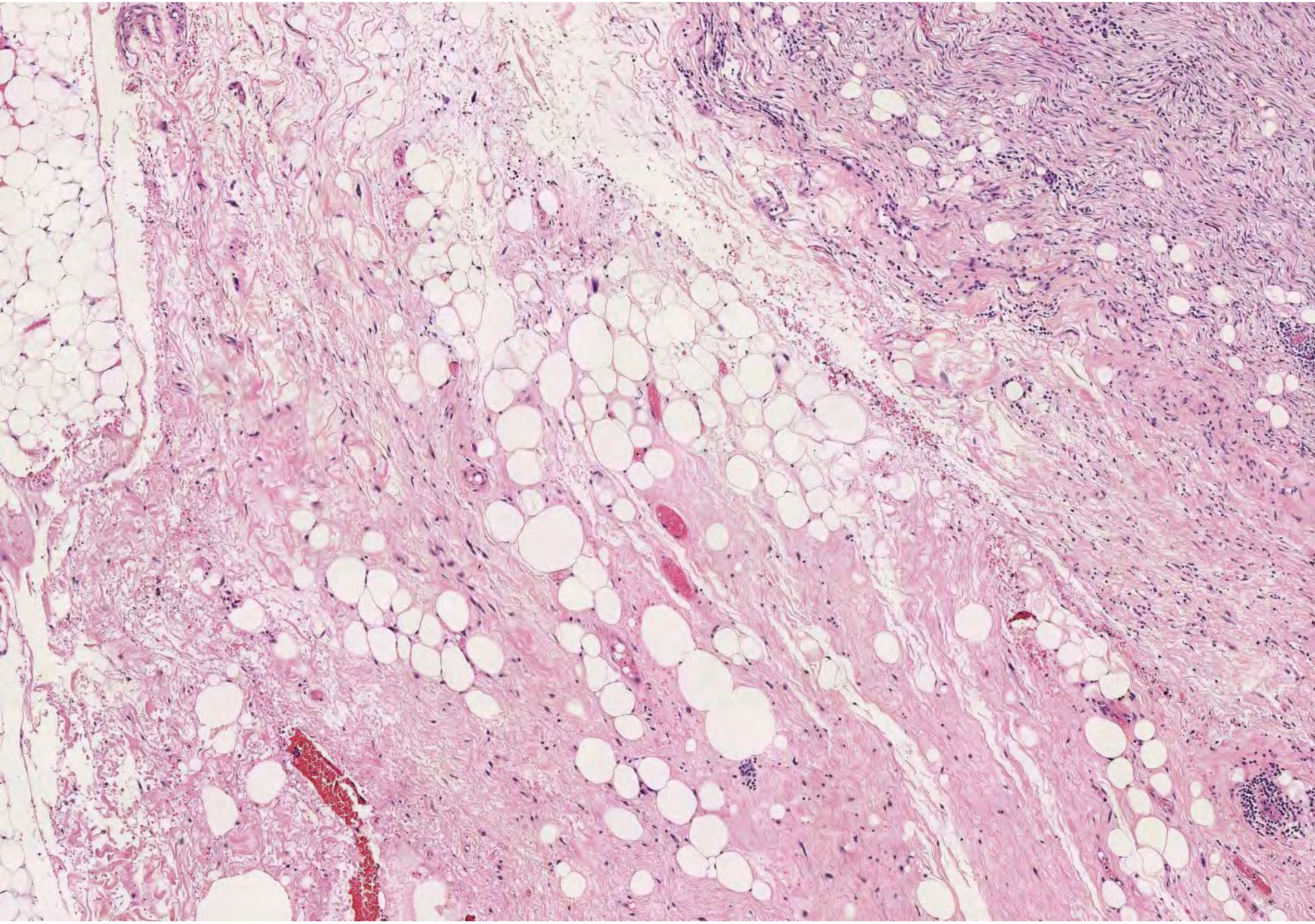

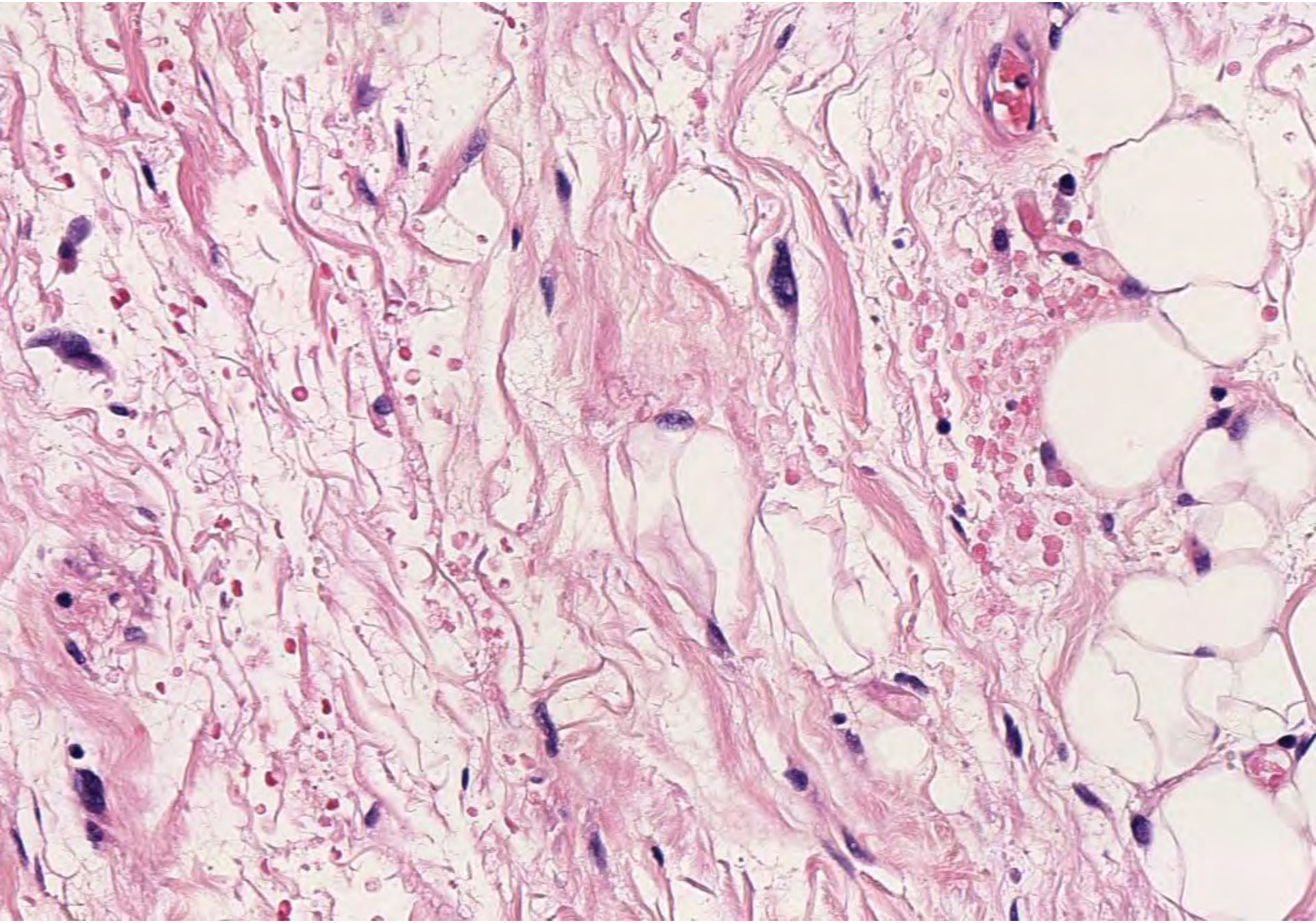

DIAGNOSIS

DDx

- Sarcomatoid renal cell carcinoma
- Sarcomatoid urothelial carcinoma
- Mucinous tubular & spindle cell carcinoma
- Angiomyolipoma
- de-differentiated liposarcoma
- Synovial sarcoma
- Solitary fibrous tumor
- Inflammatory myofibroblastic tumor
- Sclerosing epithelioid fibrosarcoma
- Leiomyosarcoma
- Melanoma
- MPNST
- metastasis

Dx

- Sarcomatoid renal cell carcinoma
- Sarcomatoid urothelial carcinoma
- Mucinous tubular & spindle cell carcinoma
- Angiomyolipoma
- **de-differentiated liposarcoma**
- Synovial sarcoma
- Solitary fibrous tumor
- Inflammatory myofibroblastic tumor
- Sclerosing epithelioid fibrosarcoma
- Leiomyosarcoma
- Melanoma
- MPNST
- metastasis

De-differentiated liposarcoma

- **"high grade" de-diff liposarcoma**
  - Cellular, marked pleomorphism
    - Looks like MFH/UPS
  - Usually >5 mites/10 hpf
  - Heterologous elements in 5-10%
- **"low grade" de-diff liposarcoma**
  - Some consider = to atypical lipomatous tumor
  - Less cellular, more bland
    - Looks like fibromatosis/fibrosarcoma spectrum
  - Usually <5 mites/10 hpf

TAKE HOME POINTS

- **Always consider de-diff liposarcoma in mesenchymal looking "renal" tumors lacking fat**
- **Sample grossly "normal" fat to look for background ALT**
- **Consider testing for MDM2/CDK4**
  - IHC, FISH, PCR